PHARMACOLOGY AND MODULATION OF ADENOSINE A_1 RECEPTORS IN THE MAMMALIAN CENTRAL NERVOUS SYSTEM

by

KEITH FINLAYSON

Submitted in accordance with the requirements for the degree

of

Doctor of Philosophy

The University of Edinburgh

Department of Pharmacology

1996

To Deborah

The candidate confirms that the work submitted is his own and that appropriate credit has been given where reference has been made to the work of others

Signed:

Date: 11 November 1996.

Abstract

Adenosine receptors are members of the G protein coupled receptor (GPCR) superfamily. Neurochemical and electrophysiological experiments point to a neuromodulatory role for adenosine. Adenosine inhibits the release of several neurotransmitters in brain by pre- and postsynaptic actions at adenosine A_1 receptors. In this thesis the pharmacology and modulation of adenosine A_1 receptors in the central nervous system (CNS) of different species was characterised. Rat renal adenosine A_1 receptors were also studied. In addition the central penetration by adenosine A_1 receptor antagonists following peripheral administration was investigated.

An *in vitro* [^{3}H]DPCPX ligand binding assay utilising a range of receptor agonists and antagonists, were used to compare the pharmacology of rat, mouse, guinea pig and human adenosine A_1 receptors. Standard xanthine-based adenosine antagonists had 10-fold lower affinity in human and guinea pig in comparison with rat and mouse. Several novel non-xanthine A_1 antagonists from the Fujisawa Pharmaceutical Co. Ltd., retained high affinity for adenosine A_1 receptors in all species, including human.

Modulation of ligand binding to adenosine A_1 and A_{2a} receptors by Gpp(NH)p and magnesium was examined. In common with other GPCRs, agonists bind to high and low affinity states, with the equilibrium modified by GTP analogues and magnesium, whereas effects on antagonist affinity are minimal. Agonist radioligands under the conditions used labelled predominantly the high affinity state of adenosine A_1 and A_{2a} receptors. Gpp(NH)p and magnesium have essentially inverse effects on radioligand (agonists and antagonists) binding to both adenosine A_1 and A_{2a} receptors. In addition their effects on [^{3}H]agonist and [^{3}H]antagonist binding are generally opposite, which is consistent with effects observed for other

GPCRs.

To act centrally, compounds must cross the blood brain barrier (BBB). A modified radioreceptor assay, involving a denaturation step to overcome the lipophilic nature of adenosine A_1 receptor antagonists was developed. This assay accurately measures the central penetration of adenosine A_1 receptor antagonists. Adenosine A_1 antagonists administered peripherally at equipotent behavioural doses, were found to be present in brain, at concentrations between 50-500 fold greater than *in vitro* K_i values for adenosine A_1 receptors. In addition, there was an excellent association between antagonist affinity *in vitro* and antagonist brain concentrations at the equipotent behavioural dose.

Adenosine and its receptors are widely distributed throughout the body. It is important to determine if peripheral adenosine A_1 receptors are identical to those in the CNS. Renal adenosine A_1 receptors were examined using radioligand binding, *in vitro* autoradiography and *in situ* hybridisation. Even using this combined approach, identification of adenosine A_1 receptors in rat kidney was not possible.

Alzheimers disease involves a myriad of neurochemical changes and neurotransmitter deficits. By antagonising the actions of endogenous adenosine, A_1 receptor antagonists could compensate for some of these deficits, by enhancing synaptic facilitation and increasing neurotransmitter release. Analogues of FK453, a non-xanthine adenosine A_1 antagonist, which are BBB permeable and potent and selective for human adenosine A_1 receptors, could prove to be clinically useful compounds, by enhancing cognition, in conditions such as Alzheimers disease.

Publications arising from the thesis

Published Abstracts

FINLAYSON, K., SHARKEY, J., OLVERMAN, H.J. & BUTCHER. S.P. (1995). Measurement of adenosine receptor antagonists in rat brain following intraperitoneal administration using a modified radioreceptor assay. *Br. J. Pharmacol. Proc. Suppl*, **116**, 307P.

MAEMOTO, T., FINLAYSON, K., OLVERMAN, H.J. & BUTCHER. S.P. (1995). Pharmacological characterisation of adenosine A_1 receptors in human brain membranes using a [^{3}H]DPCPX binding assay. *Br. J. Pharmacol. Proc. Suppl*, **116**, 308P.

ITO, H., MAEMOTO, T., FINLAYSON, K., OLVERMAN, H.J. & BUTCHER. S.P. (1995). Effects of adenosine receptor antagonists on CCPA-stimulated guanosine-5'-O-(3-[^{35}S]-thio)triphosphate binding to rat cerebral cortical membranes. *Br. J. Pharmacol. Proc. Suppl*, **116**, 306P.

FINLAYSON, K., MAEMOTO, T., OLVERMAN, H.J. & BUTCHER. S.P. (1995). Effects of Gpp(NH)p on adenosine A_1 receptor binding in rat cortical membranes. (A3.58-Abstracts of the Fourth IBRO World Congress of Neuroscience, Kyoto, Japan).

MAEMOTO, T., FINLAYSON, K., ATKINS, J.M., PERRY, R.C., OLVERMAN, H.J. & BUTCHER. S.P. (1994). Regional and species differences in brain adenosine A_1 receptors. *Can. J. Physiol. Pharmacol.* **72**. Suppl.1, P17.2.17.

FINLAYSON, K., MAEMOTO, T., OLVERMAN, H.J. & BUTCHER. S.P. (1994). The effect of Gpp(NH)p on adenosine A_1 receptor binding in rat cortical membranes. *Br. J. Pharmacol. Proc. Suppl*, **113**, 108P.

MAEMOTO, T., FINLAYSON, K., ATKINS, J.M., PERRY, R.C., OLVERMAN, H.J. & BUTCHER. S.P. (1994). Regional and species differences in [^{3}H]DPCPX binding to brain adenosine A_1 receptors. *Br. J. Pharmacol. Proc. Suppl*, **113**, 53P.

Papers

FINLAYSON, K., SHARKEY, J., OLVERMAN, H.J. & BUTCHER. S.P. (1996). Measurement of adenosine receptor antagonists in rat brain using a modified radioreceptor assay. (To be submitted- *J. Neurosci. Methods*).

MARSTON, H., FINLAYSON, K., MAEMOTO, T., OLVERMAN, H.J., SHARKEY, J. & BUTCHER. S.P. (1996). Correlation between the locomotor effects of adenosine receptor agonists and antagonists and drug levels in rat brain. (In preparation- *J. Pharmacol. Exp. Ther*).

MAEMOTO, T., FINLAYSON, K., OLVERMAN, H.J., AKAHANE, A., HORTON, R. & BUTCHER. S.P. (1996). Species differences between brain adenosine A_1 receptors studied using xanthine and pyrazolopyridine based antagonists. (In preparation- *Br. J. Pharmacol.*).

ITO, H., MAEMOTO, T., FINLAYSON, K., OLVERMAN, H.J., AKAHANE, A. & BUTCHER. S.P. (1996). Pyrazolopyridine derivatives act as competitive antagonists of brain adenosine A_1 receptors; guanosine-5'-0-(3-[^{35}S]thio)triphosphate binding studies. (In preparation- *Br. J. Pharmacol.*).

Acknowledgements

The studies reported in this thesis were carried out in the Department of Pharmacology, University of Edinburgh, in conjunction with the Fujisawa Institute of Neuroscience, University of Edinburgh. Neither this thesis or any part of it has been submitted to any other University.

I would like to thank a number of people who have helped and supported me during these studies:

-Professor J.S. Kelly for allowing me to work in the Department of Pharmacology and for his personal interest in my future development.

-My supervisors Dr H.J. Olverman and Dr S.P. Butcher for their direction and guidance throughout the thesis (I am sure there was?) and for their abilities to make 5 min conversations last 1 hr or 20 sec, respectively.

-My friend and colleague Taku Maemoto for his contribution to the work in Dr. Horton's lab and for his Apple Macintosh (most of the time!).

-Dr. H.M. Marston and Dr. J. Sharkey for explaining the intricacies of behavioural pharmacology and autoradiography.

-Dr T. Takaya and Dr K. Yoshida for their interest and kindness and for the use of Fujisawa compounds from the adenosine programme.

-Friends and colleagues in both Dr. Horton's and Dr. Eidne's laboratories for their invaluable help and assistance.

-I would like to thank my dad, mum and sister for always providing support and encouragement in everything I've done (and latterly some concern, especially when chapter 2 crashed!).

-Finally, to Deborah (my wife!), to whom this thesis is dedicated, for encouraging me to do a PhD (since Australia 1992, when I carelessly mooted the possibility) and for latterly doing everything I've not been aware of, remembered, or had time to do.

Contents

GENERAL INTRODUCTION

I. Historical Perspective

The physiological roles of extracellular purine nucleosides and nucleotides have been investigated since Drury and Szent-Györgi, (1929) first described a range of biological effects, including bradycardia and vasodilation. Research for the next three decades centred around physiological rather than pharmacological studies, and in the 1950's the cardiovascular effects of ATP (Green & Stoner, 1950) were examined in geriatric patients (Boettge *et al.*, 1957, quoted in Burnstock, 1993). In the 1960's, adenosine's role in regulating coronary blood flow associated with myocardial hypoxia was postulated (Berne, 1963; Gerlach *et al.*, 1963, quoted in Fredholm *et al.*, 1994a), generating a wider interest. The possible existence of an adenosine receptor was noted when the cardiovascular effects of adenosine were found to be blocked by caffeine (De Gubareff & Sleator, 1965). The vasodilatory role of ATP was not discovered until much later (De May & Vanhoutte, 1981). Receptors for the nucleotide ADP were also recognised several decades ago from work on blood platelets (Gaarder *et al.*, 1961), as summarised by Haslam & Cusack, (1981). Effects in the central and peripheral nervous system were implied when it was shown that ATP could be released from sensory nerves (Holton, 1959). With evidence accumulating, Burnstock (1972) in a pivotal review on "purinergic nerves" postulated the existence of central ATP receptors and that the principal substance released from nonadrenergic noncholinergic (NANC) nerves was ATP. At the same time, experiments in the CNS showed adenosine could stimulate the accumulation of cAMP in brain slices, an effect blocked by methylxanthines (Sattin & Rall, 1970). The release of endogenous adenosine from brain slices at concentrations sufficient to increase cAMP provided further evidence for the existence of adenosine receptors in the CNS (McIlwain, 1972). In the 25 years since these seminal observations an array of both central and peripheral effects, mediated through

a variety of purinergic receptors, have been attributed to both nucleosides and nucleotides (Olsson & Pearson, 1990; Jacobson *et al.*, 1992a; Burnstock, 1993; Collis & Hourani, 1993; Jacobson *et al.*, 1996). In light of the myriad of effects produced by these compounds, this review concentrates primarily on the role of adenosine receptors in the CNS.

II. Regulation of Adenosine

Adenosine is part of the metabolic machinery of all living cells and is central to the balance of energy supply and demand (Williams, 1987). Intracellular production of adenosine is via two distinct metabolic pathways, both involving hydrolases (Olsson & Pearson, 1990; Bruns, 1990). The major pathway involves the hydrolysis of the nucleotide AMP to adenosine by 5´-nucleotidase (Figure I.1), and the other involves catabolism of S-adenosylhomocysteine (SAH). Adenosine is released under conditions of stress, such as hypoxia, when cellular energy is depressed and acts locally as a metabolic regulator. The consequence of receptor activation is to restore the tissue or cell to a normal state and to protect from over-activation. Once released, adenosine can be eliminated by a variety of pathways, including transport back into the cell by specific nucleoside transporters, six of which have now been characterised (Kwong *et al.*, 1988; Gu *et al.*, 1995; Glass *et al.*, 1996; Parkinson *et al.*, 1996), passage across the membrane by simple diffusion and deamination to the receptor inactive compound inosine by adenosine deaminase (Olsson & Pearson, 1990). Adenosine's half-life of a few seconds or less in the circulation (Moser *et al.*, 1989), ensures a local action, diffusing perhaps a millimetre from the site of release. As highlighted above, adenosine once released acts on a range of adenosine receptors, regulating a wide variety of physiological functions throughout the body including, CNS, cardiovascular, renal, respiratory, immunological, gastrointestinal and

Purine Metabolism

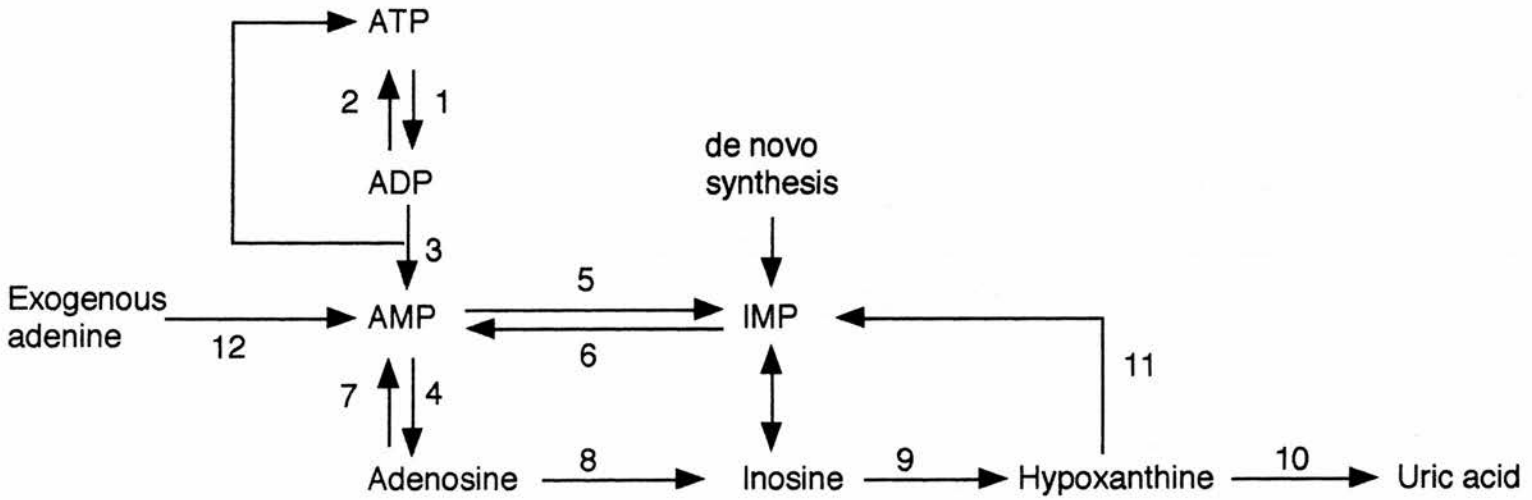

Figure I.1 Purine metabolism (from Olsson & Pearson, 1990). 1, ATP-consuming reactions; 2, oxidative phosphorylation; 3, myokinase; 4, 5´-nucleotidase; 5, AMP deaminase; 6, adenylosuccinate synthase and lyase; 7, adenosine kinase; 8, adenosine deaminase; 9, purine nucleoside phosphorylase; 10, xanthine dehydrogenase; 11, guanine phosphoribosyl transferase; 12, adenine phosphoribosyl transferase.

metabolic effects (Daly, 1982; Williams, 1987, 1993; Olsson & Pearson, 1990; Jacobson *et al.*, 1992a, 1996; Burnstock, 1993; Collis & Hourani, 1993).

III. A Neuromodulatory Role for Adenosine

Adenosine and ATP are both local regulators of physiological functions; i.e. they act within the same organs and perhaps even on the very cells that are the site of production. For over 50 years, ATP and adenosine have been proposed to function as neuromodulators or neurohormones. Interest in the role of purine receptors in the CNS was rekindled by the discovery that the methylxanthines, caffeine and theophylline may exert stimulatory actions by blocking the action of endogenous adenosine at adenosine receptors (Daly *et al.*, 1981). That caffeine was an adenosine receptor antagonist made it clear that adenosine receptors are the target for the most commonly used drug in the world (Jacobson *et al.*, 1996). Adenosine has been characterised as an inhibitory neuromodulator at biochemical, electrophysiological and behavioural levels (Williams, 1987, 1993). However, the question of whether purinergic transmission occurs in the CNS is controversial, because unlike classical neurotransmitters such as acetylcholine (Snyder, 1985), well circumscribed purinergic neuronal pathways have been difficult to identify (Williams, 1987). The most convincing evidence for discrete effects of adenosine in the CNS was the heterologous distribution of recognition sites in mammalian brain sections (Goodman & Snyder, 1982), suggesting as originally hypothesised, that purines play a significant role in controlling neuronal function (Snyder, 1985).

Historical precedent has defined a set of criteria which a compound should fulfil for it to be considered a neurotransmitter (Snyder, 1985). Classical neurotransmitters are produced by neurons, stored in synaptic vesicles, have mechanisms for synthesis and degradation, and the effects of nerve

stimulation should be mimicked by tissue application of the putative transmitter. Many neurotransmitters (e.g. acetylcholine at the neuromuscular junction) are very short acting (msec to sec) and are inactivated in the synapse (< 1 micron from the site of release). At the opposite end of the scale, classical circulating hormones are produced by glands and distributed by the circulation, acting for long periods (min to hr) at distant locations throughout the body. Based on the prototypic neurotransmitter, acetylcholine, adenosine was classified as a neuromodulator (Snyder, 1985). Adenosine is produced by many cell types, has well characterised synthetic and degradative pathways (Olsson & Pearson, 1990) and is released from nervous tissue *per se*, although evidence for vesicular storage is weak (Sweeney, 1996). The mechanism by which adenosine is released from neurons has still to be fully elucidated. There is evidence for Ca^{2+} dependent release, which is indicative of release of adenosine itself, rather than just by the dephosphorylation of ATP (Cahill *et al.*, 1993; Umemiya & Berger, 1994; Sweeney, 1996). Modulation of synaptic transmission by adenosine is mediated via both pre- and postsynaptic receptors (Swanson *et al.*, 1995; Von Lubitz *et al.*, 1996). Early experiments showed both adenosine and ATP reduced spontaneous and evoked release of acetylcholine, producing evidence for the existence of prejunctional purinergic receptors (Ginsborg & Hirst, 1972). Adenosine has subsequently been shown to inhibit the release of a variety of neurotransmitters (Fredholm & Dunwiddie, 1988; Von Lubitz *et al.*, 1996). Long term potentiation (LTP), which is postulated to be an underlying event in learning and memory is also inhibited by adenosine (Daval *et al.*, 1991; Suzuki *et al.*, 1993; Von Lubitz *et al.*, 1993). The presynaptic inhibition of neurotransmitter release, the postsynaptic decrease in excitability and the inhibition of LTP, an electrophysiological correlate of learning, all point to a negative neuromodulatory role for adenosine in the brain.

IV. Receptor Classification

Extensive analysis of the literature led to a proposal which forms the basis of currently accepted nomenclature for purinergic receptors (Burnstock, 1978). The initial receptor classification was based on the preference of receptors for binding adenosine (P_1 receptors) or adenine nucleotides (P_2 receptors). Inhibition of P_1 receptors by methylxanthines such as caffeine and theophylline was used to further distinguish between P_1 and P_2 receptors. Biochemical evidence showing differing effects of adenosine analogues on cAMP accumulation in different preparations and different agonist potencies pointed to the existence of multiple adenosine (P_1) receptors (Londos & Wolff, 1977; Van Calker *et al.*, 1979; Londos *et al.*, 1980). The two classes of receptor were named A_1 and A_2, based on their ability to inhibit or stimulate adenyl cyclase respectively (Van Calker *et al.*, 1979). This nomenclature was used in preference to the terminology, R_i (inhibition of adenyl cyclase) and R_a (activation of adenyl cyclase) proposed by Londos *et al.*, (1980). Traditionally, this type of receptor classification was based on relative potencies and the selectivities of agonists and antagonists. The criteria are: (1) antagonist affinity, (2) agonist potency ratio, (3) agonist affinity and (4) relative intrinsic agonist efficacy. The subsequent development of selective ligands (Jacobson *et al.*, 1992a; Suzuki *et al.*, 1992, 1993; Peet *et al.*, 1993), and the recent isolation of multiple cDNA clones for both P_1 and P_2 receptors (reviewed in, Fredholm *et al.*, 1994; Palmer & Stiles, 1995; Olah & Stiles, 1995), has necessitated expansion of the original classification.

The general advances in pharmacological and molecular techniques over the last 15 years have resulted in the on going identification of a large number of new receptor subtypes. In response, the International Union of Pharmacology (IUPHAR) Committee on Receptor Nomenclature and Drug

Classification have attempted to define how receptors should now be classified. Pharmacological classification of receptors should be based on combined structural and pharmacological information, with emphasis on antagonists rather than agonists, as agonist potency is dependent on agonist binding to the receptor and the entire signal transduction machinery (Kenakin *et al.*, 1992). These problems were highlighted with reference to purinoreceptors (Abbracchio *et al.*, 1993), where lack of selective antagonists has resulted in a classification heavily dependent on the relative potency of agonists. The IUPHAR subcommittee on purinoreceptors have attempted to clarify the situation (Fredholm *et al.*, 1994). Clarification was necessary, as there is debate over how many different subtypes of both P_1 and P_2 receptors exist. The controversy was exemplified by an almost simultaneous paper in which further potential subtypes of both P_1 and P_2 receptors were shown to exist, plus a separate class of P_3 purinoreceptors (Dalziel & Westfall, 1994). As well as the classified purinergic receptors, other proteins capable of binding adenosine include the P-site, adenosine transporters, adetonin and SAH, a site for the dinucleotide, diadenosinetetraphosphate and CD26 (Hutchison *et al.*, 1990; Schwabe *et al.*, 1991; Olsson & Pearson, 1990; Fredholm *et al.*, 1994; Dalziel & Westfall, 1994; Ciruela *et al.*, 1996).

Detailed discussion of P_2 receptors are not relevant to this thesis. Reviews on the classification and potential roles of P_2 receptors can be found (Burnstock, 1993; Fredholm *et al.*, 1994; Dalziel & Westfall, 1994; Abbracchio & Burnstock, 1994; Boarder *et al.*, 1995; Kennedy & Leff, 1995).

V. Adenosine (P_1) Receptors

All adenosine receptors have a general structure similar to that of bacteriorhodopsin (Henderson *et al.*, 1990) and are members of the G protein coupled receptor superfamily. To date, four adenosine receptors subtypes, A_1, A_{2a}, A_{2b} and A_3 have been structurally and pharmacologically characterised (Stiles, 1992; Jacobson *et al.*, 1992a; reviewed in Palmer & Stiles, 1995; Olah & Stiles, 1995). These receptors are distributed widely throughout the body giving a variety of potential therapeutic targets for both adenosine agonists and antagonists (Jacobson *et al.*, 1992a; Williams, 1993). The various subtypes and their extensive distribution necessitate that any therapeutic usefulness will require agonists and antagonists which are selective in their actions. Compounds used to identify the various subtypes of P_1 purinoreceptors have been summarised, along with some general information (Table I.1). This will be discussed in more detail in the following sections with each receptor described structurally, pharmacologically and functionally as these parameters define the subtypes and have physiological implications.

VI. The Adenosine A_1 Receptor

P_1 receptors were initially divided by the ability of adenosine to inhibit (A_1) or stimulate (A_2) cAMP production (Van Calker *et al.*, 1979; Londos *et al.*, 1980), and their relative sensitivity to methylxanthines. The rank order of potency of adenosine analogues in producing this effect was used to classify these receptor subtypes, A_1: R-PIA > NECA > S-PIA and A_2: NECA > R-PIA > S-PIA. This agonist order of potency is still important in the classification of adenosine receptors (Table I.1). However, extensive studies on the structure activity relationships of adenosine receptor ligands have identified structural features that produce selective high affinity agonists and antagonists, suitable

Table I.1 Adenosine Receptor Classification

Subtype	A_1	A_{2a}	A_{2b}	A_3
Potency order	R-PIA>NECA>S-PIA	NECA>R-PIA>S-PIA	NECA>R-PIA>S-PIA	R-PIA=NECA>S-PIA
Selective agonists	CPA, CCPA	CGS21680, APEC	--	APNEA, ABMECA
Selective antagonists	DPCPX, XAC, CPT	CSC, KF17837, SCH58261	--	I-ABOPX
Agonist radioligands	[^{3}H]CCPA, [^{3}H]R-PIA	[^{3}H]CGS21680, [^{3}H]NECA	--	[^{125}I]APNEA
Antagonist radioligands	[^{3}H]DPCPX, [^{3}H]XAC	[^{3}H]KF17837S, [^{3}H]SCH58261	--	[^{125}I]ABOPX
Species of cDNA isolation	Dog, Rat, Human, Mouse, Cow, G.pig, Rabbit, Chick	Dog, Rat, Human, Mouse, G.pig	Rat, Human, Mouse	Rat, Human, Sheep
Molecular mass-amino acids	37 kDa, 324-328 AA	45 kDa, 409-412 AA	36 kDa, 328-332 AA	36 kDa, 317-320 AA
G protein coupling	Gi / Go	Gs	Gs	Yes
Effectors	↓ cAMP, ↑ IP3 ↑ K^+, ↓ Ca^{2+}	↑ cAMP	↑ cAMP	↓ cAMP PLC, PKC

Abbreviations: R-PIA, R(-)-N^6-(2-Phenylisopropyl)adenosine; NECA, 5´-N-Ethylcarboxamidoadenosine; S-PIA, S(-)-N^6-(2-Phenylisopropyl)adenosine; CPA, N^6-Cyclopentyladenosine; CCPA, 2-Chloro-N^6-cyclopentyladenosine; DPCPX, 8-Cyclopentyl-1,3-dipropylxanthine; XAC, xanthine amine congener; CPT, 8-Cyclopentyl-1,3-dimethylxanthine; APEC, 2-[(2-aminoethylamino)carbonylethylphenylethylamino]-5´-N-ethylcarboxamidoadenosine; CGS21680, (2-*p* -carboxyethyl)phenylamino-5´N-carboxamidoadenosine; CSC, 8-(3-Chlorostyryl)caffeine; KF17837, (E)-1,3-Dipropyl-8-(3,4-dimethoxystyryl)-7-methylxanthine; SCH58261, 5-Amino-7-(2-phenylethyl)-2-(2-furyl)-pyrazolo[4,3-e]-1,2,4-triazolo[1,5-c]pyrimidine; APNEA, N^6-[2-(4-amino-3-iodophenyl)-ethyl]adenosine; ABMECA, N^6-(4-amino-3-iodobenzyl)adenosine-5´-N-methyluronamide; I-ABOPX, 3-(3-iodo-4-aminobenzyl)-8-(4-oxyacetate)-1-propylxanthine.

for A_1 and A_2 receptor characterisation (Jacobson *et al.*, 1992a) (Table I.1). The action of adenosine on A_1 receptors and the subsequent inhibitory effect on adenylate cyclase was shown to be G protein linked, with the A_1 receptor coupling to multiple G proteins, including G_i and G_o (Fredholm *et al.*, 1994; Palmer & Stiles, 1995; Asano *et al.*, 1995). In producing its effects, the A_1 receptor couples not only to different G proteins but to multiple effector systems (Olsson & Pearson, 1990; Collis & Hourani, 1993; Murthy & Makhlouf, 1995). A_1 receptors are linked to potassium channels, calcium channels, phospholipases A_2 and C (PLC) and perhaps guanylyl cyclase, although evidence for the latter is weak (Linden, 1991; Stiles, 1992; Olah & Stiles, 1992; Iredale *et al.*, 1994; Olah & Stiles, 1995). Based on evidence from other G protein coupled receptors (GPCRs), it is likely that these effects are produced by both the α and $\beta\gamma$ subunits of the G protein (Birnbaumer, 1992; Tang & Gilman, 1992; Freund *et al.*, 1994; Jockers *et al.*, 1994; Murthy & Makhlouf, 1995). For the A_1 receptor, knowledge of these effector systems is important as species homologues of the receptor can differentiate between related G protein α-subunits (Jockers *et al.*, 1994) and the same receptor can use multiple effectors (Akbar *et al.*, 1994; Freund *et al.*, 1994).

Structural characteristics of the A_1 receptor were investigated using ligand based radioprobes. The two approaches involved labelling adenosine receptors by indirect photoaffinity crosslinking (radiolabelled receptor ligand contains a chemically active group, e.g. aryl amine) and direct photoaffinity labelling (ligand preactivated for photolysis, e.g. using azido-derivatives) (reviewed in Stiles, 1990; Jacobson *et al.*, 1992a). The A_1 receptor binding protein was identified in rat as having a molecular weight of ~38 kDa (Klotz *et al.*, 1985; Stiles, 1985, 1986; Lohse *et al.*, 1986; Leung *et al.*, 1988) and was subsequently purified to homogeneity using affinity chromatography from a

variety of sources (Nakata, 1990; Freissmuth *et al.*, 1991a). The purified protein had the appropriate pharmacology (R-PIA > NECA > S-PIA), was functionally coupled to G proteins (Nakata, 1990; Freissmuth *et al.*, 1991a) and appeared to be identical across tissues and species as shown by the consistent labelling of a 38 kDa protein (Olah & Stiles, 1992). The size of the protein was confirmed by radiation inactivation analysis (Reddington *et al.*, 1989). The distribution of the A_1 receptor in a number of tissues and species has been examined using receptor autoradiography, with varying levels expressed in brain and peripheral tissues of various mammalian species (Goodman & Snyder, 1982; Fastbom *et al.*, 1986; Weber *et al.*, 1988, 1990a).

The introduction of molecular biology into the field of adenosine research has produced an explosion of information in the last five years. The adenosine A_1 receptor originally cloned from dog (Libert *et al.*, 1989, 1991a), has now been cloned from rat (Mahan *et al.*, 1991; Reppert *et al.*, 1991; Ungerer *et al.*, 1992), cow (Olah *et al.*, 1992; Tucker *et al.*, 1992), human (Libert *et al.*, 1992; Townsend-Nicholson & Shine, 1992; Ren & Stiles, 1994a), rabbit (Bhattacharya *et al.*, 1993), guinea pig (Meng *et al.*, 1994a), mouse (Marquardt *et al.*, 1994) and chick (Aguilar *et al.*, 1995) tissue (Table I.1 and Figure I.2). The clones encode a protein of 326 amino acids (AA) with the exception of rabbit which has 328 AA (Bhattacharya *et al.*, 1993) and chick (324 AA) (Aguilar *et al.*, 1995), corresponding to a protein of ~36.7 kDa, similar to that determined using photoaffinity labelling (Stiles, 1990) and immunological studies (Nakata, 1993). The amino acid sequence of the homologues from different mammalian species and tissues is very similar, showing approximately 90% homology in the transmembrane region but lower homology with the chick receptor (80%). The cloned receptor has similar properties to native receptors when expressed in mammalian cell lines, with the same rank order of potency for adenosine agonists: R-PIA > NECA >

Figure I.2 Rat Adenosine A_1 Receptor

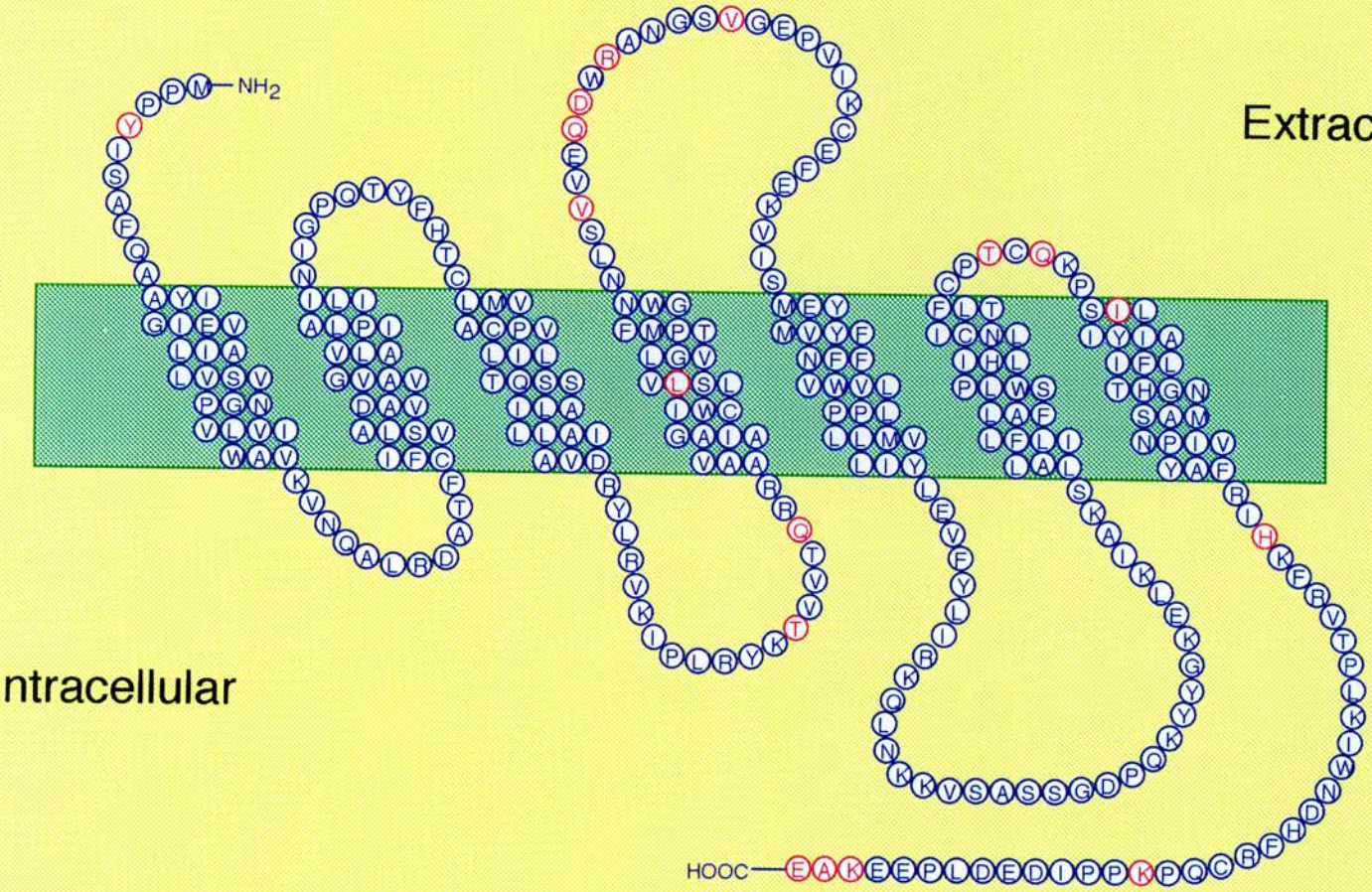

○ : Common sequence with human

S-PIA, except the bovine A_1 receptor, which has a unique pharmacology in both native and cloned receptors: R-PIA > S-PIA > NECA, (Olah *et al.*, 1992; Tucker *et al.*, 1992; Tucker & Linden, 1993). The distribution of adenosine A_1 receptor mRNA in rat tissue has been analysed using Northern blotting, *in situ* hybridisation and RT-PCR and is similar to that seen in comparable autoradiographic (Goodman & Snyder, 1982; Weber *et al.*, 1990a) and immunohistochemical studies (Rivkees *et al.*, 1995c; Ciruela *et al.*, 1995). The A_1 receptor is highly expressed in rat brain (cortex, cerebellum, thalamus and hippocampus), spinal cord and testis, with lower levels in heart and kidney (Mahan *et al.*, 1991; Reppert *et al.*, 1991; Johansson *et al.*, 1993; Rivkees, 1994). This distribution in rat of mRNA for all four adenosine receptors (for A_{2a}, A_{2b} and A_3, see below) has recently been expanded in an extensive study using *in situ* hybridisation and RT-PCR (Dixon *et al.*, 1996). There would appear to be species differences in tissue distribution, although brain and heart are consistently labelled in dog (Libert *et al.*, 1989), cow (Olah *et al.*, 1992), guinea pig (Meng *et al.*, 1994a), chick (Aguilar *et al.*, 1995) and human (Ren & Stiles, 1994a; Rivkees *et al.*, 1995b). A clue to perhaps understanding tissue and species variation in the properties of the adenosine A_1 receptor has recently been published (Ren & Stiles, 1994a, b). They demonstrated that control of human A_1 receptor gene expression can occur in the 5′ untranslated region by alternative splicing. The human A_1 gene has six exons and five introns, of which exons 1, 2, 3, 4 and part of 5 encode 5′ untranslated regions. This complexity is unusual with many other GPCRs not reported to have introns (Ren & Stiles, 1994a). The differential use of exons 3 or 4 directly effected levels of receptor expression in different tissues, with levels considerably reduced when exon 4 is present. This exon contained two ATG codons (and an in frame termination codon) which when mutated relieved the

inhibition of expression. The lack of exons 1 and 2 in mature mRNA from mammalian tissue has led recently to the renumbering of these exons (Ren & Stiles, 1995). Techniques such as site directed mutagenesis and production of chimeric receptors may help in understanding the amino acid residues involved in ligand recognition, perhaps leading to the development of new compounds (Klotz *et al.*, 1988; Tucker *et al.*, 1994; Olah *et al.*, 1994; Townsend-Nicholson & Schofield, 1994; Rivkees *et al.*, 1995a). This is of greater importance for the other adenosine receptors, as lack of selective antagonists still hampers our understanding of their pharmacological properties. The A_1 receptor was originally thought to be localised to chromosome 22 (Libert *et al.*, 1991b), but has now been correctly identified on chromosome 1 (Libert, 1994; Townsend-Nicholson *et al.*, 1995; Deckert *et al.*, 1995; Rivkees *et al.*, 1995b).

There is a great deal of evidence pointing to a functional role for the adenosine A_1 receptor in a number of physiological systems. Adenosine itself has been approved for the treatment of supraventricular tachycardia (Daval *et al.*, 1991; Jacobson *et al.*, 1992a). There is also evidence for a potential role for adenosine A_1 agonists in the treatment of epilepsy, stroke and pain (Daval *et al.*, 1991; Jacobson *et al.*, 1992a; Williams, 1993). Adenosine A_1 antagonists have potential roles in both renal protection and as diuretics (Jacobson *et al.*, 1992a; Burnstock, 1993; Jacobson *et al.*, 1996). Their role as cardiac stimulants and anti-asthmatic compounds has also been investigated (Daval *et al.*, 1991; Jacobson *et al.*, 1992a). In the mammalian CNS, calcium influx via different calcium channels contributes to the release of neurotransmitters at the presynaptic terminal. Presynaptic inhibition by adenosine action on A_1 receptors has been shown to inhibit predominantly N-type calcium channels (Yawo & Chuhma, 1993; Mogul *et al.*, 1993; Umemiya & Berger, 1994), leading to inhibition of neuronal calcium uptake and

decreased release of several neurotransmitters, such as acetylcholine, dopamine, norepinephrine, serotonin and glutamate (Fredholm & Dunwiddie, 1988; Arvin *et al.*, 1989; Lupica *et al.*, 1989; Von Lubitz *et al.*, 1996). Stimulation of postsynaptic A_1 receptors activates potassium and chloride conductances resulting in membrane hyperpolarisation and decreased neuronal excitability and firing rate. Adenosine A_1 antagonists enhance the release of various neurotransmitters and prevent hyperpolarisation of postsynaptic neurons. This mechanism may provide a way to treat cognitive deficits in humans, such as those associated with Alzheimers disease.

VII. The Adenosine A_{2a} Receptor

The A_{2a} receptor is positively linked to adenylate cyclase and is also G protein coupled. Unlike the A_1 receptor, coupling is unifocally to the stimulatory protein G_s and to its effector adenylate cyclase (Peterfreund *et al.*, 1996). Whereas A_1 selective ligands have been available for many years (Jacobson *et al.*, 1992a), selective A_2 ligands have only recently become available. The initial characterisation of the A_2 receptor was heavily dependent on the use of the non-selective agonist NECA, with various strategies used to block the A_1 component (Bruns *et al.*, 1986). The NECA derivative and agonist CGS21680 (Jarvis *et al.*, 1989a) exhibits high A_{2a} affinity and selectivity, and has become the radioligand of choice when examining this receptor subtype (Jarvis *et al.*, 1989a; Stehle *et al.*, 1992; Zhou *et al.*, 1992) (Table I.1). This ligand also helped confirm the existence of the A_2 receptor subtypes, A_{2a} and A_{2b} (Hide *et al.*,1992; Gurden *et al.*, 1993). The lack of highly selective A_{2a} antagonists has hindered receptor characterisation, as agonists like [^{3}H]CGS21680 label both high and low affinity states of the receptor in striatum (Wan *et al.*, 1990; Mazzoni *et al.*, 1993). However, three selective antagonists KF17837, 2-[2-(4-

amino-3-iodophenyl)ethylamino]adenosine (I-APE) and SCH58261, which have recently been developed as radioligands may help in further characterising the A_{2a} receptor (Nonaka *et al.*, 1994; Palmer *et al.*, 1995c; Zocchi *et al.*, 1996) (Table I.1).

Using an agonist photoaffinity probe (an azide derivative of ^{125}I-PAPA-APEC) and techniques similar to those described for the A_1 receptor, the mass of the A_2 receptor in native tissues was found to be ~45 kDa (Barrington *et al.*, 1990; Nanoff & Stiles, 1993). Autoradiographic distribution in different species demonstrated high expression in striatum with small amounts in cortex and midbrain (Jarvis & Williams, 1987; Jarvis *et al.*, 1989b, c; Martinez-Mir *et al.*, 1991). The striatum has therefore been the tissue of choice in which the functional and pharmacological characteristics of the A_{2a} receptor have been examined, with the properties of the non-striatal A_{2a} receptors initially ignored. The recent characterisation and classification of non-striatal A_{2a} receptor binding sites would appear controversial (Kirk & Richardson, 1995; Luthin & Linden, 1995; Johansson & Fredholm, 1995; Cunha *et al.*, 1996), and may in part be due to use of different agonist radioligands and incubation conditions. The use of the high affinity, selective antagonist radioligands will clarify this situation (Nonaka *et al.*, 1994; Palmer *et al.*, 1995c; Zocchi *et al.*, 1996).

The A_{2a} adenosine receptor has been cloned from canine (Maenhaut *et al.*, 1990), rat (Fink *et al.*, 1992; Chern *et al.*, 1992), human (Furlong *et al.*, 1992), mouse (Marquardt *et al.*, 1994) and guinea pig (Meng *et al.*, 1994b) cDNA libraries (Table I.1 and Figure I.3). There is a high level of homology (82-93%) comparing the overall amino acid sequence of canine and other receptors. Within the transmembrane domains there is 51% sequence homology at the amino acid level between the two originally identified canine A_1 and A_{2a} receptors (Libert *et al.*, 1989). The A_{2a} receptor is larger than the

Figure I.3 Rat Adenosine A_{2a} Receptor

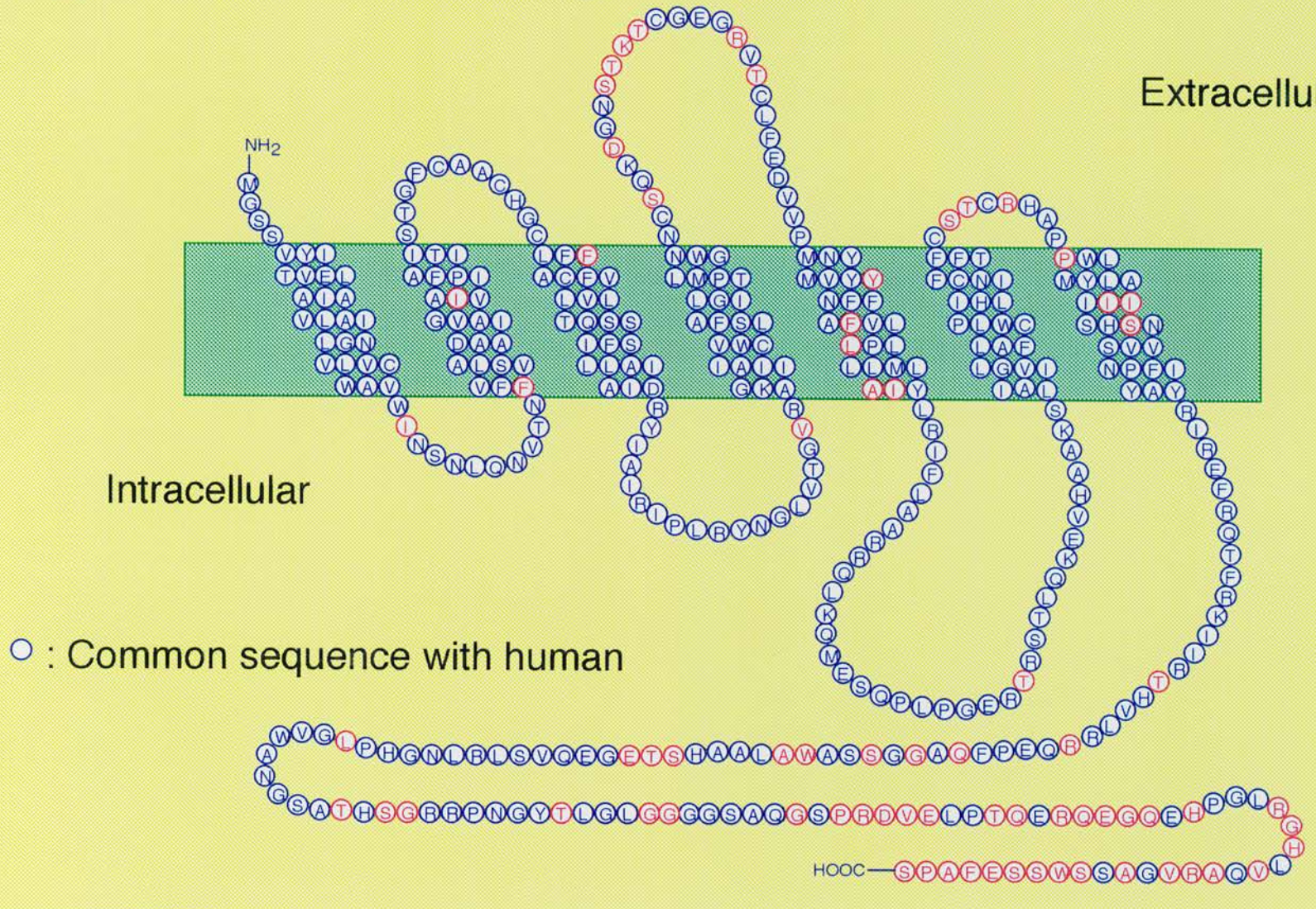

other three receptor subtypes (409-412 AA), corresponding to a protein of ~45 kDa, confirming photoaffinity labelling data (Stiles, 1986; Barrington *et al.*, 1990) (Table I.1). The functional significance of the 80-90 AA located on the carboxy terminus has not been elucidated. Truncation of the tail produced no appreciable difference in agonist pharmacology (Piersen *et al.*, 1994). Residues responsible for both agonist and antagonist binding have recently been identified in studies using site directed mutagenisis (Kim *et al.*, 1995). The pharmacology of the cloned receptors on stable expression was similar to that of native receptors (Fink *et al.*, 1992; Furlong *et al.*, 1992). The distribution in different species of the A_{2a} receptor message in brain, as analysed by Northern blotting and *in situ* hybridisation studies (Fink *et al.*, 1992; Furlong *et al.*, 1992; Meng *et al.*, 1994b) was similar to the autoradiographic distribution (Jarvis & Williams, 1989b, c). The receptor is highly expressed in striatum with small amounts in cortex and midbrain. Interestingly, the discrete localisation in adult animals of A_{2a} mRNA to the striatum, contrasts with a widespread expression during development (Weaver, 1993). In peripheral tissues, the A_{2a} receptor transcript is present in human heart, kidney, spleen, lung, thymus and leukocytes (Peterfreund *et al.*, 1996). In guinea pig, the distribution was similar with hybridisation signals in heart, kidney and spleen, however, there was no signal in lung (Meng *et al.*, 1994b). The A_{2a} receptor in human has recently been reported to be localised to chromosome 22 (Peterfreund *et al.*, 1996). As with the A_3 receptor (see below) and unlike the A_1 receptor, it contains only two exons and one intron. The intron occurs in the sequence corresponding to the second intracellular loop, which lies between transmembrane domains 3 and 4. This may be a feature common to the adenosine receptor gene family as it is present in human A_1 (Ren & Stiles, 1994a), rabbit A_1 (Bhattacharya *et al.*, 1993), chick A_1 (Aguilar *et al.*, 1995) and rat and human A_3 (Zhou *et al.*,

1993; Murrison *et al.*, 1995, 1996).

Evidence for a functional role for the A_{2a} receptor in multiple physiological systems is increasing. The role of adenosine in regulating blood flow (Olsson & Pearson, 1990), and the vasodilation associated with activation of A_{2a} receptors, led to the proposal that selective agonists may have a role in hypotensive therapy (Hutchison *et al.*, 1989; Collis and Hourani, 1993). The co-localisation of A_{2a} receptors with dopamine receptors (Fink *et al.*, 1992) in striatum, and the effects of adenosine on dopamine receptor density (Williams, 1993), imply a potential therapeutic role in Parkinsons disease, schizophrenia and Huntingtons disease (Williams, 1993; Kim *et al.*, 1995). A potential role for the A_{2a} receptor in facilitating synaptic transmission through P-type calcium channels at the presynaptic terminal may also exist (Umemiya & Berger, 1994). Expression of the receptor in mast cells, spleen, thymus and leukocytes also indicates a potential role in immune responses (Marquardt *et al.*, 1994; Peterfreund *et al.*, 1996).

VIII. The Adenosine A_{2b} Receptor

The separation of the A_2 receptor into two subtypes (Daly *et al.*, 1983; Bruns *et al.*, 1986), was based on differences observed in agonist and antagonist binding affinities for rat striatal (A_{2a}) (Bruns *et al.*, 1986) and human fibroblast (A_{2b}) adenosine receptors (Bruns, 1980, 1981). The A_{2a} and A_{2b} receptors are both positively linked to adenylate cyclase, presumably through G_s. While the high affinity A_{2a} receptor was found primarily in striatum, the low affinity A_{2b} receptor is found throughout the brain (Daly *et al.*, 1983; Bruns *et al.*, 1986). Although the availability of compounds like CGS21680 has enabled the classification to be tentatively confirmed in functional studies using different tissues and species (Jarvis *et al.*, 1989a; Wan *et al.*, 1990; Gurden *et al.*,

1993), pharmacological data is still minimal due to the lack of receptor selective compounds for the A_{2b} receptor in particular.

The A_{2b} receptor has been cloned from rat (Stehle *et al.*, 1992; Rivkees & Reppert, 1992), mouse (Marquardt *et al.*, 1994) and human (Pierce *et al.*, 1992) cDNA libraries with >85% homology in the transmembrane spanning regions across species (Table I.1). There is a reasonable level of homology (73%) between the A_{2b} and A_{2a} receptors in the transmembrane regions (Stehle *et al.*, 1992), despite being smaller than the A_{2a} receptor and more similar in size to the A_1 and A_3 receptors, at 36.4 kDa. Identification and characterisation of clones which potentially encode for the A_{2b} receptor and assessment of their functional significance is still limited by the lack of selective compounds. Identification is generally by excluding the involvement of the other adenosine receptor subtypes. For the A_{2b} receptor, stimulation of adenylate cyclase is less sensitive to adenosine agonists and more sensitive to xanthine antagonists than the A_{2a} receptor (Bruns *et al.*, 1986). This combined with specific binding using [^{3}H]NECA (non-selective agonist) and the lack of [^{3}H]CGS21680 (A_{2a} agonist) or [^{3}H]CCPA (A_1 agonist) binding is used to identify the existence of A_{2b} receptors (Stehle *et al.*, 1992; Rivkees & Reppert, 1992; Pierce *et al*, 1992). Distribution of rat A_{2b} receptor mRNA as assessed by Northern blot analysis is very distinct from A_1 and A_{2a} receptors, with greatest expression of transcripts in caecum, large intestine and urinary bladder and lesser amounts in brain, spinal cord and lung (Stehle *et al.*, 1992). Localisation of the receptor using a polyclonal antibody to the human A_{2b} receptor has confirmed and extended this distribution map (Puffinbarger *et al.*, 1995). The identification and use of tissues which highly and specifically express the A_{2b} receptor may help to clarify the pharmacological and functional characteristics of the receptor and confirm possible roles, such as

mediation of the secretory action of adenosine on mast cells (Marquardt *et al.*, 1994). Recently the chromosomal localisation of the human A_{2b} receptor gene and a potential pseudogene, which shares 79% homology, has been reported (Jacobson *et al.*, 1995). The A_{2b} receptor was reported to be localised to chromosome 17p12 and the pseudogene to 1q32, both of which are distinct from the chromosomal localisation of A_1 and A_{2a} receptors. The presence of potential pseudogene transcripts, despite their inability to produce functional receptors, may lead to a misinterpretation of results from *in situ* hybridisation and Northern blot studies on the potential localisation of the A_{2b} receptor.

IX. The Adenosine A_3 Receptor

Based on radioligand binding studies and the physiological effects of adenosine analogues on various tissues, the existence of A_1, A_{2a} and A_{2b} receptors was postulated before cloning of the relevant cDNA sequences. This was not the case for the A_3 receptor, as screening of cDNA libraries with degenerate oligonucleotide probes resulted in the isolation of a further and unexpected adenosine receptor subtype. A clone isolated from a rat testis cDNA library encoded a protein of 320 AA that displayed an overall homology of 47 and 42% to the canine A_1 and A_{2a} receptors respectively (Meyerhof *et al.*, 1991). Pharmacological characterisation of a clone from a rat brain cDNA library which was 99.5% identical to the clone from rat testis, showed a pharmacological profile different from characterised adenosine receptors and was called the A_3 receptor (Zhou *et al.*, 1992). Competition binding studies using membranes from transfected cells showed that, in comparison with the A_1 receptor, agonists had a lower affinity and a different order of potency and that xanthine antagonists were uncharacteristically poor inhibitors. In cells transfected with the putative A_3 receptor, adenosine analogues also inhibited

forskolin stimulated accumulation of cAMP through an interaction with a pertussis toxin sensitive G protein, in a manner similar to the A_1 receptor (Zhou *et al.*, 1992).

A_3 receptors were subsequently cloned from sheep (Linden *et al.*, 1993) and human (Salvatore *et al.*, 1993; Sajjadi & Firestein, 1993) cDNA libraries and were more similar to each other (85%) than to rat (73%) in terms of overall amino acid identity. The A_3 receptor is similar in size to the A_1 and A_{2b} receptors (317-320 AA, depending on species) and encodes a protein of approximately 36.6 kDa (Table I.1). The A_3 receptor is unlike the other three receptors because it has N-linked glycosylation sites on both the amino terminus and the second extracellular loop; the relevance of these sites is not known. A_3 receptor homologues from different species have a greater variation at the amino acid level than other adenosine receptors, and vary substantially in their pharmacological characteristics and tissue distribution (Salvatore *et al.*, 1993). Development of selective agonists and antagonists for the A_3 receptor has confirmed these pharmacological differences, and a binding site model has been proposed for the A_3 receptor (van Galen *et al.*, 1994; Kim *et al.*, 1994) (Table I.1). Significant species differences have been confirmed in both agonist affinity (Ji *et al.*, 1994) and tissue distribution (Linden, 1994). In rat, the most abundant message is in testis (Meyerhof *et al.*, 1991; Zhou *et al.*, 1992), with moderate amounts of A_3 receptor mRNA found in lung, kidney and heart and lower levels in brain (Zhou *et al.*, 1992). In sheep, higher levels were found in brain, lung and spleen with low levels in kidney (Linden *et al.*, 1993). In human (Salvatore *et al.*, 1993), the distribution profile of A_3 receptor mRNA was: lung = liver >> brain = aorta > testis > heart, with none in spleen and kidney. In contrast, Sajjedi & Firestein (1993), despite showing A_3 receptor mRNA in lung, liver and heart, did not detect transcript in brain but found a

strong signal in kidney. The physiological role of this receptor has still not been clearly defined although the localisation in rat testis implies a role in reproduction (Meyerhof *et al.*, 1991; Mazzoni *et al.*, 1995). The abundance of receptor mRNA in lung suggests a role in allergic responses in the pulmonary system (Linden *et al.*, 1993), however roles in mediating cardiovascular and CNS effects have also been implied (Jacobson *et al.*, 1992b; Kim *et al.*, 1994; Abbracchio *et al.*, 1995; Von Lubitz *et al.*, 1995). A very recent study in which the tissue distribution of receptor mRNA for all four adenosine receptors was examined, suggested a similar distribution of the A_3 receptor in rat, sheep and human, with previous differences attributable to quantitative differences in abundance (Dixon *et al.*, 1996). Initial studies showed adenosine analogues mediated effects at the A_3 receptor through a pertussis toxin sensitive effect on adenylate cyclase (Zhou *et al.*, 1992). However, a variety of effector systems have recently been linked with the A_3 receptor. Like the A_1 receptor, there is evidence that the A_3 receptor couples to different G protein subtypes (Palmer *et al.*, 1995b) and thus to protein kinase C (PKC) (Kim *et al.*, 1994), PLC (Abbracchio *et al.*, 1995) and G protein coupled receptor kinases (Palmer *et al.*, 1995a). The human A_3 receptor gene has been characterised (Murrison *et al.*, 1995, 1996), containing two exons separated by one intron as in rat (Zhou *et al.*, 1992). Unlike the A_1 receptor (Ren & Stiles, 1994a, b), the A_3 receptor is unlikely to undergo alternative splicing in the 5′ untranslated region. However, considerable variation in tissue expression would imply a transcriptional control of A_3 mRNA at some level. The human A_3 receptor gene (ADORA3) has been localised to chromosome 1p and may help in determining whether mutant A_3 receptor genes are candidates for diseases of the lung, vasculature or nervous systems that map to that area (Monitto *et al.*, 1995). Interestingly the mouse A_3 receptor gene has been chromosomally located and mapped to chromosome

3, which has a high homology with human chromosome 1 (Zhao *et al.*, 1995).

The cloned A_3 receptor discussed here is distinct from the other putative adenosine A_3 receptor described for the frog neuromuscular junction (Ribeiro & Sebastiao, 1986). The classification of these receptor subtypes has been the subject of much debate (Carruthers & Fozard, 1993; Ribeiro & Sebastiao, 1994; Beaven *et al.*, 1994; Linden, 1994). Evidence for the neuromuscular A_3 receptor (Ribeiro & Sebastiao, 1986) was considered not compelling, whereas that of the cloned A_3 receptor (Zhou *et al.*, 1992) was and consequently it has been accepted as a distinct adenosine receptor subtype (Abbracchio *et al.*, 1993; Fredholm *et al.*, 1994).

X. Aims of the Research Project

Neurochemical and electrophysiological experiments have led to the proposal that adenosine may act as a inhibitory neuromodulator in the CNS. Basal CNS concentrations of adenosine in the low micromolar range suggest that adenosine receptors are tonically activated and perhaps contribute to the mediation of a general inhibitory tone. Adenosine is known to inhibit the release of several neurotransmitters in brain by acting upon adenosine A_1 receptors. The neuromodulatory role of adenosine may exert a specific protective effect under conditions of enhanced neuronal activity (Schwabe *et al.*, 1991), but it may exacerbate the problem of neurotransmitter deficit in conditions such as Alzheimers disease. Reversal of this tonic inhibition by an adenosine A_1 receptor antagonist may enhance neurotransmitter levels, leading to synaptic facilitation at both pre- and postsynaptic sites and perhaps leading to some restoration of neuronal function in diseases such as Alzheimers (Daval *et al.*, 1991; Suzuki *et al.*, 1993; Von Lubitz *et al.*, 1993).

The purpose of the work described in this thesis was to identify a

selective, high affinity, blood brain barrier permeable adenosine A_1 receptor antagonist, using a series of novel non-xanthine antagonists (Terai *et al*, 1995a; Balakrishnan *et al.*, 1996). In order to achieve this goal the following three main areas were investigated:

In chapters 1 and 2, basic aspects of adenosine receptor pharmacology were examined. In chapter 1, *in vitro* radioligand binding assays were used to comprehensively characterise the affinity and selectivity of agonists and antagonists for adenosine A_1 receptors in rat brain. With species differences in adenosine A_1 receptor pharmacology characterised and as the ultimate goal of this study is the discovery of a drug for use in man, adenosine A_1 receptor pharmacology was studied in human brain tissue. Adenosine receptors are members of the G protein coupled receptor superfamily. As the ligand binding properties of other members of the receptor family are sensitive to the effects of cations and guanine nucleotides, chapter 2 involved an extensive examination of the modulation of ligand binding to both adenosine A_1 and A_{2a} receptors by the stable GTP analogue Gpp(NH)p and magnesium.

In Chapter 3, a modified radioreceptor assay was developed and characterised to measure the concentration of adenosine A_1 receptor antagonists in rat brain following intraperitoneal administration. All drugs were given at doses known to produce a centrally mediated behavioural effect and drug concentrations were determined in brain and serum.

Finally, in chapter 4, peripheral adenosine A_1 receptors were examined in order to determine whether they are identical to those in the CNS. A centrally selective adenosine A_1 receptor antagonist devoid of peripheral activity would be of obvious benefit. The pharmacology and localisation of renal adenosine A_1 receptors were examined using a combined approach of radioligand binding, *in vitro* autoradiography and *in situ* hybridisation.

CHAPTER ONE

SPECIES DIFFERENCES IN ADENOSINE A_1 RECEPTOR PHARMACOLOGY

1.1. Introduction

It has been emphasized that antagonists rather than agonists should be used for the pharmacological classification of receptors (Kenakin *et al.*, 1992). Until the late 1980s, this was not the case for purinergic receptors, with stable adenosine analogues like N^6-cyclohexyladenosine (CHA), R-PIA, 2-chloroadenosine (CADO) and NECA (Bruns *et al.*, 1980; Murphy & Snyder, 1982; Yeung & Green, 1984) used for receptor classification. These agonists were central to identifying the pharmacological characteristics of A_1, A_{2a} and A_{2b} receptors (Jacobson *et al.*, 1992a; Abbracchio *et al.*, 1993; Collis and Hourani, 1993). Extensive studies on the structure activity relationships of adenosine receptor ligands identified further modifications on both adenosine based agonists and xanthine antagonists that produced selective high affinity compounds for the A_1 receptor (Daly *et al.*, 1985; Jacobson *et al.*, 1992a; Peet *et al.*, 1993; Suzuki *et al.*, 1993). The agonist, CCPA (Klotz *et al.*, 1989; Monopoli *et al.*, 1994) and antagonist, DPCPX (Bruns *et al.*, 1987), with subnanomolar affinity and marked selectivity for A_1 receptors were developed. [^{3}H]DPCPX is now the ligand of choice when studying adenosine A_1 receptors, exhibiting consistent and marked selectivity for the A_1 versus the A_{2a} receptor (>600 fold) and being devoid of affinity for other receptors (Bruns *et al.*, 1987; Lohse *et al.*, 1987; Weber *et al.*, 1990a; Bisserbe *et al.*, 1992). As with other GPCRs, agonists can bind to a high and low affinity state of the adenosine A_1 receptor, whose equilibrium is modified by ionic conditions and the presence of guanine nucleotides. In contrast, antagonists have the advantage of recognising both states with equal affinity (Gilman, 1987; Collis & Hourani, 1993; Casado *et al.*, 1994). Unlike A_1 receptors, studies into A_{2a}, A_{2b} and the recently cloned A_3 adenosine receptor have been hindered by a dearth of useful compounds. Binding properties of the A_2 receptor were initially

examined using the non-selective agonist [^{3}H]NECA, with contaminating A_1 sites blocked using selective A_1 antagonists or agonists, thereby increasing the complexity of the assay (Bruns *et al.*, 1986). The synthesis of CGS21680, which has high affinity and selectivity for rat striatal A_{2a} receptors, removed this complexity and is presently the radioligand of choice when investigating this receptor subtype (Jarvis *et al.*, 1989a). The lack of selective A_{2a} antagonists has hindered the pharmacological characterisation of this receptor, and until recently the high affinity, non-selective antagonist 9-chloro-2-(2-furyl)[1,2,4]triazolo[1,5-c]quinazolin-5-amine (CGS15943) was the only useful compound (Jarvis *et al.*, 1989a; Griebel *et al.*, 1991). New styryl based A_{2a} antagonists like CSC (Jacobson *et al.*, 1993) and KF17837 (Shimada *et al.*, 1992; Nonaka *et al.*, 1993), with reasonable affinity and selectivity are now available, however neither is very stable. These compounds have recently been superseded by a new generation of stable, high affinity and selective A_{2a} receptor antagonists, which when commercially available, will no doubt provide useful pharmacological tools (Nonaka *et al.*, 1994; Palmer *et al.*, 1995c; Zocchi *et al.*, 1996). The development of selective agonists (e.g. ABMECA) and antagonists (e.g. I-ABOPX) for the A_3 receptor (Van Galen *et al.*, 1994; Kim *et al.*, 1994), would appear to be proceeding faster than that of the A_{2b} receptor, which although recognised for more than 10 years, still lacks any suitable ligands (Olah & Stiles, 1995).

The classification of the adenosine receptors has been complicated not only by the lack of receptor selective ligands but by well documented species differences in adenosine receptor pharmacology, characterised in radioligand binding studies (Murphy & Snyder, 1982; Ferkanky *et al.*, 1986; Ukena *et al.*, 1986; Stone *et al.*, 1988; Ji *et al.*, 1994). N^6-substituted adenosine analogues like CHA and R-PIA have a higher affinity for the adenosine A_1 receptor in

bovine, rat and mouse brain tissue compared with guinea pig and human tissue (Murphy & Snyder, 1982; Ferkanky *et al.*, 1986; Ukena *et al.*, 1986). In contrast, the presence of the 5′-ethylcarboxamido moiety in compounds like NECA, resulted in almost equipotency across species (Ferkanky *et al.*, 1986; Ukena *et al.*, 1986). These species difference have also been visualised for adenosine A_1 receptors in both central and peripheral tissues using autoradiographic studies; for example, adenosine A_1 receptors are localised in the cortex of human kidney but are found in the medulla of guinea pig kidney (Fastbom *et al.*, 1986, 1987a; Palacios *et al.*, 1987; Araki *et al.*, 1992).

In assessing the therapeutic potential of Fujisawa's novel non-xanthine adenosine A_1 receptor antagonists (Terai *et al.*, 1995a; Balakrishnan *et al.*, 1996), it is necessary to determine both affinity and selectivity for adenosine A_1 receptors in brain tissue. The inherent problems associated with agonist ligands (Kenakin *et al.*, 1992), prompted the establishment of a radioligand binding assay in rat brain using the antagonist [^{3}H]DPCPX in a method similar to Bruns *et al.*, (1987). To establish whether compounds were selective for the A_1 receptor, affinity for rat striatal A_{2a} receptors was examined using [^{3}H]CGS21680 in a method similar to Jarvis *et al.*, (1989a). Unfortunately when these studies were conducted no antagonist radioligands for the A_{2a} receptor were commercially available. The potential for species differences (Ferkanky *et al.*, 1986; Stone *et al.*, 1988; Ji *et al.*, 1994), and the lack of a comprehensive pharmacological study using antagonist radioligands, prompted modification of the [^{3}H]DPCPX binding assay for use in human tissue in order to study species selectivity.

1.2. Methods and Materials

1.2.1. Animals

Unless otherwise stated, animals used in these studies were male Sprague Dawley rats (250-350 g; Charles River). Animals were given food and water *ad libitum* and maintained on a 12hr light/12hr dark cycle.

1.2.1.1. Rat Brain Membrane Preparation

Crude synaptosomal P_2 membranes were prepared from rat cerebral cortex and striatum using the following procedure. Rats were killed by decapitation, brains removed and placed in ice cold saline. Following dissection of appropriate brain areas, tissues were dried briefly, rolled on filter paper to remove superficial blood vessels and weighed. Tissues were homogenised using a teflon glass homogeniser in 15 vol. (v/w) of ice cold 0.32 M sucrose and the homogenate was centrifuged at 1000 g for 10 min at 4°C in a Burkard Coolspin. The supernatant was centrifuged at 17000 g for 20 min at 4°C and the resultant P_2 pellet was lysed in 30 vol. (v/w) of ice cold glass distilled water for 30 min. Membranes were centrifuged at 50000 g for 10 min at 4°C in a Centrikon T-2070. The pellet was resuspended in 30 vol. (v/w) of 50 mM Tris-HCl buffer, pH 7.4 (Tris-buffer) at 4°C and centrifuged at 50000 g for 10 min at 4°C. The final pellet was resuspended in 5 vol. (v/w) of Tris-buffer and stored in 1.4 ml aliquots in 1.8 ml microcentrifuge tubes at -20°C until required.

On the day of the assay membranes were resuspended in 30 vol. (v/w) of Tris-buffer and centrifuged at 50000 g for 10 min at 4°C. The final pellet was resuspended in 200 vol. (v/w) of Tris-buffer, then kept on ice prior to use in the assay.

1.2.1.2. Human Brain Membrane Preparation

All studies using human brain tissue were performed in collaboration with Dr R.W. Horton, St. George's Hospital Medical School, London. All procedures were carried out with strict adherence to rules laid down by the hospital in regard to handling human tissue.

Human parietal cortex (Brodmann Area 7) (9.6 g) collected from five separate individuals was stored separately at -20°C and was pooled for preparation of a P_2 synaptosomal fraction. All subjects were male between the ages of 47 and 62. Death was by myocardial infarction, pulmonary embolism or a ruptured aneurism and tissues were received with a post mortem delay of between 17 to 68 hr. P_2 synaptosomal membranes were prepared exactly as for animal tissue (Section 1.2.1.1.), with the final pellet stored in 5 vol. (v/w) of Tris-buffer at -20°C.

1.2.2. General Experimental Methodology for Binding Assays

1.2.2.1. Competition Experiments

For competition experiments, incubation time, membrane (receptor) concentration and radioligand concentration are kept constant, whereas the concentration of competing drug is varied. As the concentration of competing drug is increased the amount of bound radioligand decreases. It is possible to then calculate the concentration of competing drug which inhibits 50% of specific radioligand binding (IC_{50}) (see p37). The slope of competition binding curves, known as the "Hill slope" or "Hill coefficient" (nH), may indicate the type of binding model appropriate for data analysis. If nH=1, the data are probably consistent with a simple one site model and increasing the concentration of competing drug from one tenth to 10 times the IC_{50} value, should reduce the specific binding of the radioligand from 90.9% to 9.1%. A Hill slope of less than

unity indicates binding is not consistent with a single population of non-interacting sites and a 2-site model may be more appropriate. As the IC_{50} is an experimentally determined parameter, an inhibition constant (K_i) for the inhibitor, which is independent of radioligand concentration can be calculated (see p37). It is possible to determine the equilibrium dissociation constant (K_D) and the number of binding sites (B_{max}) (see p37) using the unlabelled version of the radioligand. In this case when inhibitor is identical to radioligand, competition (cold saturation) and 'hot' saturation experiments (see below) are the same and should give the same K_D and B_{max}.

1.2.2.2. 'Hot' Saturation Experiments

As for competition experiments, receptor concentration and time are constant and the amount of bound radioligand is measured as a function of the free radioligand concentration at various concentrations of the radioligand. Hot saturation, like competition experiments, when using unlabelled ligand allows the determination of K_D and B_{max} with Hill slopes again indicative of the type of receptor binding. Ideally, concentrations of radioligand should go from 10 fold below to 10 fold above the K_D.

1.2.2.3. Time Course Experiments: Association & Dissociation

In association experiments, receptor and radioligand concentration are constant, with radioligand bound to the receptor measured as a function of time. To calculate the association rate constant (k_{+1}), a pseudo first order method is used in which the radioligand concentration is assumed to be constant, i.e. less than 10% of radioligand is bound. These time course experiments allow us to determine when equilibrium has been reached, enabling saturation and competition experiments to be performed correctly. As

$K_D=k_{-1}$ / k_{+1} (k_{-1} is the dissociation rate constant), time course experiments provide an independent estimate of the K_D which should agree with the K_D from equilibrium studies.

In dissociation experiments, radioligand and receptor are incubated until equilibrium is achieved. Further association of the radioligand is prevented by the addition of excess unlabelled drug (usually 100 x IC_{50}) so the dissociation of the radioligand from the receptor can be monitored and the k_{-1} measured.

1.2.3. Adenosine Receptor Binding Assays

All drugs used in the study of adenosine receptor binding were dissolved and diluted in DMSO, whose final assay concentration did not exceed 1%. (R)-1-((E)-3-(2-phenylpyrazolo(1,5-a)pyridin-3-yl)acryloyl)-2-piperidine ethanol (FK453) and some related compounds are light sensitive and can undergo a photochemical *trans-cis* isomerisation, so great care was taken to minimise exposure to light. Drugs and membrane preparations were stored for up to 3 months at -20°C. Buffers were prepared in Milli-Q distilled water (d.H_2O) and stored at 4°C. Adenosine deaminase (ADA) was added to all adenosine receptor binding assays to remove endogenous adenosine. Radioligands were diluted in d.H_2O to appropriate concentrations and stored at -70°C under liquid N_2 in aliquots sufficient for one experiment. Binding assays were generally conducted at 25°C (final volume, 0.5-2 ml) in 5 ml round bottomed polypropylene tubes (Sterlin (RT35), U.K.). A Brandel cell harvester was used to separate bound from free ligand (with the exception of microcentrifugation assays). The harvester can filter 24 samples simultaneously under a vacuum pressure of 15-25 mm Hg. Whatman GF/B filters, pre-wetted with filtration buffer, were used to separate bound radioligand from free radioligand unless otherwise stated. Filter disks were

transferred to scintillation vials and were incubated with 100 µl of 100% formic acid for 10 min. Emulsifier Safe scintillant (4 ml) was then added and equilibrated overnight. For each binding assay eight samples of the radioactivity added to the assay were used as standards. Radioactivity was determined in a Packard 2500TR scintillation counter with automatic quench correction (counting efficiency approximately 50%), with samples counted for 4 min unless otherwise stated and results expressed as disintegrations per minute (dpm) per sample.

1.2.3.1. [^{3}H]DPCPX Binding Assay - Rat Cortex

[^{3}H]DPCPX ([^{3}H]-8-cyclopentyl-1,3-dipropylxanthine) (98.1 Ci mmol^{-1}; NEN) binding was carried out under equilibrium conditions by preincubating 10 µl of DMSO or test drug, 290 µl of Tris-buffer and 100 µl of ADA (1u ml^{-1}) with 100 µl of 1 nM [^{3}H]DPCPX for 2 min at 25°C. Test drugs were diluted in DMSO to give 10 duplicate or 20 single concentrations. Total binding was determined in the presence of 1% DMSO and 10 µM R-PIA was used to determine non-specific binding. Addition of P_2 membrane suspension (500 µl; 10-20 µg), which gave a final volume of 1 ml, initiated a 20 min incubation at 25°C. Bound and free ligand were separated using a Brandel cell harvester and this was followed by 3 washes (3 ml) in ice cold Tris-buffer over GF/B filters. Filter disks were then transferred to scintillation vials and the procedure followed as described above.

1.2.3.2. [^{3}H]DPCPX Binding Assay - Human Cortex

The [^{3}H]DPCPX binding assay was carried out as described for rat cortex except the [^{3}H]DPCPX concentration was increased to 7 nM (final 0.7 nM) and the incubation period was extended to 120 min. Total binding was

determined in the presence of 1% DMSO and 10 μM R-PIA was used to determine non-specific binding.

1.2.3.3. [^{3}H]CGS21680 Binding Assay - Rat Striatum

[^{3}H]CGS21680 ([^{3}H](2-p-carboxyethyl)phenylamino-5'-N-carboxamido adenosine) (40.5 Ci mmol^{-1}; NEN) binding was carried out under equilibrium conditions by preincubating 10 μl of DMSO or test drug, 290 μl of Tris-buffer (+10 mM $MgCl_2$, pH 7.4) and 100 μl of ADA (1u ml^{-1}) with 100 μl of 20 nM [^{3}H]CGS21680 for 2 min at 25°C. Test drugs were diluted in DMSO to give 10 duplicate or 20 single concentrations. Total binding was determined in the presence of 1% DMSO and 10 μM CADO was used to determine non-specific binding. Addition of P_2 rat striatal membrane suspension (500 μl; 20-40 μg), which gave a final volume of 1 ml, initiated a 60 min incubation at 25°C. Bound and free ligand were separated using a Brandel cell harvester and this was followed by 3 washes (3 ml) in ice cold Tris-buffer over GF/B filters. Filter disks were transferred to scintillation vials and the procedure followed as described above.

1.2.4. Data Analysis

1.2.4.1. Competition Experiments

Competition binding curves generally comprised of 2 duplicate tubes for both total and non-specific binding and either 10 duplicate concentrations of competing drug or 20 single concentrations when fitting the data to a two site model (see below). Stock drugs were diluted 1 in 10 and 1 in 3.33 followed by serial 10 fold dilutions of both to give a series of concentrations one half a log unit apart. The range of concentrations used in the assay were altered in accordance with the IC_{50} of each compound. Data were analysed using a

iterative, non-linear least squares curve fitting programme (Sigma Plot) to a one site logistic model (Barlow, 1983);

$$Y=(M \times K^P) / (X^P + K^P) + B$$

where Y: is the bound [^{3}H]ligand (dpm) at [X], [X]: is the inhibitor concentration (M), M: is the specifically bound [^{3}H]ligand in the absence of inhibitor (dpm), K: is the concentration of inhibitor (M) giving 50% (IC_{50}) inhibition of binding, P: is the Hill slope (nH) and B: is the calculated non-specific binding (dpm). The calculated specific binding (M) and non-specific binding (B) were compared with experimentally determined values. Values were accepted if within 10%.

For agonists and antagonists K_i values were calculated using the Cheng Prusoff approximation (Cheng and Prusoff, 1973);

$$K_i=IC_{50} / 1 + ([^3H]ligand / K_D)$$

where IC_{50} (M): is that of the compound being tested, [^{3}H]ligand (M) is the concentration in the assay and K_D is the affinity of the radioligand.

When the inhibitor was the unlabelled form of the [^{3}H]ligand (a 'cold' saturation experiment) the K_D and B_{max} were determined using;

$$K_D=IC_{50} - [^3H]ligand$$

where IC_{50} (M): is that of the unlabelled ligand and [^{3}H]ligand (M) is the concentration in the assay.

B_{max} values (mol mg^{-1} protein) were calculated by converting specific

binding (M) of the radioligand bound into the number of moles bound using the specific activity and the following equation;

$$B_{max}=(b \times IC_{50}) / ([^3H]ligand \times Pr)$$

where b: is the specific binding (moles) at the [^{3}H]ligand concentration used in the assay, IC_{50} (M) is that of the unlabelled ligand, [^{3}H]ligand (M) is the concentration in the assay and Pr: is the amount of protein added to assay tube (mg).

1.2.4.2. 'Hot' Saturation Experiments

Radioligands were diluted to give a range of concentrations 10 fold above and below the expected K_D. Generally 8 concentrations in duplicate were used to determine total binding and 8 single concentrations used to determine non-specific binding. Specific binding (bound [^{3}H]ligand) was determined for each point by subtracting non-specific binding from total binding. The free [^{3}H]ligand at equilibrium was calculated by subtracting specifically bound [^{3}H]ligand from [^{3}H]ligand added for each concentration. Using the specific activity of the radioligand the concentration (M) of both free and bound [^{3}H]ligand was calculated. The data were fitted using the iterative, non-linear least squares curve fitting programme (Sigma Plot) to a hyperbolic model and K_D and B_{max} values estimated;

$$b=(B_{max} \times L) / (L + K_D)$$

where b: is the specifically bound [^{3}H]ligand (M), L: is the free [^{3}H]ligand (M) concentration, K_D (M) the affinity of the ligand and B_{max} (M). B_{max} was

expressed in mol mg^{-1} protein by determining the amount of protein used in the assay (mg) of each sample.

1.2.4.3. Two-Site Model

Data were initially analysed using a one site logistic model. Data with Hill slopes of less than unity (nH~0.5-0.7) were analysed using a 2-site model. In determining the proportions and affinity of these two states for a select set of drugs, 20 different concentrations of competing drug were added across an extended range using 3 concentrations per log cycle and data fitted to a 2-site hyperbolic model using the following equation (Barlow, 1983);

$$b_I = b_{I1} + b_{I2} = ((M_1 \times K_1) / (K_1 + X)) + ((M_2 \times K_2) / (K_2 + X))$$

where b_I: is the bound [^{3}H]ligand (dpm) at [X], [X]: is the inhibitor concentration (M), b_{I1} and b_{I2}: is the bound [^{3}H]ligand for the high and low affinity states (dpm) and K_1 and K_2 are the IC_{50} (M) values for the high and low affinity states.

A partial *F* test was used to determine whether the 2-site model provided any statistical improvement over the one site model. The differential *F* value was calculated using the following equation;

$$F=(SS_1 - SS_2) / (df_1 - df_2) / (SS_2 / df_2)$$

SS_1: the sum of the square of the errors for the single site, SS_2: the sum of the square of the errors for the two site model and df_1 and df_2 are the degrees of freedom for the one and two site models respectively. A two site fit was assumed to be significantly better than a single site fit if the determined *F*

value was significant ($P < 0.05$) (De Lean *et al.*, 1981).

1.2.4.4. Time Course Experiments - Association Rate Constant (k_{+1})

Experiments were carried out under conditions such that pseudo-first order kinetics were applicable by ensuring that less than 10% of radioligand added is bound through the time course. Specific binding at each time point was determined by subtracting non-specific binding from total binding and data fitted to a single exponential function (Bylund & Yamamura, 1990);

$$B_t = B_e - (B_e / \exp(k_{obs.t}))$$

where t: is time (min), B_t: is bound [^{3}H]ligand (dpm) at time t, B_e: total specific binding (dpm) at equilibrium and k_{obs} (min^{-1}) is the observed constant.

The association rate constant (k_{+1}) was determined by estimating the free [^{3}H]ligand concentration (M) when maximum binding is observed and calculated using the following equation;

$$k_{+1} = (k_{obs} - k_{-1}) / L$$

where: k_{obs} (min^{-1}) is the observed constant, k_{-1} (min^{-1}) (see below) is the dissociation rate constant and L: is the free concentration of [^{3}H]ligand (M).

1.2.4.5. Time Course Experiments - Dissociation Rate Constant (k_{-1})

The dissociation rate constant (k_{-1}) was calculated from a dissociation

time course experiment. Specific binding at each time point determined by subtracting non-specific binding from total binding and data fitted to the following equation (Bylund & Yamamura, 1990);

$$B_t=(B_o / \exp(k_{-1}.t))$$

where t: is time (min), B_t: is bound [^{3}H]ligand (dpm) at time t, B_o: total specific binding (dpm) at time 0 and k_{-1} (min^{-1}) is the dissociation rate constant.

1.2.4.6. Equilibrium Dissociation Constant (K_D)

The K_D (M) was calculated from the time course data using the following equation;

$$K_D=k_{-1} / k_{+1}$$

where k_{-1} (min^{-1}) and k_{+1} (min^{-1} M^{-1}) are the dissociation and association rate constants respectively.

1.2.5. Protein Assay

The amount of protein was determined using a Bradford Assay (Bradford, 1976). Standard curves were constructed using serial dilutions of bovine serum albumin (BSA) ranging from of 10 to 200 μg ml^{-1} of protein. 50 μl aliquots of standards or test sample were added to Nunclon 96 well plates followed by 250 μl of Bradford reagent (10% coomassie blue (v/w), 5% of 95% ethanol (v/v), 10% of 85% orthophosphoric acid (v/v) in d.H_2O; filtered twice through Whatman filter paper and stored at 4°C). Using a Dynatech plate reader, samples were mixed by shaking for 20 sec and absorbance measured at an optical density of 595 nM (OD_{595}) after 20 min. (OD_{595}) measurements for BSA samples fitted to a straight line through the linear portion of the curve

and the amount of protein in each sample determined.

1.2.6. Statistical Analysis

The majority of figures displayed in the thesis are a representation of one experiment, all of which have been carried out at least three times, unless otherwise stated. Data in tables and text are shown as mean ± the standard error (S.E.M.) for at least three separate experiments. Statistical tests used in the thesis were the Students t-test, a one-way analysis of variance (ANOVA), a two-way anova and a Dunnett's test (JMP and Sigma Stat).

1.2.7. Materials

Radioligands were purchased from New England Nuclear (NEN) and adenosine deaminase (Type VIII) from Sigma. FK453, (R)-1-[(E)-3-(2-phenylpyrazolo[1,5-a]pyridin-3-yl)acryloyl]-piperidin-2-yl acetic acid (FK352), 6-oxo-3-(2-phenylpyrazolo[1,5-a]pyridin-3-yl)acryloyl]-1(6H)-pyridazinebutylic acid (FK838) and all FR compounds were synthesised by the Fujisawa Pharmaceutical Co. Ltd, as were 8-(noradamantan-3-yl)-1,3-dipropylxanthine (KW3902/FR144942), (R)-3,7-dihydro-8-(1-phenylpropyl)-1,3-dipropyl-1*H*-purine-2,6-dione) (MDL102234/FR160502), 1-benzyl-1-6-(4-methoxyphenyl)-3-propyl-1,2,3,4-tetrahydro-5*H*-imidazol[2',1':5,1]pyrazolo[3,4-d]pyrimidin-2,4-dione (Takeda/FR160492) and (E)-1,3-dipropyl-8-(3,4-dimethoxystyryl)-7-methylxanthine, (KF17837/FR179123). Standard adenosine agonists and antagonists were purchased from Research Biochemicals Inc. (RBI), with the exception of APEC and CSPA which were supplied courtesy of the NIMH chemical synthesis programme. All other standard laboratory chemicals were from Sigma, Fisons or BDH and were of the highest grade available.

1.3. Results

Receptor binding assays to rat brain membranes using the potent and selective adenosine A_1 receptor antagonist [^{3}H]DPCPX and the A_{2a} selective adenosine receptor agonist [^{3}H]CGS21680, had been established in the laboratory prior to my arrival. As a consequence, limited time course and saturation analysis was necessary to confirm attainment of equilibrium and to determine appropriate radioligand concentrations required for use in competition studies. Compounds were tested in both binding assays to determine their affinity and selectivity for the adenosine A_1 receptor.

1.3.1. [^{3}H]DPCPX Binding to Rat Cerebral Cortical Membranes

1.3.1.1. Time Course of [^{3}H]DPCPX Binding to Rat Cerebral Cortical Membranes

A time course (0-60 min) of [^{3}H]DPCPX (0.1 nM) binding to rat cerebral cortex was carried out at 25°C, with equilibrium attained by 20 min (Figure 1.1). Curve fitting using non linear regression gave an observed constant (k_{obs}) of 0.141 ± 0.017 min^{-1} (n=3). Dissociation (0-60 min) of [^{3}H]DPCPX binding was carried out after 60 min and initiated by the addition of 1 mM R-PIA. Dissociation followed first order kinetics with a $t_{1/2}$ of 4.75 min (Figure 1.2) and a dissociation rate constant (k_{-1}) of 0.123 ± 0.012 min^{-1} (n=3). Subsequent calculation gave an association rate constant (k_{+1}) of 0.212 ± 0.051 min^{-1} M^{-1}. The data from these time course experiments gave an equilibrium dissociation constant (K_D) of 0.652 ± 0.152 nM. In the following competition experiments [^{3}H]DPCPX (0.1 nM) binding to rat cortical membranes was carried out at 25°C for 20 min.

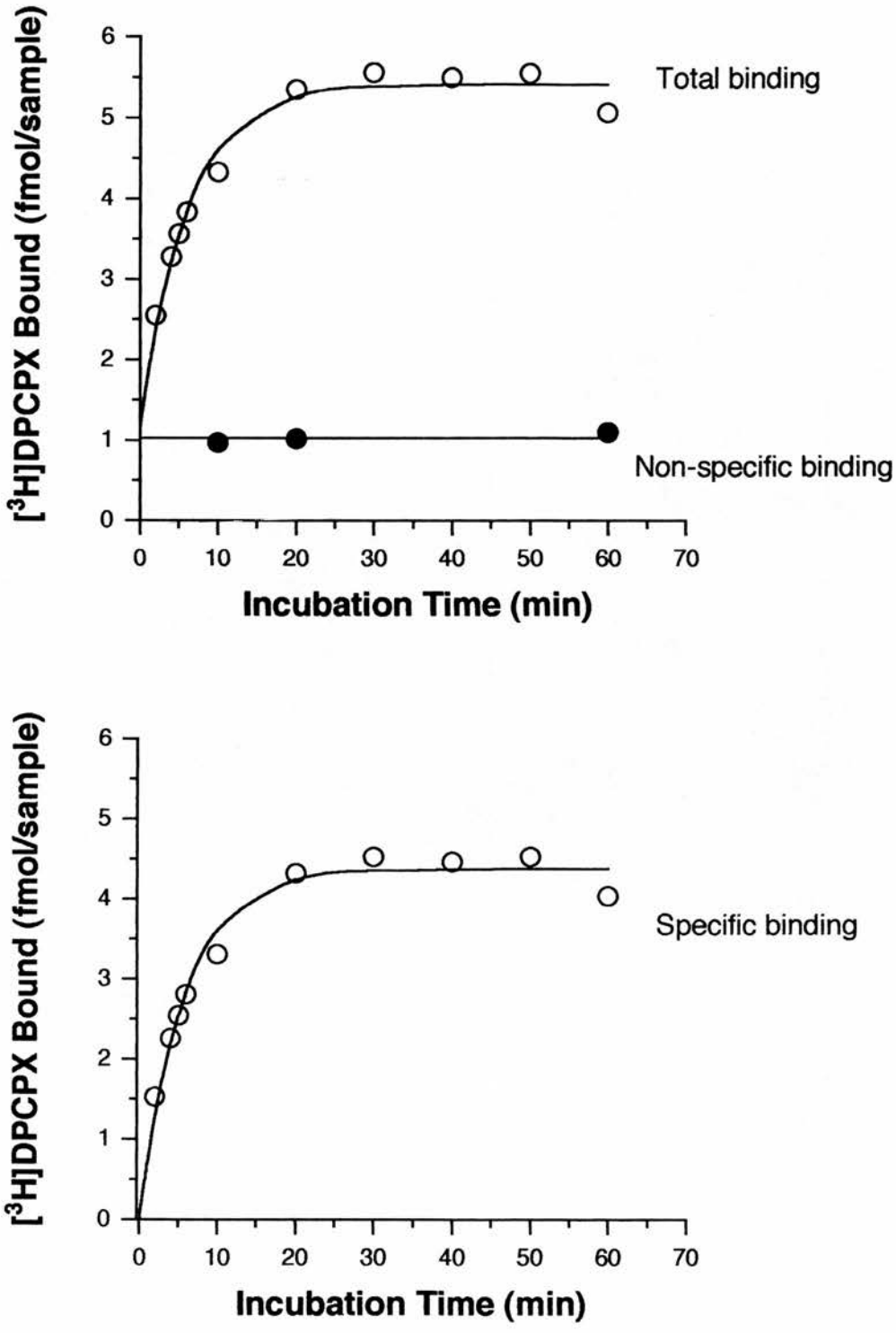

Figure 1.1 Time Course of [^{3}H]DPCPX BInding to Rat Cerebral Cortical Membranes.

The data represent a typical time course experiment. Membranes were incubated with 0.1 nM [^{3}H]DPCPX for various times at 25°C. Total binding was determined in the presence of DMSO and non-specific binding in the presence of 10 μM R-PIA. Experiments performed as described in text with mean data obtained from three experiments (text for mean values).

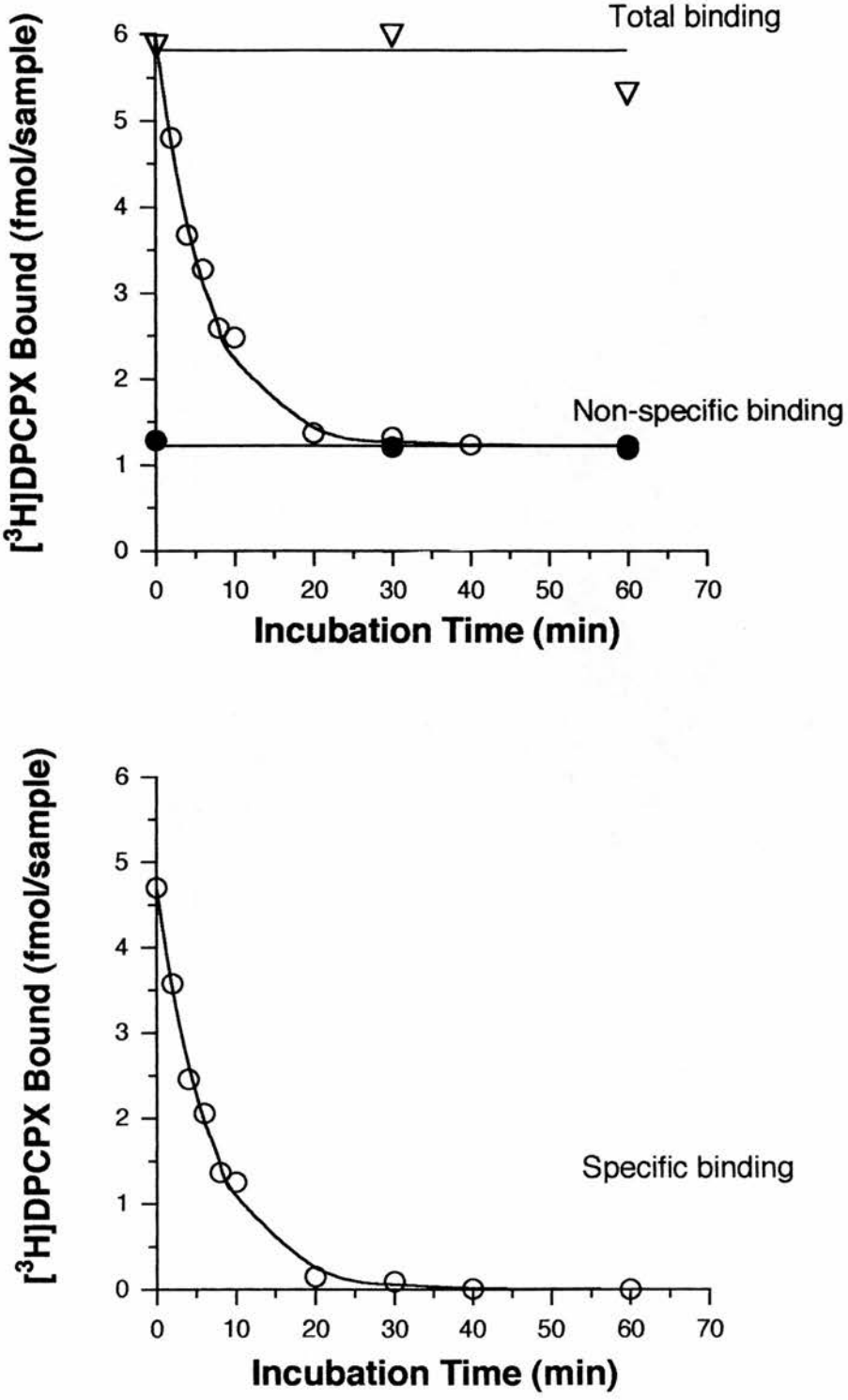

Figure 1.2 Time Course of [^{3}H]DPCPX Binding to Rat Cerebral Cortical Membranes.

The data represent a typical dissociation experiment. Membranes were incubated with 0.1 nM [^{3}H]DPCPX for 60 min prior to the addition of 1 mM R-PIA to initiate dissociation. Experiments performed as described in text with mean data obtained from three experiments (text for mean values).

1.3.1.2. Concentration Dependence of [^{3}H]DPCPX Binding to Rat Cerebral Cortical Membranes

Hot saturation analysis of [^{3}H]DPCPX binding to rat cerebral cortex was carried out once using increasing concentrations of [^{3}H]DPCPX (Figure 1.3a). Curve fitting using a hyperbolic model gave an equilibrium dissociation constant (K_D) of 0.22 nM and a B_{max} of 3.37 pmol mg^{-1} protein.

Competition binding studies using 0.1 nM [^{3}H]DPCPX and increasing concentrations of unlabelled DPCPX (0.003-100 nM) (Figure 1.3b), gave a K_D of 0.29 ± 0.01 nM and a B_{max} of 1.60 ± 0.09 pmol mg^{-1} protein (n=44), which is in reasonable agreement with data obtained from time course and saturation studies.

1.3.2. [^{3}H]CGS21680 Binding to Rat Striatal Membranes

1.3.2.1. Time Course of [^{3}H]CGS21680 Binding to Rat Striatal Membranes

A time course of [^{3}H]CGS21680 (2 nM) binding to rat striatum was carried out at 25°C, with equilibrium attained by 60 min (Figure 1.4). In all other competition experiments [^{3}H]CGS21680 (2 nM) binding to rat striatal membranes was carried out at 25°C for 60 min unless otherwise stated.

1.3.2.2. Concentration Dependence of [^{3}H]CGS21680 Binding to Rat Striatal Membranes

Hot saturation analysis of [^{3}H]CGS21680 binding to rat striatal membranes was carried out once (Figure 1.5a). Curve fitting using a hyperbolic model gave an equilibrium dissociation constant (K_D) of 10.66 nM and a B_{max} of 4.65 pmol mg^{-1} protein.

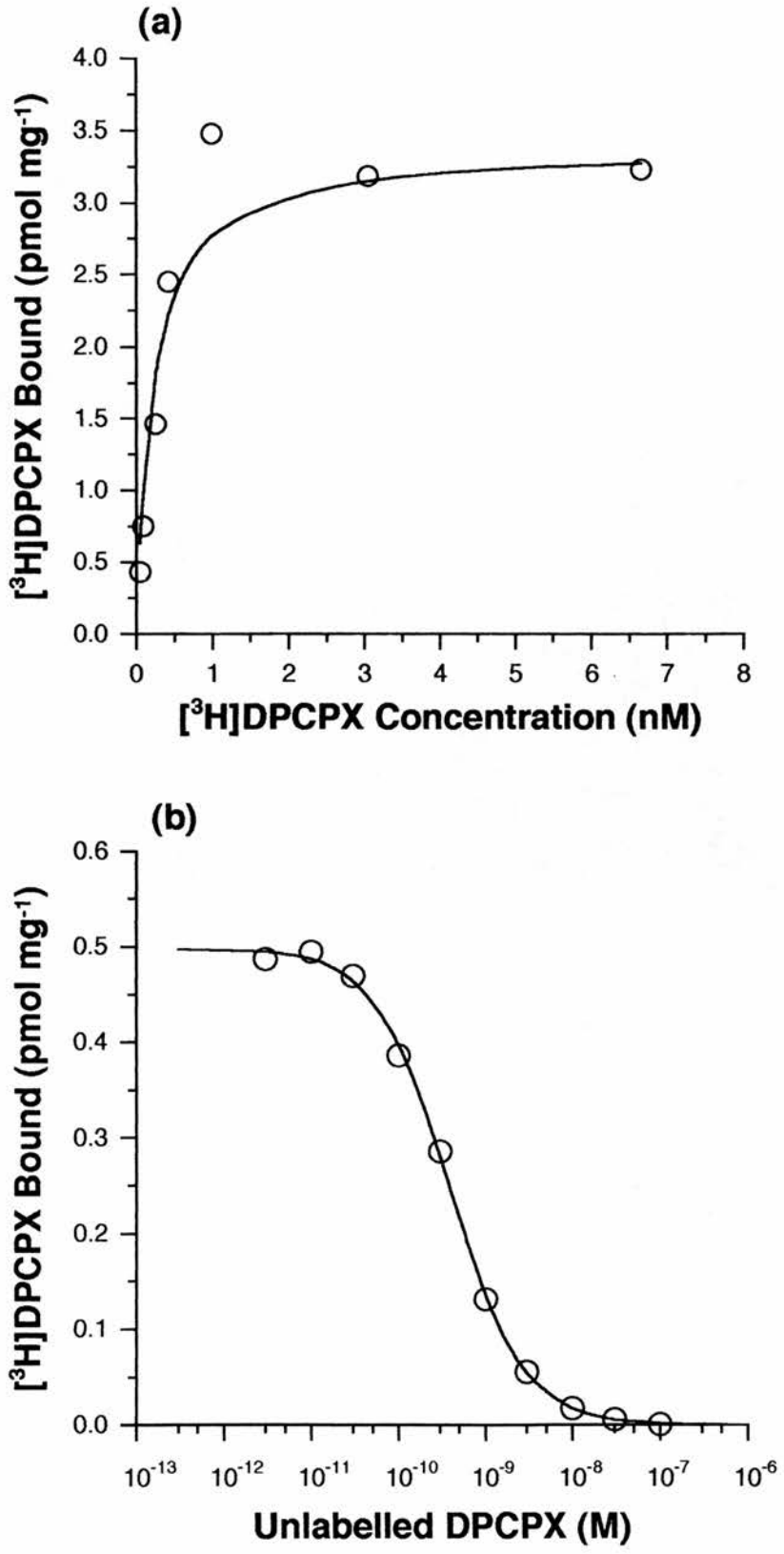

Figure 1.3 Concentration Dependence of Specific [^{3}H]DPCPX Binding to Rat Cerebral Cortical Membranes.

The results represent a single (a) hot saturation and a typical (b) cold saturation experiment with each point performed in duplicate. For the cold saturation see text for mean values.

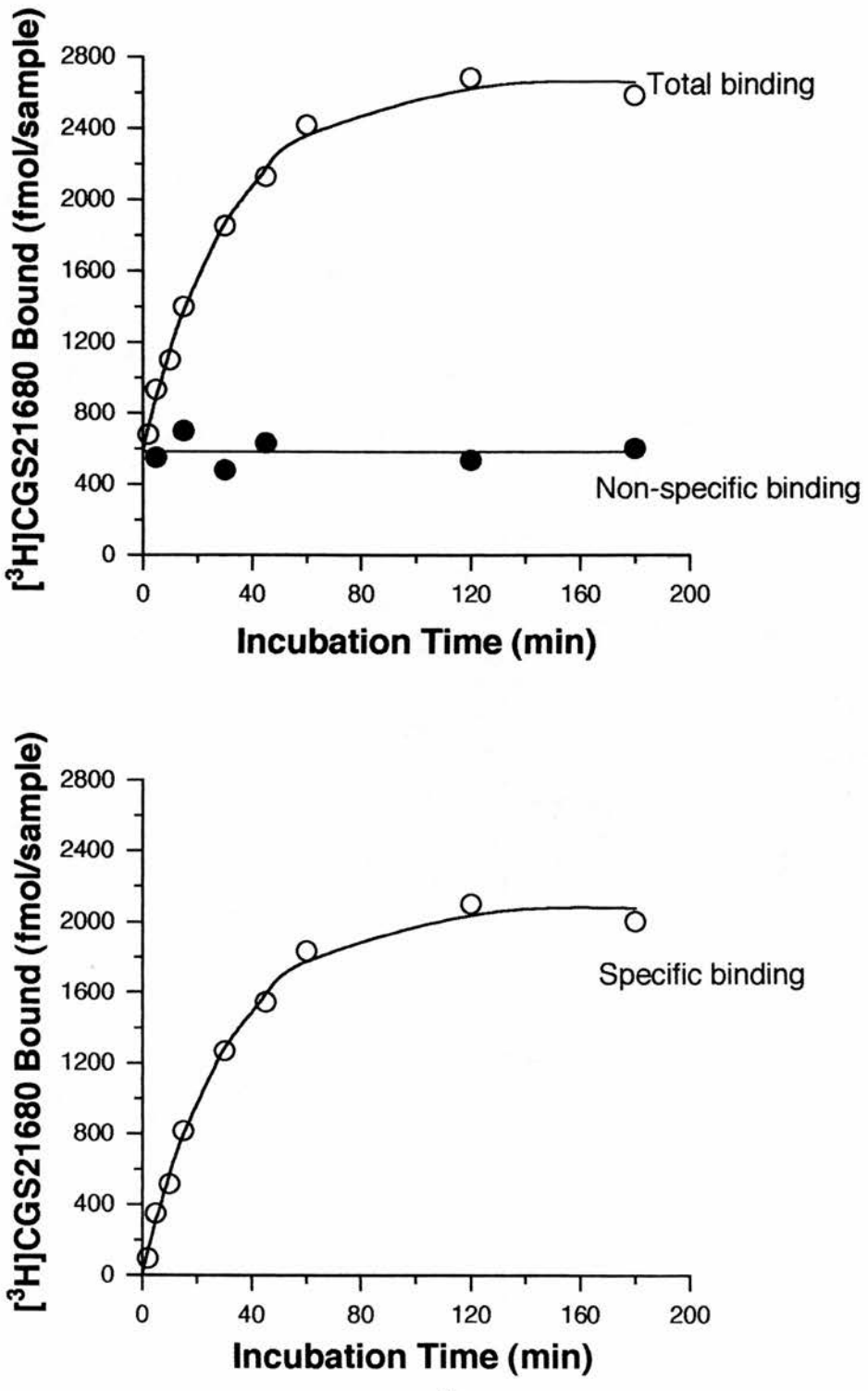

Figure 1.4 Time Course of [^{3}H]CGS21680 Binding to Rat Striatal Membranes.

The data represent a typical time course experiment. Membranes were incubated with 2 nM [^{3}H]CGS21680 for various times at 25°C. Total binding was determined in the presence of DMSO and non-specific binding in the presence of 10 μM CADO. Experiments performed as described in text with data obtained from at least three experiments.

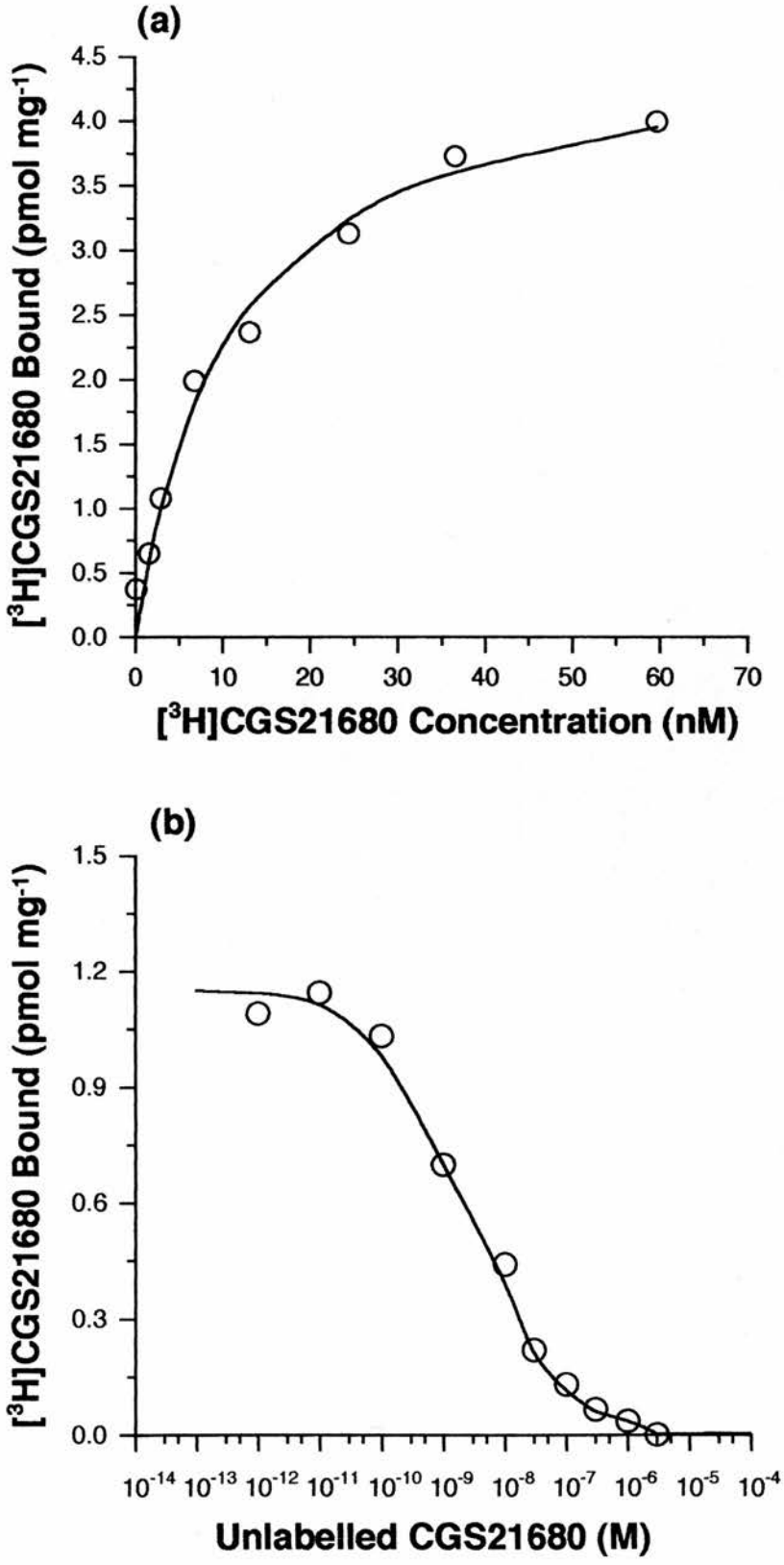

Figure 1.5 Concentration Dependence of Specific [^{3}H]CGS21680 Binding to Rat Striatal Membranes.

The results represent a single (a) hot saturation and a typical (b) cold saturation experiment with each point performed in duplicate. For the cold saturation see text for mean values.

Competition binding studies using 2 nM [^{3}H]CGS21680 and increasing concentrations of unlabelled CGS21680 (0.001 nM-300 μM) (Figure 1.5b), gave a K_D of 9.64 ± 0.85 nM and a B_{max} of 4.99 ± 0.86 pmol mg^{-1} protein (n=6), which was in good agreement with data from the saturation experiment.

1.3.3. Pharmacological Profile of [^{3}H]DPCPX & [^{3}H]CGS21680 Binding Sites in Rat Brain Membranes

1.3.3.1. Adenosine Receptor Antagonist Pharmacology

Competition studies using both adenosine receptor binding assays were used to characterise adenosine antagonist receptor pharmacology. Figure 1.6 shows the structure of some of the antagonists tested and Figure 1.7 shows inhibition of [^{3}H]DPCPX and [^{3}H]CGS21680 binding by a select number of antagonists.

Antagonists exhibited the typical adenosine A_1 pharmacological profile for [^{3}H]DPCPX binding sites in rat cortical membranes with the following order of potency: DPCPX > CGS15943 > CPT > 1,3-diethyl-8-phenylxanthine (DPX) > 8-phenyltheophylline (8-PT) > 1,3-dipropyl-8-sulphophenylxanthine (DPSPX) = KF17837 > 8-(*p*-sulphophenyl)theophylline (8-PST) > theophylline > CSC > caffeine, with K_i values shown in Table 1.1. DPCPX and CGS15943 were the most potent A_1 antagonists with nanomolar affinity, while caffeine had the lowest affinity. Hill slopes were close to unity for all antagonists.

Antagonists also exhibited the typical adenosine A_{2a} pharmacological profile for [^{3}H]CGS21680 binding sites in rat striatal membranes with the following order of potency: CGS15943 > KF17837 > CSC > DPCPX > DPX > DPSPX = 8-PT > CPT > 8-PST > theophylline > caffeine, with K_i values shown in Table 1.1. CGS15943 and the styryl compounds KF17837 and CSC had nanomolar affinity with caffeine having the lowest affinity. Hill slopes were

Figure 1.6.- Adenosine Agonists

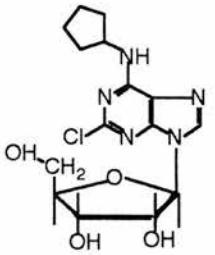

CCPA

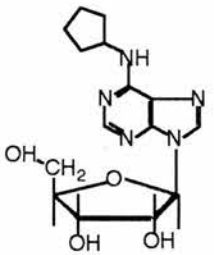

CPA

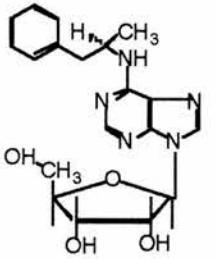

R-PIA

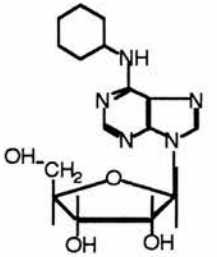

CHA

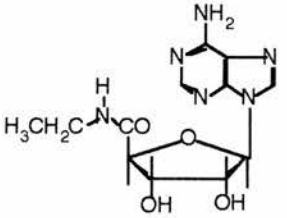

NECA

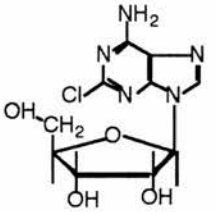

CADO

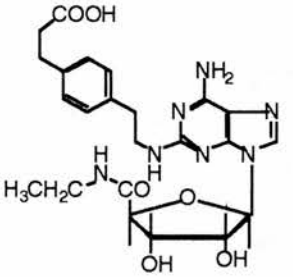

CGS21680

Adenosine Antagonists

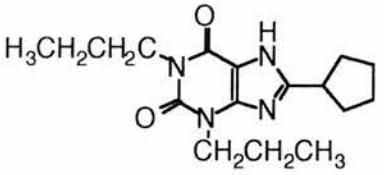

DPCPX

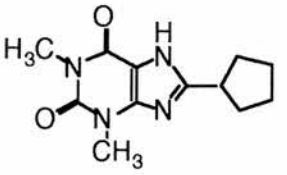

CPT

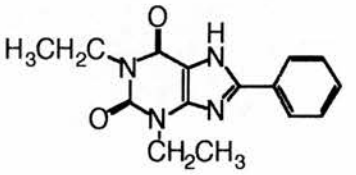

DPX

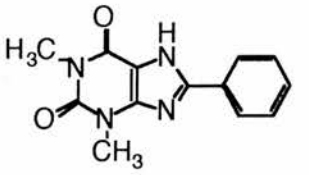

8-PT

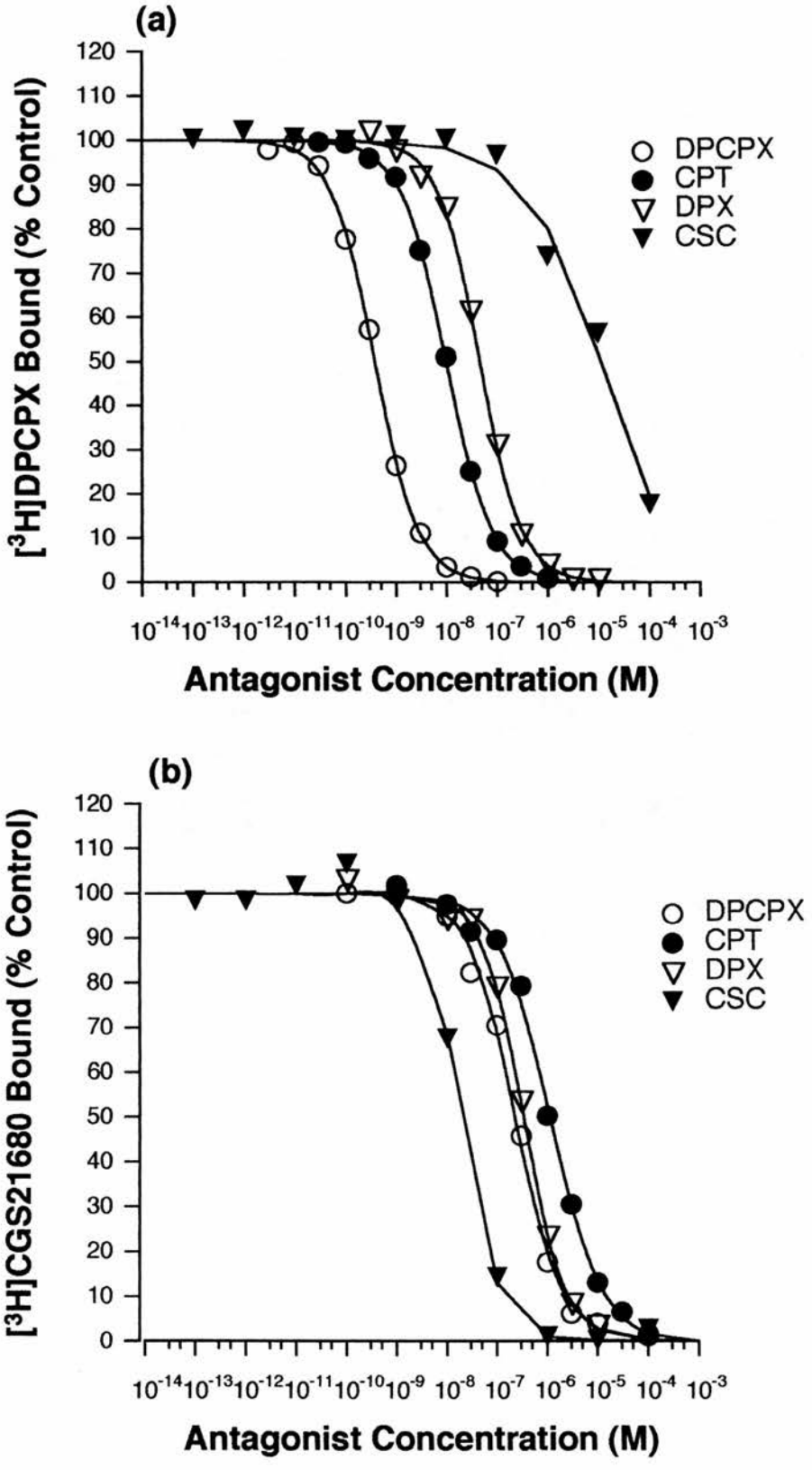

Figure 1.7 Inhibition of (a) [^{3}H]DPCPX and (b) [^{3}H]CGS21680 Binding to Rat Brain Membranes by Adenosine Receptor Antagonists.

The data represent a typical experiment, each point performed in duplicate with mean data obtained from at least three experiments (Table 1.1).

Table 1.1 Inhibition of [^{3}H]DPCPX and [^{3}H]CGS21680 Binding to Rat Brain Membranes by Adenosine Receptor Antagonists

	[^{3}H]DPCPX		[^{3}H]CGS21680		
Compound	**K_i (nM)**	**(nH)**	**K_i (nM)**	**(nH)**	**K_i Ratio**
DPCPX	0.28 ± 0.01	0.99 ± 0.02	192 ± 17.2	0.91 ± 0.06	686
CGS15943	1.35 ± 0.24	0.98 ± 0.03	0.38 ± 0.09	0.86 ± 0.04	0.28
CPT	6.49 ± 0.87	1.01 ± 0.05	845 ± 32.2	0.88 ± 0.05	130
DPX	33.1 ± 2.01	1.05 ± 0.03	289 ± 13.7	1.09 ± 0.09	8.73
8-PT	45.0 ± 1.37	1.07 ± 0.03	391 ± 12.2	1.09 ± 0.05	8.69
DPSPX	76.1 ± 3.43	0.97 ± 0.05	386 ± 29.0	0.78 ± 0.01	5.07
KF17837	80.6 ± 4.16	0.93 ± 0.03	2.32 ± 0.25	0.86 ± 0.04	0.029
8-PST	1020 ± 93.0	0.94 ± 0.06	4100 ± 624	1.05 ± 0.07	4.02
Theophylline	4330 ± 790	0.98 ± 0.03	6770 ± 499	1.16 ± 0.12	1.56
CSC	10600 ± 1140	0.92 ± 0.02	14.0 ± 0.87	1.01 ± 0.15	0.001
Caffeine	25300 ± 2100	1.07 ± 0.04	13800 ± 960	1.08 ± 0.16	0.545

K_i values and Hill slope (nH) determined for competition assays as described in the methods. Values expressed as mean ± S.E.M. ($n \geq 3$). K_i ratio shown between [^{3}H]CGS21680 binding in rat striatal membranes & [^{3}H]DPCPX binding in rat cortical membranes.

close to unity for all antagonists.

Antagonist receptor selectivity was assessed by comparing the respective affinities (K_i ratio) of each antagonist in the two receptor binding assays (Table 1.1). DPCPX and CPT were the most A_1 receptor selective compounds, whereas CSC and KF17837 were A_{2a} selective antagonists.

1.3.3.2. Adenosine Receptor Agonist Pharmacology

Competition studies using both adenosine receptor binding assays were used to characterise adenosine agonist receptor pharmacology. Figure 1.6 shows the structure of some of the agonists tested and Figure 1.8 shows inhibition of [^{3}H]DPCPX and [^{3}H]CGS21680 binding by a select number of agonists.

Agonists exhibited the typical adenosine A_1 pharmacological profile for [^{3}H]DPCPX binding sites in rat cortical membranes with the following order of potency: CCPA = CPA ≥ R-PIA > CHA > NECA = CADO > S-PIA > N^6-*p*-sulfophenyladenosine (CSPA) = APEC > CGS21680, with K_i values shown in Table 1.2. CPA and CCPA were the most potent A_1 agonists with nanomolar affinity, while CGS21680 had the lowest affinity. Hill slopes were significantly less than unity for all agonists, indicating the presence of two different affinity states for the adenosine A_1 receptor.

Agonists also exhibited the typical adenosine A_{2a} pharmacological profile for [^{3}H]CGS21680 binding sites in rat striatal membranes with the following order of potency: NECA = APEC > CGS21680 > CADO > R-PIA > CPA = CHA > CCPA > S-PIA > CSPA, with K_i values shown in Table 1.2. NECA, CGS21680 and the recently available A_{2a} agonist APEC had nanomolar affinity, while CSPA exhibited the lowest affinity. Hill slopes for agonists were closer to unity than for [^{3}H]DPCPX binding, with three values

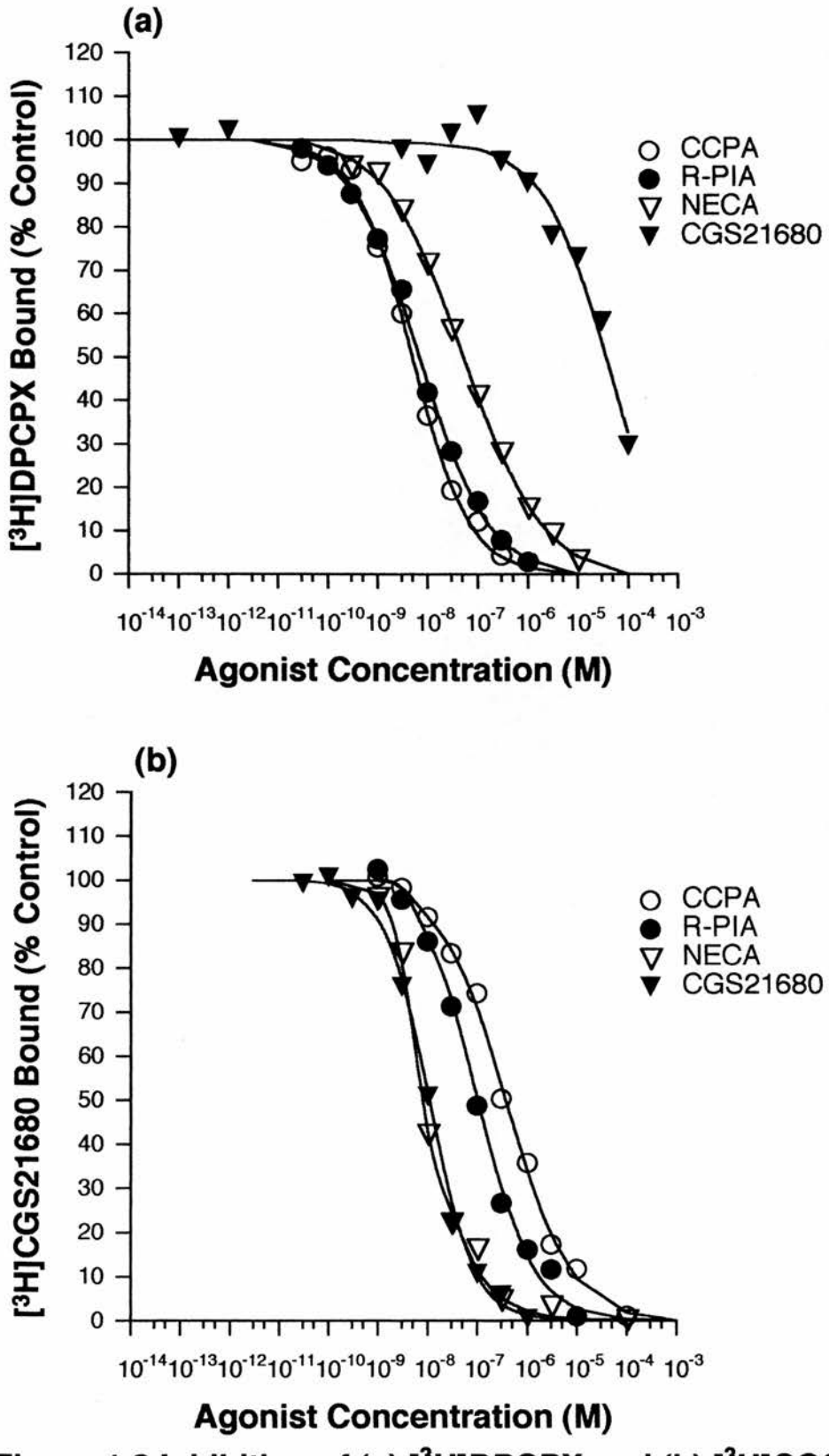

Figure 1.8 Inhibition of (a) [^{3}H]DPCPX and (b) [^{3}H]CGS21680 Binding to Rat Brain Membranes by Adenosine Receptor Agonists.

The data represent a typical experiment, each point performed in duplicate with mean data obtained from at least three experiments (Table 1.2).

Table 1.2 Inhibition of [^{3}H]DPCPX and [^{3}H]CGS21680 Binding to Rat Brain Membranes by Adenosine Receptor Agonists

	[^{3}H]DPCPX		[^{3}H]CGS21680		
Compound	**K_i (nM)**	**(nH)**	**K_i (nM)**	**(nH)**	**K_i Ratio**
CCPA	3.39 ± 0.40	0.65 ± 0.02	331 ± 30.7	0.73 ± 0.02	97.6
CPA	4.02 ± 0.59	0.63 ± 0.02	220 ± 21.5	0.74 ± 0.06	54.7
R-PIA	4.56 ± 0.28	0.59 ± 0.02	91.4 ± 16.2	0.79 ± 0.11*	20.0
CHA	7.16 ± 1.26	0.62 ± 0.06	248 ± 0.21	0.63 ± 0.05	34.6
NECA	39.1 ± 7.84	0.58 ± 0.06	4.92 ± 0.56	0.79 ± 0.05	0.126
CADO	41.0 ± 4.51	0.60 ± 0.02	28.1 ± 4.81	0.69 ± 0.06	0.685
S-PIA	212 ± 28.4	0.59 ± 0.02	1680 ± 375	0.89 ± 0.11*	7.92
CSPA	583 ± 111	0.64 ± 0.04	3640 ± 987	0.79 ± 0.06	6.24
APEC	602 ± 112	0.63 ± 0.04	5.57 ± 1.36	0.90 ± 0.08*	0.009

K_i values and Hill slope (nH) determined for competition assays as described in the methods. Values expressed as mean ± S.E.M. ($n \geq 3$). K_i ratio shown between [^{3}H]CGS21680 binding in rat striatal membranes & [^{3}H]DPCPX binding in rat cortical membranes. * Hill slope was not significantly ($P < 0.05$) different from unity in a t-test.

(R-PIA, S-PIA and APEC) not significantly different from unity.

Agonist receptor selectivity was assessed by comparing the respective affinities (K_i ratio) of each agonist in the two binding assays (Table 1.2). CCPA and CPA were found to be the most A_1 receptor selective compounds, whereas APEC and CGS21680 were A_{2a} selective agonists.

1.3.3.3. Fujisawa Adenosine Receptor Antagonist Pharmacology

Fujisawa kindly supplied over 150 compounds from their adenosine receptor programme. Mr T. Maemoto tested these compounds in a 2 point screen to assess preliminary A_1 receptor affinity and selectivity. Three development compounds (FK453, FK352 and FK838), five pre-clinical compounds (FR129946, FR160537, FR171562, FR182303 and FR182394) and three adenosine receptor antagonists from other companies (KW3902, Takeda (FR160492) and MDL102234) were chosen for further pharmacological characterisation. With the exception of KW3902 and MDL102234, all the antagonists are non-xanthines, in contrast to the standard adenosine antagonists which are all xanthines (Figures 1.9 & 1.10).

Competition studies using the [^{3}H]DPCPX and [^{3}H]CGS21680 binding assays were used to characterise Fujisawa adenosine antagonist receptor pharmacology. Figure 1.11 shows inhibition of [^{3}H]DPCPX binding in rat cortical membranes and [^{3}H]CGS21680 binding in rat striatal membranes by a select number of antagonists. The pharmacological profile of the antagonists for [^{3}H]DPCPX binding sites was: KW3902 > FR160537 > DPCPX = FR171562 > FK453 > FR129946 > FR182394 > FR182303 > FK838 > FR160492 = MDL102234 > FK352, with K_i values shown in Table 1.3. A range of affinities were found in the nanomolar range with some compounds slightly

Figure 1.9

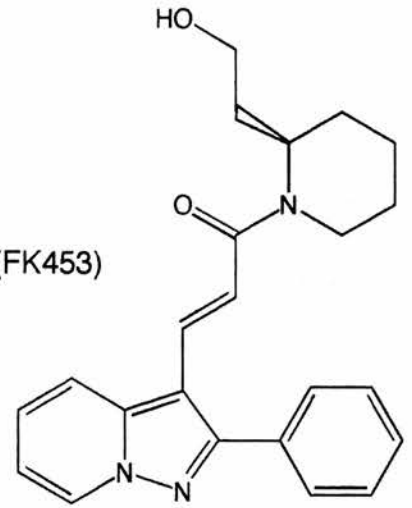

FR113453 (FK453)

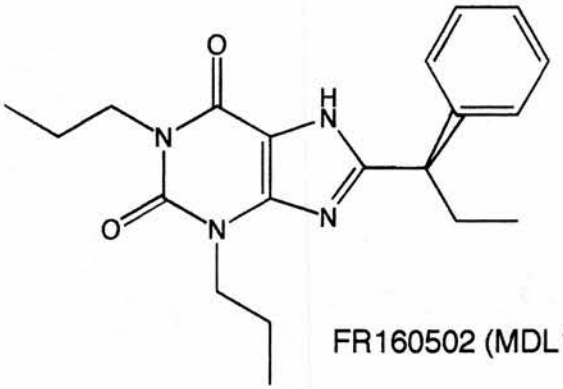

FR160502 (MDL102234)

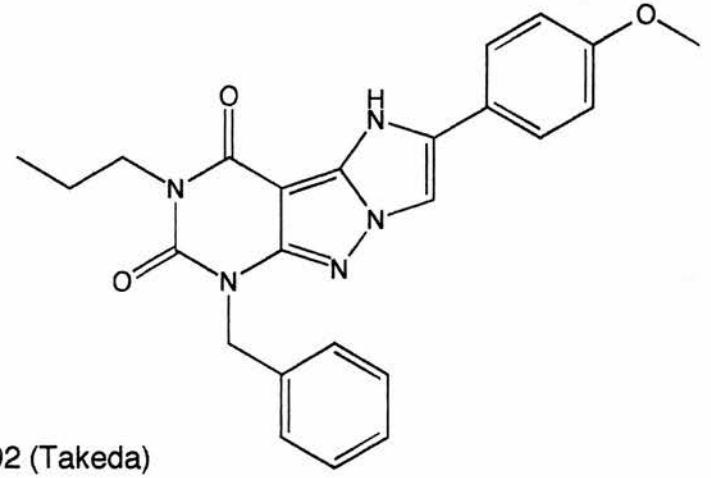

FR160492 (Takeda)

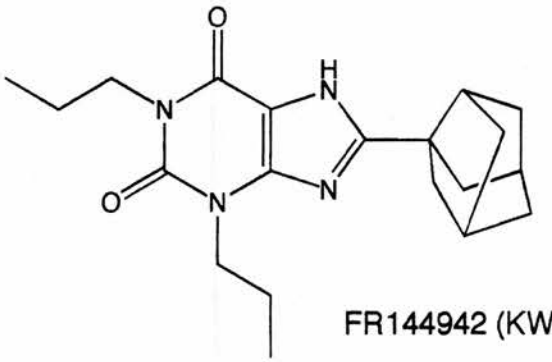

FR144942 (KW3902)

Figure 1.10

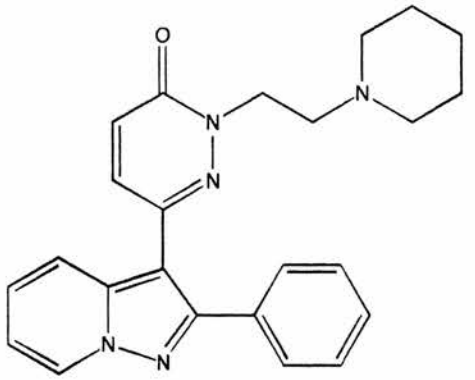

FR129946

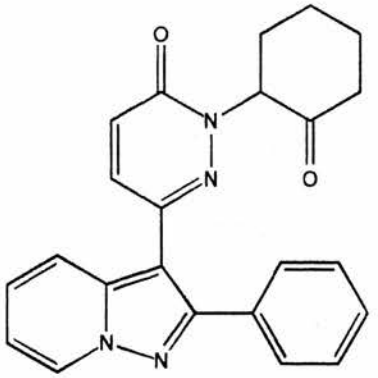

FR160537

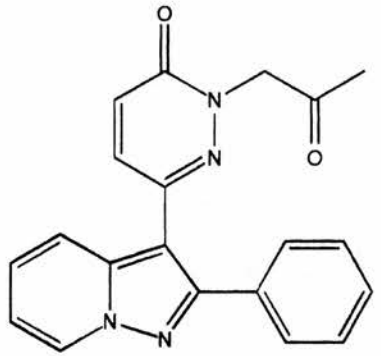

FR171562

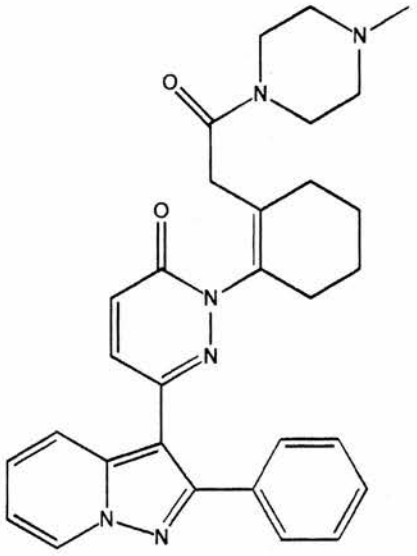

FR182303

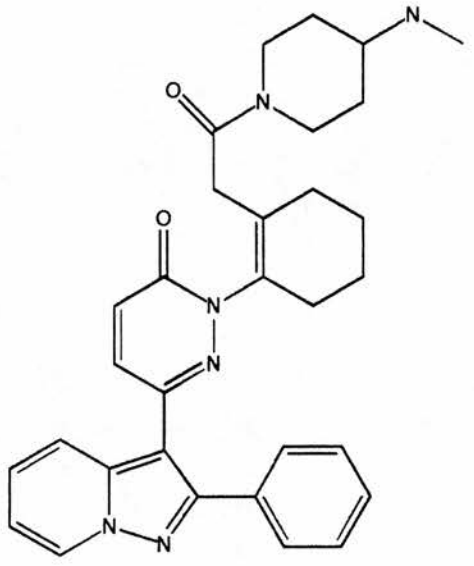

FR182394

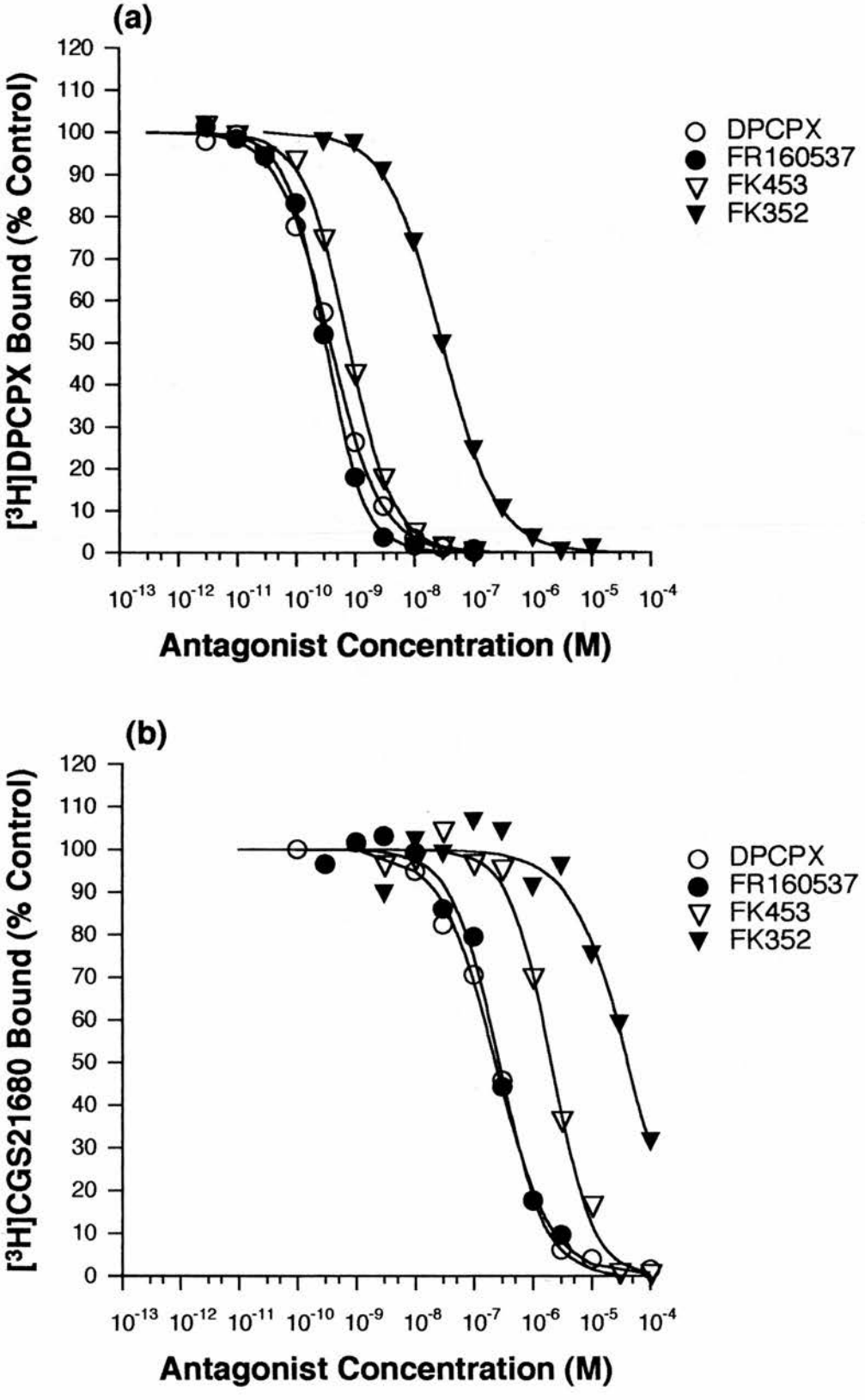

Figure 1.11 Inhibition of (a) [^{3}H]DPCPX and (b) [^{3}H]CGS21680 Binding to Rat Brain Membranes by Fujisawa Adenosine Receptor Antagonists.

The data represents a typical experiment, each point performed in duplicate with mean data obtained from at least three experiments (Table 1.3).

Table 1.3 Inhibition of [^{3}H]DPCPX and [^{3}H]CGS21680 Binding to Rat Brain Membranes by Fujisawa Adenosine Receptor Antagonists

	[^{3}H]DPCPX		[^{3}H]CGS21680		
Compound	**K_i (nM)**	**(nH)**	**K_i (nM)**	**(nH)**	**K_i Ratio**
DPCPX	0.28 ± 0.01	0.99 ± 0.02	192 ± 17.2	0.91 ± 0.06	686
FR160537	0.21 ± 0.01	1.22 ± 0.03	179 ± 34.2	0.83 ± 0.08	852
FR171562	0.29 ± 0.03	1.21 ± 0.07	272 ± 12.6	0.84 ± 0.06	938
FK453	0.54 ± 0.02	1.14 ± 0.03	1300 ± 158	0.98 ± 0.08	2410
FR129946	1.08 ± 0.07	1.02 ± 0.06	726 ± 157	1.05 ± 0.05	672
FR182394	1.73 ± 0.35	0.95 ± 0.03	4630 ± 220	0.87 ± 0.12	2680
FR182303	3.46 ± 0.50	1.12 ± 0.04	524 ± 38.0	0.92 ± 0.06	151
FK838	5.58 ± 0.34	0.99 ± 0.03	1210 ± 18.7	1.01 ± 0.07	217
FK352	23.6 ± 0.70	1.01 ± 0.02	51400 ± 12000	1.01 ± 0.25	2180
KW3902	0.16 ± 0.01	1.21 ± 0.03	184 ± 14.6	0.90 ± 0.03	1150
FR160492	7.94 ± 0.59	1.24 ± 0.09	55.8 ± 14.8	0.97 ± 0.13	7.03
MDL102234	8.00 ± 0.37	1.02 ± 0.03	722 ± 115	0.93 ± 0.11	90.2

K_i values and Hill slope (nH) determined for competition assays as described in the methods. Values expressed as mean ± S.E.M. (n≥3). K_i ratio shown between [^{3}H]CGS21680 binding in rat striatal membranes & [^{3}H]DPCPX binding in rat cortical membranes.

more potent than DPCPX. As with standard antagonists, Hill slopes were close to unity in all cases.

The pharmacological profile of the antagonists for [^{3}H]CGS21680 binding sites was: FR160492 > FR160537 = KW3902 = DPCPX > FR171562 > FR182303 = MDL102234 = FR129946 > FK838 = FK453 > FR182394 > FK352, with K_i values shown in Table 1.3. A range of affinities were found both higher and lower than DPCPX. Hill slopes as for standard antagonists were close to unity.

Antagonist receptor selectivity was assessed by comparing the respective affinities (K_i ratio) of each antagonist in the two binding assays (Table 1.3). FK453, FR182394 and FK352 were the most A_1 receptor selective compounds being 3 fold more selective than DPCPX, with a K_i ratio of greater than 2000. FR160537, FR171562 and FR129946 had similar affinities and selectivity for the A_1 receptor compared with DPCPX, whereas FR182303 and FK838 were slightly less selective. The three other antagonists varied with KW3902 being both more potent and selective than DPCPX, MDL102234 showing moderate selectivity and FR160492 showing the least selectivity of all the non-xanthines tested.

1.3.4. Pharmacological Profile of [^{3}H]DPCPX Binding Sites in Human Cortical Membranes

As the ultimate goal of this study is the discovery of a drug for use in man, it is essential to examine receptor pharmacology in human tissue. All studies using human brain tissue were carried out in collaboration with Dr R.W. Horton at St George's Hospital Medical School, London.

1.3.4.1. Time Course of [^{3}H]DPCPX Binding to Human Cortical Membranes

A time course of [^{3}H]DPCPX (0.7 nM) binding to human cerebral cortex was carried out at 25°C, with equilibrium attained by 20 min (Figure 1.12). In subsequent competition experiments [^{3}H]DPCPX (0.7 nM) binding to human cortical membranes was carried out at 25°C for 120 min.

1.3.4.2. Concentration Dependence of [^{3}H]DPCPX Binding to Human Cortical Membranes

Hot saturation analysis of [^{3}H]DPCPX binding to human cerebral cortex was carried out (Figure 1.13a). Curve fitting using a hyperbolic model gave an equilibrium dissociation constant (K_D) of 2.49 ± 0.85 nM and a B_{max} of 5.68 ± 1.25 pmol mg^{-1} protein (n=3).

Competition binding studies using 0.7 nM [^{3}H]DPCPX and increasing concentrations of unlabelled DPCPX gave a K_D of 2.18 ± 0.35 nM and a B_{max} of 4.97 ± 0.98 pmol mg^{-1} protein (n=3) (Figure 1.13b), which is in good agreement with data obtained from the hot saturation studies.

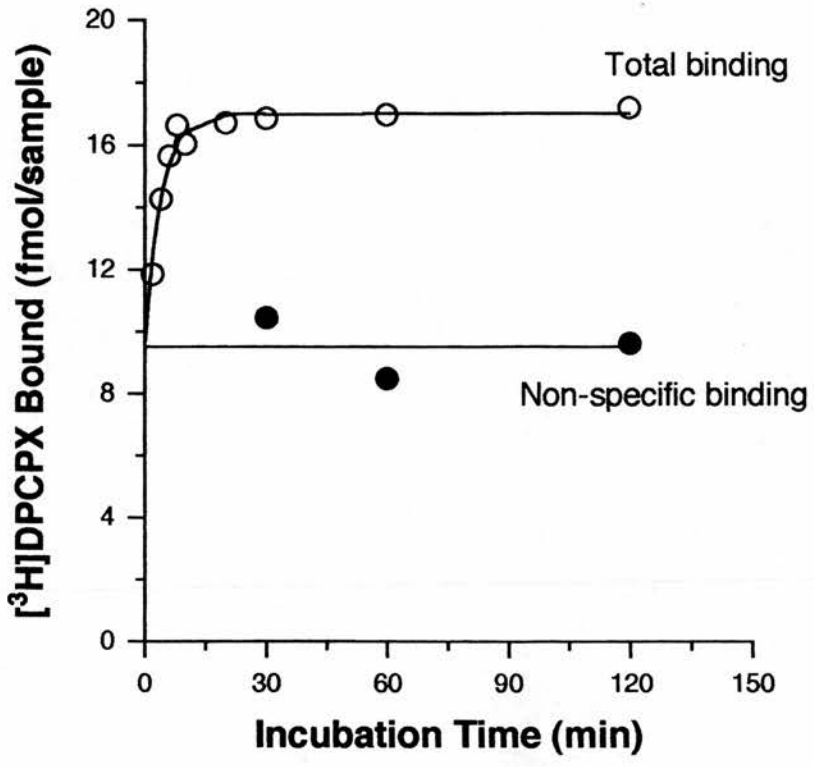

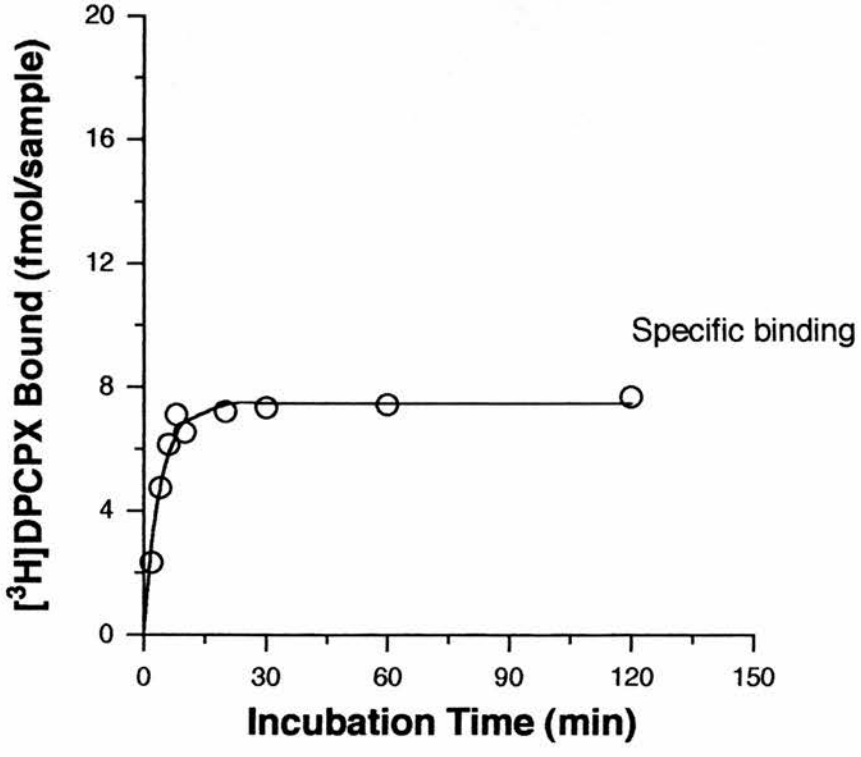

Figure 1.12 Time Course of [^{3}H]DPCPX Binding to Human Cerebral Cortical Membranes.

The data represent a typical time course experiment. Membranes were incubated with 0.7 nM [^{3}H]DPCPX for various times at 25°C. Experiments were performed as described in text with mean data obtained from two experiments (text for mean values).

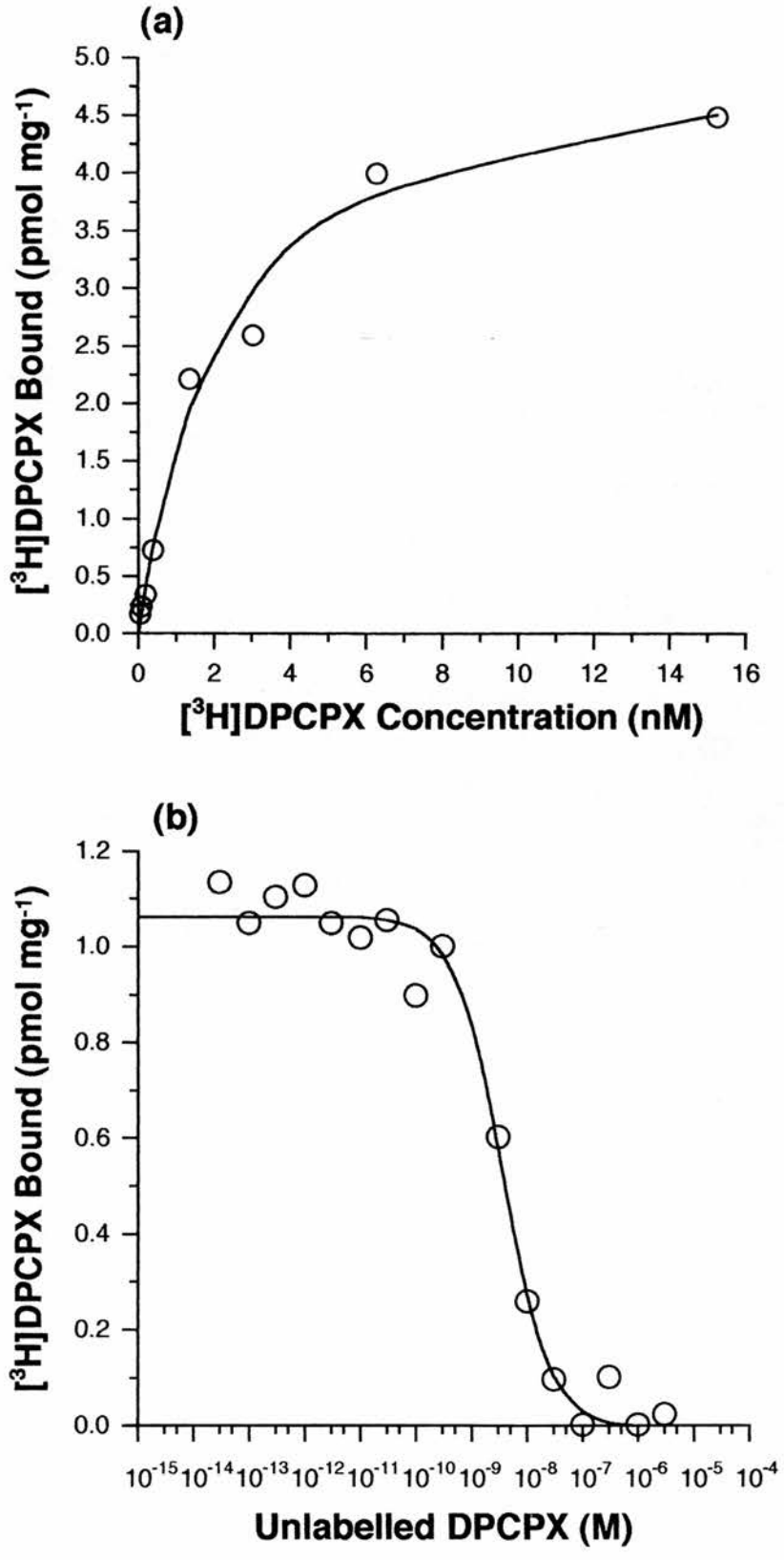

Figure 1.13 Concentration Dependence of Specific [^{3}H]DPCPX Binding to Human Cerebral Cortical Membranes.

The results represent a typical (a) hot and (b) cold saturation experiment with mean data obtained from three experiments (text for mean values).

1.3.4.3. Adenosine Receptor Antagonist and Agonist Pharmacology in Human Cortex

Adenosine receptor antagonists and agonists exhibited the typical adenosine A_1 pharmacological profile for [^{3}H]DPCPX binding sites in human cortical membranes. Antagonists had the following order of potency: DPCPX > CPT > DPX > 8-PT, with K_i values shown in Table 1.4. Agonists had the following order of potency: CCPA = CPA ≥ R-PIA > CHA > NECA ≥ CADO > CGS21680, with K_i values shown in Table 1.4. The affinity of antagonists and agonists in human cortex were lower than in rat (7-25 fold) as shown by the K_i ratio (Table 1.4), with the exception of CGS21680 at 2.9 fold lower. The K_i of CCPA on addition of the stable GTP analogue Gpp(NH)p (100 μM), was reduced to 378 ± 36 nM (nH=0.78 ± 0.02). Hill slopes were near unity for antagonists and significantly less than unity for all agonists.

1.3.4.4. Fujisawa Adenosine Receptor Antagonist Pharmacology in Human Cortex

In comparison with rat brain membranes, Fujisawa and xanthine based antagonists had a slightly different adenosine A_1 pharmacological profile for [^{3}H]DPCPX binding sites in human cortical membranes. The pharmacological profile of Fujisawa antagonists for [^{3}H]DPCPX binding sites was: FR160537 > FR171562 = KW3902 > FK453 = FR182303 > FR182394 = FR129946 > FK838 = FR160492 > FK352 = MDL102234, with K_i values shown in Table 1.5. In contrast to standard agonists and xanthine based antagonists, these non-xanthine compounds showed very little alteration in affinity between the two species, as shown by a selective comparison in Figure 1.14 and by the K_i ratio in Table 1.5. Results for the two xanthines, KW3902 and MDL102234 differed with the former xanthine having a similar affinity in both rat and human

Table 1.4 Inhibition of [^{3}H]DPCPX Binding to Human and Rat Brain Cortical Membranes by Adenosine Receptor Antagonists and Agonists

	[^{3}H]DPCPX - Human		[^{3}H]DPCPX - Rat		
Compound	**K_i (nM)**	**(nH)**	**K_i (nM)**	**(nH)**	**K_i Ratio**
DPCPX	2.18 ± 0.35	0.91 ± 0.10	0.28 ± 0.01	0.99 ± 0.02	7.79
CPT	49.1 ± 3.23	1.31 ± 0.13	6.49 ± 0.87	1.01 ± 0.05	7.57
DPX	467 ± 120	0.91 ± 0.07	33.1 ± 2.01	1.05 ± 0.03	14.1
8-PT	730 ± 141	0.86 ± 0.05	45.0 ± 1.37	1.07 ± 0.03	16.2
CCPA	47.6 ± 10.9	0.50 ± 0.06	3.39 ± 0.40	0.65 ± 0.02	14.0
CPA	64.0 ± 13.3	0.46 ± 0.05	4.02 ± 0.59	0.63 ± 0.02	15.9
R-PIA	88.4 ± 20.6	0.53 ± 0.04	4.56 ± 0.28	0.59 ± 0.02	19.4
CHA	184 ± 27.1	0.58 ± 0.04	7.16 ± 1.26	0.62 ± 0.06	25.7
NECA	312 ± 67.7	0.61 ± 0.04	39.1 ± 7.84	0.58 ± 0.06	7.98
CADO	338 ± 133	0.53 ± 0.05	41.0 ± 4.51	0.60 ± 0.02	8.24
CGS21680	112000± 4900	0.87 ± 0.15	39000 ± 9400	0.65 ± 0.04	2.87

K_i values and Hill slope (nH) determined for competition assays as described in the methods. Values expressed as mean ± S.E.M. ($n \geq 3$). K_i ratio shown between human & rat [^{3}H]DPCPX binding.

Table 1.5 Inhibition of [^{3}H]DPCPX Binding to Human and Rat Brain Cortical Membranes by Fujisawa Adenosine Receptor Antagonists

	[^{3}H]DPCPX - Human		[^{3}H]DPCPX - Rat		
Compound	**K_i (nM)**	**(nH)**	**K_i (nM)**	**(nH)**	**K_i Ratio**
DPCPX	2.18 ± 0.35	0.91 ± 0.10	0.28 ± 0.01	0.99 ± 0.02	7.79
FR160537	0.07 ± 0.01	1.10 ± 0.09	0.21 ± 0.01	1.22 ± 0.03	0.33
FR171562	0.20 ± 0.04	0.90 ± 0.09	0.29 ± 0.03	1.21 ± 0.07	0.69
FK453	0.50 ± 0.07	0.90 ± 0.16	0.54 ± 0.02	1.14 ± 0.03	0.93
FR129946	2.16 ± 0.43	0.78 ± 0.06	1.08 ± 0.07	1.02 ± 0.06	2
FR182394	1.67 ± 0.20	0.95 ± 0.06	1.73 ± 0.35	0.95 ± 0.03	0.97
FR182303	0.67 ± 0.06	1.22 ± 0.06	3.46 ± 0.50	1.12 ± 0.04	0.19
FK838	12.9 ± 3.06	1.02 ± 0.04	5.58 ± 0.34	0.99 ± 0.03	2.31
FK352	32.0 ± 7.39	1.13 ± 0.07	23.6 ± 0.70	1.01 ± 0.02	1.36
KW3902	0.30 ± 0.04	0.89 ± 0.12	0.16 ± 0.01	1.21 ± 0.03	1.88
FR160492	17.9 ± 2.19	1.05 ± 0.13	7.94 ± 0.59	1.24 ± 0.09	2.25
MDL102234	36.7 ± 1.88	1.33 ± 0.11	8.00 ± 0.37	1.02 ± 0.03	4.59

K_i values and Hill slope (nH) determined for competition assays as described in the methods. Values expressed as mean ± S.E.M. ($n \geq 3$). K_i ratio shown between human & rat [^{3}H]DPCPX binding.

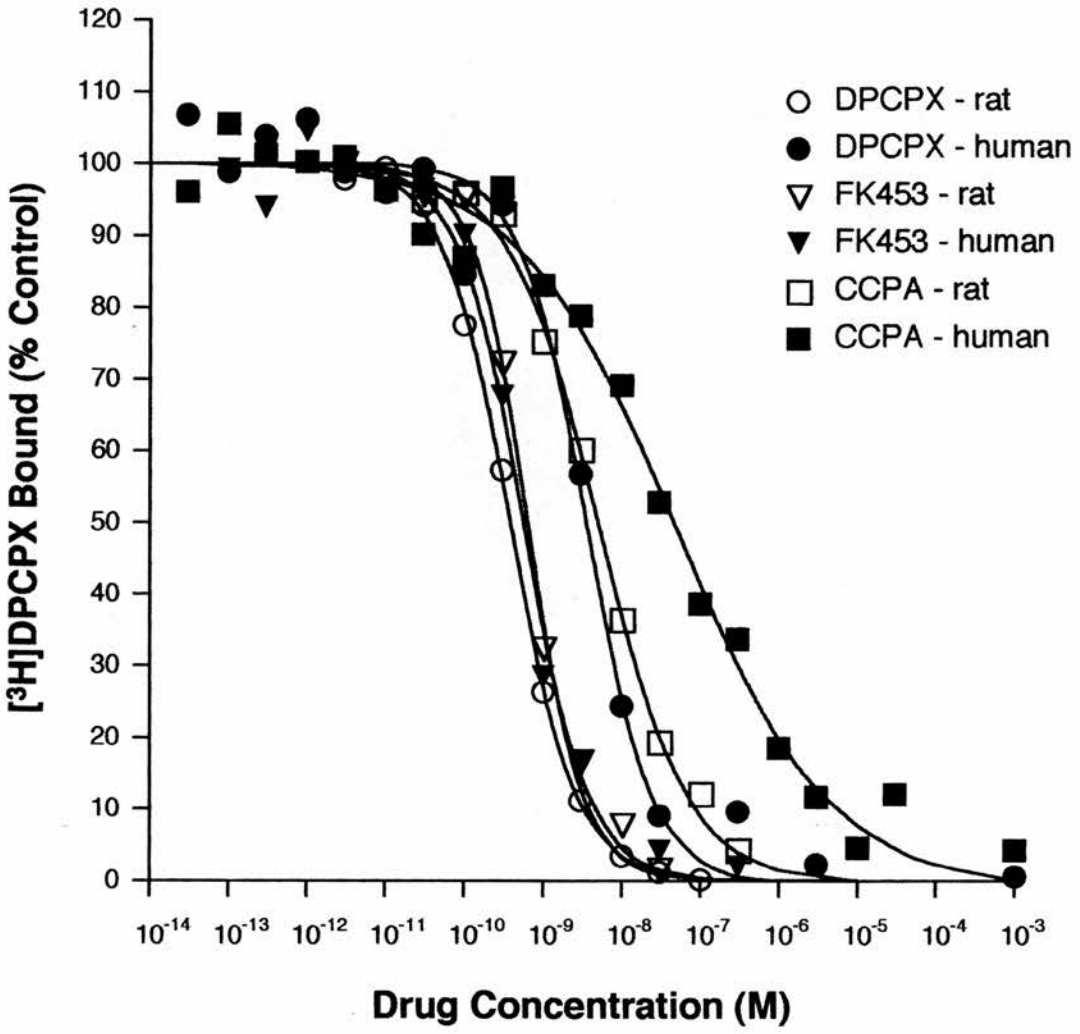

Figure 1.14 Inhibition of [^{3}H]DPCPX Binding to Human and and Rat Brain Cortical Membranes by DPCPX, FK453 and CCPA.

The data represents a typical experiment. Experiments were performed as described in text with mean data obtained from at least three experiments (Table 1.4; 1.5).

brain membranes and the latter showing a decrease in affinity consistent with the other xanthines. Hill slopes for all antagonists tested were close to unity.

1.3.5. Species Differences in Adenosine Receptor Pharmacology

In comparing the data from different species I would like to acknowledge that the data shown for mouse and guinea pig tissues were generated by Mr T. Maemoto. Following the discovery that the Fujisawa antagonists showed a similar affinity in rat and human cortical membranes, Mr T. Maemoto tested a limited number of compounds against [^{3}H]DPCPX binding to cortical membranes from mouse and guinea pig brain.

1.3.5.1. Standard Adenosine Receptor Antagonists and Agonists

Table 1.6 shows the affinity of both xanthine based antagonists (DPCPX, CPT, DPX, 8-PT) and adenosine based agonists (CCPA, CPA, R-PIA, CHA, NECA, CADO, CGS21680) in four species. As shown in Figure 1.15a, there is a direct correlation between rat and mouse K_i values with the data best described by the equation y=0.88x+0.17 and a correlation coefficient (r) of 0.99. The antilog of the intercept represents the average difference in affinity of the compounds between the two species. For rat and mouse the antilog of the intercept is equal to 1.48 with compounds having a similar affinity in both species. Figure 1.15b shows a good correlation between rat and human K_i values with the data best described by the equation y=0.87x+1.20 and a correlation coefficient (r) of 0.98. For rat and human the antilog of the intercept is equal to 15.8 with compounds being about an order of magnitude less potent in human membranes. Figure 1.15c shows a good correlation

Table 1.6 Species Differences in Inhibition of [^{3}H]DPCPX Binding to Brain Cortical Membranes by Adenosine Receptor Antagonists and Agonists

	K_i (nM)			
Compound	**Rat**	**Mouse***	**Human**	**Guinea pig***
DPCPX	0.28 ± 0.01	0.42 ± 0.03	2.18 ± 0.35	1.45 ± 0.13
CPT	6.49 ± 0.87	7.19 ± 0.42	49.1 ± 3.23	29.7 ± 1.38
DPX	33.1 ± 2.01	42.8 ± 5.07	467 ± 120	308 ± 10.8
8-PT	45.0 ± 1.37	52.4 ± 4.74	730 ± 141	366 ± 10.4
CCPA	3.39 ± 0.40	5.15 ± 0.86	47.6 ± 10.9	26.3 ± 4.04
CPA	4.02 ± 0.59	4.42 ± 1.98	64.0 ± 13.3	33.3 ± 6.92
R-PIA	4.56 ± 0.28	6.28 ± 0.58	88.4 ± 20.6	53.1 ± 11.7
CHA	7.16 ± 1.26	7.78 ± 2.59	184 ± 27.1	77.4 ± 18.6
NECA	39.1 ± 7.84	15.1 ± 1.37	312 ± 67.7	57.2 ± 13.7
CADO	41.0 ± 4.51	60.5 ± 28.2	338 ± 133	131 ± 26.0
CGS21680	39000 ± 9400	14900 ± 3200	112000 ± 4900	23400 ± 6300

K_i values determined for competition assays as described in the methods. Values expressed as mean ± S.E.M. (n≥3). * Data from mouse and guinea pig provided by Mr T. Maemoto.

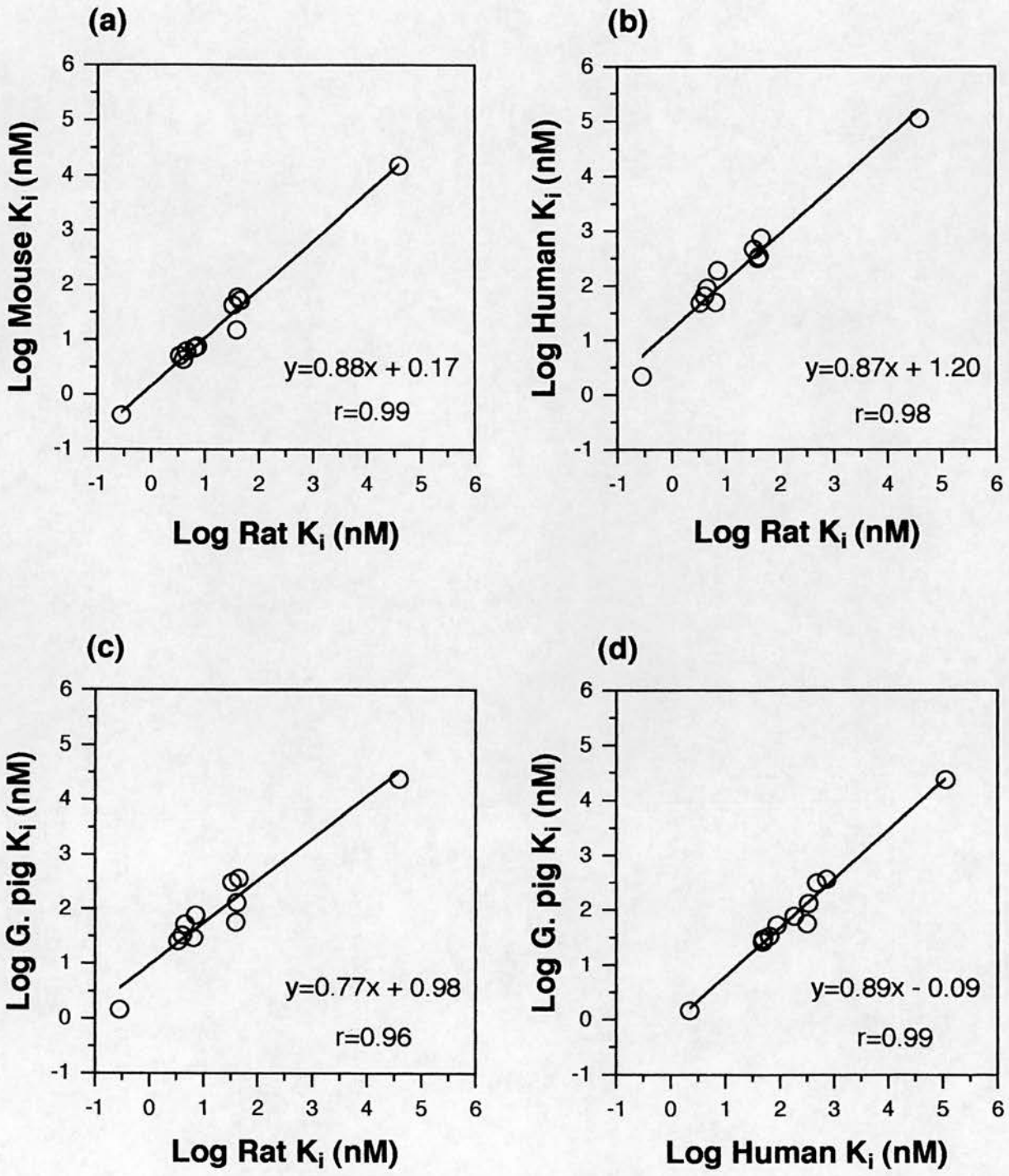

Figure 1.15 Correlation of the K_i values of Adenosine Antagonists and Agonists for [^{3}H]DPCPX Binding Sites in Cortical Membranes from Four Different Species.

The solid line represents a linear regression through the data presented in Table 1.6.

between rat and guinea pig K_i values with the data best described by the equation y=0.77x+0.98 and a correlation coefficient (r) of 0.96. For rat and guinea pig the antilog of the intercept is equal to 9.55 with compounds being about an order of magnitude less potent in guinea pig membranes. Figure 1.15d shows a very good correlation between human and guinea pig K_i values with the data best described by the equation y=0.89x-0.09 and a correlation coefficient (r) of 0.99. With the antilog of the intercept equal to 0.81, compounds would appear to have similar affinities in human and guinea pig membranes.

1.3.5.2. Fujisawa Adenosine Receptor Antagonists

Figure 1.16 shows a good correlation between rat and human K_i values for non-xanthine antagonists (FR160537, FR171562, FK453, FR129946, FR182394, FR182303, FK838, FK352), with the data best described by the equation y=1.18x-0.11 and a correlation coefficient (r) of 0.92. With a correlation coefficient of 0.92 and the antilog of the intercept equal to 0.78, compounds exhibit similar affinities in rat and human membranes. Table 1.7 shows the affinity of a limited number of Fujisawa antagonists tested in the four different species. Figure 1.17a shows a very good correlation between rat and mouse K_i values with the data best described by the equation y=1.09x+0.09 and a correlation coefficient (r) of 0.99. With the antilog of the intercept equal to 1.23, compounds would appear to have similar affinities in both species. Figure 1.17b shows a good correlation between rat and human K_i values with the data best described by the equation y=1.27x-0.01 and a correlation coefficient (r) of 0.98. With the antilog of the intercept equal to 0.98, compounds would appear to have similar affinities in both species. Figure 1.17c shows a very good correlation between rat and guinea pig K_i values with

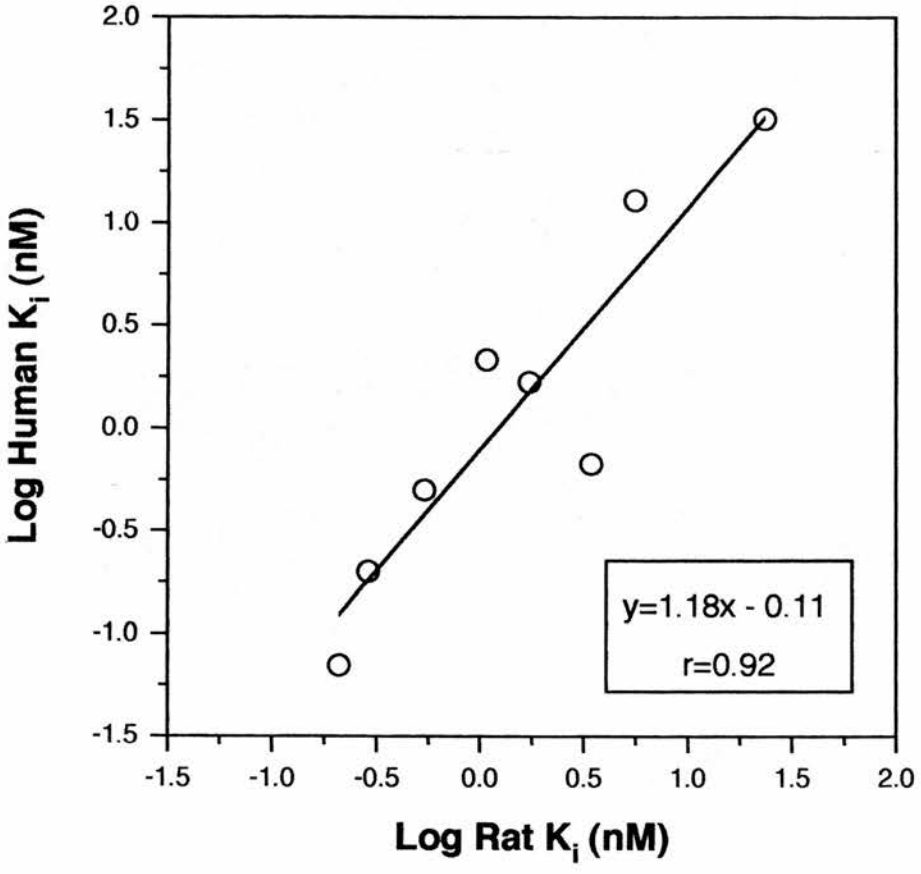

Figure 1.16 Correlation of the K_i Values of Fujisawa Antagonists for [^{3}H]DPCPX Binding Sites in Rat and Human Cortical Membranes.

The solid line represents a linear regression through the data from Table 1.5 for FR160537, FR171562, FK453, FR129946, FR182394, FR182303, FK838 and FK352.

Table 1.7 Species Differences in Inhibition of [^{3}H]DPCPX Binding to Brain Cortical Membranes by Fujisawa Adenosine Receptor Antagonists

	K_i (nM)			
Compound	**Rat**	**Mouse***	**Human**	**Guinea pig***
DPCPX	0.28 ± 0.01	0.42 ± 0.03	2.18 ± 0.35	1.45 ± 0.13
FR160537	0.21 ± 0.01	N.D.	0.07 ± 0.01	0.24 ± 0.01
FR171562	0.29 ± 0.03	N.D.	0.20 ± 0.04	0.37 ± 0.01
FK453	0.54 ± 0.02	0.57 ± 0.10	0.50 ± 0.07	0.64 ± 0.04
FR129946	1.08 ± 0.07	N.D.	2.16 ± 0.43	1.31 ± 0.04
FK838	5.58 ± 0.34	10.3 ± 0.33	12.9 ± 3.06	10.1 ± 0.53
FK352	23.6 ± 0.70	32.9 ± 6.49	32.0 ± 7.39	22.2 ± 0.98
KW3902	0.16 ± 0.01	0.17 ± 0.06	0.30 ± 0.04	0.37 ± 0.02
FR160492	7.94 ± 0.59	7.44 ± 1.31	17.9 ± 2.19	26.7 ± 3.16
MDL102234	8.00 ± 0.37	10.3 ± 3.91	36.7 ± 1.88	28.2 ± 7.95

K_i values determined for competition assays as described in the methods. Values expressed as mean ± S.E.M (n>3), (N.D. = not determined). *Data from mouse and guinea pig provided by Mr T. Maemoto.

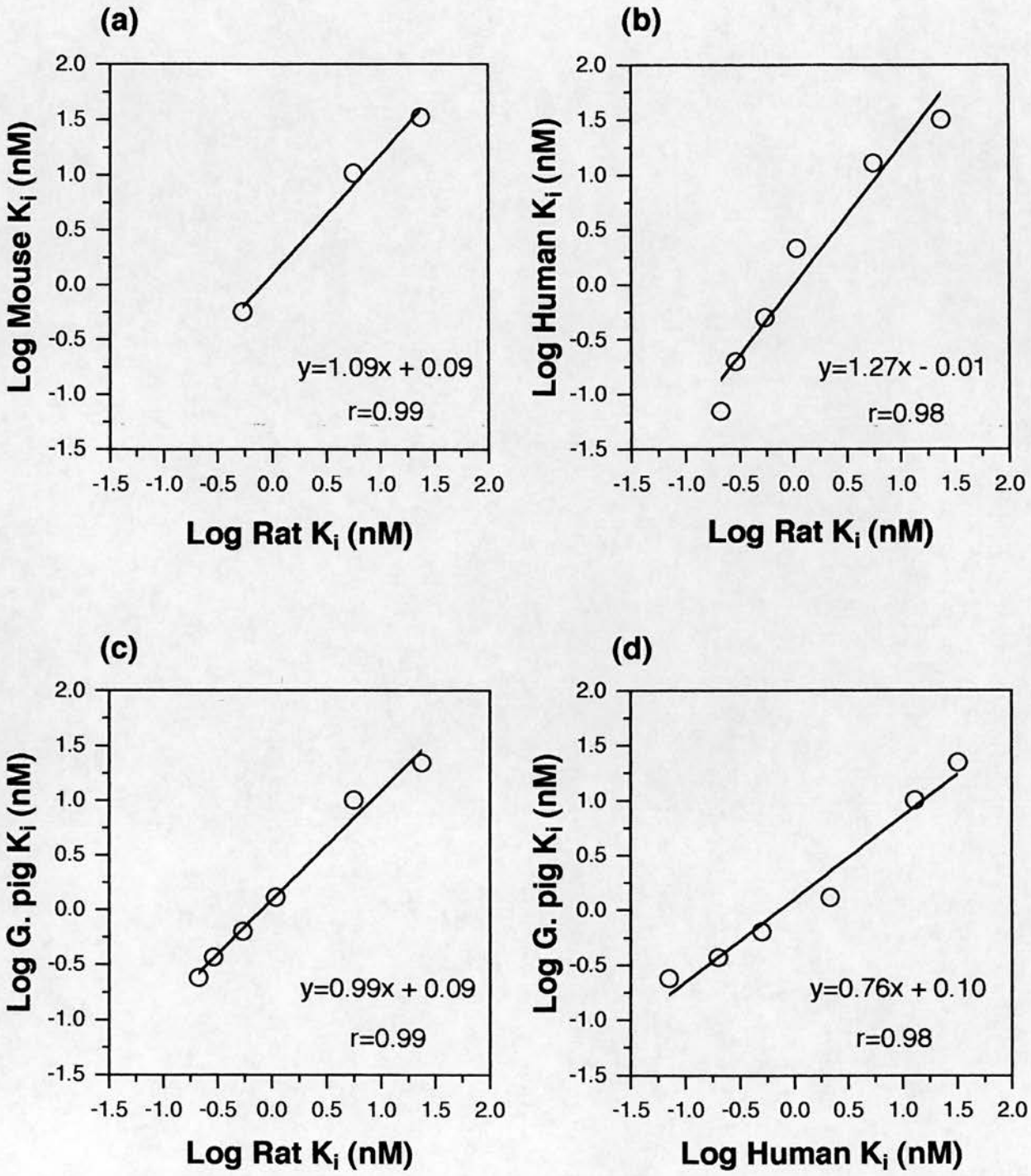

Figure 1.17 Correlation of the K_i values of Fujisawa Antagonists for [^{3}H]DPCPX Binding Sites in Cortical Membranes from Four Species.

The solid line represents a linear regression through the data from Table 1.7 for FR160537, FR171562, FK453, FR129946, FK838 and FK352 where appropriate.

the data best described by the equation y=0.99x+0.09 and a correlation coefficient (r) of 0.99. With the antilog of the intercept equal to 1.23, compounds would appear to have similar affinities in both species. Figure 1.17d shows a good correlation between human and guinea pig K_i values with the data best described by the equation y=0.76x+0.10 and a correlation coefficient (r) of 0.98. With the antilog of the intercept equal to 1.26, compounds would appear to have similar affinities in both species.

1.4. Discussion

[^{3}H]DPCPX and [^{3}H]CGS21680 binding assays have been used to determine the adenosine A_1 receptor affinity and selectivity in rat brain of a range of adenosine agonists, xanthine based antagonists and Fujisawa's novel non-xanthine antagonists. The A_1 receptor affinities of a select group of compounds were determined in the brain of three other species; mouse, guinea pig and human.

The binding of [^{3}H]DPCPX and [^{3}H]CGS21680 to rat brain membranes was reversible, saturable and of high affinity. The K_D and B_{max} values for the individual radioligands were similar in their respective kinetic, saturation and competition studies. These data from kinetic and saturation studies are in good agreement to those calculated in the original characterisation of [^{3}H]DPCPX (Bruns *et al.*, 1987) and [^{3}H]CGS21680 (Jarvis *et al.*, 1989a) binding sites. The reference xanthine antagonists exhibited the typical adenosine A_1 pharmacological profile for [^{3}H]DPCPX binding sites in rat cortical membranes, with Hill slopes not significantly different from unity and with an order of potency identical to Bruns *et al.*, (1987). Table 1.8 shows antagonist affinities determined using [^{3}H]DPCPX binding were similar to values obtained using the agonist radioligands [^{3}H]CHA and [^{3}H]R-PIA and to data from cloned rat

Table 1.8 A_1 Receptor Affinity for Adenosine Receptor Agonists and Antagonists

	[^{3}H]DPCPX Present Study	[^{3}H]DPCPX[a] Rat	[^{3}H]CHA Rat	[^{3}H]RPIA[e] Rat
CCPA	3.39			0.4[h]
CPA	4.02	7.9	1[c]	0.34
R-PIA	4.56	16	2[c]	1.2
CHA	7.16	27	2[c]	1.0
NECA	39.1	90	6[c]	7.8
CADO	41.0		14[c]	7.5
S-PIA	212	520	29[d]	50
CSPA	583			
APEC	602			235[g]
CGS21680	39000		2600[c]	
DPCPX	0.28	0.56/0.18[b]		1.2
CGS15943	1.35		22[c]	
CPT	6.49	11/6.3[b]		10
DPX	33.1	37	135[d]	
8-PT	45.0		176[d]	76
DPSPX	76.1			140
KF17837	80.6	390[i]		
8-PST	1020		1275[d]	1000
Theophylline	4330	5600[b]	10960[d]	12800
CSC	10600			28000[f]
Caffeine	25300		28000 [c]	44000

Data taken from: [a]Bruns *et al.*, (1987), [b]Klotz *et al.*, (1991), [c]Jarvis *et al.*, (1989a), [d]Ferkanky et *al.*, (1986), [e]Ukena *et al.*, (1986), [f]Jacobson *et al.*, (1993), [g]Nikodijevic et *al.*, (1991), [h]Lohse *et al.*, (1988) and [i]Nonaka *et al.*, (1993).

brain A_1 receptors (Mahan *et al.*, 1991; Freund *et al.*, 1994). These antagonists also exhibited the typical adenosine A_{2a} pharmacological profile for [^{3}H]CGS21680 binding sites in rat striatal membranes, with Hill slopes not significantly different from unity and with an order of potency identical to Jarvis *et al.*, (1989a) (Table 1.9). These data are consistent with the recently characterised A_{2a} receptor antagonists [^{3}H]SCH58261 (Zocchi *et al.*, 1996) and [^{3}H]KF17837S (Nonaka *et al.*, 1994) (Table 1.9). Receptor selectivity, as determined by the K_i ratio, was almost identical to that described by Bruns *et al.*, (1987), for DPCPX (686 vs 607), CPT (130 vs 127) and DPX (8.7 vs 23.2). For the recently characterised A_{2a} receptor selective antagonists CSC (Jacobson *et al.*, 1993) and KF17837 (Shimada *et al.*, 1992; Nonaka *et al.*, 1993), values were very similar at (0.001 vs 0.002) and (0.029 vs 0.018) respectively.

The reference adenosine agonists exhibited the typical adenosine A_1 pharmacological profile for [^{3}H]DPCPX binding sites in rat cortical membranes, with Hill slopes significantly less than unity (nH=0.58-0.65) and with an order of potency identical to Bruns *et al.*, (1987) (Table 1.8). As with other G protein coupled receptors, the shallow Hill slope is indicative that agonists recognise high and low affinity states of the receptor, reflecting the receptor being coupled to and uncoupled from G proteins (Gilman, 1987; Birnbaumer *et al.*, 1990). The lower affinity of agonists in the [^{3}H]DPCPX binding assay in comparison with the agonist radioligands [^{3}H]CHA and [^{3}H]R-PIA (Table 1.8), is because agonist radioligands recognise almost exclusively the high affinity state of the receptor. The standard agonists exhibited the typical adenosine A_{2a} pharmacological profile for [^{3}H]CGS21680 binding sites in rat striatal membranes, with an order of potency identical to Jarvis *et al.*, (1989a) (Table 1.9). Jarvis and colleagues reported Hill slopes not significantly different from

Table 1.9 A_{2a} Receptor Affinity for Adenosine Receptor Agonists and Antagonists

	Present Study	[^{3}H]CGS21680[a] Rat	[^{3}H]SCH58261[b] Rat	[^{3}H]KF17837S[c] Rat	[^{3}H]CGS21680[c] Rat	[^{3}H]CGS21680[d] Human
NECA	4.92	12	61	59	3.1	15
APEC	5.57					
CGS21680	9.64	14	111	130	4.5	18
CADO	28.1	120				36
R-PIA	91.4	410	992	510	54	153
CPA	220	890		1500	230	
CHA	248	685	2840			465
CCPA	331		3260			
S-PIA	1680	3020	8504	6400	660	1539
CSPA	3640					
CGS15943	0.38	3	0.38	0.39	0.39	
KF17837	2.32		9.4			
CSC	14					
DPCPX	192	260	234	160	120	
DPX	289	490				
DPSPX	386					
8-PT	391	550	383			
CPT	845	1050				
8-PST	4100	3320				
Theophylline	6770	21000				
Caffeine	13800	37000		11000	19000	

Data taken from: [a]Jarvis *et al.*, (1989a), [b]Zocchi *et al.*, (1996), [c]Nonaka *et al.*, (1994) and [d]Wan *et al.*, (1990).

unity for agonists and antagonists and hence one binding component. Our data indicate that the majority of agonist Hill slopes were steeper than those in the [^{3}H]DPCPX binding assay but were still significantly less than unity, suggesting that [^{3}H]CGS21680 labels two affinity states. These data are consistent with the recently characterised A_{2a} antagonist [^{3}H]KF17837S (Nonaka *et al.*, 1994), with shallow Hill slopes for agonists supporting the concept that A_{2a} receptors exist in two agonist coupling states. In the same study [^{3}H]CGS21680 was reported to label a large proportion of high affinity receptors (Table 1.9). This is consistent with the present data as when CGS21680 was examined over an extended concentration range and data fitted to a 2-site model (although this model provided no significant improvement using a partial *F* test, $P > 0.05$), a high affinity site of 7.5 ± 1.6 nM (84%) and a low affinity site of 176 ± 132 nM were identified. The lack of improvement on fitting the data to a 2-site model is perhaps not surprising as studies indicate that 2-site models are only likely to improve the fit when the difference in affinity between two sites is greater than the 30 fold observed in the present study (Bruns *et al.*, 1986, 1987). There is however controversy as the A_{2a} antagonist [^{3}H]SCH58261 (Zocchi *et al.*, 1996), labels only one low affinity component for agonists, despite similar affinities to those obtained for [^{3}H]KF17837S (Nonaka *et al.*, 1994) (Table 1.9). The reason for this discrepancy remains to be elucidated. Receptor selectivity as determined by the K_i ratio was almost identical to that described by Bruns *et al.*, (1987), for CPA (54.7 vs 58.2), CHA (34.6 vs 19.0) and R-PIA (20 vs 7.5). For the recently characterised A_{2a} receptor selective agonists CGS21680 (Jarvis *et al.*, 1989a) and APEC (Nikodijevic *et al.*, 1991), values were very similar at (0.0002 vs 0.005) and (0.023 vs 0.029) respectively.

Species differences in A_1 (Murphy & Snyder, 1982; Ferkanky *et al.*,

1986; Ukena *et al.*, 1986; Klotz *et al.*, 1991) and A_{2a} (Stone *et al.*, 1988) receptor pharmacology have been characterised. These studies have predominantly used agonist radioligands, with the exception of Klotz *et al.*, (1991), who used [^{3}H]DPCPX to characterise a limited number of compounds. This is the first comprehensive study in which an antagonist radioligand has been used to assess adenosine receptor pharmacology. To complement and extend these studies, Mr T. Maemoto used [^{3}H]DPCPX to examine the A_1 receptor affinity of 11 standard agonists and antagonists in cerebral cortical membranes of the two other most commonly used laboratory animals, the mouse and guinea pig (Maemoto *et al.*, 1994). The K_D and B_{max} values for [^{3}H]DPCPX in mouse cortex were very similar to rat, as were the rank order of potency and affinity of both agonists and antagonists. Similarities in the pharmacological properties of rat and mouse brain membranes were also observed using the agonist radioligand, [^{3}H]CHA (Ferkanky *et al.*, 1986). However, for guinea pig cortex the K_D was approximately 5 fold lower than rat, the B_{max} 2 fold higher and the rank order of potency similar, with the exception of NECA which had a similar affinity in all three species. These data are consistent with previous data (Ferkanky *et al.*, 1986; Ukena *et al.*, 1986; Klotz *et al.*, 1991; Alexander *et al.*, 1994). The low affinity of the guinea pig receptor for agonists and antagonists was also studied using hippocampal tissue (Maemoto *et al.*, 1994). Recently an adenosine A_1 receptor from guinea pig brain was cloned and expressed, with agonist affinities even lower than native tissues (Meng *et al.*, 1994a). Further studies will be required to define whether this is a distinct low affinity subtype or an artifact of the expression system.

This solid database for adenosine receptor pharmacology in different species allowed us to confidently examine a series of novel non-xanthine antagonists from Fujisawa. Over 150 compounds were screened using rat

brain membranes and a two point screen for both A_1 and A_{2a} receptor binding assays (Mr T. Maemoto, unpublished data). Eight compounds were chosen for further characterisation. For comparison we examined three compounds from other companies: the xanthines KW3902 (Nonaka *et al.*, 1996) and MDL102234 (Peet *et al.*, 1993) and a non-xanthine Takeda compound (FR160492). In rat brain membranes, all the compounds had high affinity and selectivity for the A_1 receptor, with the exception of the Takeda compound which showed only 7 fold selectivity for the A_1 receptor. The Fujisawa antagonists had a range of affinities from 0.21 nM for FR160537 to 23.6 nM for FK352. Three compounds FK453, FR182394 and FK352 were three times more selective (> 2000 fold) than DPCPX. The K_i value for FK453 is slightly higher than that found by Terai *et al.*, (1995a). The affinity and selectivity for KW3902 and MDL102234, were however in excellent agreement with that found by Nonaka *et al.*, (1996) and Peet *et al.*, (1993) respectively.

The ultimate goal of the project is to develop a clinically useful drug. In light of characterised and reported species differences, it was therefore essential to examine the pharmacology of the adenosine A_1 receptor in human brain tissue. In collaboration with Dr R.W. Horton, we examined adenosine A_1 receptor pharmacology in human parietal cortex (Brodmann area 7). With tissue in short supply, only a limited kinetic characterisation was carried out. The binding of [^{3}H]DPCPX to human brain membranes was saturable, of high affinity and equilibrium was attained after a 20 min incubation. The K_D and B_{max} values were similar in saturation (K_D=2.49 ± 0.85 nM; B_{max}=5.68 ± 1.25 pmol mg^{-1} protein) and competition studies (K_D=2.18 ± 0.35 nM; B_{max}=4.97 ± 0.98 pmol mg^{-1} protein). The K_D in human cortex was approximately 8 fold lower than in rat cortex and the B_{max} three fold higher. These data are consistent with Murphy & Snyder, (1982) and Ferkanky *et al.*, (1986) who

found a lower K_D in human brain membranes in comparison with rat; however, the latter study demonstrated no difference in B_{max}. The K_D of [^{3}H]DPCPX in human cortical membranes in the present study is comparable to values obtained for the cloned (Libert *et al.*, 1992; Townsend-Nicholson & Shine, 1992; Jockers *et al.*, 1994) and purified human brain A_1 adenosine receptor (Nakata, 1992). These data contrast with Rivkees *et al.*, (1995b), who demonstrated a similar affinity and binding capacity for cloned rat and human adenosine A_1 receptors using [^{3}H]CCPA as the radioligand. The data from cloned studies must be interpreted with caution as work within our own laboratory (Mr T. Maemoto, personal communication), has indicated that agonist affinity can be radically altered by changing the expression level of the receptor. Standard agonists and antagonists inhibited [^{3}H]DPCPX binding to human cortical membranes with the typical adenosine A_1 pharmacological profile. However, agonist and antagonist affinities for the human receptor were at least 7 fold lower than rat, with the exception of CGS21680 which had negligible affinity. The differences between rat and human are larger than the decrease shown by Murphy and Snyder, (1982) for R-PIA (2 fold) and CHA (4 fold) but are almost identical for DPX at 14.3 fold. The data is consistent with that of the cloned brain A_1 receptor (Libert *et al.*, 1992). These data do however contrast with Ferkanky *et al.*, (1986), who showed a variable profile of effects when comparing rat and human receptor pharmacology. The possibility that the receptor is functionally uncoupled from its G protein would seem unlikely, as the Hill slope for agonists is significantly less than unity and addition of Gpp(NH)p, the stable GTP analogue, produced an 8 fold decrease in affinity for CCPA. This 8 fold decrease in affinity in the presence of Gpp(NH)p was accompanied by an increase in Hill slope. However, the value was still significantly less than unity, presumably reflecting an incomplete shift

to the low affinity state. In contrast, Libert *et al.*, (1992) and Nanoff *et al.*, (1995), demonstrated a complete shift to the low affinity state for the cloned human A_1 receptor. Interestingly when the cloned human brain A_1 receptor was expressed in *E. coli* that contain no endogenous G proteins (Jockers *et al.*, 1994) and therefore only the low affinity state for agonists is detectable, the affinity of CPA, R-PIA, NECA and CADO was 5-7 fold lower than our data and is similar to values we would expect on addition of Gpp(NH)p.

The pharmacological profile of the 8 non-xanthine Fujisawa antagonists in human brain tissue was the same as rat. In contrast to adenosine based agonists and xanthine based antagonists, the affinity of these novel compounds in rat and human brain tissue was almost identical. The non-xanthine Takeda compound (FR160492) also had a similar affinity in rat and human brain tissue. As with the other xanthine based antagonists, MDL102234 (Peet *et al.*, 1993) had a K_i value approximately 5 fold lower in human brain tissue than in rat. However, the xanthine KW3902 (Nonaka *et al.*, 1996) had a similar affinity in both rat and human tissue.

The rank order of potency for adenosine agonists and xanthine based antagonists in inhibiting [^{3}H]DPCPX binding to brain membranes was similar in all four species. There was however differences in affinity for agonists and antagonists, with guinea pig pharmacology sharing the closest resemblance to human. This is consistent with Ferkanky *et al.*, (1986), who despite having different values for the affinity of the compounds, reached a similar conclusion. It may therefore be more appropriate to assess the pharmacology of these compounds in guinea pig tissue rather than rat or mouse when trying to extrapolate to man. For the non-xanthine Fujisawa adenosine antagonists so far examined, it would appear that pharmacological characteristics can be assessed in rat, mouse and guinea pig, as the affinity of these compounds in brain tissue was almost identical to that of human cortex. The cloning of

multiple adenosine receptor subtypes, now makes it possible to identify the receptor domains responsible for binding certain functional groups present on specific ligands. Compared with other GPCRs, the understanding of how ligands bind to adenosine A_1 receptors and which amino acids are involved in the binding of agonists and antagonists is still in its infancy. It has been shown for the 5-HT_{1b} receptor that a single amino acid is responsible for major pharmacological differences between human and rodent receptors (Oksenberg *et al.*, 1992). Replacement of threonine at residue 355 in the human 5-HT_{1b} receptor by the equivalent asparagine residue in the rodent 5-HT_{1b} receptor renders agonist and antagonist pharmacology almost identical. This is not uncommon for GPCRs, with single amino acids important for conferring species specificity in pharmacological properties of α_2-adrenergic, 5-HT_2, cholecystokinin and neurokinin receptors (Link *et al.*, 1992; Kao *et al.*, 1992; Jensen *et al.*, 1993). Binding models postulate that the ligand binding sites of adenosine A_1 receptors are within the transmembrane regions, as with adrenergic (α and β), muscarinic, dopamine and serotonin receptors (Ostrowski *et al.*, 1992; Olah *et al.*, 1994). Unlike these biogenic amines, adenosine is uncharged at physiological pH and is bulkier, so all the features required for binding may not be conserved (Palmer & Stiles, 1995). One example of this would be the aspartate residue (Asp113), which is conserved in all GPCRs that bind biogenic amines but is not present in adenosine receptors (Tota *et al.*, 1991). The role of histidine residues in adenosine A_1 receptor ligand binding was first investigated in a study in which rat brain membranes were chemically modified by treatment with diethylpyrocarbonate (Klotz *et al.*, 1988). This study provided the first evidence for agonists and antagonists occupying separate domains at the binding site and a role for multiple histidine residues within the transmembrane domains. A more specific

study, where the two histidine residues in transmembrane six and seven (TM6 and TM7) were altered by site directed mutagenesis, again pointed to a role for the residues in agonist and antagonist binding (Olah *et al.*, 1992). Recent studies, using site directed mutagenesis and chimeric receptors, have indicated a role for multiple regions of the adenosine A_1 receptor in ligand recognition. This has included regions within the transmembrane domains and on the extracellular loops, with a considerable degree of overlap in structural features for agonist and antagonist binding (Olah *et al.*, 1994; Tucker *et al.*, 1994; Townsend-Nicholson & Schofield, 1994). This is unlike the β_2-adrenergic receptor where discrete sequences have been found to be responsible for binding specific functional groups (Ostrowski *et al.*, 1992). There are, however, differences with individual amino acids important in the binding of ligands to adenosine A_1 receptors in different species. The amino acid at position 277 is able to interact with the 5´-ribose moiety (Townsend-Nicholson & Schofield, 1994; Tucker *et al.*, 1994) and amino acid 270 is able to interact with the N^6-substituted adenosine analogues and C^8-substituted xanthines (Tucker *et al.*, 1994). These two amino acids have been reported to be important in conferring species selectivity in ligand binding to A_1 receptors. As with the 5-HT_{1b} receptor (Oksenberg *et al.*, 1992), these amino acids are located in TM7. In the case of the 5-HT_2 and α_2-adrenergic receptors, important structural amino acids are located in TM5 (Link *et al.*, 1992; Kao *et al.*, 1992). Consistent with amino acid 270 being important for C^8 and N^6-substituted ligands, the rat and mouse adenosine A_1 receptors have the same residue as the bovine receptor, whereas the human and guinea pig receptors, which show lower affinities for these compounds both have threonine residues (Townsend-Nicholson & Shine, 1992; Meng *et al.*, 1994a; Marquardt *et al.*, 1994). The canine receptor, which has an even lower affinity, has a methionine residue at

amino acid 270 (Townsend-Nicholson & Shine, 1992; Tucker *et al.*, 1994). These observations are consistent with our data, in that the affinity of agonists and xanthine based antagonists, were similar in human and guinea pig membranes and higher in rat and mouse brain membranes. These studies primarily focused on sites within TM's 5-7, with species dependent binding properties conferred primarily by the carboxyl third of the receptor. However a very recent study, has pointed to a role for TM's 1-4, which also contain important determinants for adenosine A_1 receptor agonist and antagonist binding and ligand specificity (Rivkees *et al.*, 1995a). It is not difficult to speculate that these regions may also contain determinants important in conferring species selectivity. It is also tempting to speculate that the non-xanthine Fujisawa antagonists do not interact with amino acid 270, thereby explaining the maintenance of affinity across species, although confirmation of this requires further studies at the molecular level.

Despite greater than 90% receptor identity at the amino acid level (see main introduction), this and earlier studies demonstrate that the pharmacology of adenosine A_1 receptors differs markedly between species (Murphy & Snyder, 1982; Ferkanky *et al.*, 1986; Ukena *et al.*, 1986; Stone *et al.*, 1988; Klotz *et al.*, 1991). Multiple facets may be involved in accounting for these species differences, including changes in the amino acid sequences of the different receptors (as discussed above), the ability to couple to different G proteins and hence different signal transduction pathways (Jockers *et al.*, 1994), or in the case of the human receptor posttranslational modifications (Ren & Stiles, 1994a). It may be possible to continue to identify areas involved in ligand recognition and hence explain why Fujisawa antagonists retain their affinity for the human brain adenosine A_1 receptor by using a combined approach of creating chimeric receptors and site directed mutagenisis (Tucker *et al.*, 1994; Olah *et al.*, 1994; Townsend-Nicholson & Schofield, 1994).

CHAPTER TWO

MODULATION OF LIGAND BINDING TO ADENOSINE A_1 AND A_{2a} RECEPTORS BY Gpp(NH)p AND MAGNESIUM

2.1. Introduction

Adrenergic (Ostrowski, *et al.*, 1992) and muscarinic (Hulme, *et al.*, 1990) receptors, are two extensively characterised GPCRs from which most generalities of receptor structure-function relationships are based. Adenosine receptors all fit the structural motif typical of GPCRs (Birnbaumer *et al.*, 1990). The structures have seven stretches of hydrophobic α-helical regions, composed of ~22-26 AA's, that cross the cell membrane. The amino terminus and AA's connecting the membrane spanning domains 2-3, 4-5 and 6-7 (known as extracellular loops 1, 2 and 3 respectively) are extracellular, whereas the carboxyl terminus and regions connecting transmembrane domains 1-2, 3-4 and 5-6 (intracellular loops 1, 2 and 3 respectively) are cytoplasmic. The c-terminal portion of the receptor and the third intracellular loop are supposedly important in binding G proteins (Linden, 1994). Portions of these loops may interact directly with α (Figure 2.1) and possibly $\beta\gamma$ subunits of G proteins producing receptor activation and regulation by phosphorylation (Fredholm *et al.*, 1994; Murthy & Makhlouf, 1995). In comparison with other GPCRs, A_1, A_{2b} and A_3 receptors have short amino termini and are small in size. In native tissues, A_1 and A_{2a} receptors have been identified as glycoproteins (Stiles, 1990). In common with other GPCRs, adenosine A_1 and A_{2a} receptors have two glycosylation sites on the putative second extracellular loop and none on the amino-terminal tail (Palmer & Stiles, 1995). Other common features include residues important in sodium regulation, disulphide bond formation and palmitoylation (Olah & Stiles, 1995). There are differences however; A_1, A_{2a} and A_{2b} receptors do not have an aspartic (Asp113) acid residue in the third transmembrane domain which is present in muscarinic, adrenergic, serotonergic and dopaminergic receptor proteins and is important for cationic amine ligand binding (Tota *et al.*, 1991; Stehle *et al.*, 1992). Lack of

Figure 2.1 Action of Adenosine

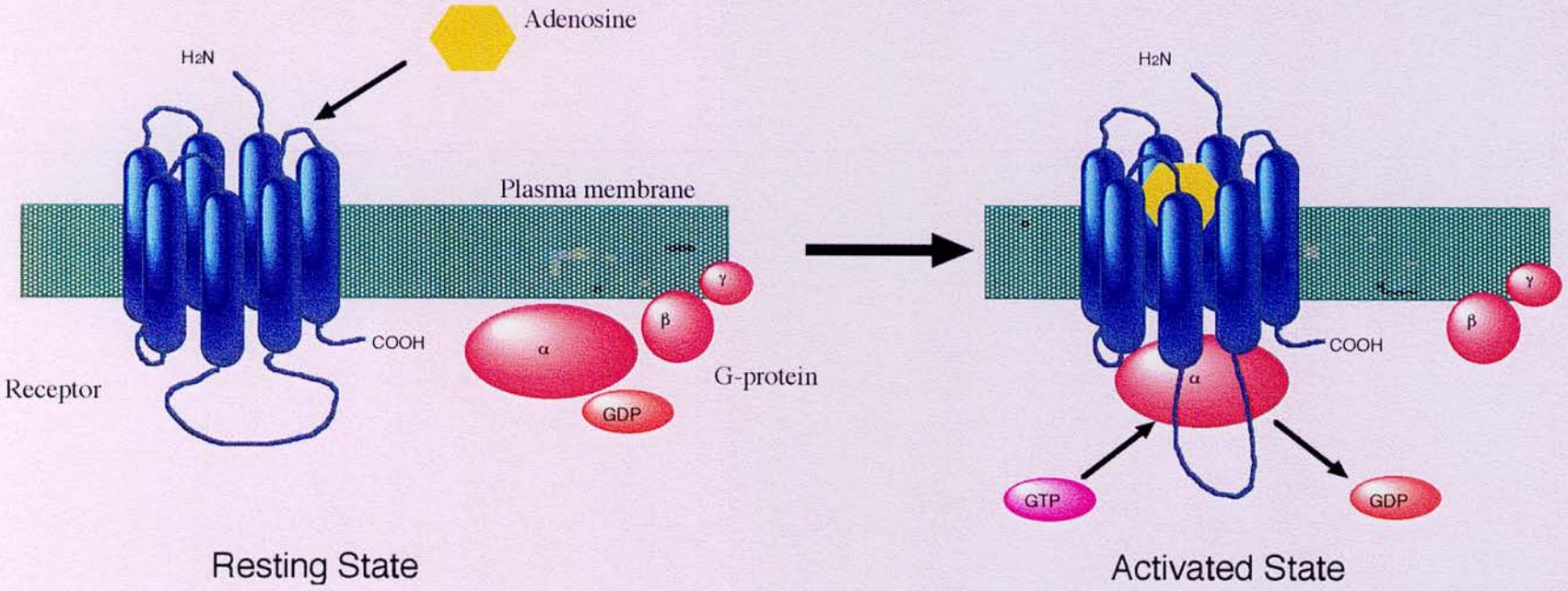

conservation in the features required for ligand binding may be due to adenosine being bulkier and uncharged at physiological pH, unlike endogenous biogenic amines (Palmer & Stiles, 1995).

On activation, adenosine receptors display a number of characteristics associated with G protein mediated transmembrane coupling (Gilman, 1987; Olah & Stiles, 1992). Two areas which have been the focus of numerous contradictory studies are the guanine nucleotide and magnesium dependence of adenosine agonist and antagonist binding. For many GPCRs including the adenosine A_1 (Lohse *et al.*, 1984; Klotz *et al.*, 1991; Casado *et al.*, 1994) and A_{2a} (Stone *et al.*, 1988; Wan *et al.*, 1990; Luthin *et al.*, 1995) receptors, two different high and low affinity states exist for agonist binding (Birnbaumer *et al.*, 1990). However, for the A_{2a} receptor this is controversial with studies reporting the existence of only one high affinity state for agonists (Jarvis *et al.*, 1989a; Kirk & Richardson, 1995). For the A_1 receptor, guanine nucleotides or their non-hydrolysable analogues uncouple the G protein from the receptor-G protein complex, so in the presence of the nucleotides the low affinity agonist state is predominant (Lohse *et al.*, 1984; Stroher *et al.*, 1989). For the A_{2a} receptor, the situation is less clear cut with the receptor apparently more resistant to the effects of guanine nucleotides (Nanoff & Stiles, 1993; Zocchi *et al.*, 1996). The finding that high affinity agonist binding for A_1 and A_{2a} receptors is not completely abolished by guanine nucleotides, or by receptor solubilisation (Gavish *et al.*, 1982; Stiles, 1985; Nanoff & Stiles, 1993), is indicative of both receptors forming a tighter association with their G proteins than other GPCRs (Stiles, 1985; Freissmuth *et al.*, 1991a). Unlike agonists, antagonists at A_1 and A_{2a} receptors recognise both coupled and uncoupled states of the receptor with equal affinity (Yeung & Green, 1983; Klotz *et al.*, 1991; Nonaka *et al.*, 1994). If true, guanine nucleotides should not modulate

antagonist binding. Preliminary studies with the new A_{2a} antagonists, [^{3}H]SCH58261 (Zocchi *et al.*, 1996) and [^{3}H]KF17837S (Nonaka *et al.*, 1994), appear consistent with this hypothesis with no alteration in K_D or B_{max} values on addition of GTP. Results for the A_1 receptor are conflicting. Some groups have shown guanine nucleotides have no effect on B_{max} or K_D (Lohse *et al.*, 1984; Klotz *et al.*, 1986; Leid *et al.*, 1988; Stiles, 1988; Olah & Stiles, 1990), whereas others found an increase in B_{max} with no change in K_D (Yeung & Green, 1983; Klotz *et al.*, 1990; Nakata, 1990; Freissmuth *et al.*, 1991a). There have also been studies demonstrating an increase in B_{max} and a decrease in K_D and vice versa (Ramkumar & Stiles, 1988; Stroher *et al.*, 1989; Lorenzen *et al.*, 1993). The possibility that antagonists unlike agonists destabilise the receptor-G protein complex and bind preferentially to the uncoupled form of the receptor (Leung & Green, 1989; Leung *et al.*, 1990), was strengthened when receptors purified using antagonist affinity chromatography were found to be uncoupled from their G proteins (Nakata, 1990). In contrast, Reddington *et al.*, (1989) found that antagonists can bind to both coupled and uncoupled receptors.

Studies on ligand-receptor-G protein interactions indicate binding reactions are strongly influenced by anions, proteins and Mg^{2+} (Gilman, 1987; Birnbaumer *et al.*, 1990; Strader *et al.*, 1994). Mg^{2+} is known to increase agonist binding at many receptors including, adrenergic (α_1, α_2 and β), dopamine and muscarinic receptors (Parkinson & Fredholm, 1992). Ligand binding studies indicate that Mg^{2+} influences both agonist and antagonist binding at A_1 and A_{2a} receptors (Goodman *et al.*, 1982; Olah & Stiles, 1990; Johansson *et al.*, 1992; Mazzoni *et al.*, 1993). As with guanine nucleotides, there are contrasting results with Mg^{2+} reported to increase (Johansson *et al.*, 1992; Mazzoni *et al.*, 1993) and decrease (Fastbom & Fredholm, 1990;

Parkinson & Fredholm, 1992) agonist binding at adenosine receptors.

The contrasting effects seen for guanine nucleotides and Mg^{2+} at A_1 and A_{2a} receptors requires further clarification. We examined the influence of the stable GTP analogue, Gpp(NH)p, which is not subject to Mg^{2+} sensitive hydrolysis (Johansson *et al.*, 1992) and $MgCl_2$ on [^{3}H]DPCPX and [^{3}H]CGS21680 binding. When these studies were conducted, the A_{2a} receptor antagonists, [^{3}H]SCH58261 (Zocchi *et al.*, 1996) and [^{3}H]KF17837S (Nonaka *et al.*, 1994), were not available to compare with [^{3}H]DPCPX. The use of [^{3}H]CCPA (Klotz *et al.*, 1989), a high affinity selective A_1 agonist radioligand, allowed us to directly compare and contrast the effects of Gpp(NH)p and $MgCl_2$ on antagonist and agonist binding at the A_1 receptor and agonist binding at both A_1 and A_{2a} receptors.

2.2. Methods and Materials

2.2.1. Membrane Preparation

P_2 synaptosomal membranes were prepared from rat cortical and striatal tissue as described in Chapter 1 (see 1.2.1.1.), for use in the following radioligand binding assays.

2.2.2. [^{3}H]DPCPX and [^{3}H]CGS21680 Binding Assays

[^{3}H]DPCPX and [^{3}H]CGS21680 binding assays were carried out as described in Chapter 1 (see 1.2.3.1. & 1.2.3.3.) and [^{3}H]CCPA binding as described below. Addition of Gpp(NH)p, Mg^{2+} or Na^{+} ions to the binding assays was accommodated by altering the volume of Tris-buffer without changing total assay volume.

2.2.3. [^{3}H]CCPA Binding Assay

[^{3}H]CCPA ([^{3}H]2-chloro-N^6-cyclopentyladenosine) (30 Ci $mmol^{-1}$; NEN) binding was carried out under equilibrium conditions by preincubating 10 μl of DMSO or test drug, 290 μl of Tris-buffer and 100 μl of ADA (1u ml^{-1}) with 100 μl of 2 nM [^{3}H]CCPA for 2 min at 25°C. Test drugs were diluted in DMSO to give 10 duplicate or 20 single concentrations. Total binding was determined in the presence of 1% DMSO and 10 μM R-PIA was used to determine non-specific binding. Addition of P_2 rat cortical membrane suspension (500 μl; 20-40 μg), which gave a final volume of 1 ml, initiated a 120 min incubation at 25°C. Bound and free ligand were separated using a Brandel cell harvester and this was followed by three washes (3 ml) in ice cold Tris-buffer over GF/B filters. Filter disks were then transferred to scintillation vials and the procedure followed as described for [^{3}H]DPCPX binding.

2.2.4. [^{3}H]CCPA Microcentrifugation Assay

[^{3}H]CCPA (30 Ci mmol^{-1}; NEN) binding was carried out under equilibrium conditions in microcentrifuge tubes, by preincubating 5 μl of DMSO or test drug, 95 μl of Tris-buffer and 50 μl of ADA (1u ml^{-1}) with 50 μl of 2 nM [^{3}H]CCPA for 2 min at 25°C. Test drugs were diluted in DMSO to give 14 single concentrations. Total binding was determined in the presence of 1% DMSO and 10 μM R-PIA was used to determine non-specific binding. Addition of P_2 rat cortical membrane suspension (300 μl; 80-100 μg), which gave a final volume of 0.5 ml, initiated a 120 min incubation at 25°C. Incubation was terminated by centrifugation at 15000 g for 2 min at 4°C in a Beckman microcentrifuge. Tubes were immediately put on ice and the clear supernatant removed under vacuum, using a fine tipped pasteur pipette. The insides of the tubes were carefully swabbed with a cotton bud, to remove residual radioactivity and wiped before transfer to scintillation vials. Pellets were digested by addition of 100% formic acid (100 μl) for 30 min and radioactivity determined as described for [^{3}H]DPCPX binding.

2.2.5. Data Analysis

Standard inhibition curves were constructed as in Chapter 1 (see 1.2.2.1.), for all radioligand binding experiments with [^{3}H]DPCPX, [^{3}H]CGS21680 and [^{3}H]CCPA. The appropriate pharmacological parameters were determined using the equations described in Chapter 1 (see 1.2.4.) and an iterative curve fitting programme (Sigma plot).

2.2.6. Statistical Analysis

Although the majority of figures displayed are a representation of one experiment, all experiments have been carried out at least three times, unless

otherwise stated. Data in tables and text are shown as mean ± the standard error (S.E.M.), for values obtained for at least three different experiments. Statistical tests used were the Students t-test, a Dunnett's test and a one-way analysis of variance (ANOVA).

2.2.7. Materials

Radioligands were purchased from New England Nuclear (NEN) and adenosine deaminase (Type VIII) from Sigma. Standard adenosine agonists and antagonists were purchased from Research Biochemicals Inc. (RBI). All FR compounds were synthesised by the Fujisawa Pharmaceutical Co. Ltd. All other standard laboratory chemicals were from Sigma, Fisons and BDH and were of the highest grade available.

2.3. Results

2.3.1. [^{3}H]DPCPX Binding to Rat Cerebral Cortical Membranes

2.3.1.1. Concentration Dependent Effect of $MgCl_2$ & Gpp(NH)p on [^{3}H]DPCPX Binding to Rat Cerebral Cortical Membranes

$MgCl_2$ produced a significant concentration dependent decrease in [^{3}H]DPCPX binding, with a maximal reduction of 44% at 10 mM $MgCl_2$ (Figure 2.2a). Gpp(NH)p produced a small but significant concentration dependent increase in [^{3}H]DPCPX binding, plateauing at concentrations above 3 μM (Figure 2.2b). Further studies to determine the effects on the affinity of adenosine receptor antagonists and agonists were carried out, in the absence or presence of 10 mM $MgCl_2$ or 10 μM Gpp(NH)p.

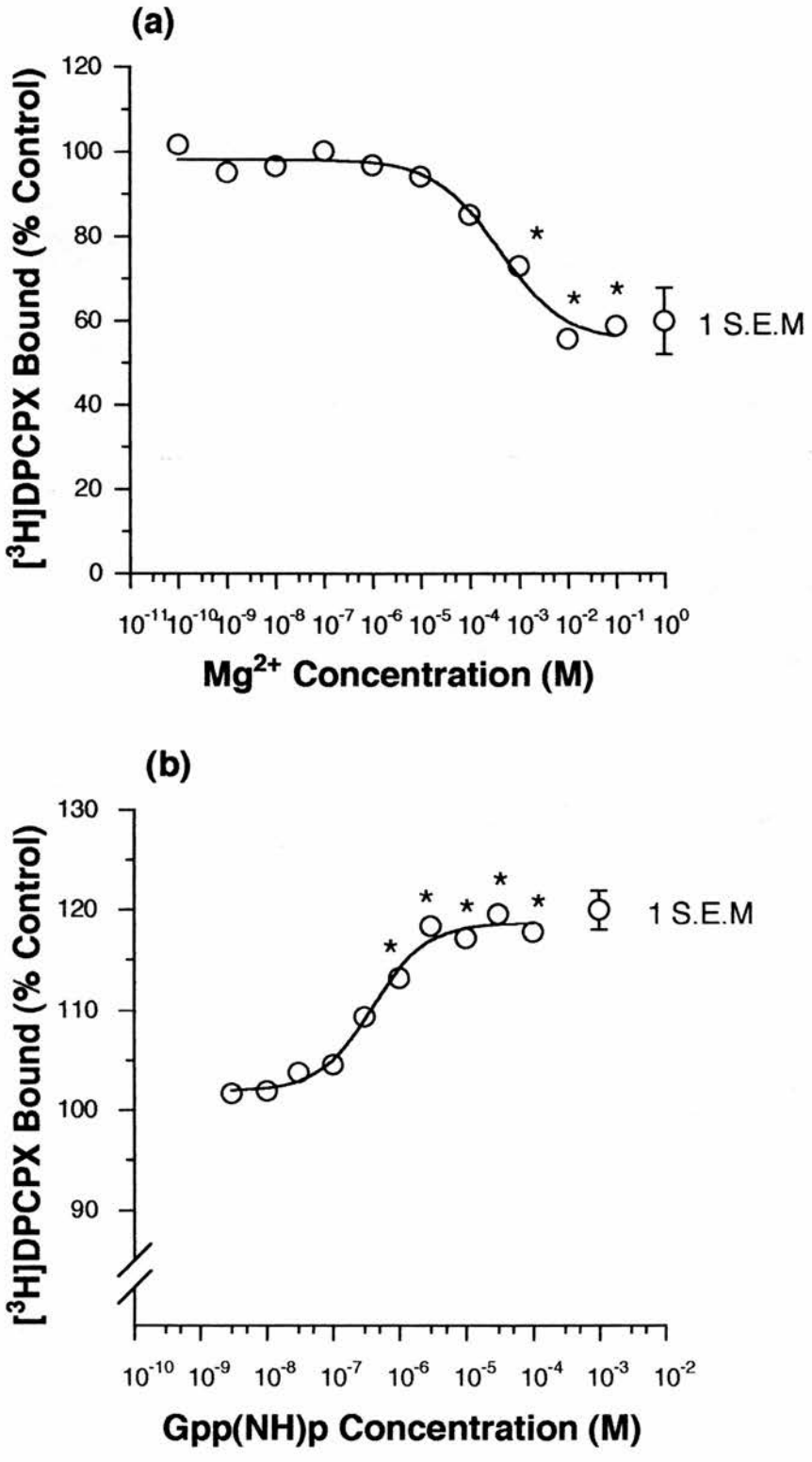

Figure 2.2 Concentration Dependence of (a) Mg^{2+} and (b) Gpp(NH)p on [^{3}H]DPCPX Binding.

The data are the mean of three experiments. The statistical comparisons were made using a one way anova followed by a Dunnett's test between control and each dose. *: $P < 0.05$.

2.3.1.2. Effect of $MgCl_2$ and Gpp(NH)p on the K_D and B_{max} of [^{3}H]DPCPX Binding Sites

Parallel binding studies using 0.1 nM [^{3}H]DPCPX and increasing concentrations of unlabelled DPCPX gave a K_D of 0.35 ± 0.04 nM (nH=0.91 ± 0.08) and a B_{max} of 2.00 ± 0.22 pmol mg^{-1} protein (n=9) in the absence of $MgCl_2$ and a K_D of 0.42 ± 0.05 nM (nH=0.91 ± 0.09) and a B_{max} of 1.28 ± 0.19 pmol mg^{-1} protein (significantly different, $P < 0.05$, in a t-test) in the presence of 10 mM $MgCl_2$.

Parallel binding studies gave a K_D of 0.25 ± 0.01 nM (nH=0.98 ± 0.03) and a B_{max} of 1.17 ± 0.07 pmol mg^{-1} protein (n=15) in the absence of Gpp(NH)p and a K_D of 0.26 ± 0.02 nM (nH=0.99 ± 0.03) and a B_{max} of 1.47 ± 0.12 pmol mg^{-1} protein (significantly different, $P < 0.05$, in a t-test) in the presence of 10 μM Gpp(NH)p.

2.3.1.3. Effect of $MgCl_2$ and Gpp(NH)p on Adenosine Antagonist and Agonist Receptor Pharmacology

The pharmacological profile of [^{3}H]DPCPX binding sites was examined in the absence and presence of 10 mM $MgCl_2$. Figure 2.3 shows inhibition of [^{3}H]DPCPX binding by DPCPX and CCPA in the absence and presence of 10 mM $MgCl_2$. Both antagonists and agonists exhibited the typical adenosine A_1 pharmacological profile for [^{3}H]DPCPX binding in the absence and presence of 10 mM $MgCl_2$. For antagonists the rank order of potency was: DPCPX > CGS15943 > CPT > DPX > 8-PT and for agonists was: CCPA = CPA ≥ R-PIA > CHA > NECA = CADO > CGS21680, with K_i values shown in Table 2.1. Antagonist affinity was not significantly different in the presence of $MgCl_2$. Hill slopes were close to unity for all antagonists under both conditions. Agonists

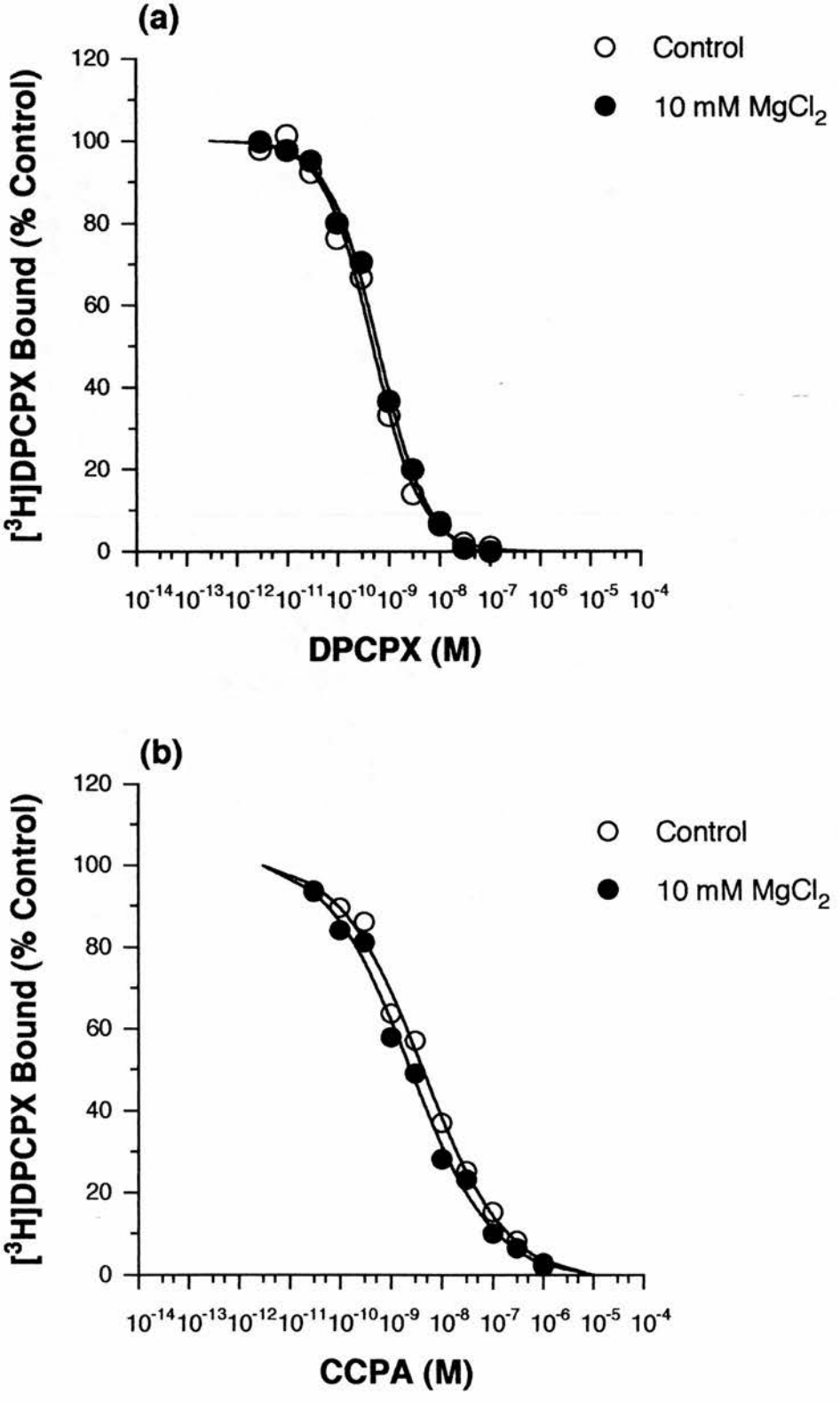

Figure 2.3 The Effect of Mg^{2+} on the Inhibition of [^{3}H]DPCPX Binding by (a) DPCPX and (b) CCPA.

The data represent a typical experiment, each point performed in duplicate with mean data obtained from at least three experiments (Table 2.1).

Table 2.1 The Effect of Mg^{2+} on [^{3}H]DPCPX Binding to Rat Brain Membranes

Compound	Control K_i (nM)	(nH)	+ 10 mM $MgCl_2$ K_i (nM)	(nH)	K_i ratio
Antagonists					
DPCPX	0.35 ± 0.04	0.91 ± 0.08	0.42 ± 0.05	0.91 ± 0.09	1.20
CGS15943	1.35 ± 0.24	0.98 ± 0.03	1.57 ± 0.11	1.09 ± 0.05	1.16
CPT	6.49 ± 0.87	1.01 ± 0.05	8.41 ± 0.63	1.04 ± 0.08	1.30
DPX	33.1 ± 2.01	1.05 ± 0.03	36.3 ± 2.19	1.10 ± 0.02	1.10
8-PT	45.0 ± 1.37	1.07 ± 0.03	49.3 ± 5.61	1.13 ± 0.04	1.10
Agonists					
CCPA	3.39 ± 0.40	0.65 ± 0.02	1.69 ± 0.07 *	0.64 ± 0.06	0.50
CPA	4.02 ± 0.59	0.63 ± 0.02	1.92 ± 0.32	0.65 ± 0.05	0.48
R-PIA	4.56 ± 0.28	0.59 ± 0.02	3.13 ± 0.57 *	0.65 ± 0.03	0.69
CHA	7.16 ± 1.26	0.62 ± 0.06	4.27 ± 0.56	0.67 ± 0.13	0.60
NECA	39.1 ± 7.84	0.58 ± 0.06	14.6 ± 2.51 *	0.59 ± 0.03	0.37
CADO	41.0 ± 4.51	0.60 ± 0.02	16.4 ± 3.38 *	0.58 ± 0.04	0.40
CGS21680	39000±9400	0.65 ± 0.04	2670 ± 430 *	0.56 ± 0.02	0.07

K_i values and Hill slope (nH) determined for competition assays as described in the methods. Values expressed as mean ± S.E.M. (n≥3). K_i ratio is between the K_i value with Mg^{2+} present and the control K_i. Statistical comparisons were made using a t-test between control and 10 mM $MgCl_2$ for each compound. *: $P < 0.05$.

showed a significant 2 fold increase in affinity with the exception of CGS21680 which increased more than 10 fold. Hill slopes were approximately 0.6 for all agonists under both conditions.

Binding studies using the [^{3}H]DPCPX binding assay in the absence and presence of 10 μM Gpp(NH)p were examined. Figure 2.4 shows the inhibition of [^{3}H]DPCPX binding by DPCPX and CCPA in the absence and presence of 10 μM Gpp(NH)p. Both antagonists and agonists exhibited the typical adenosine A_1 pharmacological profile for [^{3}H]DPCPX binding in the absence and presence of 10 μM Gpp(NH)p. For antagonists the rank order of potency was: DPCPX > CGS15943 > CPT > DPX > 8-PT and for agonists was: CCPA = CPA ≥ R-PIA > CHA > NECA = CADO > CGS21680, with K_i values shown in Table 2.2. Antagonist affinity was not significantly different in the presence of Gpp(NH)p. Hill slopes were close to unity for all antagonists under both conditions. Agonists showed a significant 5 fold decrease in affinity with the exception of CADO which decreased more than 10 fold. Hill slopes appeared to increase slightly in the presence of Gpp(NH)p but only attaining significance for R-PIA.

As Gpp(NH)p was supplied as a sodium salt, it was possible that the effects observed with Gpp(NH)p, were due to the presence of Na^+ ions. NaCl at concentrations up to 1 mM, did not affect [^{3}H]DPCPX (0.1 nM) binding. Addition of 10 μM NaCl had no effect on the affinity of CCPA, in a study where 10 μM Gpp(NH)p produced the expected decrease in affinity (data not shown).

The effect of 10 μM Gpp(NH)p was also tested using two Fujisawa non-xanthine antagonists to contrast with the xanthine antagonists shown in Table 2.2. FR129946 had a K_i of 1.10 ± 0.12 nM (nH=1.03 ± 0.13) in the absence and a K_i of 0.92 ± 0.17 nM (nH=1.06 ± 0.10) in the presence of 10 μM Gpp(NH)p. FR160537 had a K_i of 0.18 ± 0.00 nM (nH=1.19 ± 0.02) in the

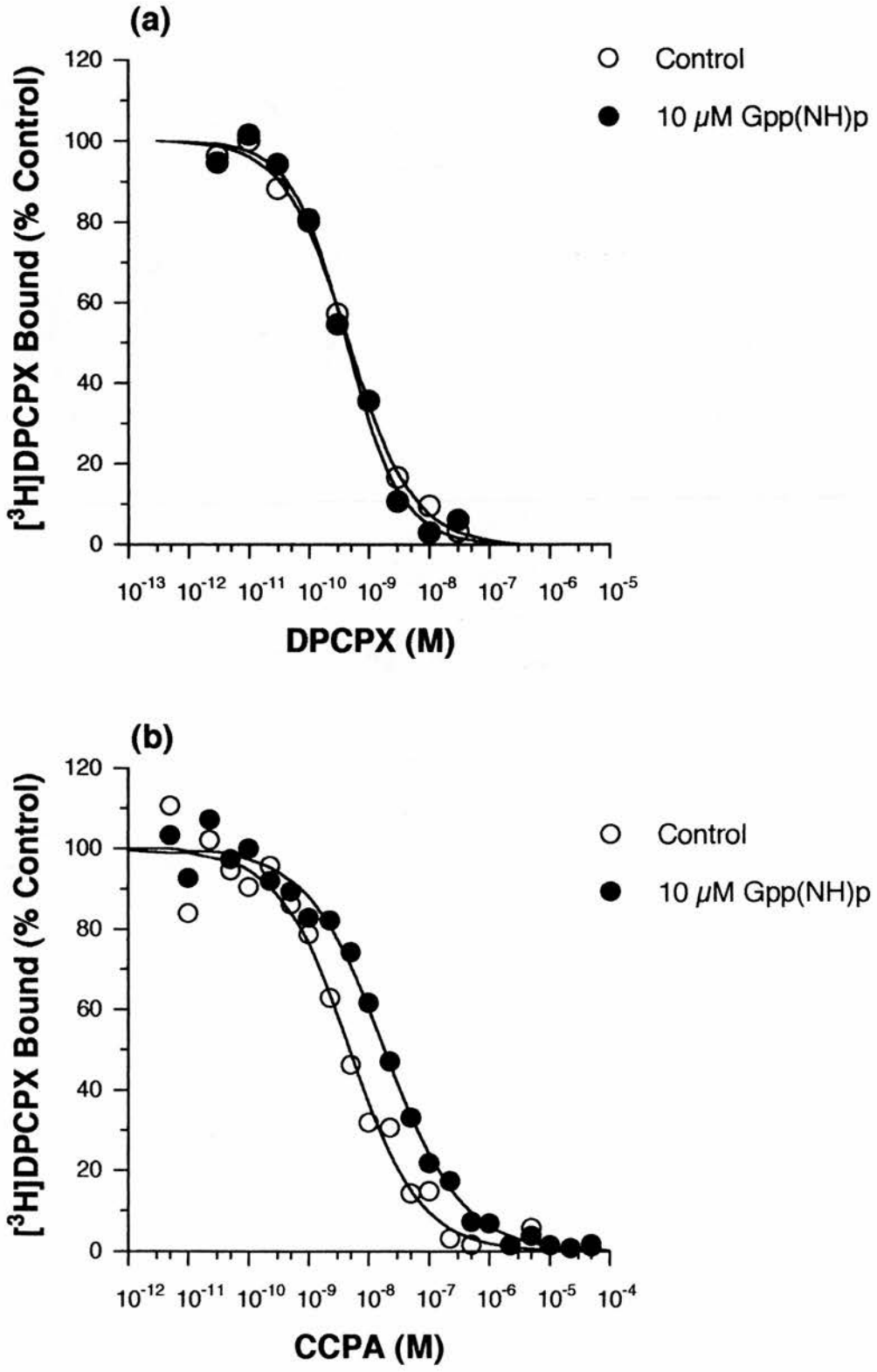

Figure 2.4 The Effect of Gpp(NH)p on the Inhibition of [^{3}H]DPCPX Binding by (a) DPCPX and (b) CCPA.
The data represent a typical experiment which was performed as described in the text. Mean data was obtained from at least three different experiments (Table 2.2).

Table 2.2 The Effect of Gpp(NH)p on [^{3}H]DPCPX Binding to Rat Brain Membranes

Compound	Control K_i (nM)	(nH)	+ 10 μM Gpp(NH)p K_i (nM)	(nH)	K_i ratio
Antagonists					
DPCPX	0.25 ± 0.01	0.98 ± 0.03	0.26 ± 0.02	0.99 ± 0.03	1.04
CGS15943	1.35 ± 0.24	0.98 ± 0.03	1.27 ± 0.06	0.99 ± 0.01	0.94
CPT	3.61 ± 0.66	0.96 ± 0.13	4.60 ± 0.29	1.05 ± 0.09	1.27
DPX	41.0 ± 4.52	1.09 ± 0.03	45.7 ± 7.11	1.12 ± 0.03	1.11
8-PT	49.3 ± 1.84	1.02 ± 0.07	44.7 ± 1.61	1.01 ± 0.08	0.91
Agonists					
CCPA	3.18 ± 0.22	0.66 ± 0.04	15.3 ± 1.07 *	0.67 ± 0.01	4.81
CPA	4.33 ± 0.68	0.61 ± 0.06	21.8 ± 2.50 *	0.71 ± 0.05	5.03
R-PIA	5.13 ± 0.35	0.59 ± 0.03	28.4 ± 3.67 *	0.70 ± 0.02 *	5.54
CHA	8.34 ± 0.66	0.62 ± 0.09	48.0 ± 3.18 *	0.72 ± 0.03	5.76
NECA	43.3 ± 13.0	0.59 ± 0.12	257 ± 30.3 *	0.67 ± 0.07	5.94
CADO	52.2 ± 2.15	0.59 ± 0.04	526 ± 71.3 *	0.76 ± 0.05	10.1
CGS21680	16650 ± 2750	0.65 ± 0.01	76000 ± 11000 *	0.74 ± 0.07	4.56

K_i values and Hill slope (nH) determined for competition assays as described in the methods. Values expressed as mean ± S.E.M. (n≥3). K_i ratio is between the K_i value with Gpp(NH)p present and the control K_i. Statistical comparisons were made using a t-test between control and 10 μM Gpp(NH)p for each compound. *: $P < 0.05$.

absence and a K_i of 0.18 ± 0.01 nM (nH=1.24 ± 0.06) in the presence of 10 μM Gpp(NH)p. Therefore the Fujisawa antagonists appeared to behave in a similar manner to xanthine antagonists with Gpp(NH)p having no significant effect on their affinity.

2.3.1.4. Effect of Gpp(NH)p on the Kinetic Parameters of [^{3}H]DPCPX Binding

For confirmation that addition of Gpp(NH)p produced no alteration in the K_D of [^{3}H]DPCPX, the kinetics of radioligand binding were studied in the absence and presence of 10 μM Gpp(NH)p. A time course of [^{3}H]DPCPX (0.1 nM) binding to rat cerebral cortex was carried out at 25°C, with equilibrium attained by 20 min (Figure 2.5a), under both conditions. Curve fitting using non linear regression gave an observed constant in the absence (K_{obs})=0.141 ± 0.017 min^{-1} (n=3) and presence (K_{obs})=0.152 ± 0.008 min^{-1} of 10 μM Gpp(NH)p, respectively.

Dissociation of [^{3}H]DPCPX binding was carried out at equilibrium (after incubation for 60 min) and initiated by the addition of 1 mM R-PIA. Dissociation followed first order kinetics (Figure 2.5b), with a dissociation rate constant in the absence (K_{-1})=0.123 ± 0.012 min^{-1} and presence (K_{-1})=0.132 ± 0.007 min^{-1} of 10 μM Gpp(NH)p, respectively. Subsequent determination gave an association rate constant in the absence of Gpp(NH)p of (K_{+1})=0.212 ± 0.051 min^{-1} M^{-1} and the resultant equilibrium dissociation constant (K_D)=0.652 ± 0.152 nM. In the presence of 10 μM Gpp(NH)p the association rate constant was (K_{+1})=0.239 ± 0.074 min^{-1} M^{-1} and the resultant equilibrium dissociation constant (K_D)=0.665 ± 0.194 nM. As with data obtained in competition studies, there was no significant difference in the K_D values on addition of Gpp(NH)p.

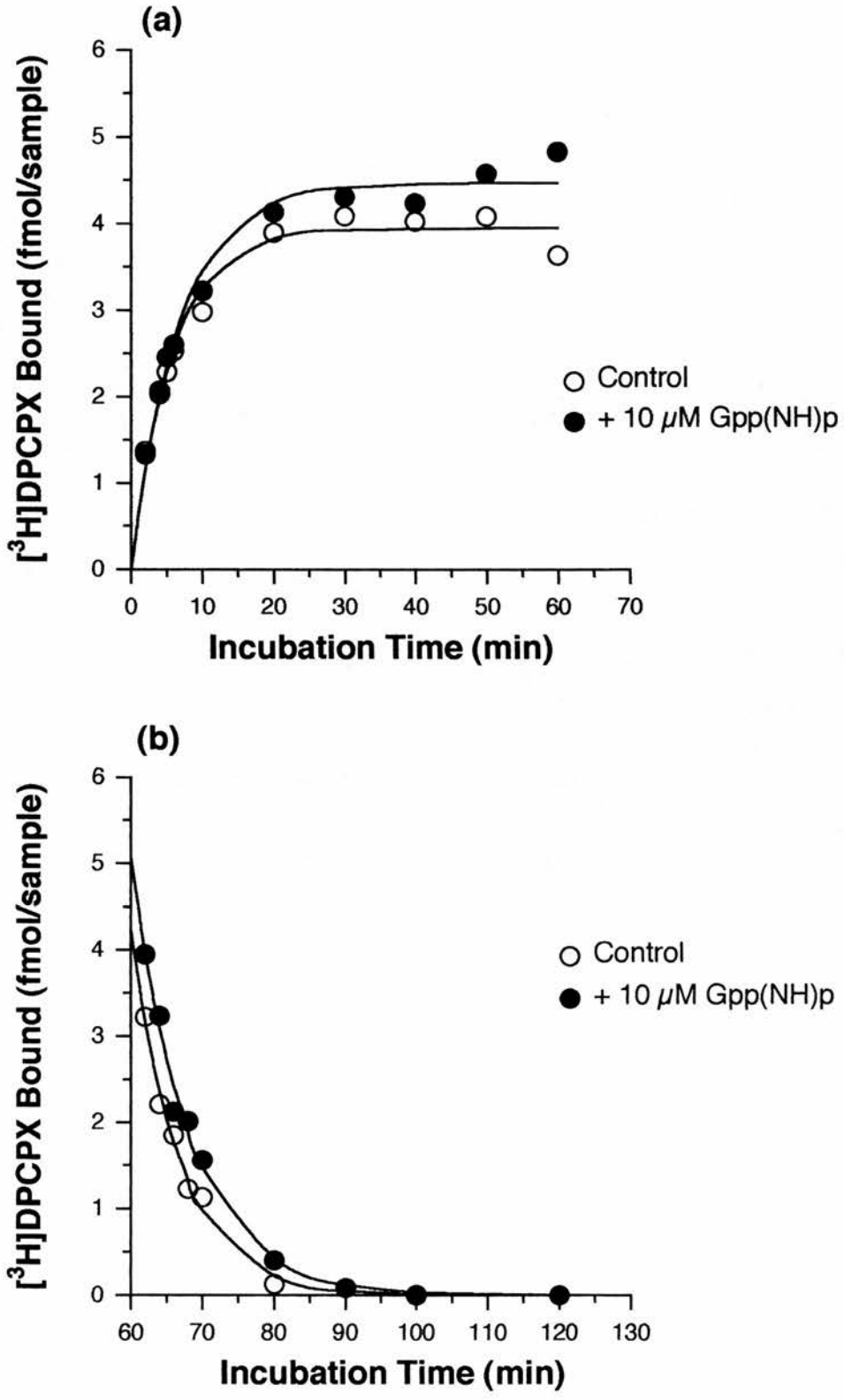

Figure 2.5 Effect of Gpp(NH)p on the (a) Association and (b) Dissociation of [^{3}H]DPCPX (0.1 nM) Binding.

The data represent a typical experiment. Dissociation initiated by adding 1 mM R-PIA after a 60 min incubation. Each point performed in duplicate with mean data obtained from three experiments (text for mean values).

2.3.1.5. Two-Site Modelling of the Effects of Gpp(NH)p and $MgCl_2$ on [^{3}H]DPCPX Binding to Rat Brain Membranes

For many GPCRs, including the adenosine A_1 receptor, high and low affinity states exist for agonist binding. The two states are supposed to reflect receptors being coupled to and uncoupled from G proteins. Shallow Hill slopes (nH~0.6) for agonist inhibition of [^{3}H]DPCPX binding may be indicative of their existence. The decrease in agonist affinity on addition of 10 μM Gpp(NH)p to the [^{3}H]DPCPX binding assay (Table 2.2) was investigated further. Increasing amounts of Gpp(NH)p (1-100 μM) were added to study the concentration dependence of the effect. The agonists CCPA and R-PIA were examined using 20 drug concentrations (3 concentrations per log cycle) to increase accuracy when trying to fit a two site model. The concentration dependent effect of Gpp(NH)p (1-100 μM) on inhibition of [^{3}H]DPCPX binding by CADO was also examined due to the large decrease in the affinity of this agonist on addition of 10 μM Gpp(NH)p (Table 2.2). For this compound, data were not examined using the two site model as only 10 duplicate concentrations were used. Table 2.3 shows the concentration dependent effect of Gpp(NH)p on the affinity of the agonists CCPA, R-PIA and CADO in the [^{3}H]DPCPX binding assay when fitted to the one site logistic model. There was a significant concentration dependent decrease in affinity in the presence of Gpp(NH)p for all three agonists. This was accompanied by a small increase in the Hill slope which attained significance for R-PIA. CADO behaved in a similar manner to CCPA and R-PIA with an approximate 5 fold decrease in affinity in the presence of 10 μM Gpp(NH)p, which is consistent with the data shown for other agonists (Table 2.2). The decrease in agonist affinity seen in rat membranes on addition of 100 μM Gpp(NH)p (Table 2.3) was similar to that for human cortical membranes with the affinity of CCPA reduced from 47.6 ± 10.9

Table 2.3 The Effect of Increasing Concentrations of Gpp(NH)p on [^{3}H]DPCPX Binding

	Gpp(NH)p	K_i (nM)	(nH)	Ratio
CCPA	Control	3.18 ± 0.22	0.66 ± 0.04	--
	1 μM	7.96 ± 1.92 *	0.66 ± 0.01	2.50
	10 μM	15.3 ± 1.07 *	0.67 ± 0.01	4.81
	100 μM	20.9 ± 1.92 *	0.71 ± 0.03	6.57
R-PIA	Control	5.13 ± 0.35	0.59 ± 0.03	--
	1 μM	14.6 ± 1.16 *	0.69 ± 0.03 *	2.85
	10 μM	28.4 ± 3.67 *	0.70 ± 0.02 *	5.54
	100 μM	43.6 ± 8.00 *	0.77 ± 0.03 *	8.50
CADO	Control	27.4 ± 2.09	0.60 ± 0.04	--
	1 μM	73.5 ± 3.30 *	0.62 ± 0.03	2.68
	10 μM	146 ± 14.3 *	0.66 ± 0.05	5.33
	100 μM	279 ± 31.2 *	0.70 ± 0.01	10.2

K_i values and Hill slope (nH) determined for competition assays as described in the methods. Data for CCPA, R-PIA and CADO were fitted to a 1 site model as described in the methods. Values expressed as mean ± S.E.M. (n≥3). Ratio shown against control K_i. Statistical comparisons were made using a t-test between control and each concentration of Gpp(NH)p for each compound. *: $P < 0.05$.

nM to 378 ± 36 nM (7.94 fold). The effect of increasing concentrations of Gpp(NH)p on [^{3}H]DPCPX binding to mouse and guinea pig cerebral cortical membranes was examined only once (data not shown). The affinity of CCPA and R-PIA in both species was reduced in a manner similar to that observed for rat.

The data for CCPA and R-PIA were fitted to a two site hyperbolic model (Figure 2.6) to determine how the addition of Gpp(NH)p resulted in a decrease in agonist affinity. The two site model provided no significant improvement ($P >$ 0.05) over the one site model when using a partial F test. The decrease in agonist affinity on addition of Gpp(NH)p was apparently due to a decrease in the proportion of the high affinity state labelled with no significant alteration in the affinity of the agonists for the high or low affinity states (Table 2.4).

Data for CCPA and R-PIA in the presence of 10 mM $MgCl_2$ were fitted to the two site hyperbolic model. The reduction in binding and greater variation in the data meant the two site model provided no significant improvement ($P >$ 0.05) over the one site model when using a partial F test. Despite this, the data indicated magnesium increased the proportion of the high affinity state labelled. For CCPA the proportion of the high affinity state labelled, increased from the control level of 65% described in Table 2.4 to 74.3 ± 4.65 (n=3), with K_i values of 0.88 ± 0.13 nM and 47.7 ± 9.69 nM for high and low affinity states respectively. For R-PIA the proportion of the high affinity state was 75.2 ± 2.18 (n=4), with K_i values of 1.81 ± 0.32 nM and 108.9 ± 24.7 nM for the high and low affinity states respectively.

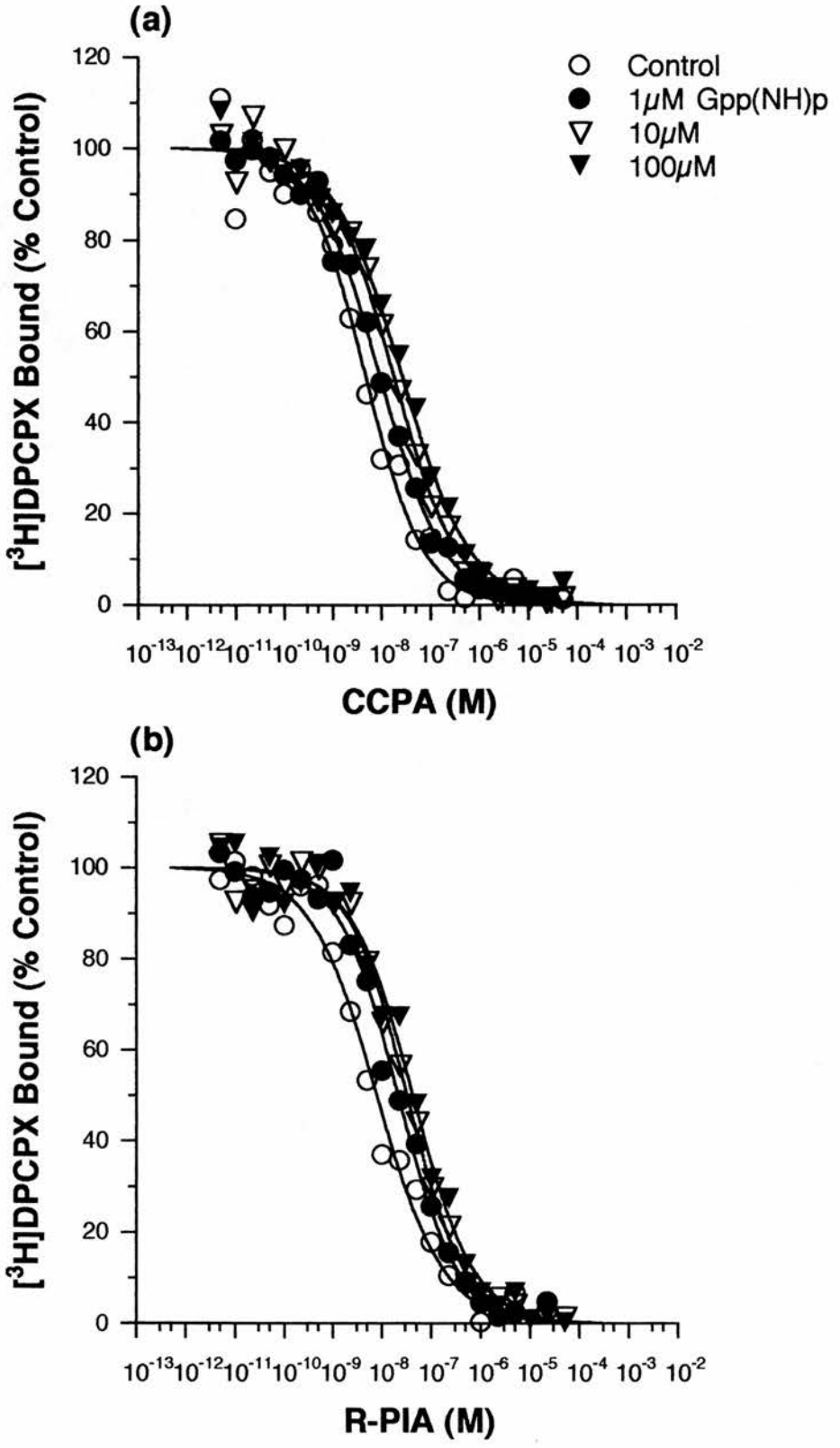

Figure 2.6 The Effect of Gpp(NH)p on the Inhibition of [^{3}H]DPCPX Binding by (a) CCPA and (b) R-PIA.

The data represent a typical experiment, with mean data obtained from three experiments (Tables 2.3 and 2.4).

Table 2.4 The Effect of Gpp(NH)p on [^{3}H]DPCPX Binding - Two Site Model

	Gpp(NH)p	b_H (fmol)	K_H (nM)	b_L (fmol)	K_L (nM)	%b_H
CCPA	Control	2.79 ± 0.22	1.20 ± 0.35	1.50 ± 0.28	31.5 ± 7.8	65.1
	1 μM	2.90 ± 0.46	2.30 ± 0.82	2.39 ± 0.67	61.4 ± 21.5	54.8
	10 μM	2.03 ± 0.33	2.02 ± 0.87	3.97 ± 0.76 *	44.4 ± 10.9	33.8
	100 μM	1.32 ± 0.15 *	1.22 ± 0.77	4.80 ± 0.41 *	39.0 ± 2.4	21.7
R-PIA	Control	2.76 ± 0.16	1.63 ± 0.48	1.45 ± 0.15	86.8 ± 28.4	65.5
	1 μM	2.93 ± 0.38	3.92 ± 0.93	2.48 ± 0.23	74.5 ± 12.0	54.2
	10 μM	2.29 ± 0.82	2.71 ± 2.09	3.40 ± 0.58 *	99.2 ± 36.0	40.2
	100 μM	1.43 ± 0.50	3.95 ± 2.05	4.25 ± 0.17 *	85.0 ± 18.2	25.3

Data for CCPA and R-PIA are fitted to a 2-site model as described in the methods. Values expressed as mean ± S.E.M. ($n \geq 3$). b_H and b_L are the total amount bound for the high and low affinity states respectively. K_H and K_L are the respective K_i values. % b_H is the percentage of total ligand bound to the high affinity state. Statistical differences between control and Gpp(NH)p treated membranes, were determined using a one way anova. *: $P < 0.05$.

2.3.2. [^{3}H]CCPA Binding to Rat Cerebral Cortical Membranes

2.3.2.1. Time Course of [^{3}H]CCPA Binding to Rat Cerebral Cortical Membranes

A time course of [^{3}H]CCPA (0.2 nM) binding to rat cerebral cortical membranes was carried out at 25°C, with equilibrium attained by 120 min (Figure 2.7). In all other experiments, [^{3}H]CCPA (0.2 nM) binding to rat cortical membranes was carried out at 25°C for 120 min, unless otherwise stated.

2.3.2.2. Concentration Dependence of [^{3}H]CCPA Binding to Rat Cerebral Cortical Membranes

Hot saturation analysis of [^{3}H]CCPA binding to rat cerebral cortical membranes was carried out once using increasing concentrations of [^{3}H]CCPA (Figure 2.8a). Curve fitting using a hyperbolic model gave an equilibrium dissociation constant (K_D) of 0.90 nM and a B_{max} of 2.35 pmol mg^{-1} protein.

Competition binding studies using 0.2 nM [^{3}H]CCPA and increasing concentrations of unlabelled CCPA (Figure 2.8b) gave a K_D of 0.47 ± 0.03 nM (nH=0.95 ± 0.03) and a B_{max} of 1.37 ± 0.14 pmol mg^{-1} protein (n=9), which is in reasonable agreement with the data obtained from the hot saturation study.

2.3.2.3. Concentration Dependent Effect of $MgCl_2$ & Gpp(NH)p on [^{3}H]CCPA Binding to Rat Cerebral Cortical Membranes

$MgCl_2$ produced a significant concentration dependent increase in [^{3}H]CCPA binding with a maximal increase of 72% at 1 mM $MgCl_2$ (Figure 2.9a). Gpp(NH)p produced a significant concentration dependent decrease in

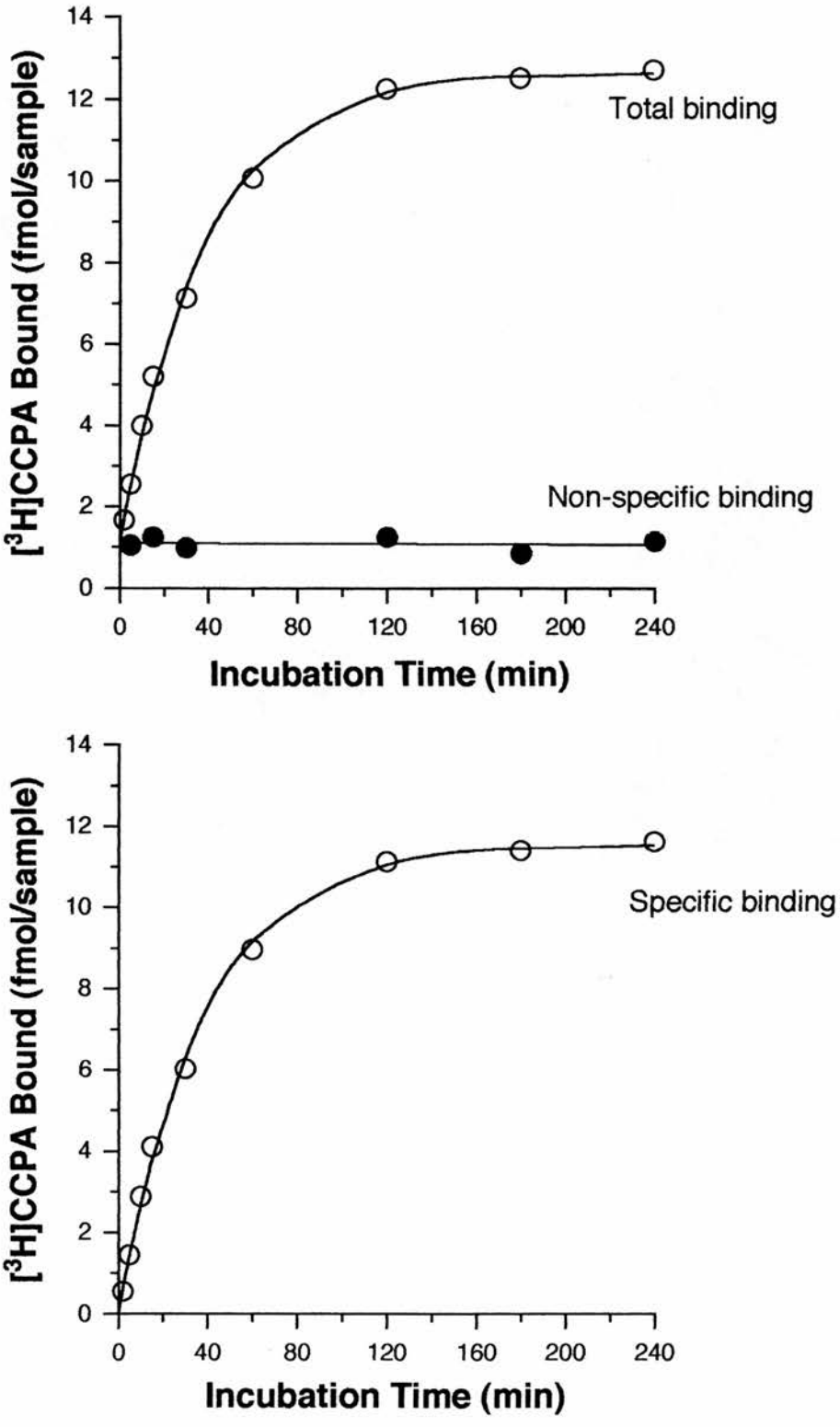

Figure 2.7 Time Course of [^{3}H]CCPA Binding to Rat Cerebral Cortical Membranes.

The data represent a typical experiment. Membranes were incubated with 0.2 nM [^{3}H]CCPA for various times at 25°C. Experiments performed as described in text with mean data obtained from three experiments.

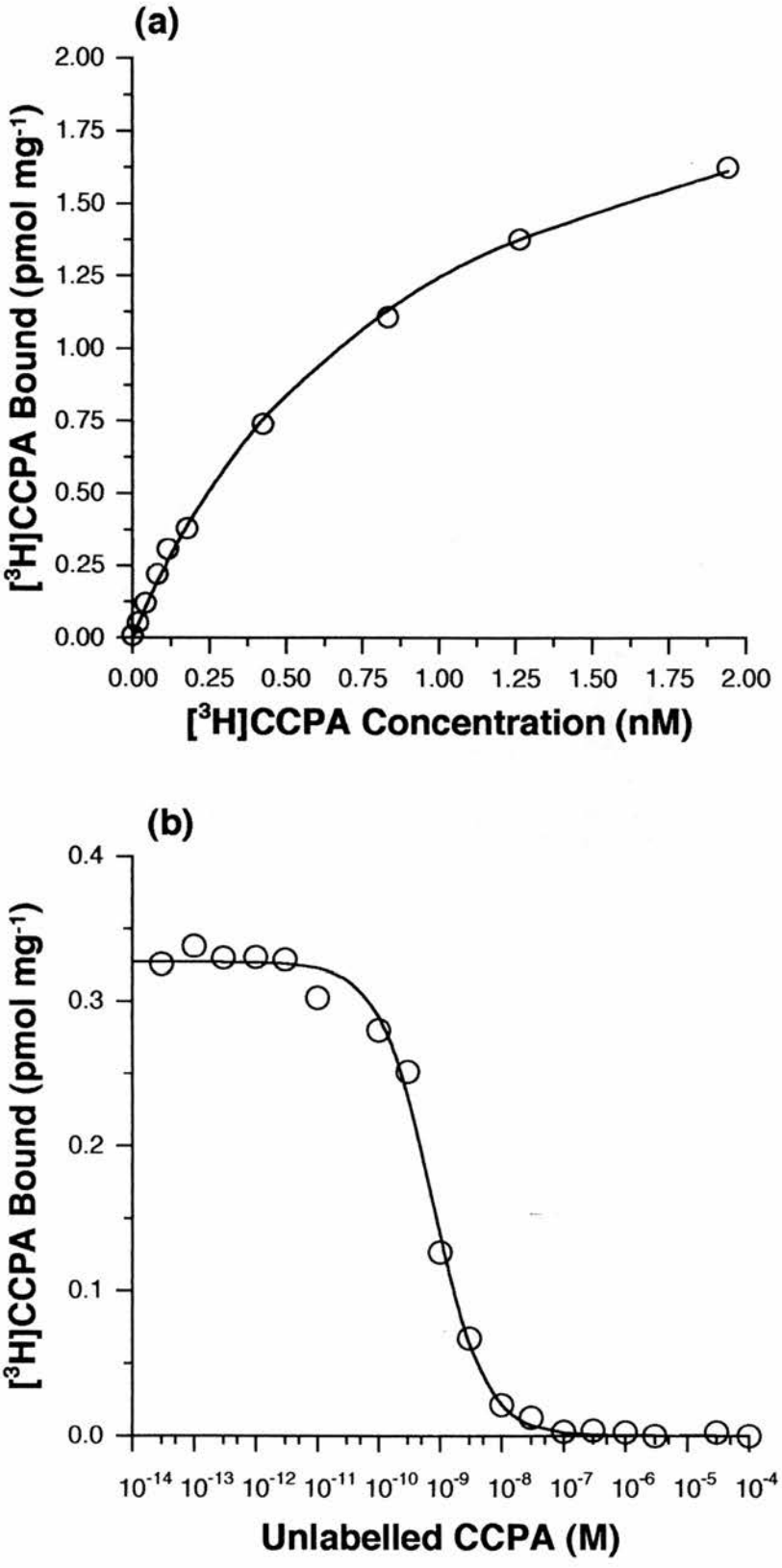

Figure 2.8 Concentration Dependence of [^{3}H]CCPA Binding to Rat Cerebral Cortical Membranes.

The results represent a single (a) hot saturation and a typical (b) cold saturation experiment. For the cold saturation experiments see text for mean values.

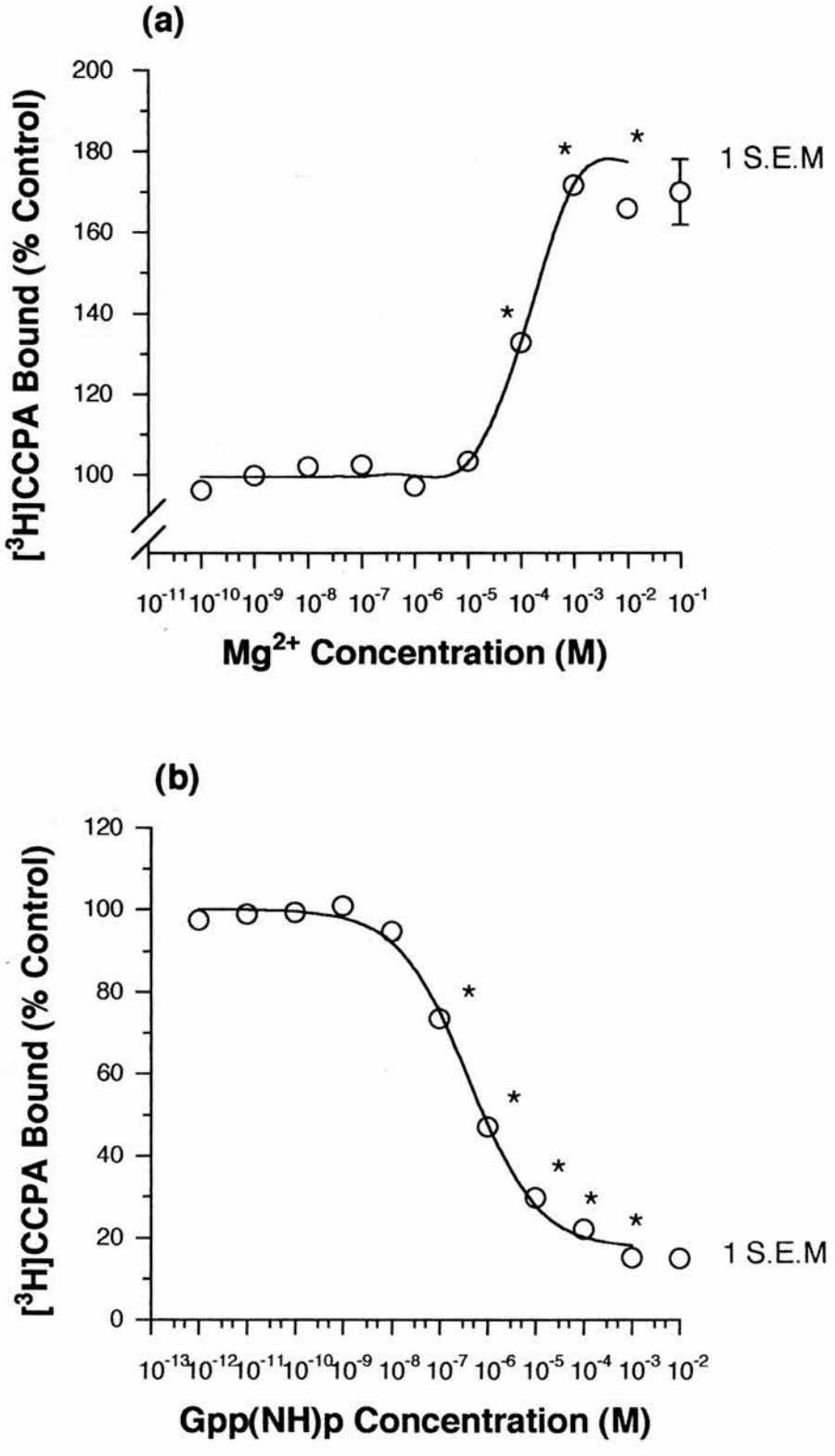

Figure 2.9 Concentration Dependence of (a) Mg^{2+} and (b) Gpp(NH)p on [^{3}H]CCPA Binding.

The data are the mean of three experiments. The statistical comparisons were made using a one way anova followed by a Dunnett's test between control and each dose. *: $P < 0.05$.

[^{3}H]CCPA binding, up to 85% at 1 mM Gpp(NH)p (Figure 2.9b). Further studies to determine the effects on the affinity of adenosine receptor antagonists and agonists were carried out in the absence or presence of 10 mM $MgCl_2$ or 10 μM Gpp(NH)p, for direct comparisons with studies using [^{3}H]DPCPX.

2.3.2.4. Effect of $MgCl_2$ and Gpp(NH)p on the K_D and B_{max} of [^{3}H]CCPA Binding Sites

Parallel binding studies using 0.2 nM [^{3}H]CCPA and increasing concentrations of unlabelled CCPA gave a K_D of 0.52 ± 0.02 nM (nH=1.03 ± 0.05) and a B_{max} of 1.21 ± 0.01 pmol mg^{-1} protein (n=3) in the absence of 10 mM $MgCl_2$ and a K_D of 0.41 ± 0.04 nM (nH=1.01 ± 0.02) (significantly different, $P < 0.05$, in a t-test) and a B_{max} of 1.42 ± 0.04 pmol mg^{-1} protein (significantly different, $P < 0.05$, in a t-test) in the presence of 10 mM $MgCl_2$.

Parallel binding studies gave a K_D of 0.41 ± 0.04 nM (nH=0.86 ± 0.03) and a B_{max} of 1.31 ± 0.36 pmol mg^{-1} protein (n=3) in the absence of 10 μM Gpp(NH)p and a K_D of 0.98 ± 0.15 nM (nH=0.80 ± 0.10) (significantly different, $P < 0.05$, in a t-test) and B_{max} of 0.66 ± 0.22 pmol mg^{-1} protein (significantly different, $P < 0.05$, in a t-test) in the presence of 10 μM Gpp(NH)p.

2.3.2.5. Effect of $MgCl_2$ and Gpp(NH)p on Adenosine Antagonist and Agonist Receptor Pharmacology

The pharmacological profile of [^{3}H]CCPA binding sites was examined in the absence and presence of 10 mM $MgCl_2$. Figure 2.10 shows inhibition of [^{3}H]CCPA binding by DPCPX and CCPA in the absence and presence of 10 mM $MgCl_2$. Both antagonists and agonists exhibited the typical adenosine A_1

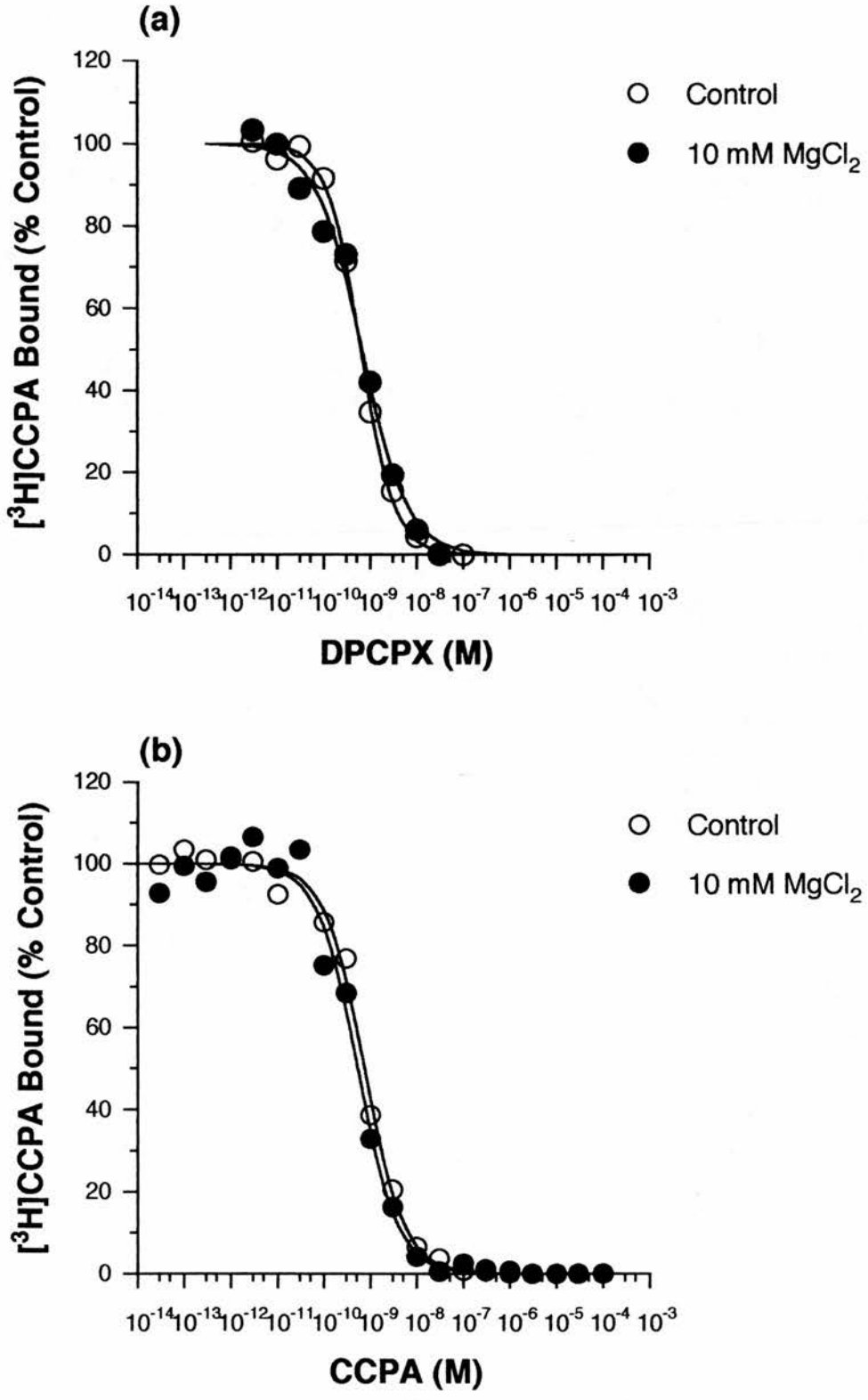

Figure 2.10 The Effect of Mg^{2+} on the Inhibition of [^{3}H]CCPA Binding by (a) DPCPX and (b) CCPA.

The data represent a typical experiment, with mean data obtained from at least three experiments (Table 2.5).

pharmacological profile for [^{3}H]CCPA binding sites, in the absence and presence of 10 mM $MgCl_2$. For antagonists the rank order of potency was: DPCPX > CGS15943 > CPT > DPX > 8-PT and for agonists was: CCPA = CPA ≥ R-PIA > CHA > NECA = CADO > CGS21680, with K_i values shown in Table 2.5. Antagonist affinity was marginally lower in the presence of $MgCl_2$, although only attaining significance for 8-PT. Hill slopes were close to unity for all antagonists under both conditions. Antagonist affinities were similar to values obtained for [^{3}H]DPCPX binding (Tables 2.1 & 2.2). Agonist affinity, despite a similar rank order of potency, was 5-17 fold higher when compared with [^{3}H]DPCPX binding (Tables 2.1 & 2.2). Hill slopes for agonists were near unity in [^{3}H]CCPA binding studies, in contrast to data from [^{3}H]DPCPX binding (nH=0.6). On addition of $MgCl_2$, agonists showed a significant 2 fold increase in affinity, with the exception of CGS21680 which increased 10 fold. Hill slopes were near unity for agonists in the presence of $MgCl_2$.

Binding studies using the [^{3}H]CCPA binding assay in the absence and presence of 10 μM Gpp(NH)p, were examined. Figure 2.11 shows inhibition of [^{3}H]CCPA binding by DPCPX and CCPA in the absence and presence of 10 μM Gpp(NH)p. Both antagonists and agonists exhibited the typical adenosine A_1 pharmacological profile for [^{3}H]CCPA binding, in the absence and presence of 10 μM Gpp(NH)p. For antagonists the rank order of potency was: DPCPX > CGS15943 > CPT > DPX > 8-PT and for agonists was: CCPA = CPA ≥ R-PIA > CHA > NECA = CADO > CGS21680, with K_i values shown in Table 2.6. Antagonist affinity was similar in the presence of Gpp(NH)p. Hill slopes were close to unity for antagonists under both conditions. Agonists showed a generally significant 2-5 fold decrease in affinity in the presence of Gpp(NH)p. The majority of Hill slopes for agonists were close to unity in [^{3}H]CCPA binding studies, in contrast to data from [^{3}H]DPCPX binding (nH=0.6).

Table 2.5 The Effect of Mg^{2+} on [^{3}H]CCPA Binding to Rat Brain Membranes

Compound	Control K_i (nM)	(nH)	+ 10 mM $MgCl_2$ K_i (nM)	(nH)	K_i ratio
Antagonists					
DPCPX	0.36 ± 0.04	0.96 ± 0.07	0.43 ± 0.11	0.95 ± 0.20	1.19
CGS15943	2.31 ± 0.31	0.98 ± 0.03	3.00 ± 0.48	0.92 ± 0.09	1.30
CPT	8.92 ± 0.90	1.02 ± 0.05	9.87 ± 1.72	0.98 ± 0.04	1.11
DPX	37.6 ± 3.52	0.93 ± 0.03	44.9 ± 4.66	0.88 ± 0.07	1.19
8-PT	64.0 ± 5.72	1.01 ± 0.04	91.1 ± 10.5 *	1.07 ± 0.09	1.42
Agonists					
CCPA	0.47 ± 0.03	1.01 ± 0.04	0.30 ± 0.06 *	0.90 ± 0.08	0.64
CPA	0.46 ± 0.10	0.92 ± 0.08	0.28 ± 0.07	0.80 ± 0.08	0.61
R-PIA	0.91 ± 0.12	0.94 ± 0.08	0.73 ± 0.18	0.86 ± 0.08	0.80
CHA	1.31 ± 0.22	0.92 ± 0.04	0.60 ± 0.08	0.91 ± 0.02	0.46
NECA	4.24 ± 0.41	0.83 ± 0.04	1.95 ± 0.14 *	0.87 ± 0.03	0.46
CADO	3.69 ± 0.40	0.86 ± 0.05	1.02 ± 0.32 *	0.82 ± 0.11	0.28
CGS21680	2300± 320	0.86 ± 0.06	220 ± 29.3 *	0.78 ± 0.01	0.10

K_i values and Hill slope (nH) determined for competition assays as described in the methods. Values expressed as mean ± S.E.M. ($n \geq 3$). K_i ratio is between the K_i value with Mg^{2+} present and the control K_i. Statistical comparisons were made using a t-test between control and 10 mM $MgCl_2$ for each compound. *: $P < 0.05$.

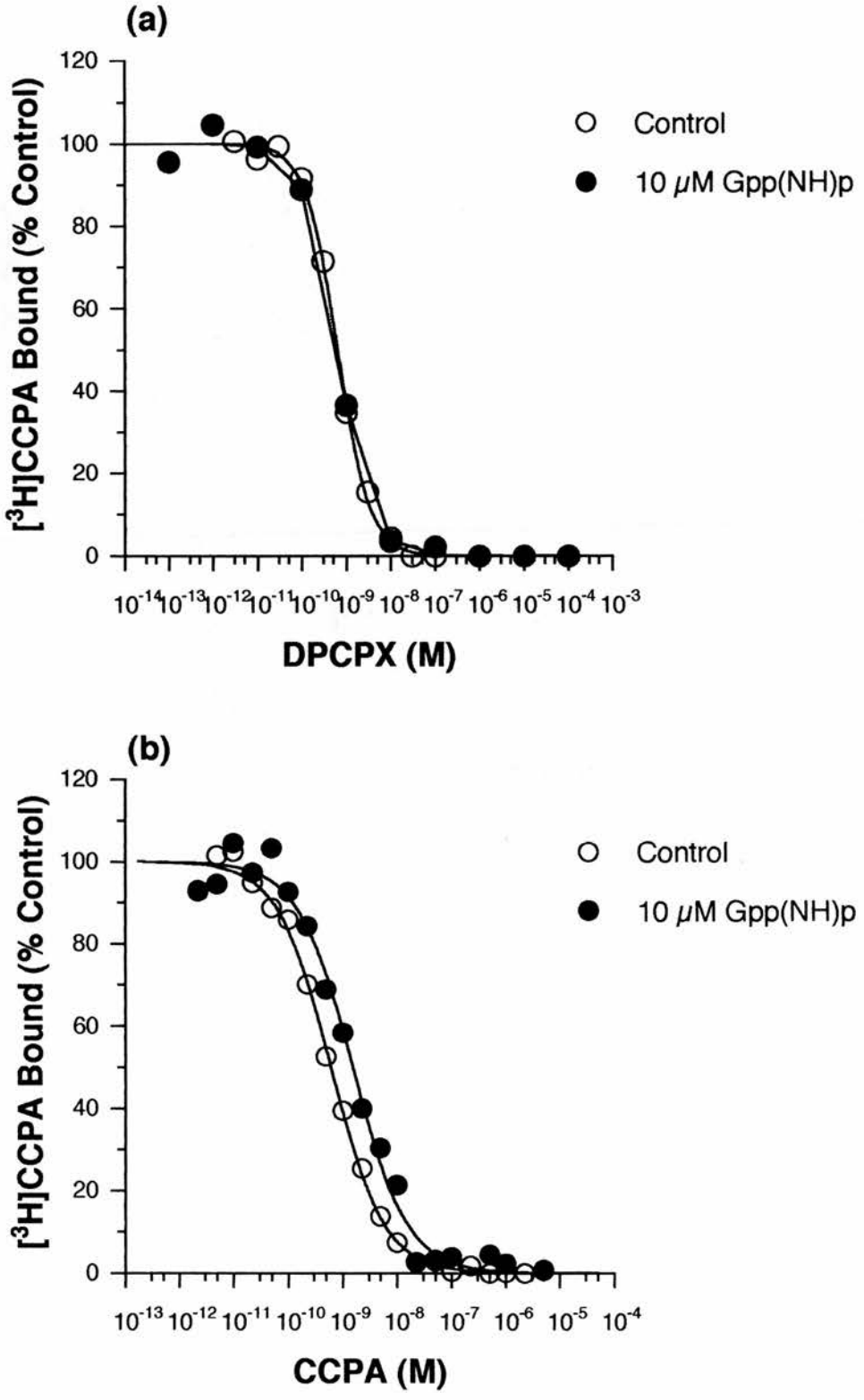

Figure 2.11 The Effect of Gpp(NH)p on the Inhibition of [^{3}H]CCPA Binding by (a) DPCPX and (b) CCPA.

The data represent a typical experiment, with mean data obtained from at least three different experiments (Table 2.6).

Table 2.6 The Effect of Gpp(NH)p on [^{3}H]CCPA Binding to Rat Brain Membranes

Compound	Control K_i (nM)	(nH)	+ 10 μM Gpp(NH)p K_i (nM)	(nH)	K_i ratio
Antagonists					
DPCPX	0.34 ± 0.07	0.94 ± 0.12	0.33 ± 0.06	1.19 ± 0.15	0.97
CGS15943	2.08 ± 0.20	0.94 ± 0.03	1.58 ± 0.05	0.84 ± 0.02 *	0.76
CPT	7.18 ± 0.89	0.96 ± 0.09	7.29 ± 2.07	0.85 ± 0.20	1.02
DPX	39.1 ± 4.81	0.92 ± 0.06	28.8 ± 1.23	1.15 ± 0.15	0.74
8-PT	60.5 ± 3.65	1.01 ± 0.11	42.7 ± 3.81*	1.23 ± 0.06	0.71
Agonists					
CCPA	0.41 ± 0.04	0.86 ± 0.03	0.98 ± 0.15	0.80 ± 0.09	2.39
CPA	0.33 ± 0.21	0.74 ± 0.15	1.17 ± 0.38	0.81 ± 0.10	3.55
R-PIA	1.10 ± 0.13	0.82 ± 0.11	4.57 ± 1.87	1.05 ± 0.22	4.15
CHA	1.07 ± 0.31	0.87 ± 0.06	3.11 ± 0.59 *	0.80 ± 0.10	2.91
NECA	4.24 ± 0.41	0.83 ± 0.04	13.9 ± 1.07 *	0.84 ± 0.08	3.28
CADO	3.69 ± 0.40	0.86 ± 0.05	17.2 ± 0.34 *	0.65 ± 0.08	4.66
CGS21680	2300± 320	0.86 ± 0.06	9330 ± 1030 *	0.78 ± 0.03	4.06

K_i values and Hill slope (nH) determined for competition assays as described in the methods. Values expressed as mean ± S.E.M. (n≥3). K_i ratio is between the K_i value with Gpp(NH)p present and the control K_i. Statistical comparisons were made using a t-test between control and 10 μM Gpp(NH)p for each compound. *: $P < 0.05$.

2.3.2.6. Two-Site Modelling of the Effects of Gpp(NH)p and $MgCl_2$ on [^{3}H]CCPA Binding to Rat Brain Membranes

The majority of Hill slopes observed for agonist inhibition of [^{3}H]CCPA binding were closer to unity than those observed in the [^{3}H]DPCPX binding assay. Under the conditions used, this may indicate that the agonist radioligand [^{3}H]CCPA predominantly labels the high affinity state rather than both the high and low affinity states labelled by [^{3}H]DPCPX. The decrease in agonist affinity on addition of 10 μM Gpp(NH)p to the [^{3}H]CCPA binding assay (Table 2.6) was investigated further. Increasing amounts of Gpp(NH)p (1-100 μM) were added to study the concentration dependence of this effect. The agonists CCPA and R-PIA were examined using 20 drug concentrations (3 concentrations per log cycle) to increase accuracy when trying to fit a two site model. With data fitted to a one site model the decrease in affinity on addition of Gpp(NH)p was not significant, with little alteration in the Hill slope (Figure 2.12; Table 2.7). This concentration dependent reduction in agonist affinity by Gpp(NH)p was more variable than that seen for [^{3}H]DPCPX binding, with no clear concentration dependence.

The data for inhibition of [^{3}H]CCPA binding by CCPA and R-PIA was fitted to a two site hyperbolic model. Under control conditions in the absence of Gpp(NH)p, this provided no significant improvement over the one site model ($P > 0.05$), when using a partial F test. Variation in the data made any interpretation of the two site data impossible. The reduction in binding in the presence of Gpp(NH)p made 2-site modelling impossible

The addition of 10 mM $MgCl_2$ and the resultant increase in [^{3}H]CCPA binding did not make it possible to fit the data for CCPA and R-PIA to the two site model. Again the two site model did not provide any significant improvement over the one site model ($P > 0.05$), when using a partial F test.

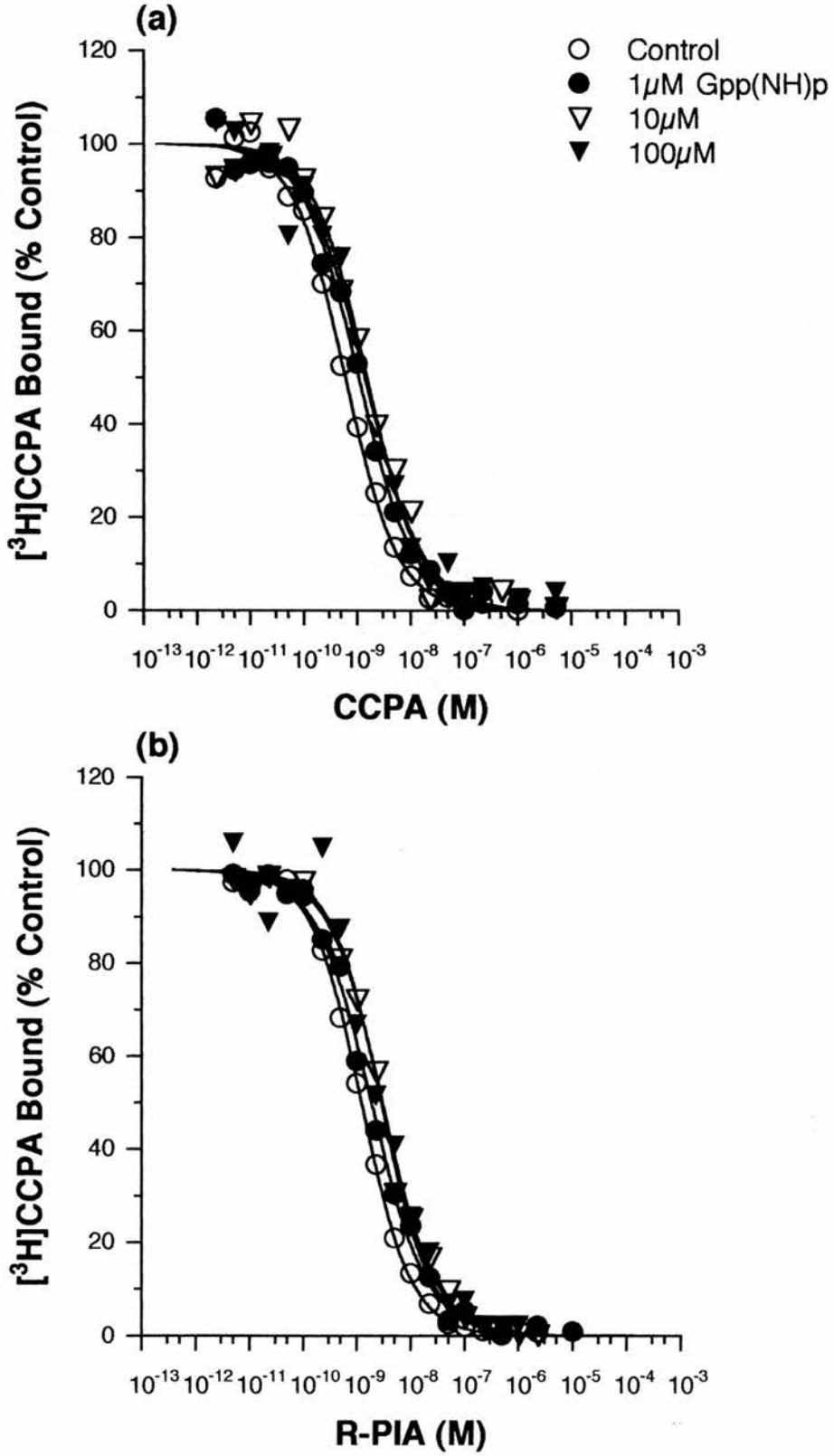

Figure 2.12 The Effect of Gpp(NH)p on the Inhibition of [^{3}H]CCPA Binding by (a) CCPA and (b) R-PIA.

The data represent a typical experiment, with mean data obtained from three experiments (Table 2.7).

Table 2.7 The Effect of Increasing Concentrations of Gpp(NH)p on [^{3}H]CCPA Binding

	Gpp(NH)p	K_i (nM)	(nH)	Ratio
CCPA	Control	0.41 ± 0.04	0.86 ± 0.03	--
	1 μM	0.64 ± 0.07	0.79 ± 0.03	1.56
	10 μM	0.98 ± 0.15	0.80 ± 0.09	2.39
	100 μM	0.80 ± 0.10	0.78 ± 0.03 *	1.95
R-PIA	Control	1.10 ± 0.13	0.82 ± 0.11	--
	1 μM	1.96 ± 0.53	0.81 ± 0.09	1.78
	10 μM	4.57 ± 1.87	1.05 ± 0.22	4.15
	100 μM	3.09 ± 0.66	0.90 ± 0.04	2.81

K_i values and Hill slope (nH) determined for competition assays as described in the methods. Data for CCPA and R-PIA are fitted to a 1 site model as described in the methods. Values expressed as the mean ± S.E.M. ($n \geq 3$). Ratio shown against control K_i. Statistical comparisons were made using a t-test between control and each concentration of Gpp(NH)p for each compound. *: $P < 0.05$.

It would appear that under the conditions used [^{3}H]CCPA predominantly labels the high affinity state of the receptor. Further data in support of this comes from competition studies using [^{3}H]CCPA and [^{3}H]DPCPX and their respective unlabelled ligands. In parallel studies the B_{max} for [^{3}H]DPCPX was 2.09 ± 0.38 pmol mg^{-1} protein (n=3) and for [^{3}H]CCPA, 1.21 ± 0.01 pmol mg^{-1} protein. The B_{max} of [^{3}H]CCPA is approximately 60% of [^{3}H]DPCPX. These data are consistent with the proportion of receptors (65%) deemed to be in the high affinity state under control conditions using [^{3}H]DPCPX (Table 2.4). The K_i value of CCPA for the high affinity state in the [^{3}H]DPCPX binding assay at approximately 1 nM (Table 2.4) is also very similar to the K_D of [^{3}H]CCPA at 0.47 nM (Section 2.3.2.2.).

2.3.2.7. [^{3}H]CCPA Microcentrifugation Assay

Inhibition of [^{3}H]DPCPX binding by CCPA gave K_i values of 1.2 and 31.5 nM, for the high and low affinity states respectively (Table 2.4). As CCPA can differentiate between both states we examined why we were unable to detect the low affinity state in the [^{3}H]CCPA binding assay, under the conditions used. A microcentrifugation assay was used which allows the separation of bound from free ligand at equilibrium, in an attempt to detect the low affinity state of the receptor-ligand complex. This method should avoid the problem of the low affinity state dissociating too rapidly to be detectable using a filtration assay.

Inhibition of [^{3}H]CCPA binding by CCPA using a microcentrifugation assay gave a K_D value of 0.84 ± 0.12 nM, (nH=0.90 ± 0.03) (n=3). Addition of 10 μM Gpp(NH)p was tested only once, with the level of [^{3}H]CCPA binding reduced by 80% and the affinity of CCPA reduced from 0.80 to 2.38 nM (2.98

fold). These data were consistent with those obtained in the filtration assay for the reduction in the level of binding (Figure 2.9) and the decrease in affinity of CCPA (Table 2.7). As with the filtration assay, the low affinity state was not detected under the conditions used.

Using the data generated for both [^{3}H]DPCPX and [^{3}H]CCPA binding assays it is possible to try and theoretically model why the low affinity state for CCPA was not measurable in the [^{3}H]CCPA binding assay. Inhibition of [^{3}H]DPCPX binding by CCPA under control conditions (Table 2.4) gave 65% of receptors in the high affinity state and 35% in the low affinity state, with respective K_i values of 1.2 and 31.5 nM. Using the following equation;

$$B_T = B_1 + B_2 = ((B_{max1} \times F) / (K_{D1} + F)) + ((B_{max2} \times F) / (K_{D2} + F))$$

where B_T is the total amount of receptors, B_1 and B_2 are the respective high and low affinity components and F is the free ligand concentration. Then at the [^{3}H]CCPA concentration used (0.2 nM) for the experiments, the amount bound to the high and low affinity states at this concentration would be;

$$= ((65\% \times 0.2) / (1.2 + 0.2)) + ((35\% \times 0.2) / (31.5 + 0.2)$$

$$= (9.29) + (0.221)$$

Therefore the relative proportion of high affinity receptors labelled at 0.2 nM [^{3}H]CCPA, would be 9.29 / (9.29 + 0.221) = 97.7%. Repeating the same calculation with [^{3}H]CCPA at ligand concentrations of 2 and 20 nM, decreases the relative proportion of high affinity receptors to 95.1% and 81.9% respectively. Detection of the low affinity state using 0.2 nM [^{3}H]CCPA would

therefore be highly unlikely.

These calculations may help explain why Gpp(NH)p has a smaller effect on agonist affinity in the [^{3}H]CCPA binding assay in comparison with the shift seen for [^{3}H]DPCPX binding. The relative proportion of low affinity receptors detectable using 0.2 nM [^{3}H]CCPA, on addition of Gpp(NH)p would remain low. As the proportion of low affinity receptors is theoretically increased to about 20% for 20 nM [^{3}H]CCPA, it might be that sensitivity to Gpp(NH)p is increased. We tested this once by comparing the effects of 10 μM Gpp(NH)p on the affinity of CCPA using [^{3}H]CCPA at 0.2 and 20 nM. Using 0.2 nM [^{3}H]CCPA, 10 μM Gpp(NH)p decreased the affinity of CCPA by 2.99 fold which is consistent with the data on Table 2.7, whereas with 20 nM [^{3}H]CCPA the decrease in affinity for CCPA was 6.84 fold.

2.3.3. [^{3}H]CGS21680 Binding to Rat Striatal Membranes

[^{3}H]CGS21680 binding is carried out in the presence of 10 mM $MgCl_2$ as described in Chapter 1 (see 1.2.3.3.), as binding is very difficult to measure in the absence of $MgCl_2$. The effects of Gpp(NH)p were therefore examined in the presence of 10 mM $MgCl_2$ unless otherwise stated. Striatal tissue is in short supply, so only seven of the eleven compounds examined previously were tested.

2.3.3.1. Concentration Dependent Effect of $MgCl_2$ & Gpp(NH)p on [^{3}H]CGS21680 Binding to Rat Striatal Membranes

$MgCl_2$ produced a significant concentration dependent increase in [^{3}H]CGS21680 binding reaching a maximum of 112% at 10 mM $MgCl_2$ (Figure 2.13a). Gpp(NH)p produced a significant concentration dependent decrease in

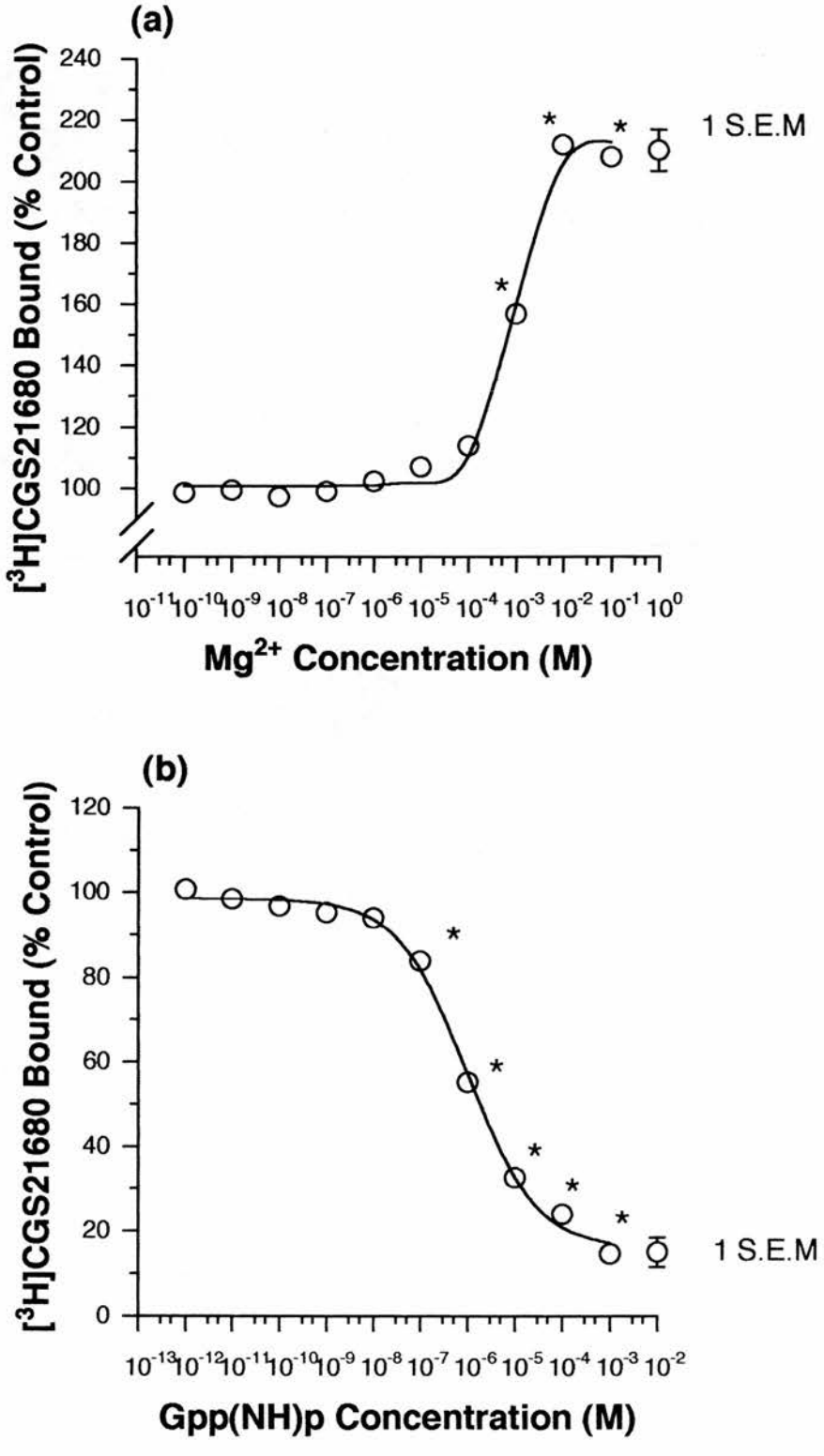

Figure 2.13 Concentration Dependence of (a) Mg^{2+} and (b) Gpp(NH)p on [^{3}H]CGS21680 Binding.

The data are the mean of three experiments. Statistical comparisons were made using a one way anova followed by a Dunnett's test between control and each dose. *: $P < 0.05$.

[^{3}H]CGS21680 binding reaching 85% at 1 mM Gpp(NH)p (Figure 2.13b). Further studies to determine the effects on the affinity of adenosine receptor antagonists and agonists were carried out as described above.

2.3.3.2. Effect of $MgCl_2$ and Gpp(NH)p on the K_D and B_{max} of [^{3}H]CGS21680 Binding Sites

Parallel binding studies using 2 nM [^{3}H]CGS21680 and increasing concentrations of unlabelled CGS21680 in the presence of 10 mM $MgCl_2$ gave a K_D of 10.8 ± 0.93 nM (nH=0.83 ± 0.05) and a B_{max} of 6.86 ± 0.08 pmol mg^{-1} protein (n=3) and in the absence of 10 mM $MgCl_2$ a K_D of 53.4 ± 8.52 nM (nH=0.77 ± 0.16) with a B_{max} of 7.13 ± 0.96 pmol mg^{-1} protein (Table 2.8).

In the same study, in the presence of both 10 mM $MgCl_2$ and 10 μM Gpp(NH)p the K_D was 34.7 ± 4.05 nM (nH=0.86 ± 0.04) with a B_{max} of 7.92 ± 0.73 pmol mg^{-1} protein (n=3). In the absence of $MgCl_2$, but in the presence of 10 μM Gpp(NH)p, the K_D was 138 ± 49.3 nM (nH=0.95 ± 0.14) with a B_{max} of 11.8 ± 3.26 pmol mg^{-1} protein (Table 2.8).

2.3.3.3. Effect of $MgCl_2$ and Gpp(NH)p on Adenosine Antagonist and Agonist Receptor Pharmacology

The pharmacological profile of [^{3}H]CGS21680 binding sites was examined in the absence and presence of 10 mM $MgCl_2$. Figure 2.14 shows inhibition of [^{3}H]CGS21680 binding by CGS15943 and CGS21680 in the absence and presence of 10 mM $MgCl_2$. Antagonists and agonists exhibited the typical adenosine A_{2a} pharmacological profile for [^{3}H]CGS21680 binding in the absence and presence of $MgCl_2$. For antagonists the rank order of potency was: CGS15943 > DPCPX and for agonists was: NECA ≥ CGS21680 > CADO

Table 2.8 Comparison of the Effects of Mg^{2+} and Gpp(NH)p on [^{3}H]CGS21680 Binding to Rat Striatal Membranes

	K_D (nM)	B_{max} (pmol mg^{-1} protein)
+ Mg^{2+} (Control)	10.8 ± 0.93	6.86 ± 0.08
- Mg^{2+}	53.4 ± 8.52*	7.13 ± 0.96
+ Mg^{2+} + Gpp	34.7 ± 4.05*	7.92 ± 0.73
- Mg^{2+} + Gpp	138 ± 49.3	11.8 ± 3.26

K_D and B_{max} values determined from competition assays as described in the methods. Data for CGS21680 fitted to a one site model as described in the methods. Values expressed as the mean ± S.E.M. ($n \geq 3$). Statistical comparisons were made using a t-test between control (+ Mg^{2+}) and each condition. *: $P < 0.05$.

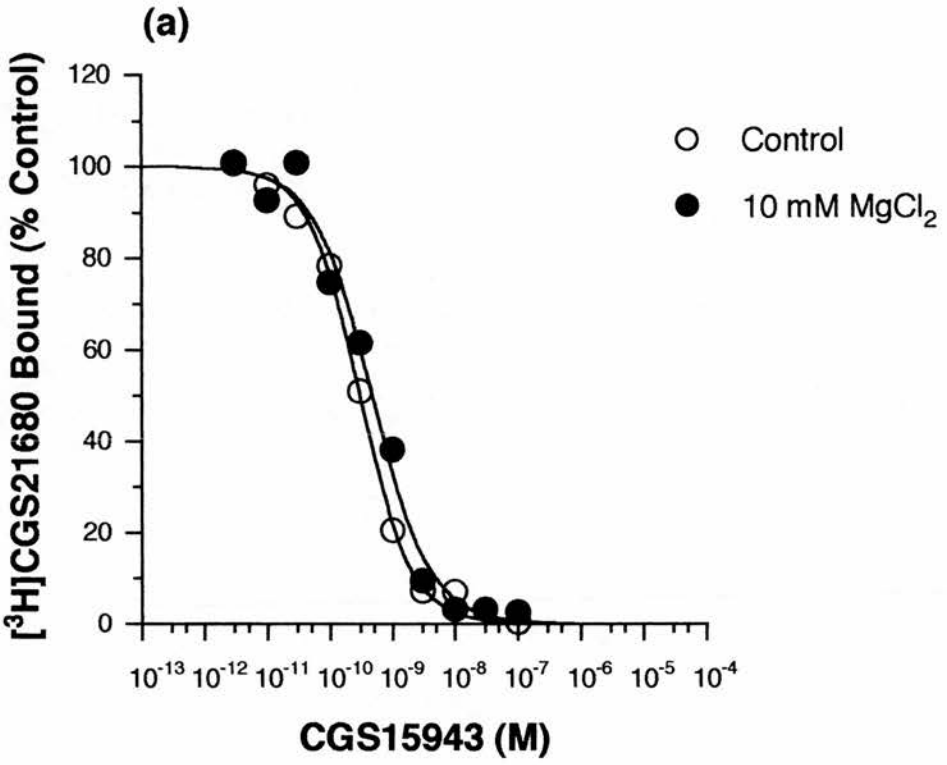

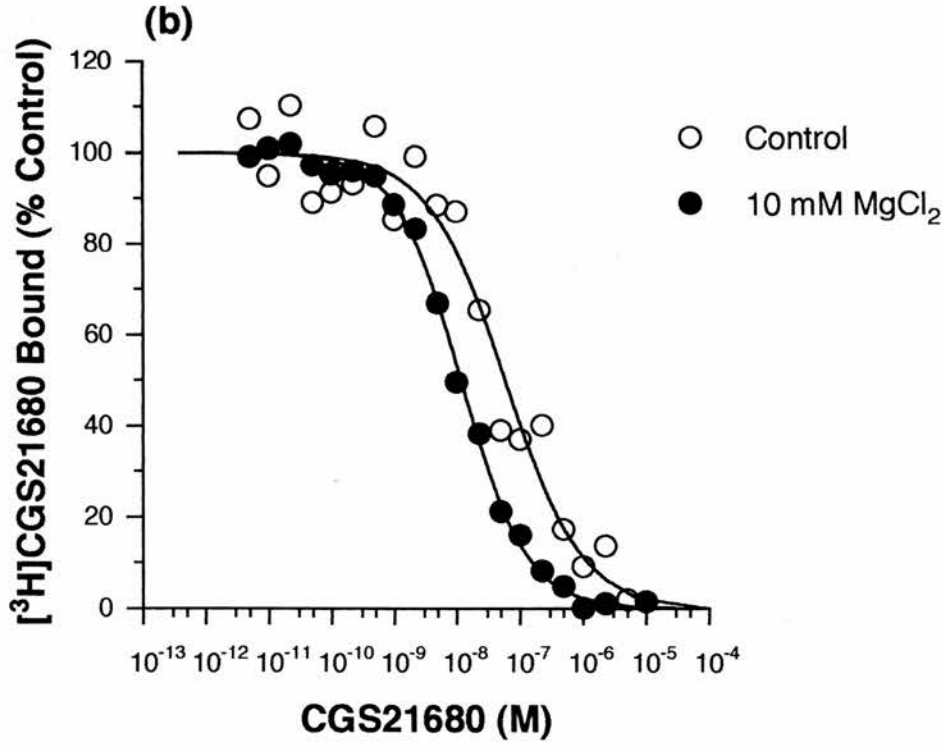

Figure 2.14 Effect of Mg^{2+} on the Inhibition of [^{3}H]CGS21680 Binding by (a) CGS15943 and (b) CGS21680.

The data represent a typical experiment, with mean data obtained from at least three different experiments (Table 2.9).

> R-PIA > CCPA, with K_i values shown in Table 2.9. CGS15943 was unaffected by the addition of $MgCl_2$ while the affinity of DPCPX decreased. Hill slopes were close to unity for antagonists under both conditions. Agonists showed a significant increase in affinity from 2 to 4.5 fold on addition of $MgCl_2$. Hill slopes were approximately 0.8 for agonists under both conditions.

Binding studies using the [^{3}H]CGS21680 binding assay (all in the presence of 10 mM $MgCl_2$) in the absence and presence of 10 μM Gpp(NH)p were examined. Figure 2.15 shows inhibition of [^{3}H]CGS21680 binding by CGS15943 and CGS21680 in the absence and presence of 10 μM Gpp(NH)p. Both antagonists and agonists exhibited the typical adenosine A_{2a} pharmacological profile for [^{3}H]CGS21680 binding sites in the absence and presence of 10 μM Gpp(NH)p. For antagonists the rank order of potency was: CGS15943 > DPCPX and for agonists was: NECA ≥ CGS21680 > CADO > R-PIA > CCPA, with K_i values shown in Table 2.10. The two antagonists had similar affinities in the absence and presence of Gpp(NH)p, with Hill slopes near unity under both conditions. Agonists showed a significant decrease in affinity from 3.2 to 8.6 fold. Hill slopes were approximately 0.8 for agonists under both conditions.

2.3.3.4. Two-Site Modelling of the Effects of Gpp(NH)p and $MgCl_2$ on [^{3}H]CGS21680 Binding to Rat Brain Membranes

Inhibition of [^{3}H]CGS21680 binding by agonists is unusual in that the Hill slope is approximately 0.8. Addition of 10 μM Gpp(NH)p (Table 2.10) decreases agonist affinity, without significant alteration in the Hill slope. To establish whether two binding components exist, CGS21680 was tested over an extended concentration range in the absence and presence of 10 mM $MgCl_2$ and 10 μM Gpp(NH)p (Figure 2.16a). Removal of $MgCl_2$ from the assay

Table 2.9 The Effect of Mg^{2+} on [^{3}H]CGS21680 Binding to Rat Striatal Membranes

	Control		+ 10 mM $MgCl_2$		
Compound	**K_i (nM)**	**(nH)**	**K_i (nM)**	**(nH)**	**K_i ratio**
Antagonists					
DPCPX	99.1 ± 11.0	0.93 ± 0.06	177 ± 9.02 *	0.94 ± 0.05	1.79
CGS15943	0.39 ± 0.08	1.19 ± 0.07	0.38 ± 0.09	0.86 ± 0.04 *	0.97
Agonists					
CCPA	670 ± 64.4	0.83 ± 0.09	331 ± 30.7 *	0.73 ± 0.02	0.49
R-PIA	232 ± 45.4	0.82 ± 0.19	91.4 ± 16.2 *	0.79 ± 0.11	0.39
NECA	16.3 ± 2.25	0.85 ± 0.09	4.92 ± 0.56 *	0.79 ± 0.05	0.30
CADO	62.2 ± 7.62	0.81 ± 0.06	28.1 ± 4.81 *	0.69 ± 0.06 *	0.45
CGS21680	43.5 ± 6.63	0.84 ± 0.08	9.64 ± 0.85 *	0.85 ± 0.04	0.22

K_i values and Hill slope (nH) determined for competition assays as described in the methods. Values expressed as mean ± S.E.M. ($n \geq 3$). K_i ratio is between the K_i value with Mg^{2+} present and the control K_i. Statistical comparisons were made using a t-test between control and 10 mM $MgCl_2$ for each compound. *: $P < 0.05$.

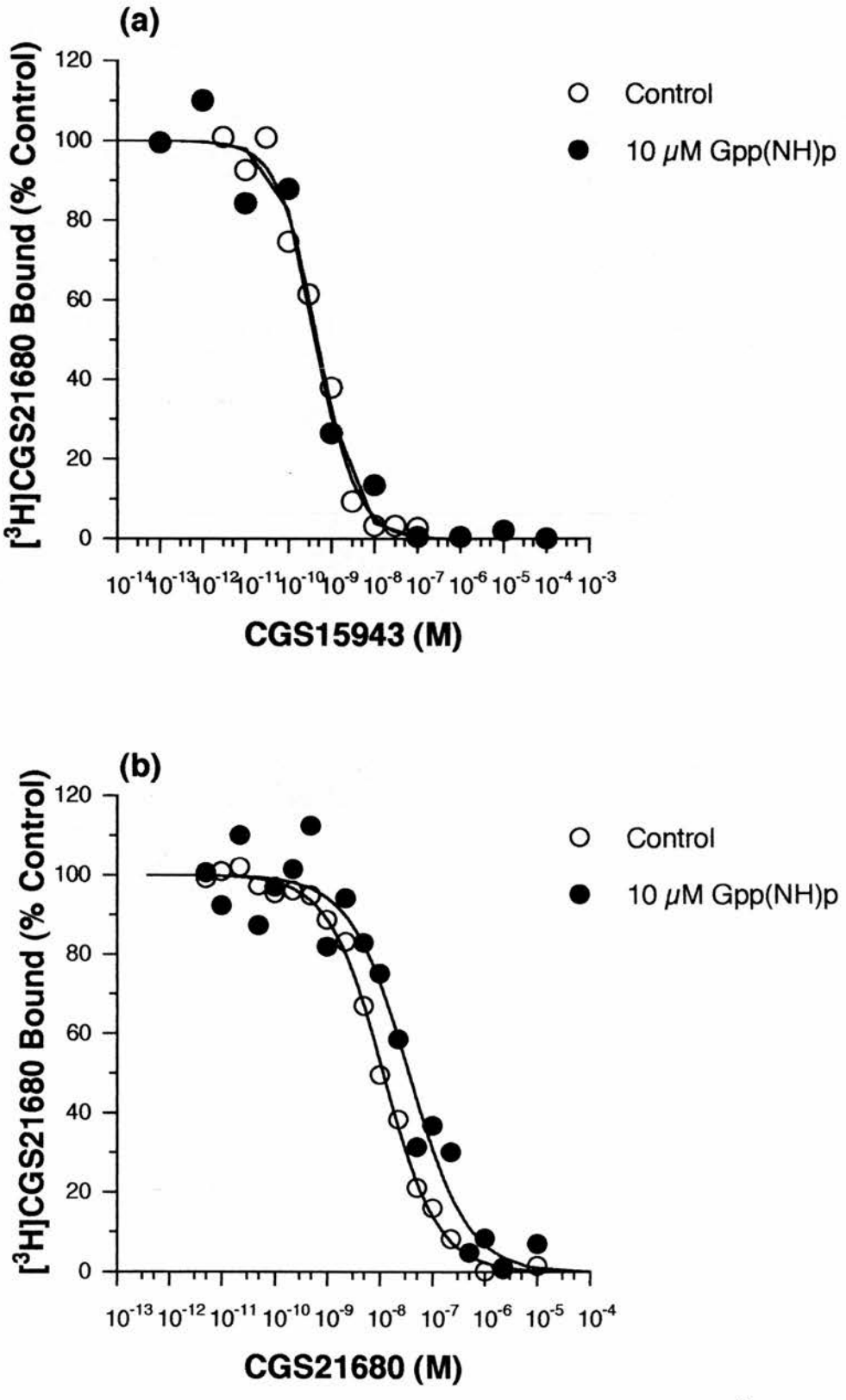

Figure 2.15 Effect of Gpp(NH)p on Inhibition of [^{3}H]CGS21680 Binding by (a) CGS15943 and (b) CGS21680.

The data represent a typical experiment, with mean data obtained from at least three different experiments (Table 2.10).

Table 2.10 The Effect of Gpp(NH)p on [^{3}H]CGS21680 Binding to Rat Striatal Membranes

	Control		+ 10 μM Gpp(NH)p		
Compound	**K_i (nM)**	**(nH)**	**K_i (nM)**	**(nH)**	**K_i ratio**
Antagonists					
DPCPX	177 ± 9.02	0.94 ± 0.05	148 ± 42.1	1.01 ± 0.08	0.84
CGS15943	0.38 ± 0.09	0.86 ± 0.04	0.36 ± 0.05	1.32 ± 0.16 *	0.95
Agonists					
CCPA	331 ± 30.7	0.73 ± 0.02	1870± 280 *	0.90 ± 0.15	5.65
R-PIA	91.4 ± 16.2	0.79 ± 0.11	723 ± 192 *	0.69 ± 0.09	7.91
NECA	6.02 ± 0.29	0.89 ± 0.06	51.6 ± 7.69 *	0.63 ± 0.10	8.57
CADO	28.1 ± 4.81	0.69 ± 0.06	234 ± 11.1 *	0.81 ± 0.12	8.33
CGS21680	10.8 ± 0.93	0.83 ± 0.05	34.7 ± 4.05 *	0.86 ± 0.04	3.21

K_i values and Hill slope (nH) determined for competition assays as described in the methods. Values expressed as mean ± S.E.M. (n≥3). [^{3}H]CGS21680 binding was carried out in the presence of 10 mM $MgCl_2$. K_i ratio is between the K_i value with Gpp(NH)p present and the control K_i. Statistical comparisons were made using a t-test between control and 10 μM Gpp(NH)p for each compound. *: $P < 0.05$.

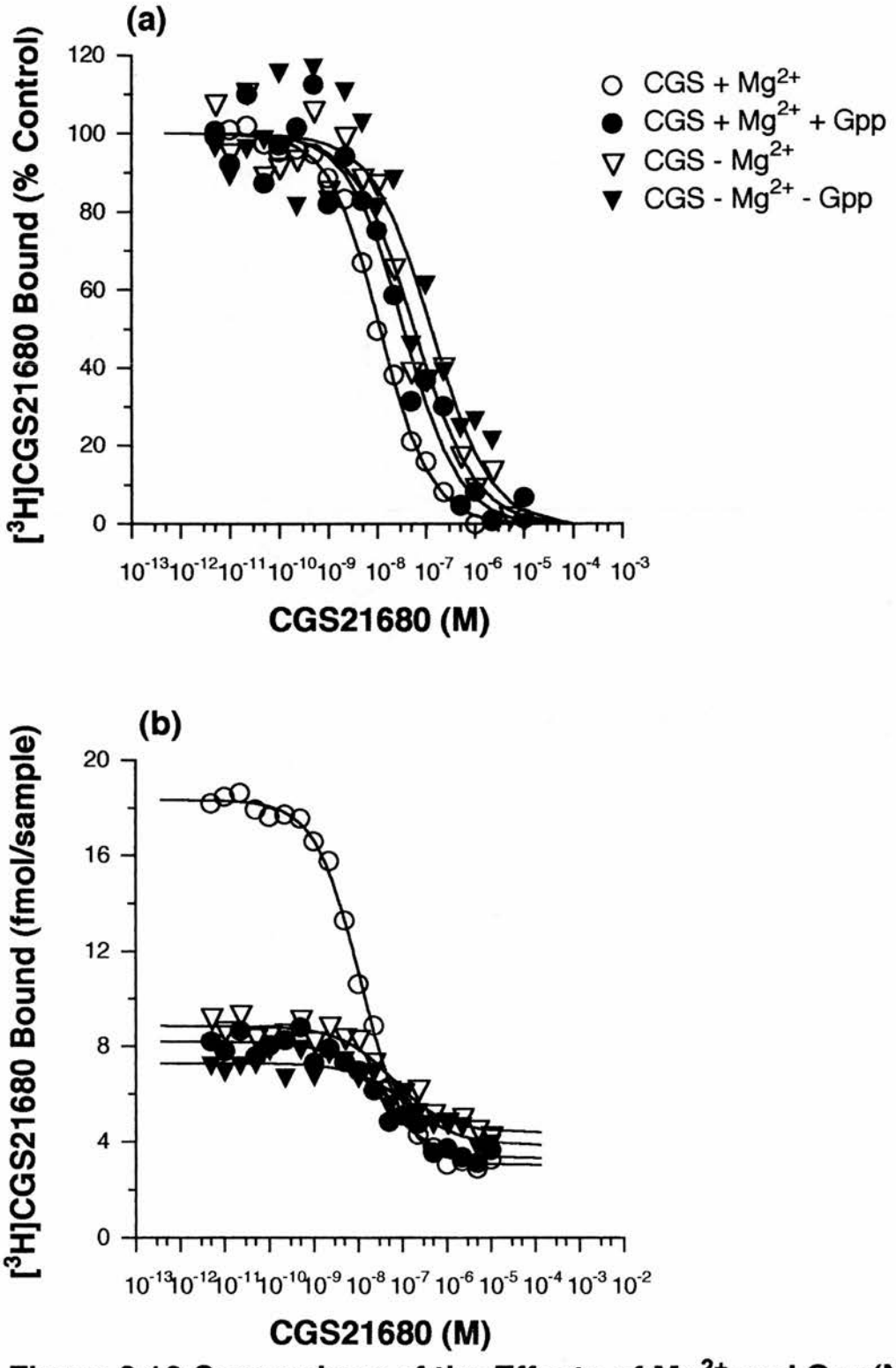

Figure 2.16 Comparison of the Effects of Mg^{2+} and Gpp(NH)p on Inhibition of [^{3}H]CGS21680 Binding by CGS21680.

The data are from the same experiment: graph (a) shows the shift in affinity and (b) shows the effect of the conditions on the level of [^{3}H]CGS21680 (0.2 nM) binding. The data represent a typical experiment, with mean data obtained from three experiments (Table 2.11).

caused a decrease in affinity of CGS21680 (Table 2.11). Gpp(NH)p caused a similar decrease in affinity for CGS21680 in the absence and presence of 10 mM $MgCl_2$ (Table 2.11). With the exception of standard conditions i.e. in the presence of 10 mM $MgCl_2$ and the absence of Gpp(NH)p, it was not possible to fit these data to the 2-site hyperbolic model due to the large reduction seen in [^{3}H]CGS21680 binding on removal of $MgCl_2$ or on addition of Gpp(NH)p (Figure 2.16b). The data indicated the proportion of high affinity receptors was 83.9 ± 2.8% (n=3) with the affinity of the high and low states equal to 7.5 ± 1.6 nM and 176 ± 132 nM, respectively. The large error in the low affinity component necessitates further experimentation to determine whether this is in fact real or an artifact of the modelling procedure.

The [^{3}H]DPCPX and [^{3}H]CCPA binding assays are routinely carried out in the absence of $MgCl_2$ unlike the [^{3}H]CGS21680 binding assay. Preliminary investigations were performed to study the effects of Gpp(NH)p in the absence of $MgCl_2$ on [^{3}H]CGS21680 binding. The concentration dependence of the effect of Gpp(NH)p on [^{3}H]CGS21680 binding in the absence of $MgCl_2$ was studied (Figure 2.17a), with the effects in the presence of $MgCl_2$ shown for comparison (Figure 2.17b). Gpp(NH)p reduced [^{3}H]CGS21680 binding in a concentration dependent manner in the absence and presence of $MgCl_2$. The larger errors in the absence of $MgCl_2$ and the resultant lack of significance, is a consequence of the 75% reduction in total binding and a reduction in specific binding from 85 to 50% of total binding.

Gpp(NH)p appeared to shift the affinity of CGS21680 to an even lower value in the absence of $MgCl_2$ (Table 2.11). The concentration dependent effect of Gpp(NH)p on agonist affinity was examined only once in the absence and presence of $MgCl_2$ for CCPA and NECA (Figures 2.18 and 2.19). As shown in Table 2.12, there appears to be a concentration dependent reduction

Table 2.11 Comparison of the Effects of Mg^{2+} and Gpp(NH)p on [^{3}H]CGS21680 Binding to Rat Striatal Membranes

	K_D (nM)	(nH)	Ratio
CGS21680			
+ Mg (Control)	10.8 ± 0.93	0.83 ± 0.05	--
+ Mg + Gpp	34.7 ± 4.05*	0.86 ± 0.04	3.21
- Mg	53.4 ± 8.52*	0.77 ± 0.16	--
- Mg + Gpp	138 ± 49.3	0.95 ± 0.14	2.58

K_D values and Hill slope (nH) determined for competition assays as described in the methods. Data for CGS21680 fitted to a one site model as described in the methods. Values expressed as the mean ± S.E.M. (n=3). Ratio shown against K_D in absence of Gpp(NH)p. Statistical comparisons were made using a t-test between control (+ Mg^{2+}) and each condition. *: $P < 0.05$.

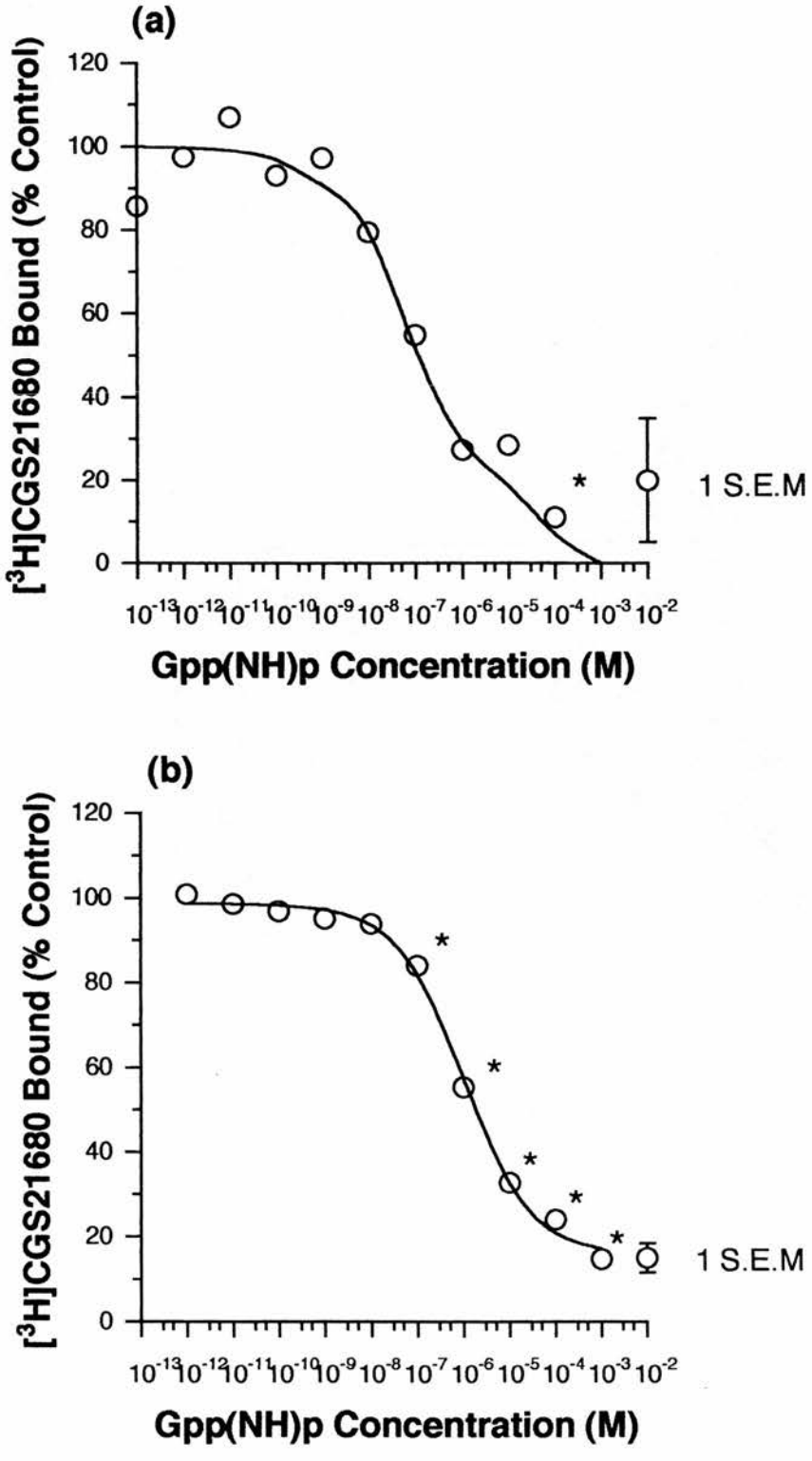

Figure 2.17 Concentration Dependence of Gpp(NH)p on [^{3}H]CGS21680 Binding in the (a) Absence and (b) Presence of 10 mM $MgCl_2$.

The data is the mean of three experiments. The statistical comparisons were made using a one way anova followed by a Dunnett's test between control and each dose. * : $P < 0.05$.

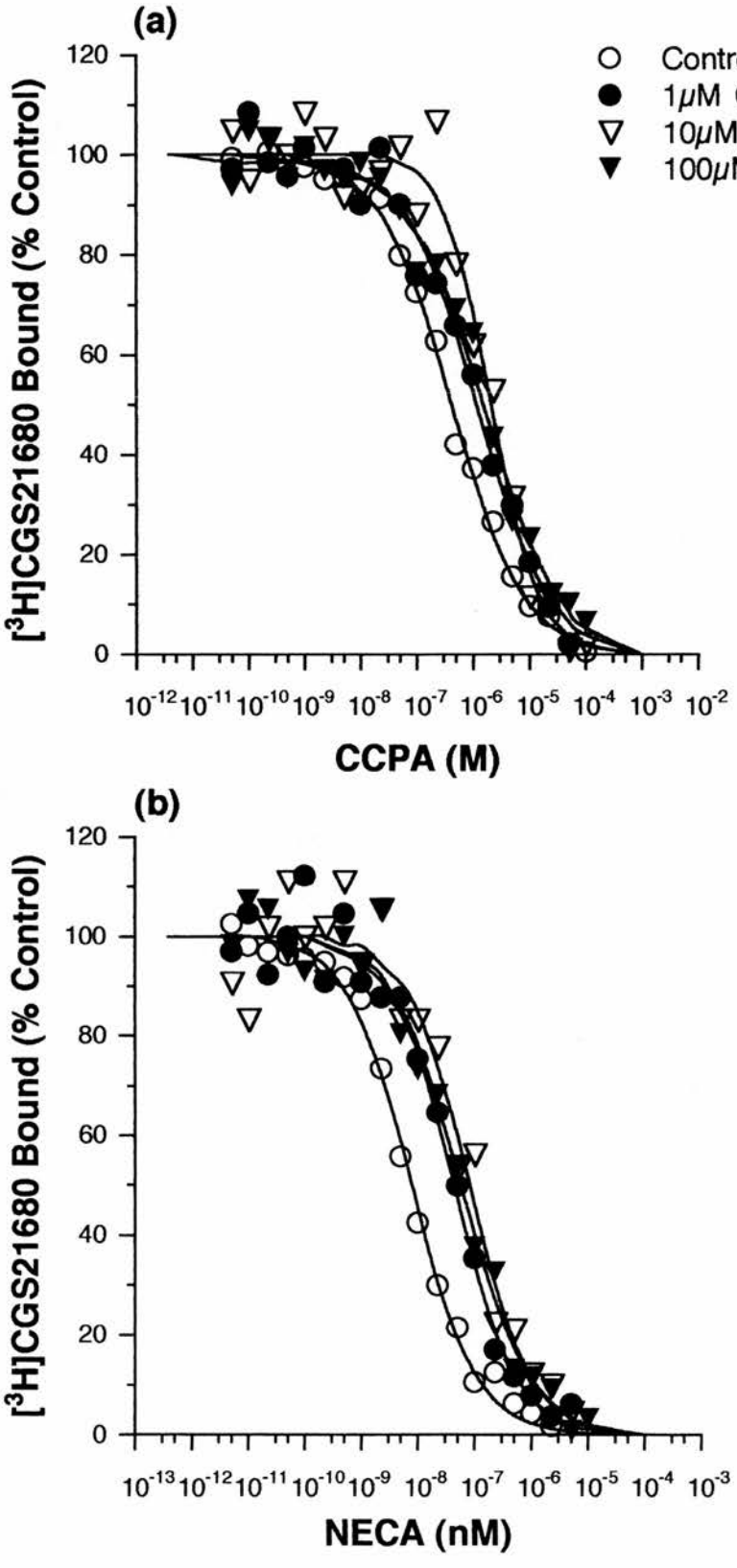

Figure 2.18 The Effect of Gpp(NH)p on the Inhibition of [^{3}H]CGS21680 Binding by (a) CCPA and (b) NECA in the Presence of $MgCl_2$.

The data represents a single experiment (Table 2.12).

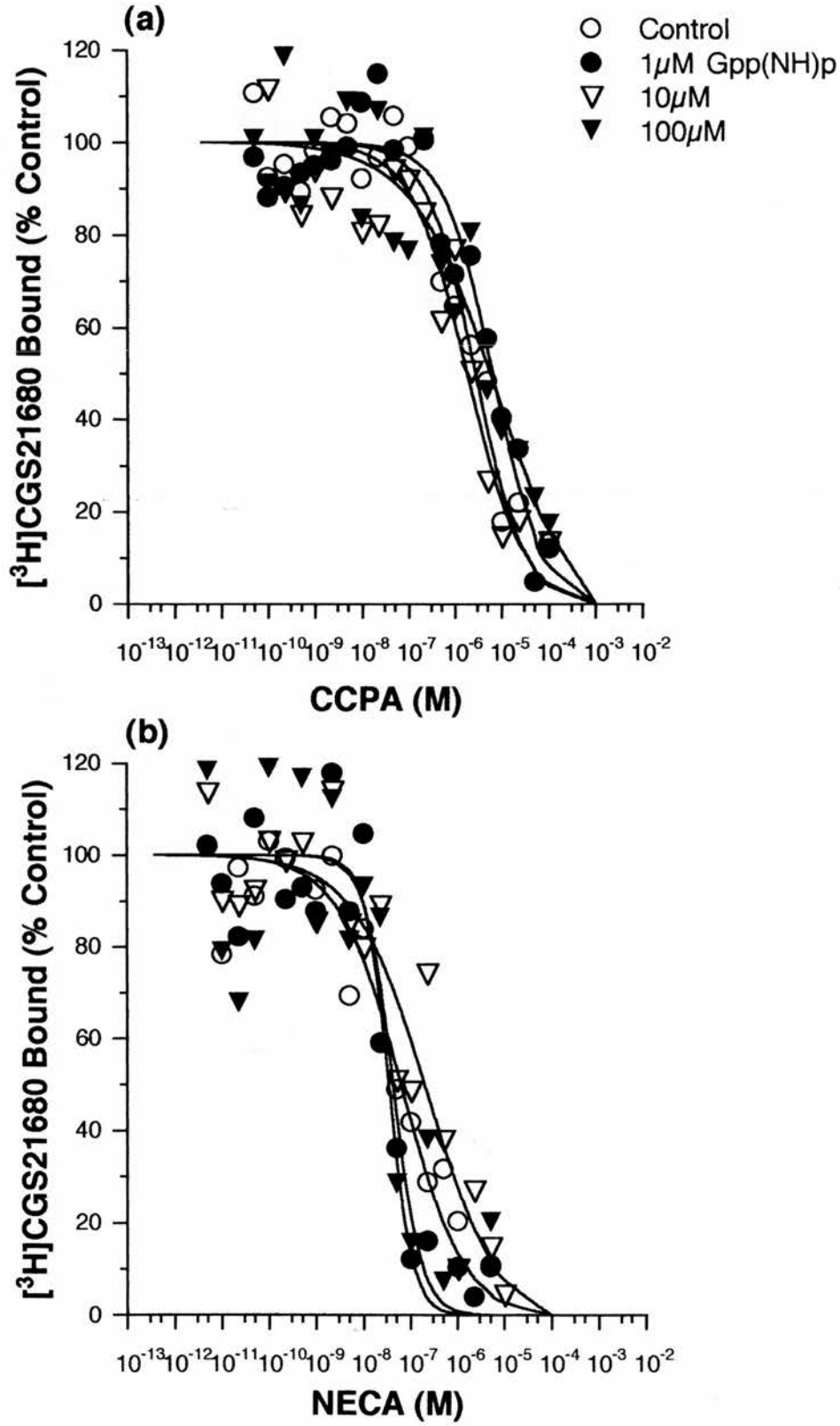

Figure 2.19 The Effect of Gpp(NH)p on the Inhibition of [^{3}H]CGS21680 Binding by (a) CCPA and (b) NECA in the Absence of $MgCl_2$.

The data represent a single experiment (Table 2.12).

Table 2.12 The Effect of Gpp(NH)p on [^{3}H]CGS21680 Binding to Rat Striatal Membranes in the Absence and Presence of $MgCl_2$

	Gpp(NH)p	K_i (nM)	(nH)	Ratio
CCPA				
+ 10 mM $MgCl_2$	Control	313	0.68	--
	1 μM	875	0.67	2.80
	10 μM	1200	0.64	3.83
	100 μM	1550	1.04	4.95
No $MgCl_2$	Control	2090	0.85	--
	1 μM	5030	0.83	2.41
	10 μM	1400	0.73	0.67
	100 μM	6410	0.48	3.07
NECA				
+ 10 mM $MgCl_2$	Control	5.66	0.77	--
	1 μM	32.3	0.81	5.71
	10 μM	41.9	0.71	7.40
	100 μM	60.0	0.81	10.6
No $MgCl_2$	Control	46.7	0.66	--
	1 μM	25.0	1.75	0.54
	10 μM	162	0.56	3.47
	100 μM	30.7	1.49	0.66

K_i values and Hill slope (nH) determined for competition assays as described in the methods. Data for CCPA and NECA are fitted to a one site logistic model as described in the methods. Values are from one experiment. Ratio shown against control K_i for each condition.

in affinity for both drugs on addition of Gpp(NH)p in the presence of $MgCl_2$; however, in the absence of $MgCl_2$ the effect is more difficult to interpret.

2.4. Discussion

In this chapter the effects of $MgCl_2$ and Gpp(NH)p on the binding of adenosine A_1 and A_{2a} antagonist and agonist radioligands have been examined. As the effects observed were different for both agonists and antagonists I will discuss each ligand separately. It has been generally agreed that antagonists recognise the coupled and uncoupled form of the receptor with equal affinity and that guanine nucleotides or their analogues have no effect on antagonist binding (Stroher *et al.*, 1989; Casado *et al.*, 1994). This has not always been the case, with guanine nucleotides producing a wide range of effects (see Introduction), including increasing the level of antagonist binding in membranes (Yeung & Green, 1983; Klotz *et al.*, 1990, 1991; Freissmuth *et al.*, 1991a; Casado *et al.*, 1994) and in cloned rat brain A_1 receptors (Mahan *et al.*, 1991). An effect of guanine nucleotides on antagonist binding has been interpreted as supporting the existence of 'negative efficacy' i.e. the concept that antagonists bind preferentially to uncoupled receptors (Leung & Green, 1989; Leung *et al.*, 1990; Freissmuth *et al.*, 1991a; Schutz & Freissmuth, 1992). For adenosine receptors, Reddington *et al.*, (1989), demonstrated that antagonists recognise both coupled and uncoupled forms of the receptor and in the present study and others (Bruns *et al.*, 1987; Lohse *et al.*, 1987; Klotz *et al.*, 1990), competition by agonists for [^{3}H]DPCPX binding, clearly shows that the radioligand recognises both G protein coupled and uncoupled receptors. That both states are recognised with equal affinity can only be assumed with caution as Casado *et al.*, (1994) demonstrated two kinetic components for [^{3}H]DPCPX binding to membranes from pig brain by

decreasing the ionic strength of the medium. The concept of 'negative efficacy' and the potential for 'inverse agonism' is the focus of current debate, with new models proposed to account for the interaction between receptors and G proteins (Bond *et al.*, 1995; Black & Shankley, 1995; Leff, 1995, Milligan *et al.*, 1995). Although our data provide no direct evidence for the concept of inverse agonism, [^{3}H]DPCPX binding was significantly higher in the presence of guanine nucleotides. The 20% increase in [^{3}H]DPCPX binding in the presence of Gpp(NH)p, with no alteration in antagonist affinity is consistent with data from other studies (Klotz *et al.*, 1990; Prater *et al.*, 1992; Casado *et al.*, 1994; Cohen *et al.*, 1996), but contrasts with groups who observed an increase in B_{max} and a decrease in K_D (Stroher *et al.*, 1989) or no effect (Klotz *et al.*, 1986; Leid *et al.*, 1988; Stiles, 1988; Olah & Stiles, 1990). The magnitude of the increase in binding is variable and appears to reflect species differences and assay conditions (Lohse *et al.*, 1984; Stiles, 1988; Klotz *et al.*, 1990; Prater *et al.*, 1992; Parkinson & Fredholm, 1992; Casado *et al.*, 1994; Nanoff *et al.*, 1995). We omitted Mg^{2+}, as cations may counteract the effects of Gpp(NH)p. Omission of a chelator in the assay could complicate interpretation of the results, as endogenous cations may have played a role. Klotz *et al.*, (1990) noted that pretreatment of rat brain membranes with EDTA did not qualitatively change the effects of guanine nucleotides on [^{3}H]DPCPX binding. It has been suggested that guanine nucleotides increase antagonist radioligand binding by decreasing the affinity of the receptor for adenosine trapped in vesicular 'cryptic' binding sites hidden from adenosine deaminase action (Prater *et al.*, 1992). If correct, the pore forming antibiotic alamethicin, which increased [^{3}H]CGS21680 binding (Luthin *et al.*, 1995), should increase [^{3}H]DPCPX binding as adenosine deaminase could access these 'cryptic pools'. However, Lorenzen *et al.*, (1996) found that alamethicin had no effect on [^{3}H]DPCPX

binding in rat brain membranes, which would indicate this cannot be the full explanation. As the authors themselves noted, there was a pool of adenosine resistant to detergent solubilisation, which could only be released by acetone (Prater *et al.*, 1992). Recently, Cohen *et al.*, (1996), investigated the effects of saponin (which can permeabilise both plasma membranes and intracellular membrane vesicles) on [^{3}H]DPCPX binding. Their interpretation of the increase in antagonist binding was that adenosine forms slowly reversible and pseudoirreversible receptor-G protein complexes, resistant to adenosine deaminase and sensitive to guanine nucleotides. Guanine nucleotides would increase the dissociation of adenosine and effectively generate an increase in receptor sites which is detected as an increase in B_{max} without changing affinity (Cohen *et al.*, 1996). It is possible that the 20% increase in binding observed in this study was due to a small increase in the affinity of [^{3}H]DPCPX that was not detected. To obtain a 20% increase in binding the K_D of the antagonist would only have to increase from 0.25 nM to 0.19 nM. Whether the increase in A_1 antagonist binding is due to one or a combination of the above effects requires further clarification.

The addition of 10 μM Gpp(NH)p to the [^{3}H]DPCPX binding assay had no effect on antagonist affinity, consistent with data from other A_1 antagonist radioligands (Goodman *et al.*, 1982; Lohse *et al.*, 1984). These data were consistent with kinetic studies, with Gpp(NH)p producing no significant alteration in association or dissociation rate constants. A similar observation was made by Klotz *et al.*, (1990).

The decrease in agonist affinity in the presence of Gpp(NH)p is characteristic of all GPCRs (Gilman, 1987). The decrease in affinity of more than 5 fold was similar to data in membranes (Goodman *et al.*, 1982; Bruns *et al.*, 1987) and cloned receptors (Mahan *et al.*, 1991). This effect was

associated with an increase in Hill slope which attained significance for R-PIA. The incomplete transition to one low affinity state for agonists in the presence of guanine nucleotides is consistent with earlier data (Stroher *et al.*, 1989; Prater *et al.*, 1992; Nanoff *et al.*, 1995) and appears to reflect tight coupling of the adenosine A_1 receptor and its G protein (Stiles, 1985; Ramkumar & Stiles, 1988; Nanoff *et al.*, 1995). These data contrast with earlier studies on adenosine (Stiles, 1986, 1988; Leung *et al.*, 1988; Klotz *et al.*, 1990; Gerwins *et al.*, 1990; Jockers *et al.*, 1994) and other G protein coupled receptors (Birnbaumer *et al.*, 1990; Samama *et al.*, 1993), in which a complete transition to the low affinity state for agonists was observed. In whole cells, intracellular GTP concentrations seem sufficient to produce a full shift (Gerwins *et al.*, 1990). Incomplete transition to a low affinity state for agonists was also observed for mouse, guinea pig (Mr K. Finlayson & Mr T. Maemoto, unpublished observations) and human cortex, with an 8 fold decrease in the affinity of CCPA on addition of 100 μM Gpp(NH)p in human cortical membranes (see Chapter 1). This effect does not seem to be organ or species specific (Stroher *et al.*, 1989). The transfer between high and low affinity states has been investigated using solubilised preparations in which the A_1 receptor retains its pharmacological properties (Stroher *et al.*, 1989; Klotz *et al.*, 1990; Olah & Stiles, 1990; Oliveira *et al.*, 1991; Prater *et al.*, 1992). Stroher *et al.*, (1989) demonstrated that the affinity of the receptor for the G protein is enhanced on solubilisation and that lower concentrations of guanine nucleotides are required for conversion to a low affinity state. Recently, Nanoff *et al.*, (1995) identified a coupling co-factor in brain membranes responsible for the incomplete transition from the high to low affinity state in rat and bovine membranes. In contrast to our data, Nanoff and colleagues suggest that the protein present in human membranes has lower affinity and does not block the complete transition to a low affinity state. A significant increase in Hill slope

was observed for CCPA on addition of Gpp(NH)p to human cortical membranes (0.52 to 0.78), however, the greater variability in binding data did not permit 2-site modelling. Interestingly, Nanoff *et al.*, (1995) noted that addition of the co-factor from human to rat or bovine membranes blocks the transition from the high to low state. Concentration response curves to Gpp(NH)p, indicate the decrease in agonist affinity is associated with a decrease in the proportion of the high affinity state labelled, with no effect on affinity for high or low states (Finlayson *et al.*, 1994). The 30 fold difference in affinity between the two states was similar in rat (20-45 fold, Bruns *et al.*, 1987) and bovine brain membranes (15-30 fold, Lohse *et al.*, 1987). The proportion and affinities of the high and low states are in good agreement with numerous authors (Lohse *et al.*, 1984; Klotz *et al.*, 1986, 1991; Stroher *et al.*, 1989; Lorenzen *et al.*, 1993, 1996) and are consistent with data from peripheral tissues (Peachey *et al.*, 1994) and cloned receptors (Mahan *et al.*, 1991; Freund *et al.*, 1994) (Table 2.13). Although examined only once, the effect of Gpp(NH)p was similar in mouse and guinea pig membranes (data not shown). The reduction in agonist affinity observed in mouse and guinea pig membranes was again due to a reduction in the proportion of the high affinity state labelled, however further studies would be required to confirm this observation. As Gpp(NH)p was supplied as the sodium salt and monovalent cations modulate binding (Gilman, 1987; Birnbaumer *et al.*, 1990), we examined the concentration dependent effect of sodium ions on [^{3}H]DPCPX binding. At concentrations up to 1 mM, NaCl had no effect on the level of binding or agonist affinity. These data are in agreement with those of Goodman *et al.*, (1982) and Casado *et al.*, (1994), but contrast with data from Stiles, (1988) and Leung *et al.*, (1988) and with data from other GPCRs (Clark & Hill, 1995). Our inability to detect any effect of this cation also contrasts with the existence of a putative sodium binding site on the cloned adenosine A_1

Table 2.13 Two Site Data for Adenosine Agonist Inhibition of Antagonist Radioligand Binding

Reference	Radioligand	Agonist	K_h	K_l	$\%b_h$
Present study	[^{3}H]DPCPX	CCPA	1.2	31.5	65.1
Present study	[^{3}H]DPCPX	R-PIA	1.6	86.8	65.5
Lohse *et al.*, (1984).	[^{3}H]DPX	R-PIA	1.3	194	72
Klotz *et al.*, (1986).	[^{3}H]DPX	R-PIA	0.34	27	52
Stroher *et al.*, (1989).	[^{3}H]DPCPX				80.1
Klotz *et al.*, (1991).	[^{3}H]DPCPX	CCPA	0.23	16.1	56
		R-PIA	0.51	20.8	56
Mahan *et al.*, (1991).	[^{3}H]DPCPX	CCPA	0.71	97.5	78
		R-PIA	0.77	61.2	69
Lorenzen *et al.*, (1993).	[^{3}H]DPCPX	R-PIA	4.5	32.4	46
Freund *et al.*, (1994).	[^{3}H]DPCPX	R-PIA	0.5	100	
Peachey *et al.*, (1994).	[^{3}H]DPCPX	R-PIA	1.52-3.04	30.2-88.1	50.2-58.6
Lorenzen *et al.*, (1996).	[^{3}H]DPCPX	R-PIA	1.3	194	72

Data for CCPA and R-PIA in the present study is taken from Table 2.4. K_h and K_l are the respective K_i values for the high and low affinity states and % b_H is the percentage of total ligand bound to the high affinity state.

receptor (Palmer & Stiles, 1995).

The effects of $MgCl_2$ on [^{3}H]DPCPX binding appear complex. The 40% decrease in [^{3}H]DPCPX binding caused by 10 mM $MgCl_2$ is accompanied by a small decrease in K_D (0.35 to 0.42 nM). In accounting for a 40% decrease in binding, the K_D of the antagonist would have to decrease from 0.35 nM to 0.65 nM. As such a shift in affinity should be detectable, other factors may be involved. It has been argued that the effect of $MgCl_2$ may be due to the promotion of the high affinity state of the receptor, a state not preferred by the antagonist (Parkinson & Fredholm, 1992; Casado *et al.*, 1994). The increase in agonist affinity and the proportion of the high affinity state labelled as shown for CCPA (65.3% to 74.3%) (Table 2.14), may reflect increased receptor-G protein coupling (Birnbaumer *et al.*, 1990). This is also consistent with the B_{max} for [^{3}H]DPCPX in the presence of 10 mM $MgCl_2$ being similar to the B_{max} of [^{3}H]CCPA (Table 2.14), which almost exclusively labels the high affinity state of the receptor (see below). The increase in affinity seen for agonists is consistent with the modulatory role of Mg^{2+} on GPCRs (Gilman, 1987; Birnbaumer *et al.*, 1990); however, it was not accompanied by an increase in Hill slope. The data from the two site model indicate that the increase in affinity is due to an increase in the proportion of high affinity states labelled with no significant alteration in affinity of either state (Table 2.14). The 10% (74.3% to 65.1%) decrease in proportion of high affinity states labelled by [^{3}H]DPCPX on removal of $MgCl_2$ (Table 2.14) is much smaller than that seen by Stroher *et al.*, (1989). This may reflect species differences or higher levels of endogenous cations in our assay. $MgCl_2$ had very little effect on antagonist affinity which is consistent with other studies using A_1 antagonist radioligands (Goodman *et al.*, 1982).

The binding of [^{3}H]CCPA to rat brain membranes was saturable, of high

Table 2.14 Comparison of the Effects of $MgCl_2$ and Gpp(NH)p on [^{3}H]DPCPX and [^{3}H]CCPA Binding

[^{3}H]DPCPX		Bmax	2 site data			
	K_D (nM)	(pmol mg^{-1})	CCPA	K_h	K_l	%B_h
Control	0.25 ± 0.01	1.17 ± 0.07		1.20 ± 0.35	31.5 ± 7.8	65.1
+ 10 μM Gpp(NH)p	0.26 ± 0.02	1.47 ± 0.12		2.02 ± 0.35	44.4 ± 10.9	33.8
Control	0.35 ± 0.04	2.00 ± 0.22				
+ 10 mM MgCl2	0.42 ± 0.05	1.28 ± 0.19		0.88 ± 0.13	47.7 ± 9.69	74.3

[^{3}H]CCPA		Bmax	2 site data			
	K_D (nM)	(pmol mg^{-1})	CCPA	K_h	K_l	%B_h
Control	0.41 ± 0.04	1.31 ± 0.36		Not possible		
+ 10 μM Gpp(NH)p	0.98 ± 0.15	0.66 ± 0.22		Not possible		
Control	0.52 ± 0.02	1.21 ± 0.02				
+ 10 mM MgCl2	0.41 ± 0.04	1.42 ± 0.04		Not possible		

	Bmax (pmol mg^{-1})	
	Control	+ 10 mM $MgCl_2$
[^{3}H]DPCPX	2.09 ± 0.38	1.21 ± 0.15
[^{3}H]CCPA	1.21 ± 0.01	1.34 ± 0.21

affinity and with equilibrium attained by 120 min. The K_D (0.47 ± 0.03 nM) and B_{max} (1.37 ± 0.14 pmol mg^{-1} protein) values were similar in both saturation and competition studies. These data are consistent with the original characterisation of [^{3}H]CCPA (K_D=0.2 nM and B_{max}=0.86 pmol mg^{-1} protein) (Klotz *et al.*, 1989) and with the K_D (0.43 nM) from cloned rat brain A_1 receptors (Rivkees *et al.*, 1995b). In contrast to [^{3}H]DPCPX, $MgCl_2$ produced a concentration dependent increase in [^{3}H]CCPA binding. This has been observed for other A_1 agonist radioligands such as [^{3}H]CHA and [^{3}H]R-PIA and for other agonist ligands binding to GPCRs (Goodman *et al.*, 1982; Klotz *et al.*, 1986; Gilman, 1987). In contrast, Traversa *et al.*, (1994), saw no increase in [^{3}H]CHA binding on addition of 1 mM $MgCl_2$. The increase in [^{3}H]CCPA binding on addition of $MgCl_2$ appears to be due to a slight increase in ligand affinity (0.52 to 0.41 nM) (Table 2.14). Agonists and antagonists exhibited the typical adenosine A_1 pharmacological profile, with agonist affinities 5-17 fold higher than values obtained using [^{3}H]DPCPX binding (Table 2.15). The data for [^{3}H]CCPA binding are consistent with Klotz *et al.*, (1989) and other agonist radioligands (Table 2.15). Both agonists and antagonists had Hill slopes not significantly different from unity, indicating the existence of predominantly one affinity state. These data are similar to other agonists radioligands like [^{3}H]R-PIA (Lohse *et al.*, 1984; Klotz *et al.*, 1986; Allende *et al.*, 1991; Casado *et al.*, 1990, 1991) and [^{3}H]CHA (Yeung & Green, 1983). The K_D of [^{3}H]CCPA is similar to the high affinity (K_h) state identified for CCPA inhibition of [^{3}H]DPCPX binding (Table 2.14). On addition of $MgCl_2$ to the [^{3}H]CCPA binding assay two site modelling was attempted and only one high affinity site could be detected. The B_{max} for [^{3}H]CCPA in the absence and presence of $MgCl_2$ is approximately 65% of that obtained using [^{3}H]DPCPX,

Table 2.15 A_1 Receptor Affinity for Adenosine Receptor Agonists and Antagonists

	[^{3}H]DPCPX	[^{3}H]CCPA	[^{3}H]DPCPX[a]	[^{3}H]CHA	[^{3}H]RPIA[e]
	Present study-Rat		Rat	Rat	Rat
CCPA	3.39	0.47			0.4[h]
CPA	4.02	0.46	7.9	1[c]	0.34
R-PIA	4.56	0.91	16	2[c]	1.2
CHA	7.16	1.31	27	2[c]	1.0
NECA	39.1	4.24	90	6[c]	7.8
CADO	41.0	3.69		14[c]	7.5
S-PIA	212		520	29[d]	50
CSPA	583				
APEC	602				235[g]
CGS21680	39000	2300		2600[c]	
DPCPX	0.28	0.36	0.56/0.18[b]		1.2
CGS15943	1.35	2.31		22[c]	
CPT	6.49	8.92	11/6.3[b]		10
DPX	33.1	37.6	37	135[d]	
8-PT	45.0	64.0		176[d]	76
DPSPX	76.1				140
KF17837	80.6		390[i]		
8-PST	1020			1275[d]	1000
Theophylline	4330		5600[b]	10960[d]	12800
CSC	10600				28000[f]
Caffeine	25300			28000 [c]	44000

Data taken from: [a]Bruns *et al.*, (1987), [b]Klotz *et al.*, (1991), [c]Jarvis *et al.*, (1989a), [d]Ferkanky *et al.*, (1986), [e]Ukena *et al.*, (1986), [f]Jacobson *et al.*, (1993), [g]Nikodijevic *et al.*, (1991), [h]Lohse *et al.*, (1988) and [i]Nonaka *et al.*, (1993).

which is in excellent agreement with the proportion of high affinity receptors identified using [^{3}H]DPCPX (Table 2.14). These data for the two radioligands are consistent with Klotz *et al.*, (1991) and all point to [^{3}H]CCPA almost exclusively labelling the high affinity state identified in the [^{3}H]DPCPX binding assay.

Gpp(NH)p caused a concentration dependent decrease in [^{3}H]CCPA binding up to 85% at 1 mM Gpp(NH)p. A similar level of reduction has been described for other A_1 agonist radioligands in membranes (Goodman *et al.*, 1982; Lohse *et al.*, 1984; Klotz *et al.*, 1986; Leung *et al.*, 1988; Freissmuth *et al.*, 1991b) and cloned receptors (Reppert *et al.*, 1991). The level of reduction probably reflects assay conditions and species differences in sensitivity to guanine nucleotides (Lohse *et al.*, 1984; Stiles, 1988; Wiener & Maayani, 1991). The 50% reduction in binding observed for CCPA is a consequence of the 58% decrease in agonist affinity, rather than a decrease in the number of binding sites (Table 2.14). This contrasts with Yeung & Green (1983), who attributed the reduction in [^{3}H]CHA binding by Gpp(NH)p to a decrease in B_{max}. The decrease in agonist affinity on addition of Gpp(NH)p was less pronounced than that observed for [^{3}H]DPCPX binding, only achieving significance for four agonists. This contrasts with Klotz *et al.*, (1989) who noted a large reduction in the affinity on addition of GTP, although levels vary depending on what is compared. The lack of significance for some agonists reflects the large reduction in [^{3}H]CCPA binding seen in the presence of Gpp(NH)p and greater variability in the data. As with [^{3}H]DPCPX binding, addition of Gpp(NH)p had very little effect on antagonist binding (Lohse *et al.*, 1984). Increasing concentrations of Gpp(NH)p reduced agonist affinities to values similar to the high affinity state identified using [^{3}H]DPCPX binding. However, the reduction in binding and variability in the data meant no

significance was obtained. The decrease in the Hill coefficient for CCPA on addition of Gpp(NH)p would be expected if agonists were being shifted from a predominantly high affinity state to a mixed high/low or low affinity state for the receptor. These data are consistent with those of Lohse *et al.*, (1984) for [^{3}H]R-PIA.

As with [^{3}H]CCPA, $MgCl_2$ increased [^{3}H]CGS21680 binding to rat striatal membranes in a concentration dependent manner. The concentration dependence and two fold increase in binding at 10 mM $MgCl_2$ is similar to that shown by Mazzoni *et al.*, (1993). This contrasts with Jarvis *et al.*, (1989a), who, when originally characterising the radioligand showed 10 mM $MgCl_2$ increased [^{3}H]CGS21680 binding by 10%. Johansson *et al.*, (1992), reported a concentration dependent increase, greater than 10 fold at 10 mM $MgCl_2$, in both ligand binding and autoradiographic studies. These researchers postulated that differences were due to the presence of a chelator in their study. This may be a factor but it cannot totally explain the variations seen, as Mazzoni *et al.*, (1993) included a chelator throughout their studies and their data was similar to the present study. The increase in specific binding can be produced by assorted divalent cations, apparently acting at the level of the receptor and not directly with the G protein (Johansson *et al.*, 1992; Mazzoni *et al.*, 1993). The addition of 10 mM $MgCl_2$ to the assay, produced a 4.9 fold increase in the K_D of CGS21680 from 53.4 to 10.8 nM, almost identical to the 4.7 fold increase (37.5 to 7.9 nM) described by Mazzoni *et al.*, (1993). They did, however, report an increase in B_{max} on addition of $MgCl_2$, whereas we noted no significant difference. The affinity of all agonists increased on addition of 10 mM $MgCl_2$. The effect being more pronounced for the A_{2a} selective compounds, CGS21680 and NECA. A similar effect is seen for other GPCRs (Birnbaumer *et al.*, 1990). The removal of $MgCl_2$ from the assay and the shift

to a low affinity state was associated with a slight increase in Hill slope, although this only attained significance for CADO. Interestingly, for antagonists, addition of $MgCl_2$ produced a significant decrease in the affinity of DPCPX which did not occur for CGS15943. The difference may be structural, as CGS15943 is a non-xanthine antagonist (Jarvis *et al.*, 1989a). However, further investigations would be required to determine the significance of this effect.

The effect of guanine nucleotides on [^{3}H]CGS21680 binding was generally investigated in the presence of 10 mM $MgCl_2$ because binding was almost undetectable in the absence. Gpp(NH)p produced a concentration dependent decrease in binding reaching 85% at 1 mM Gpp(NH)p. These data were similar to Mazzoni *et al.*, (1993), using stable GTP and GDP analogues. This reduction was greater than that described by Jarvis *et al.*, (1989a) and Johansson *et al.*, (1992). The magnitude of the effect of guanine nucleotides does appear very sensitive to cations (Mazzoni *et al.*, 1993; Luthin *et al.*, 1995). In contrast, Nanoff & Stiles (1993), reported [^{3}H]CGS21680 binding to the bovine A_{2a} receptor was insensitive to guanine nucleotides. The lack of effect of guanine nucleotides on bovine A_{2a} striatal binding had been described previously using the A_{2a} agonist [^{125}I]PAPA-APEC (Barrington *et al.*, 1990) and was confirmed by Mazzoni *et al.*, (1993). These results indicate that the bovine A_{2a} receptor is even more tightly coupled to a G protein than in rat (Nanoff & Stiles, 1993). The addition of 10 μM Gpp(NH)p produced a 3.2 fold decrease in the K_D of CGS21680 from 10.8 to 34.7 nM. A similar decrease in affinity with no alteration in B_{max} was reported by other groups (Hide *et al.*, 1992; Mazzoni *et al.*, 1993; Cunha *et al.*, 1996). The addition of 10 μM Gpp(NH)p produced a significant decrease in affinity for all agonists tested, being marginally smaller for CGS21680. The shift towards a low affinity state

for agonists in the presence of Gpp(NH)p was even more pronounced on removal of $MgCl_2$ from the assay. The decrease in agonist affinity on addition of Gpp(NH)p to the [^{3}H]CGS21680 binding assay, was similar to the shift seen for [^{3}H]DPCPX binding but was larger than for [^{3}H]CCPA binding. The affinity of CCPA, R-PIA and NECA in the presence of Gpp(NH)p is similar to the low affinity state observed with the A_{2a} antagonists [^{3}H]SCH58261 (Zocchi *et al.*, 1996) and [^{3}H]KF17837S (Nonaka *et al.*, 1994) (Table 1.9). The affinity of CGS21680 is not as similar but this is probably a reflection of Gpp(NH)p having a smaller effect. The shift towards the low affinity state, is not accompanied by a significant increase in Hill slope. The low level of specific binding in the presence of Gpp(NH)p and larger variations in data, make accurate determination of Hill slopes more difficult. As with the other radioligand binding assays, addition of Gpp(NH)p produced no significant alteration in antagonist affinity. Since [^{3}H]CGS21680 binding is strongly influenced by both guanine nucleotides and Mg^{2+}, we examined the interdependence of these effects using a extended concentration range for CGS21680. In the absence and presence of 10 mM $MgCl_2$, addition of 10 μM Gpp(NH)p produced a similar 3 fold decrease in affinity for CGS21680. These effects may therefore be independent of each other (Johansson *et al.*, 1992). In contrast, Mazzoni *et al.*, (1993), showed no effect of stable GTP analogues in the absence of $MgCl_2$. The lack of a chelator in our assay and the presence of residual divalent cations may account for these differences. In attempting to model the interconversion between high and low affinity states, in the absence and presence of both $MgCl_2$ and Gpp(NH)p, we fitted the data to a 2-site model, despite no significant improvement ($P > 0.05$) when assessed using a partial F test. Only under control conditions when $MgCl_2$ was present were we able to generate any data, as removal of $MgCl_2$ or addition of Gpp(NH)p

significantly reduced binding. In the presence of 10 mM $MgCl_2$, 82.3 ± 1.4% of the receptors were in the high affinity state, with K_i values of 7.5 ± 1.6 and 176 ± 132 nM for the high and low affinity states respectively. These data, although variable, appear consistent with those of Mazzoni *et al.*, (1993) and Luthin *et al*, (1995). The low affinity state appears different to the very low affinity state described by Wan *et al.*, (1990). The latter site probably reflects labelling of A_1 and possibly A_{2b} receptors. The K_i value for the low affinity state appears to correlate with the low affinity site labelled by antagonist radioligands (Nonaka *et al.*, 1994; Zocchi *et al.*, 1996) (Table 1.9). It is also very similar to the affinity of CGS21680 in the absence of $MgCl_2$ and the presence of Gpp(NH)p. As Gpp(NH)p appeared to shift the affinity for CGS21680 to a even lower value in the absence of $MgCl_2$, preliminary studies were performed to examine this effect. Gpp(NH)p produced a similar concentration dependent decrease in [^{3}H]CGS21680 binding in the absence of $MgCl_2$. However, due to low levels of binding and the reduction in specific binding, significance was only obtained at the highest concentration of Gpp(NH)p. One study using CCPA and NECA, showed that in the presence of $MgCl_2$, Gpp(NH)p reduced the affinity of both agonists in a concentration dependent manner, to values similar to that determined by antagonist radioligands (Nonaka *et al.*, 1994; Zocchi *et al.*, 1996) (Table 1.9). However in the absence of $MgCl_2$, no consistent reduction in affinity was seen and further studies would be required to examine this effect. Contrasting results on the existence of this low affinity state have been demonstrated for the antagonist radioligands, with Nonaka *et al.*, (1994), showing GTP produced a further shift to the right for CGS21680 (130 to 340 nM) and Zocchi *et al.*, (1996), reporting no effect.

It is clear that the guanine nucleotide and magnesium dependence of adenosine receptor binding is highly variable and dependent on the system

and species used (Wiener & Maayani, 1991; Jockers *et al.*, 1994). Whether this is due to an atypically tight coupling of the receptor (Stiles, 1985; Nanoff & Stiles, 1993), or perhaps factors like vesicle formation (Prater *et al.*, 1992; Luthin *et al.*, 1995), pH (Askalan & Richardson, 1994) or temperature (Borea *et al.*, 1991; Luthin & Linden, 1995; Lorenzen *et al.*, 1996) still requires to be elucidated. The final identification of the 'coupling cofactor', (Nanoff *et al.*, 1995), or the use of saponins may help clarify the situation (Cohen *et al.*, 1996). The new selective adenosine A_{2a} antagonist ligands (Nonaka *et al.*, 1994; Palmer *et al.*, 1995; Zocchi *et al.*, 1996), when commercially available, will undoubtedly help in the further characterisation of the A_{2a} receptor.

CHAPTER THREE

MEASUREMENT OF ADENOSINE RECEPTOR ANTAGONISTS IN RAT BRAIN USING A MODIFIED RADIORECEPTOR ASSAY

3.1. Introduction

Electrophysiological and functional evidence (Fredholm & Dunwiddie, 1988; Jacobson *et al.*, 1992a; Suzuki *et al.*, 1993) have pointed to a neuromodulatory role for adenosine at pre- and postsynaptic adenosine A_1 receptors (Snyder, 1985; Williams, 1993). The inhibition by adenosine of LTP and the release of several neurotransmitters is strong evidence for an inhibitory neuromodulatory role (Fredholm & Dunwiddie, 1988). These actions of adenosine and the central stimulation produced by caffeine (Daly *et al.*, 1981; Jarvis & Williams, 1988), imply that selective and potent adenosine A_1 antagonists may be beneficial in enhancing cognition by enhancing synaptic transmission (Jacobson *et al.*, 1992a; Suzuki *et al.*, 1993). Central stimulation by adenosine A_1 antagonists and the reversal of behavioural depression induced by adenosine agonists (Nikodijevic *et al.*, 1991), ensures a continuing interest in the development of adenosine A_1 antagonists (Peet *et al.*, 1993; Suzuki *et al.*, 1993; Terai *et al.*, 1995a). In attributing any beneficial effect to adenosine A_1 antagonists in behavioural models, it is essential to demonstrate the presence of drugs in brain tissue, at concentrations sufficient to mediate pharmacological effects. A number of different techniques have been used to measure central penetration of drugs, including HPLC, *ex vivo* binding and radioreceptor assays (Janis *et al.*, 1983). HPLC is limited for use as a high throughput assay capable of making quick and easy determinations, as conditions need to be established for individual compounds and active metabolites (Patel *et al.*, 1994a). On the other hand, *ex vivo* binding and radioreceptor assays are quick, simple and relatively easy to establish if suitable radioligand binding assays are available. The principles behind *ex vivo* binding and radioreceptor assays are similar to radioimmunoassays. They are based on the fact that specific binding of a radioactive ligand to a receptor site

is a quantitative function of the amount of unlabelled ligand present. In essence, drugs which interact with receptors *in situ* can be detected after tissue homogenisation and incubation *in vitro* (Burki, 1986). There are, however, a number of major differences between the two assays. In *ex vivo* binding assays the tissue in which the drug concentration is to be determined must be capable of binding a suitable radioligand for the system under investigation. A standard curve can be generated by conducting a binding assay using control (i.e. untreated) tissue in the presence of known quantities of ligand which interferes with radioligand binding to the receptor. The amount of ligand in a drug treated tissue sample can then be estimated by determining the level of binding in the treated sample and comparing this to the standard curve. The method assumes that the tissue used from each animal has the same density of receptors and ligand affinity for those receptors (Heffez *et al.*, 1985). Radioreceptor assays avoid these problems by 'extraction' of the ligand from the treated tissue. The ligand is then added as a 'competing drug' in a conventional *in vitro* radioligand binding assay, where one standard source of membranes is used. The amount of ligand can then be estimated by determining the percent inhibition of binding and comparing this to an appropriate standard curve generated by the addition of known quantities of unlabelled ligand. The use of one standard source of membranes to determine drug concentrations in treated samples should avoid variations in both affinity and receptor density. The radioreceptor assay also allows the determination of drug concentrations in tissues or preparations such as serum or plasma which may contain no endogenous receptors for the system under investigation. Unfortunately, neither radioreceptor or *ex vivo* binding assays are capable of distinguishing between parent drug and pharmacologically active metabolites. The use of both techniques is widespread, with *ex vivo* binding used to determine the blood brain barrier (BBB) permeability of calcium antagonists

(Heffez *et al.*, 1985; Watson *et al.*, 1994), opioids (Richards & Sadee, 1985; Barber *et al.*, 1994), muscarinic agents (Sethy & Francis, 1988; Freedman *et al.*, 1989; Bymaster *et al.*, 1993a, b), psychoactive drugs (Burki, 1986; Hyttel *et al.*, 1992), angiotensin antagonists (Marshall *et al.*, 1993), histamine antagonists (Taylor *et al.*, 1992; Barnes *et al.*, 1993), CCK_B antagonists (Patel *et al.*, 1994a, b) and adenosine antagonists (Baumgold *et al.*, 1992). Radioreceptor assays have been used to measure a variety of substances (reviewed in Enna, 1978; Gould *et al.*, 1983; Janis *et al.*, 1983), with γ-aminobutyric acid (GABA), the first neurotransmitter measured (Enna & Snyder, 1976). For GABA, a water soluble compound, extraction from tissue samples is by simple centrifugation (Enna, 1978). Unfortunately, adenosine receptor antagonists show varying degrees of lipophilicity and therefore centrifugation of tissue samples may not result in all the drug appearing in the supernatant. To avoid developing separate extraction procedures for every drug, we attempted to develop a procedure in which the drug is left intact in the tissue sample and any other factors capable of interfering with binding are eliminated. This allows drug concentrations present in tissue samples to be assayed by simple addition to an *in vitro* radioligand binding assay.

Drug present in the vascular system of the brain may contaminate tissue samples taken from brain (Patel *et al.*, 1994a). We incorporated a transcardiac perfusion step to minimise the presence of drug from the vascular system of the brain. Transcardiac perfusions have been used in studies on calcium antagonists (Heffez *et al.*, 1985), muscarinic agents (Freedman *et al.*, 1989), angiotensin antagonists (Marshall *et al.*, 1993), histamine antagonists (Taylor *et al.*, 1992; Barnes *et al.*, 1993) and CCK_B antagonists (Patel *et al.*, 1994a, b) but not when adenosine receptor antagonists were measured in mouse brain using *ex vivo* binding (Baumgold *et al.*, 1992). This chapter describes the development and characterisation of a modified radioreceptor

assay capable of measuring central penetration of adenosine receptor antagonists in rat brain following intraperitoneal administration.

3.2. Methods and Materials

3.2.1. *Ex vivo* Binding

Rats were injected intraperitoneally (i.p.) with vehicle or appropriate dose of DPCPX (0.01-1.0 mg kg^{-1}). Animals were anaesthetised with 4% halothane in oxygen and nitrous oxide (30:70 v:v). At 20 min the cortex was immediately dissected and rolled on filter paper to remove superficial blood vessels, weighed and homogenised in 9 vol. (v:w) of Tris-buffer using a teflon glass homogeniser. Appropriate volumes were removed for experimentation on fresh homogenate and samples were stored in microcentrifuge tubes in 1 ml aliquots at -20°C. Prior to use in the assay, brain homogenate was incubated for 60 min at 37°C in the presence of ADA (6 u ml^{-1}), to remove endogenous adenosine (Baumgold *et al.*, 1992).

[^{3}H]DPCPX *ex vivo* binding was carried out under equilibrium conditions by preincubating 10 μl of DMSO or DPCPX and 840 μl of Tris-buffer with 100 μl of 1 nM [^{3}H]DPCPX for 2 min at 25°C. DPCPX was diluted in DMSO to give 10 duplicate concentrations. Total binding was determined in the presence of DMSO and 10 μM R-PIA was used to determine non-specific binding. Addition of brain homogenate (50 μl: 10 vol. (v:w)) to give a final volume of 1 ml, initiated a 20 min incubation at 25°C. Bound and free ligand were separated using a Brandel cell harvester and this was followed by 3 washes (3 ml) in ice cold Tris-buffer over GF/B filters. Filter disks were transferred to scintillation vials and incubated with 100 μl of 100% formic acid for 10 min prior to addition of Emulsifier Safe scintillant (4 ml) and equilibrated overnight. Radioactivity was determined using the Packard 2500TR scintillation counter, with samples

counted for 4 min and results expressed as dpm per sample.

For *ex vivo* binding, [^{3}H]DPCPX standard curves were constructed by incubating 50 μl of control brain homogenate (10 vol. (v:w)) from vehicle treated rats, with increasing concentrations of DPCPX (0.003-100 nM) as above. Estimation of the DPCPX concentration in each brain sample from treated animals was done by determining total and non-specific binding for that sample and comparing the level of specifically bound [^{3}H]DPCPX to the standard curve. For each DPCPX dose given to treated animals, DPCPX concentrations in brain were determined in duplicate using at least three animals. Taking into account dilutions within the assay and assuming the drug is freely distributed within the tissue and hence 1.05 g of brain tissue corresponds to 1 ml, potential concentrations in the brain were calculated.

3.2.2. Radioreceptor Binding Assay

Standard and Modified [^{3}H]DPCPX Binding Assays

P_2 synaptosomal membranes were prepared from rat cortical tissue as described in Chapter 1 (see 1.2.1.1.), for use in the [^{3}H]DPCPX binding assays.

Rats were injected i.p. with vehicle or the appropriate dose of drug. At various times post-injection and 2 min prior to the collection of tissue samples animals were anaesthetised with 4% halothane in oxygen and nitrous oxide (30:70 v:v). Venous blood (7 ml) was collected from the inferior vena cava, 1 min before removal of cortex; the blood was left to clot at 4°C overnight in tubes containing glass beads and the resultant serum was stored in 200 μl aliquots at -20°C (serum samples were subsequently diluted 10 fold in Tris-buffer before any procedure, unless otherwise stated). Immediately prior to removal of the cortex, animals received a transcardiac perfusion of saline for

30 seconds (flow rate: 35 ml min^{-1}), by inserting a needle through the left ventricle and into the aorta, unless otherwise stated. After perfusion, the cortex was immediately removed and the tissue homogenate prepared as described for the *ex vivo* binding assay. In some experiments, tissue supernatant was collected and tested, by centrifugation of brain homogenate samples at 17000 g for 20 min at 4°C.

The standard [^{3}H]DPCPX binding assay was carried as described in Chapter 1 (see 1.2.3.1.). Briefly, 10 μl of DMSO or test drug, 290 μl of Tris-buffer, 100 μl of ADA (1 u ml^{-1}) and 100 μl of 1 nM [^{3}H]DPCPX were preincubated for 2 min at 25°C. Test drugs were diluted in DMSO to give 10 duplicate concentrations. Total binding was determined in the presence of DMSO and 10 μM R-PIA was used to determine non-specific binding. Addition of P_2 rat cortical membrane suspension (500 μl; 20-40 μg), which gave a final volume of 1 ml, initiated a 20 min incubation at 25°C. Bound and free ligand were separated using a Brandel cell harvester and this was followed by 3 washes (3 ml) in ice cold Tris-buffer over GF/B filters. Filter disks were transferred to scintillation vials and the procedure followed as for *ex vivo* binding.

The brain tissue from vehicle and drug treated animals contains adenosine A_1 receptors and hence has [^{3}H]DPCPX binding capacity. This [^{3}H]DPCPX binding capacity must be removed in order to determine the drug concentration in brain homogenate. Complete denaturation of vehicle and drug treated samples should remove this [^{3}H]DPCPX binding capacity, allowing the amount of drug present in treated samples to be determined in the standard [^{3}H]DPCPX binding assay. A number of conditions were tested including heating samples to 56°C for 60 min and sonication for 30 min. Removal of the [^{3}H]DPCPX binding capacity of the vehicle and drug treated brain

homogenates was achieved by incubation of homogenates at 80°C for 15 min. Although not strictly necessary for serum or tissue supernatant samples, which should have no intrinsic binding, consistency was maintained by treating all samples at 80°C. Drug stability at 80°C was checked by constructing two [^{3}H]DPCPX standard curves using washed P_2 membranes over an appropriate concentration range for each drug, with one set of drugs having been preincubated at 80°C for 15 min in the presence of Tris-buffer. Following treatment at 80°C, samples were left to cool on ice and then incubated for 60 min at 37°C in the presence of ADA (6 u ml^{-1}) to remove endogenous adenosine (Baumgold *et al.*, 1992). [^{3}H]DPCPX binding in the presence of denatured samples was carried out as described above for the standard assay, by reducing the volume of buffer to 240 µl and adding 50 µl of denatured brain homogenate, serum or tissue supernatant. To increase sensitivity, the volume of the assay was reduced to 0.5 ml, without altering the amount of denatured sample added.

Two [^{3}H]DPCPX standard curves using washed P_2 membranes were constructed for each drug over an appropriate concentration range in the absence and presence of denatured control brain homogenate, serum or tissue supernatant from vehicle treated rats as appropriate. The standard curve for each drug which contained no denatured brain homogenate, serum or tissue supernatant acted as an internal control to check that addition of denatured samples from vehicle treated animals had no effect on drug affinity or the level of specific binding. Estimation of drug concentrations in brain homogenate, serum or tissue supernatant samples from treated animals was calculated as for *ex vivo* binding by determining the total and non-specific binding for that sample and comparing the percent of specifically bound [^{3}H]DPCPX for each sample with the appropriate standard curve. For each

drug dose given to treated animals, drug concentrations in brain, serum and tissue supernatant were determined in duplicate using at least three animals. Taking into account dilutions within the assay and assuming the drug is freely distributed within the tissue and hence 1.05 g of brain tissue corresponds to 1 ml, potential concentrations in the brain were calculated.

3.2.3. [^{14}C]Inulin Tracer Study

[^{14}C]Inulin (2.6 mCi g^{-1}; NEN) was used as a trace marker for blood plasma in a method similar to Patel *et al.*, (1994a). Rats were anaesthetised with 4% halothane in oxygen and nitrous oxide (30:70 v:v) and placed in a incubator on a heated blanket to maintain body temperature. PE50 catheters were inserted into the femoral vein for [^{14}C]inulin infusion and the ipsilateral femoral artery for removal of blood samples. Animals were injected with 2.5 μCi of [^{14}C]inulin in 600 μl of saline over a 30 sec period, followed by a 100 μl flush with saline. At 3 min, blood samples were removed from the femoral artery; for whole blood and plasma preparations, samples were collected in pre-heparinised (10 u ml^{-1}) Beckman microcentrifuge tubes and for serum preparation, blood was collected in microcentrifuge tubes containing glass beads. Plasma was obtained by centrifugation of blood at 10000 g for 2 min in a Beckman microcentrifuge. For each animal duplicate (50 μl) aliquots of whole blood and plasma sample were pipetted onto 1 cm glass fibre filter disks and transferred to 20 ml glass scintillation vials. Hydrogen peroxide (200 μl) was added dropwise, followed 30 min later by soluene (1 ml). Hionic Fluor scintillant was added (20 ml) two hours later. Serum was prepared by leaving blood samples overnight at 4°C, followed by centrifugation (10000 g, 2 min at 4°C), with 50 μl aliquots of serum added to small filter disks and treated as above.

At 4 min after [^{14}C]inulin infusion, animals were perfused with saline via the aorta for 15, 30 or 60 sec. The cortex was immediately dissected and a tissue sample from either side of the brain (approximately, 100 mg) was removed from each animal, placed in glass scintillation vials and tissue weight determined. Following addition of soluene (1 ml), samples were incubated at 56°C for 120 min then left overnight at room temperature before addition of Hionic Fluor scintillant (20 ml). Radioactivity in blood samples and brain tissue was measured in a 2500TR Packard scintillation counter using automatic quench correction, with samples counted for 10 min and results expressed as dpm per sample.

3.2.4. *In Vivo* Distribution of the Radioligands [^{3}H]DPCPX and [^{3}H]Flunitrazepam

The *in vivo* distribution in brain of [^{3}H]DPCPX was assessed and compared with [^{3}H]flunitrazepam, a compound known to cross the BBB. [^{3}H]DPCPX (98.1 Ci mmol^{-1}; NEN) and [^{3}H]flunitrazepam (84 Ci mmol^{-1}; NEN) were diluted with their respective cold ligands and were given at doses known to be pharmacologically active. Rats were anaesthetised with 4% halothane in oxygen and nitrous oxide (30:70 v:v) and placed in a incubator on a heated blanket to maintain body temperature. PE50 catheters were inserted into the femoral vein and animals infused with 20 μCi of [^{3}H]DPCPX (0.25 mg kg^{-1}) or 10 μCi of [^{3}H]flunitrazepam (0.17 mg kg^{-1}) in 500 μl of saline over a 30 sec period. At 20 and 60 min for [^{3}H]DPCPX, and 20 min for [^{3}H]flunitrazepam, blood samples (7 ml) were removed from the inferior vena cava through heparinised syringes and collected in heparinised (10 u ml^{-1}) blood pots. Duplicate (50 μl) aliquots of whole blood were added to 20 ml glass scintillation vials. Hydrogen peroxide (200 μl) was added dropwise, followed 30 min later

by soluene (1 ml). Hionic Fluor scintillant (20 ml) was added two hours later.

After collection of blood samples, the brain was removed and seven different brain regions (frontal cortex, rear cortex, hippocampus, striatum, brain stem, midbrain and cerebellum) were immediately dissected and tissue samples from each side of the brain (approximately, 30-200 mg per area) were removed from each animal, placed in glass scintillation vials and tissue weight determined. Following addition of soluene (1 ml), samples were incubated at 56°C for 120 min and left overnight at room temperature, before addition of Hionic Fluor scintillant (20 ml). Radioactivity in blood and brain tissue was measured in a 2500TR Packard scintillation counter using automatic quench correction, with samples counted for 10 min and results expressed as dpm per sample.

3.2.5. Data Analysis

For all competition experiments, the appropriate [^{3}H]DPCPX standard curves were constructed for test compounds, IC_{50} values were determined using the iterative curve fitting programme Sigma plot and K_i values were calculated (Cheng and Prusoff, 1973). Drug concentrations in samples from treated animals were calculated as described in the methodology of each assay. For each drug dose given to treated animals, drug concentrations in brain, serum and tissue supernatant were determined in duplicate using at least three animals and shown as a mean ± SE.M.

For the [^{14}C]inulin data, results were expressed as dpm g^{-1} brain tissue. The amount of plasma in the brain (brain plasma) was determined at each timepoint by dividing dpm g^{-1} (brain samples) by dpm μl^{-1} (plasma samples). Values for serum and whole blood were obtained in a similar manner to plasma. Statistical analysis was conducted by a one-way analysis of variance

(ANOVA) followed by a Dunnett's test.

For the [^{3}H]DPCPX and [^{3}H]flunitrazepam *in vivo* distribution studies, results were expressed as percent injected dose per gram of brain tissue. Values for each brain area were obtained from both halves of four animal brains and expressed as a mean ± S.E.M. Using the specific activity of each radioligand and the exact tissue weight, values were then expressed as a potential concentration in brain tissue.

3.2.6. Statistical Analysis

Data in tables and text are shown as mean ± the standard error (S.E.M.) for at least three separate experiments for K_i values and for three animals or more for drug concentrations. Statistical analyses used were the Students t-test, a one-way analysis of variance (ANOVA), a two-way anova and a Dunnett's test (JMP and Sigma Stat).

3.2.7. Materials

Radioligands were purchased from New England Nuclear (NEN) and adenosine deaminase (Type VIII) from Sigma. All FK and FR compounds were synthesised by the Fujisawa Pharmaceutical Co. Ltd, as were KW3902 (FR144942), MDL102234 (FR160502) and Takeda (FR160492). Standard adenosine agonists and antagonists were purchased from Research Biochemicals Inc. (RBI). The vehicles in which drugs were dissolved for intraperitoneal injection were Oil of Arachis (DPCPX, FR144942, FR160492, FR160502), cyclodextrin (DPSPX, 8-PST, DPX, CPT, 8-PT, FK838, FK453, FR160537, FR171562) and saline (FK352, FR129946, FR182303, FR182394). All other standard laboratory chemicals were from Sigma, Fisons and BDH and were of the highest grade available.

3.3. Results

3.3.1. Measurement of Adenosine Receptor Antagonists in Rat Brain Using *Ex Vivo* Binding

A pilot study was conducted to assess if DPCPX, when given at behaviourally relevant doses (i.e. doses known to produce a reversal of the hypolocomotion induced by the adenosine agonist CPA, Dr H.M. Marston, personal communication), could be measured in rat brain following i.p. administration. Four groups of animals were given vehicle or DPCPX (0.01, 0.1 and 1.0 mg kg^{-1}), the brain removed and the cortex dissected and homogenised 20 min post-injection. In order to estimate DPCPX concentrations in brain homogenate from treated animals, four [^{3}H]DPCPX standard inhibition curves using increasing concentrations of unlabelled DPCPX and control brain homogenate from four separate vehicle treated animals were constructed and results averaged to generate one standard curve. DPCPX (0.01 mg kg^{-1}) was not detectable in brain homogenate, however, at the higher doses of 0.1 and 1.0 mg kg^{-1}, brain concentrations were 69.7 ± 2.3 nM and 202.8 ± 10.7 nM respectively (Figure 3.1). The final concentrations shown take into account the initial 10 fold dilution of the homogenate and the 20 fold dilution in the assay; i.e. concentrations determined from the standard curve are multiplied 200 fold. The use of this crude cortical homogenate for generating standard curves, rather than P_2 cortical synaptosomes, used in our standard [^{3}H]DPCPX binding assay (K_D=0.33 ± 0.02 nM; B_{max}=1.90 ± 0.08 pmol mg^{-1} protein), gave different pharmacological parameters with a K_D of 0.61 ± 0.01 nM and a B_{max} of 2.32 ± 0.10 pmol mg^{-1} protein. Since drug levels measured are dependent on the affinity of the compound and the level of specific binding from standard curves, variations in these parameters may effect the level of drug measured. It is also

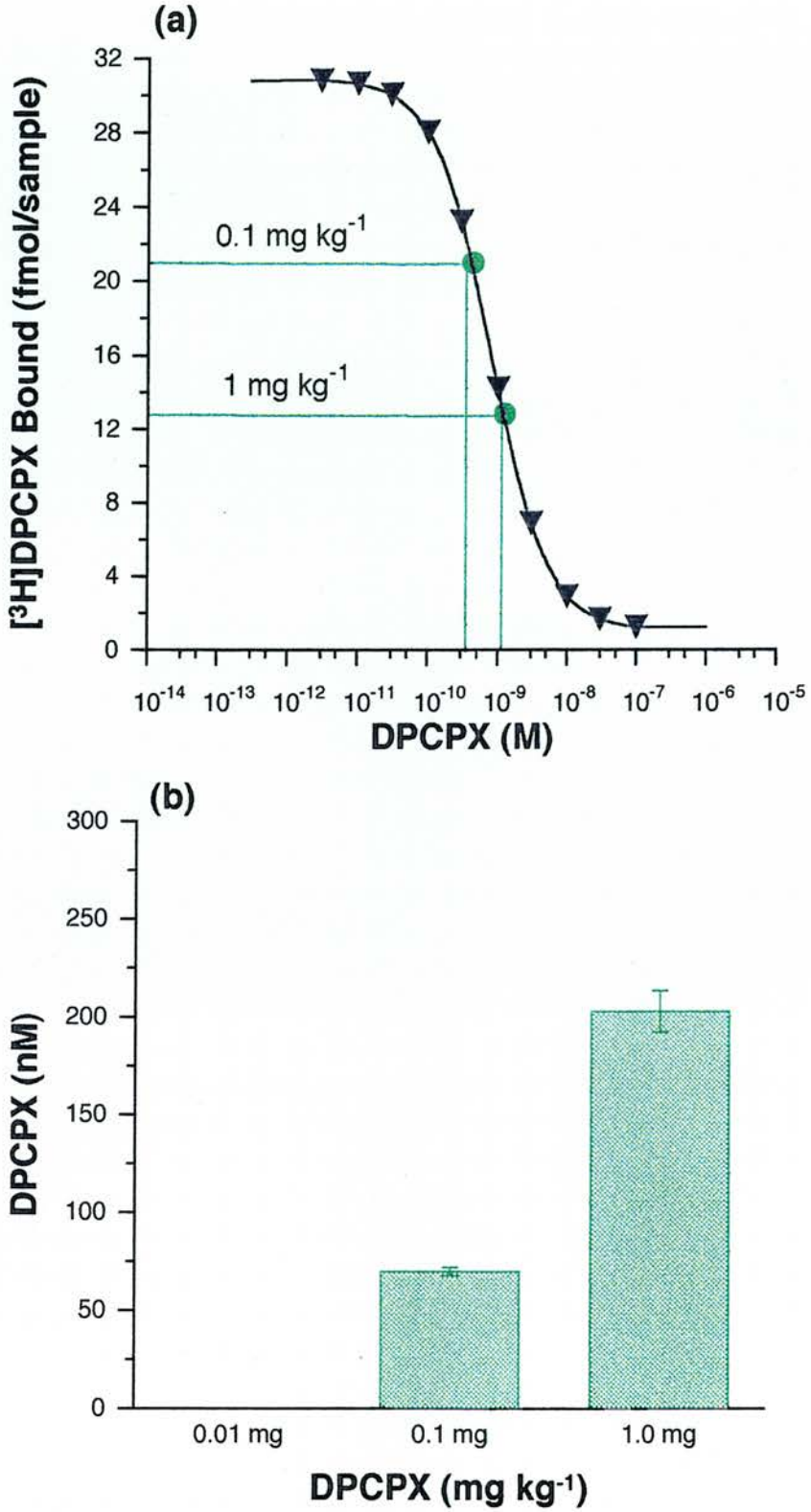

Figure 3.1 DPCPX Concentration in Brain Tissue Measured at 20 min After i.p. Injection by *Ex Vivo* Binding.

Drug concentrations for each dose are determined from the (a) standard curve with (b) mean values ± S.E.M. for four animals shown.

very difficult to modify this assay to allow the detection of samples which fall below the detection limit of the assay. In an attempt to enhance sensitivity, to avoid potential inter-animal variation and to be able to determine drug concentrations in other tissues we developed a modified radioreceptor assay.

3.3.2. [^{14}C]Inulin Tracer Study

Contamination of brain tissue by drug present in residual cerebral blood may complicate determination of drug concentrations. A transcardiac perfusion step can be used to reduce potential contamination. The efficiency of perfusion and the minimum time required to remove maximal blood from brain vasculature was assessed using [^{14}C]inulin, a non-penetrating marker for blood plasma. Measurements of [^{14}C]inulin were made for brain tissue, whole blood, plasma and serum. In control (unflushed) rats, assuming radioactivity present is due solely to the presence of residual blood within the CNS, the blood content in brain was 21.5 ± 0.17 μl g^{-1} (n=3) (Figure 3.2). A maximal reduction was seen after perfusion with saline for 30 sec, with the blood content of brain significantly reduced to 8.15 ± 0.72 μl g^{-1} (n=3: $P < 0.05$). Results for plasma and serum were almost identical, following a similar profile to that of blood. The reason for the [^{14}C]inulin content in whole blood per gram of brain tissue being approximately double that of plasma and serum is because of the cellular content of blood. The level of contamination of brain tissue drug concentrations from drug present in residual cerebral blood would therefore be in the order of 1-2% with this being reduced a further 62% by the introduction of a transcardiac flush. In measuring the drug concentrations in brain tissue of treated animals we assumed free penetration within tissues and a specific gravity of 1.05 g ml^{-1}. Based on the assumption of free penetration within tissues, drug concentrations in blood would be equivalent to that of

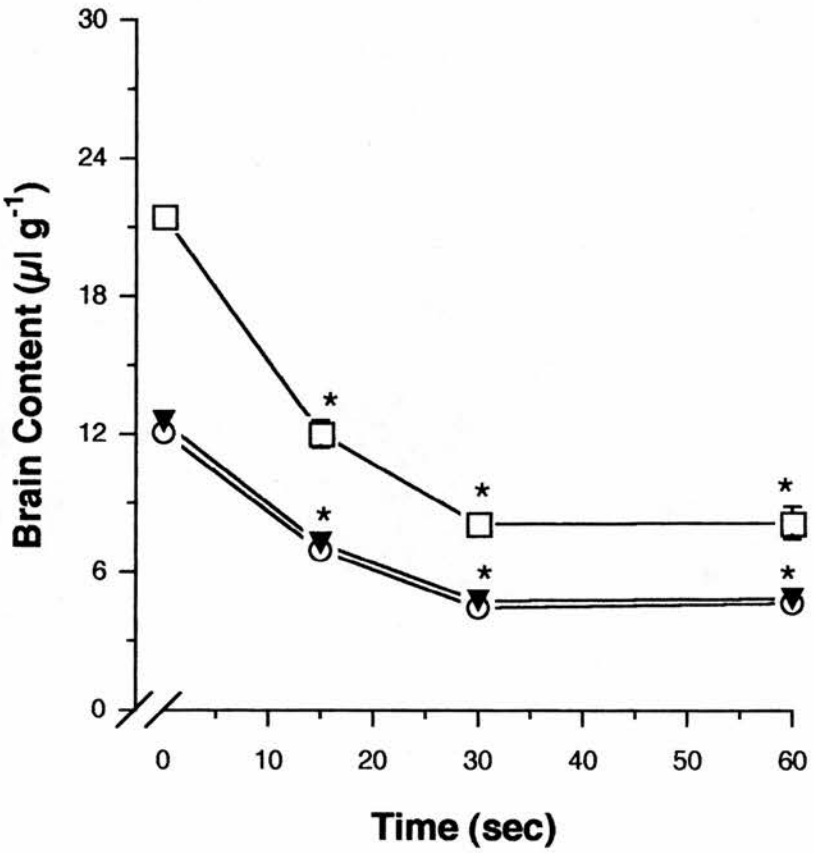

Figure 3.2 Effect of Increasing Transcardiac Perfusion Time.

[^{14}C]Inulin content in ○ plasma, ▼ serum and □ whole blood of rat brain. Brain content calculated as described in methods. Results expressed as mean ± S.E.M at each time point. Statistical comparisons made using a Dunnett's test between non-perfused (time 0 s) and each time point, within each group, *: $P < 0.05$.

plasma and serum and as a consequence serum concentrations were routinely determined for all treated animals. Subsequently all animals routinely received a transcardiac flush unless otherwise stated.

3.3.3. Measurement of Adenosine Receptor Antagonists in Rat Brain Using a Modified Radioreceptor Assay

Competition studies using the standard [^{3}H]DPCPX binding assay and rat brain P_2 cortical membranes showed binding was to a single population of receptors (nH=1), with a B_{max} of 1.90 ± 0.08 pmol mg^{-1} protein and a K_D of 0.327 ± 0.024 nM. K_i values for DPCPX, DPSPX and 8-PST were consistent with binding to the adenosine A_1 receptor (Table 3.1).

Addition of brain homogenate from vehicle and drug treated animals as a 'competing drug' to the [^{3}H]DPCPX binding assay is complicated as the tissue also binds [^{3}H]DPCPX. To remove the intrinsic binding capacity of this brain homogenate, sonication for 30 min and treatment at 56°C for 60 min was assessed. Neither treatment completely abolished the binding capacity of brain homogenate (data not shown). However, incubation at 80°C for 15 min completely abolished the specific [^{3}H]DPCPX binding capacity of brain homogenate. Treatment at 80°C did not, however, affect drug stability (Figure 3.3).

Addition of denatured control brain homogenate or serum from vehicle treated animals to [^{3}H]DPCPX standard curves using washed P_2 membranes did not alter the total amount of specific binding despite a 30% increase in non-specific binding for the brain homogenate (Figure 3.4), or the affinity of test drugs, as shown for DPCPX (Table 3.1).

Known concentrations of DPCPX were added to denatured control brain homogenate from vehicle treated animals. These samples were then added to

Table 3.1. [^{3}H]DPCPX Receptor Pharmacology

	K_i (nM)	(nH)
DPCPX	0.33 ± 0.02 *	1.04 ± 0.01
DPSPX	91.6 ± 2.73	0.97 ± 0.05
8-PST	1380± 86.5	0.94 ± 0.06
DPCPX + control brain	0.35 ± 0.03 * (n=7)	0.96 ± 0.06
DPCPX + control serum	0.36 ± 0.02 * (n=10)	1.08 ± 0.03

K_i and Hill slope (nH) determined from competition experiments, as described in the methods. Values expressed as mean ± S.E.M ($n \geq 3$). K_i values for DPCPX in the presence of denatured control brain homogenate and serum from vehicle treated animals were determined as for competition experiments. Numbers shown in brackets are for direct comparisons with DPCPX alone. Not significantly different in a t-test. *: $P < 0.05$.

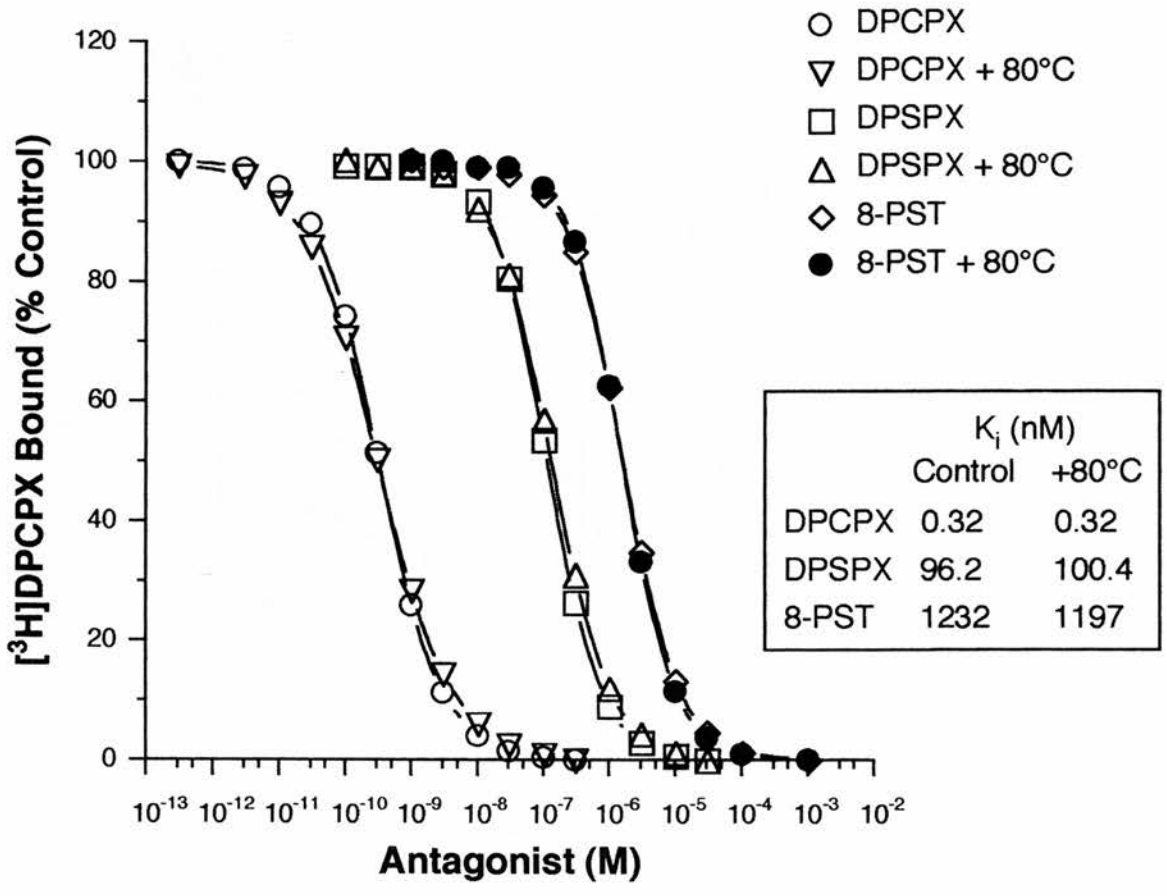

Figure 3.3 Effect of Treatment at 80°C on Adenosine Antagonists.

The data represent a typical experiment, each point performed in duplicate. Drugs were treated in the presence of buffer for 15 min at 80°C with K_i values determined as in methods. Data shown in inset is from parallel experiments.

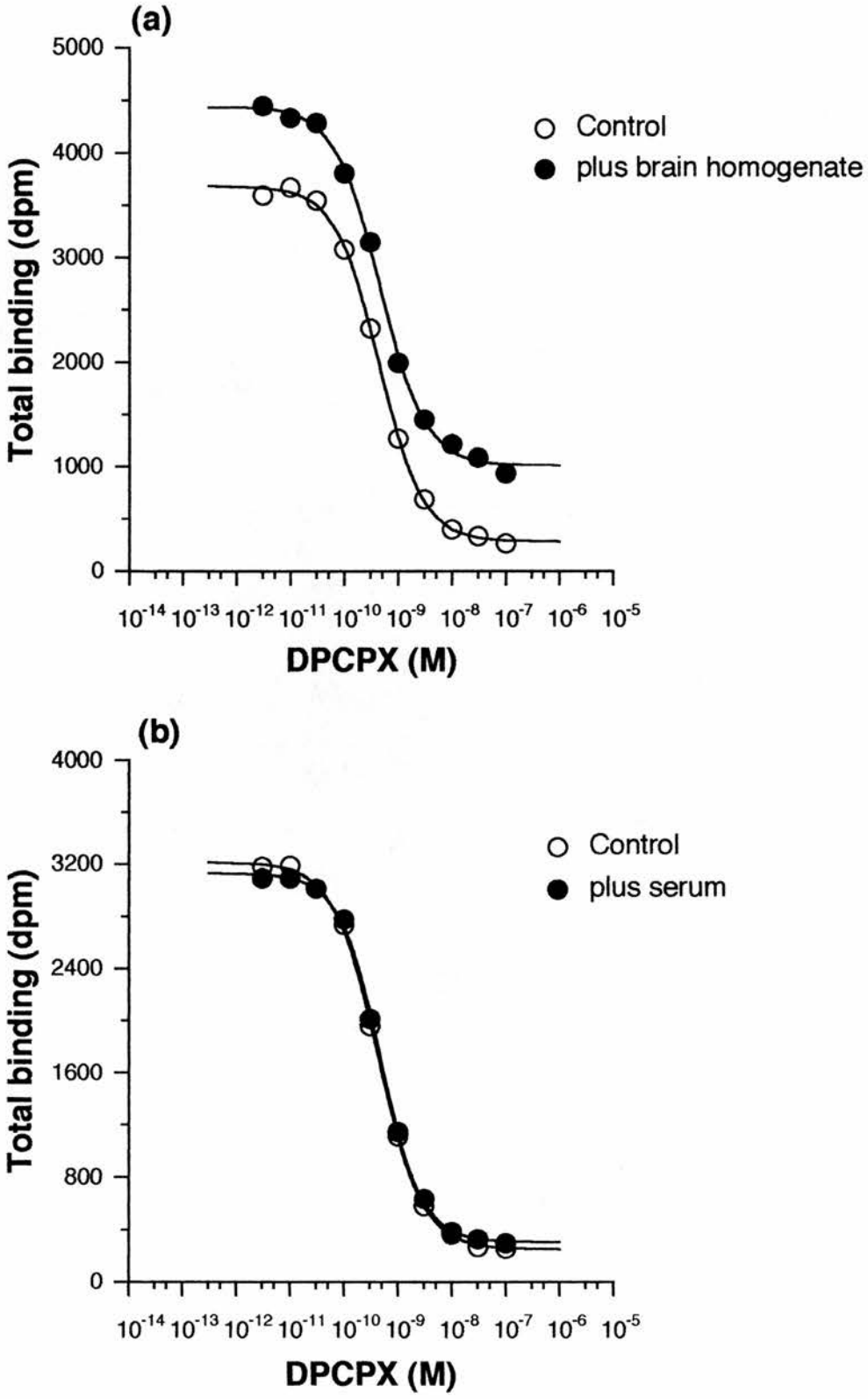

Figure 3.4 Effect of Denatured Control (a) Brain Homogenate and (b) Serum Samples on Inhibition of [^{3}H]DPCPX Binding.
The data represent a typical experiment, each point performed in duplicate with mean data obtained from at least three experiments (Table 3.1).

the [^{3}H]DPCPX binding assay to determine the detection limits for the assay. Addition of DPCPX to denatured control brain homogenate at concentrations causing < 10% or > 90% inhibition of [^{3}H]DPCPX binding in the standard (1 ml) assay were less reliable (Table 3.2). Brain and serum concentrations for drugs were subsequently accepted for samples which gave between 10% and 90% inhibition of [^{3}H]DPCPX binding, giving a 100 fold concentration range over which drug concentration can be reliably measured. For samples of DPCPX treated control brain homogenate causing < 10% or > 90% inhibition of [^{3}H]DPCPX binding, assay conditions were altered. For samples of DPCPX treated control brain homogenate causing > 90% inhibition of [^{3}H]DPCPX binding, a simple 10 fold dilution of the homogenate with untreated control brain homogenate could be used to accurately determine drug concentration (Table 3.2). For samples causing < 10% inhibition, attempts were made to increase sensitivity by (a) reducing the volume of the assay and by (b) adding increased amounts of homogenate. Reducing the assay volume from 1 ml to 0.5 ml, without altering the amount of homogenate added was attempted. A concentration of DPCPX (0.3 nM) which caused approximately 50% inhibition was initially tried (Table 3.2). As the results of the 1 ml and 0.5 ml assays were similar when compared directly, this would appear to be a valid way of doubling the sensitivity of the assay (Table 3.2). An upper limit is reached on adding increasing volumes of homogenate as anything above 70 μl of 10 vol. of brain homogenate blocks filtration. Alteration from GF-B to GF-C filters provided no further improvement (data not shown). To overcome this problem, brain homogenate with known concentrations of DPCPX added was centrifuged and DPCPX concentration measured in tissue supernatant as described for GABA (Enna, 1978). Detection of DPCPX in tissue supernatant was possible at 0.3 and 1 nM, however, supernatant concentrations were only 41.6 and 30.9% of respective brain homogenate concentrations. DPCPX

Table 3.2 Validation of the Assay Limitations for the Radioreceptor Assay

DPCPX added (nM)	Standard Assay (1 ml) DPCPX (nM)	± Error	% Inhibition	0.5 ml Assay DPCPX (nM)	± Error	% Inhibition
0.003	0.026 ± 0.007	+8.66	3.45 ± 0.92	N.T.	--	N.T.
0.01	0.036 ± 0.011	+3.60	7.06 ± 2.18	N.T.	--	N.T.
0.03	0.062 ± 0.023	+2.07	7.80 ± 3.21	0.027 ± 0.012	-0.90	5.70 ± 2.34
0.1	0.121 ± 0.010	+1.21	20.4 ± 1.27	0.099 ± 0.011	-0.99	17.6 ± 1.46
0.3	0.331 ± 0.004	+1.10	40.9 ± 0.30	0.270 ± 0.013	-0.90	35.4 ± 1.04
1	0.972 ± 0.043	-0.97	59.0 ± 1.09	**Diluted Assay (10 fold dilution)**		
3	3.105 ± 0.23	+1.04	86.0 ± 0.99	0.316 ± 0.011	+1.05	39.7 ± 0.83
10	9.11 ± 2.53	-0.91	95.6 ± 0.91	1.054 ± 0.009	+1.05	61.0 ± 0.20
30	267 ± 203	+8.90	99.4 ± 0.28	3.196 ± 0.227	+1.07	89.7 ± 0.70

DPCPX concentration measured in standard (1ml), diluted and 0.5 ml [^{3}H]DPCPX radioreceptor binding assays. For the 0.5 ml assay the amount of homogenate added was unaltered while the amount of drug, P_2 membranes, ADA and [^{3}H]DPCPX were halved and the volume of buffer adjusted accordingly. In the diluted assay the brain homogenate containing DPCPX was diluted 10 fold with control homogenate. Values expressed as mean ± S.E.M ($n \geq 4$). Each concentration determined is shown with ± the fold error on the individual value and its associated level of inhibition in the assay (N.T. - not tested).

concentration in serum samples was determined in the same way as brain homogenate. For serum samples which cause > 90% inhibition of [^{3}H]DPCPX binding, samples were diluted. For those causing < 10% inhibition of [^{3}H]DPCPX binding, adding increased amounts of serum did not block filtration. However, data indicate that unless serum samples receive a 5 fold dilution before addition to the assay (hence a 100 fold final dilution) specific binding is reduced (data not shown).

DPCPX (0.01-1.0 mg kg^{-1}) was administered i.p. to two groups of animals, with one group receiving a transcardiac perfusion with saline. Standard [^{3}H]DPCPX inhibition curves using washed P_2 membranes were constructed in the absence and presence of denatured control brain homogenate or serum from vehicle treated rats using a range of DPCPX concentrations (0.003-100 nM). The DPCPX concentration in samples of brain homogenate and serum from drug treated animals were determined from the appropriate standard curve and values multiplied by 200 fold to take into account the dilutions of brain and serum in the assay. In both groups, there was a dose dependent increase in DPCPX concentration measured in brain and serum (Figure 3.5). For both groups, DPCPX concentrations in brain tissue were measured using the *ex vivo* binding and radioreceptor assays (Table 3.3). For flushed and unflushed rats (groups 1 & 2), DPCPX was undetectable at 0.01 and 0.03 mg kg^{-1} using *ex vivo* binding (as in the pilot study: see 3.3.1.), whereas using the radioreceptor assay DPCPX concentrations were measurable at all five doses in brain tissue for both groups (Table 3.3). In groups 1 (unflushed rats) and 2 (flushed rats), for concentrations of DPCPX that were measurable in brain by both methods, there was no significant difference between methods when assessed using a two-way anova ($P > 0.05$). There was, however, a significant dose dependent

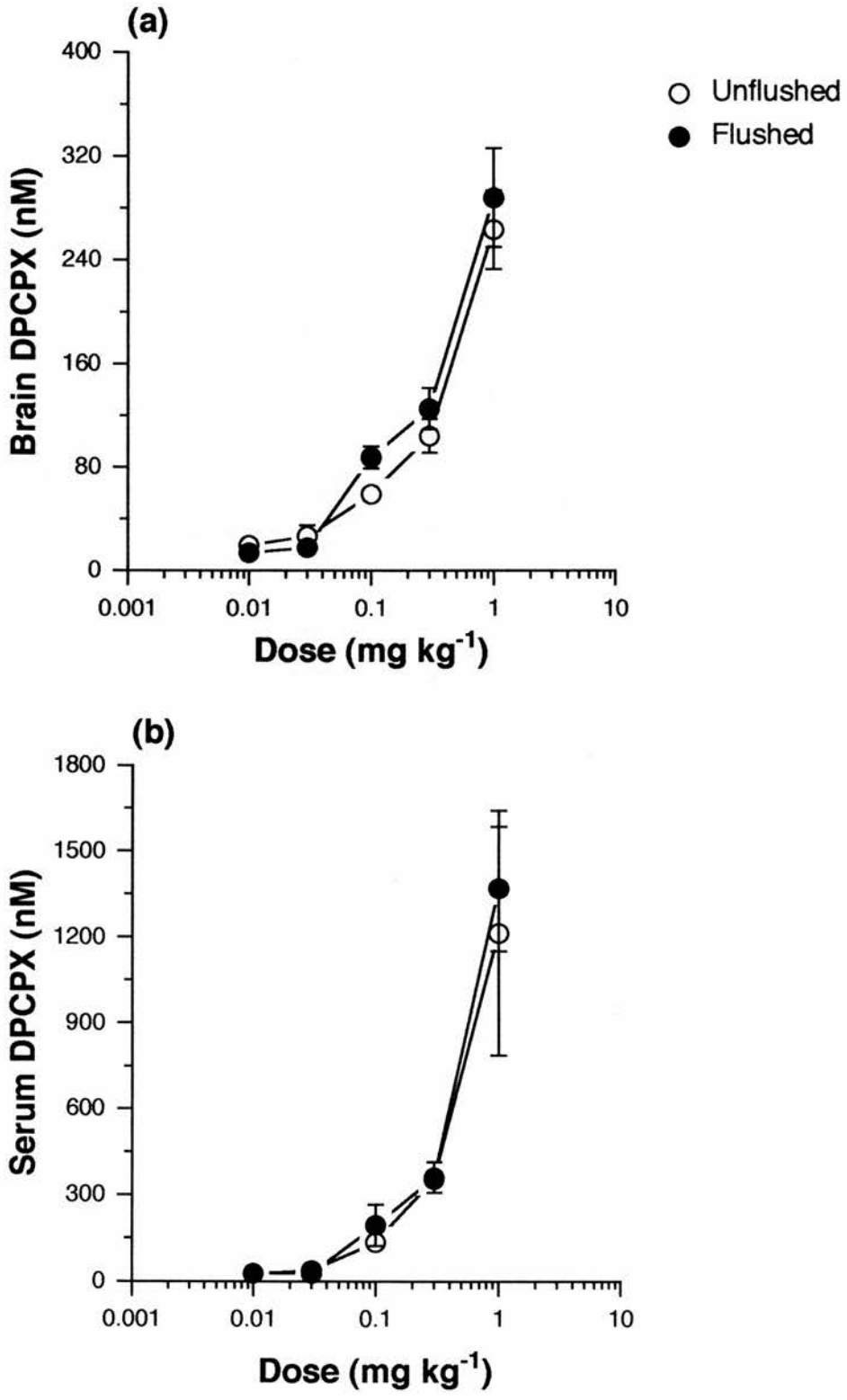

Figure 3.5 Dose Dependence of DPCPX Concentration in (a) Brain and (b) Serum in Flushed and Unflushed Animals.

The data represent the mean ± S.E.M. of duplicate determinations from at least three different animals for all concentrations. Concentrations were determined as described in the methods at 20 min after i.p. injection.

Table 3.3 DPCPX Concentration in Brain Tissue and Serum as Determined by *Ex Vivo* Binding and Radioreceptor Assay

	Group 1 (Unflushed)				Group 2 (Flushed)			
	Ex vivo Assay	Radioreceptor Assay			*Ex vivo* Assay	Radioreceptor Assay		
Dose (mg kg^{-1})	Brain (nM)	Brain (nM)	Serum (nM)	Ratio	Brain (nM)	Brain (nM)	Serum (nM)	Ratio
0.01	N.D.	19.7 ± 2.62	26.3 ± 5.71	0.75	N.D.	13.8 ± 2.41	26.5 ± 2.60	0.52
0.03	N.D.	26.7 ± 8.61	37.1 ± 14.7	0.72	N.D.	17.7 ± 2.05	26.5 ± 5.40	0.67
0.1	44.4 ± 2.57	53.5 ± 3.07	136 ± 28.6	0.39	83.0 ± 4.40	87.7 ± 4.60	195 ± 72.5	0.45
0.3	87.2 ± 8.32	87.2 ± 7.27	355 ± 31.2	0.25	106 ± 14.4	126 ± 16.0	362 ± 53.7	0.35
1	204 ± 29.0	238 ± 41.6	1210± 430	0.20	297 ± 21.9	288 ± 38.0	1370± 217	0.21
1*	N.T.	N.T.	N.T	--	259 ± 30.2*	257 ± 63.2*	N.T.	--

DPCPX concentration measured in the [^{3}H]DPCPX *ex vivo* and radioreceptor binding assays for two groups of animals, only one of which had received a transcardiac flush (N.B. * was unflushed). Values expressed as mean ± S.E.M of duplicate determinations for at least three different animals. Ratio is the brain to serum ratio for each group as determined using the radioreceptor assay. (N.D. - not detectable within assay limitations). (N.T. - not tested).

increase in DPCPX concentration for groups 1 ($F_{(2,44)}$=165.4, $P < 0.05$) and 2 ($F_{(2,26)}$=55.7, $P < 0.05$). Taking the radioreceptor assay and comparing flushed and unflushed groups of animals there appears to be a reasonable overall agreement in DPCPX concentrations in brain and serum (Table 3.3). However, DPCPX concentrations in brain are lower at 0.01 and 0.03 mg kg^{-1} and higher at 0.1 and 0.3 mg kg^{-1} in the flushed group than the unflushed group. Higher values in the flushed group would be unexpected as flushing should reduce the overall brain concentration by either reducing the contribution from drug in blood or possibly by reversing the blood-brain concentration gradient and flushing drug out of the brain. A similar pattern to brain was also observed with serum concentrations for the two groups of animals. As the brain to serum ratios in the radioreceptor assay are quite similar in both flushed and unflushed groups for DPCPX, any differences observed may be attributable to differences between the groups rather than an effect of the flushing. The possibility of drug being flushed out of the brain seems unlikely as DPCPX concentrations in unflushed rats in group 2 at 1mg kg^{-1} were not significantly different from flushed rats (in a t-test, $P < 0.05$) (Table 3.3). This was also observed for FR129946, FR160537 and FR171562 (see 3.3.5. & Table 3.5). Fresh and frozen brain and serum samples from treated animals gave similar results (data not shown). All animals subsequently received a 30 sec transcardiac perfusion with saline prior to the removal of cortex and the radioreceptor assay was routinely used to measure brain homogenate and serum concentrations of drugs.

Animals were given DPCPX (1 mg kg^{-1}) to determine the DPCPX concentration in brain homogenate and serum at various time points. There was a time dependent decrease (Figure 3.6) in DPCPX concentration in brain and serum, measured over the period of 20-180 min with $t_{1/2}$ values of 35.2

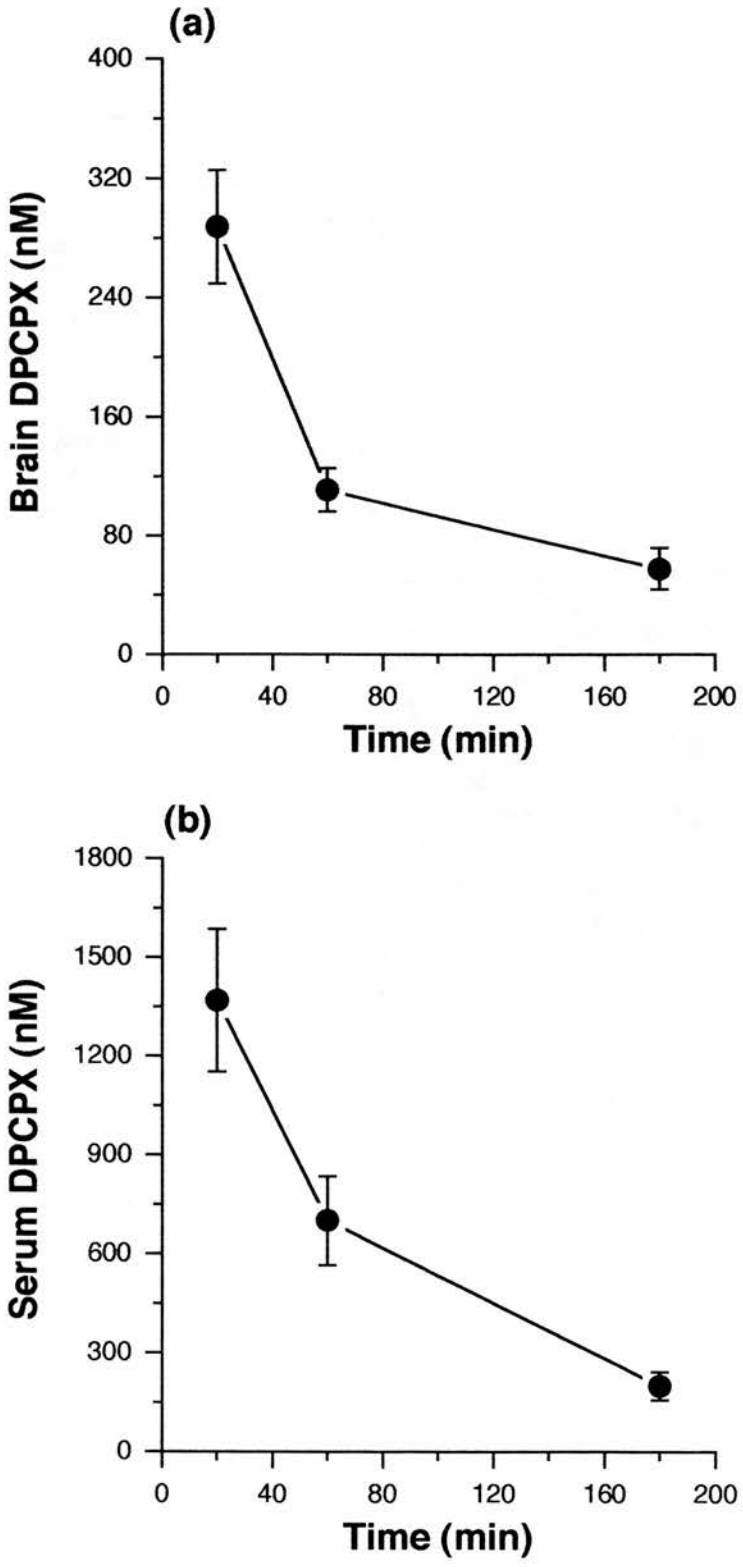

Figure 3.6 Time Dependence of DPCPX (1 mg kg^{-1}) Concentration in (a) Brain and (b) Serum.

The data represent the mean ± S.E.M. of duplicate determinations from at least three different animals for each time point. The DPCPX concentrations were determined as described in the methods.

min and 47.1 min respectively.

The brain penetration of DPSPX and 8-PST, two adenosine receptor antagonists reported not to cross the BBB, was tested to further validate the assay. Standard [^{3}H]DPCPX inhibition curves using washed P_2 membranes were constructed in the absence and presence of denatured control brain homogenate or serum from vehicle treated rats using an appropriate concentration range for DPSPX and 8-PST. Injection (i.p.) of DPSPX (5.6 mg kg^{-1}) and 8-PST (20 mg kg^{-1}), gave serum concentrations of 56 ± 3 μM and 52 ± 8.3 μM respectively, when measured 20 min post-injection. Despite high serum concentrations, neither drug was detectable in brain at this time point. Estimated brain to serum ratios were calculated on the basis that samples of brain homogenate containing DPSPX and 8-PST caused < 1% inhibition of [^{3}H]DPCPX binding (Table 3.4).

3.3.4. *In Vivo* Distribution of [^{3}H]DPCPX & [^{3}H]Flunitrazepam

An independent assessment of DPCPX penetration into the CNS was made by giving [^{3}H]DPCPX intravenously. [^{3}H]Flunitrazepam, a compound known to cross the BBB, was used as a positive control, with both compounds measured in various brain regions. DPCPX (0.25 mg kg^{-1}) and flunitrazepam (0.17 mg kg^{-1}) when given at pharmacologically active doses crossed the BBB as shown for frontal cortex (Figure 3.7). DPCPX concentration decreased with time in frontal cortex, however blood levels were not significantly different at the two time points. A brain to blood ratio at 20 min of 0.18, is similar to values for unflushed (0.25) and flushed (0.35) animals, at a comparable dose of 0.3 mg kg^{-1}, determined using the radioreceptor assay (Table 3.3). The brain to blood ratio of 0.08 at 60 min, is similar to that of 0.16 in the radioreceptor assay (Figure 3.6), despite a four fold difference in dose. For flunitrazepam,

Table 3.4 Relationship Between Brain and Serum Concentrations for Adenosine Receptor Antagonists

	Dose (mg kg^{-1})	Concentration (nM) Brain	Serum	K_i (nM)	Ratio Brain / Serum
DPSPX	5.6	< 238	56300 ± 2930	91.6	< 0.004
8-PST	20	< 3580	51960 ± 8260	1380	< 0.068
DPCPX	0.01	13.8 ± 2.4	26.5 ± 2.6	0.33	0.52
	0.1	87.7 ± 8.6	195 ± 72.5	--	0.45
	1	288 ± 38.0	1370 ± 220	--	0.21

Drug concentrations were measured in the [^{3}H]DPCPX radioreceptor binding assay for both brain and serum samples. Values for DPSPX and 8-PST in brain correspond to the concentration of drug in brain tissue which would cause <1% inhibition of [^{3}H]DPCPX binding in the radioreceptor assay. Brain and serum concentrations expressed as mean ± S.E.M of duplicate determinations for at least three different animals. K_i values determined in competition binding assays as described in the methods and values expressed as mean ± S.E.M. ($n \geq 4$). Ratio is brain concentration divided by serum concentration for each dose.

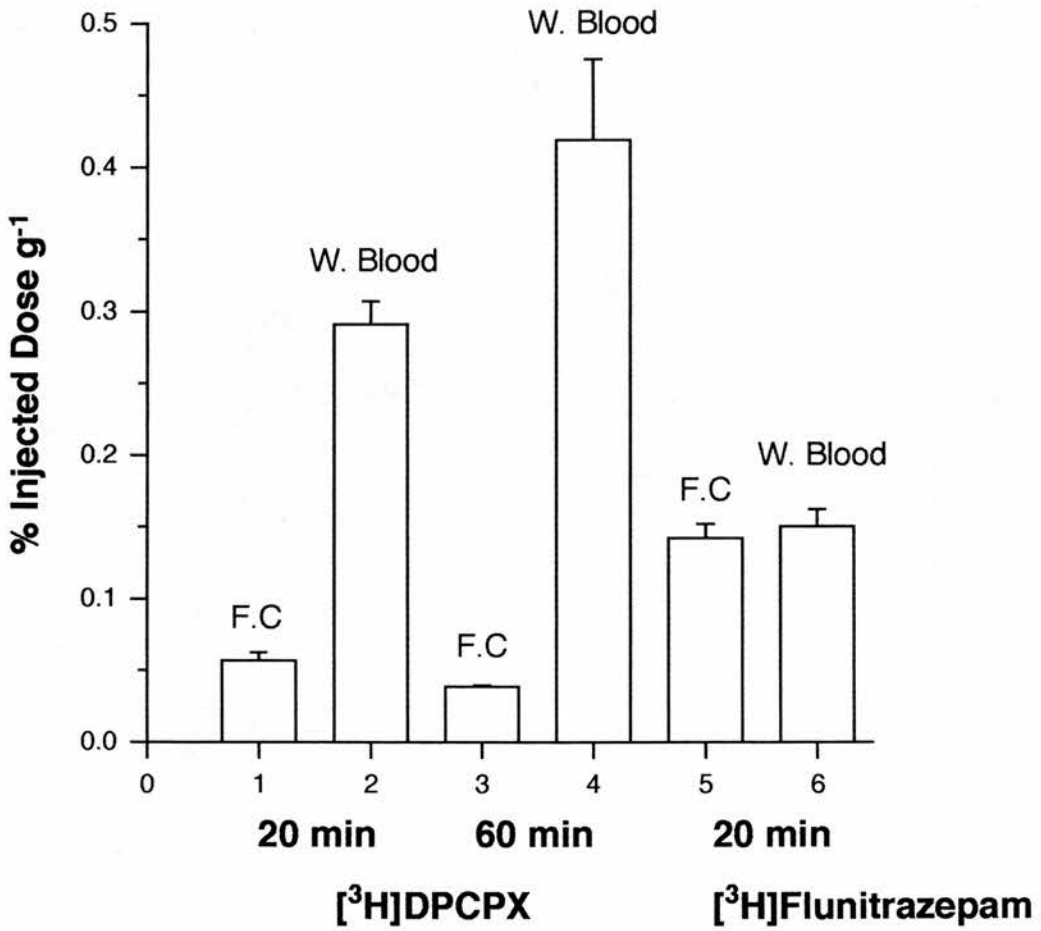

Figure 3.7 [^{3}H]DPCPX and [^{3}H]Flunitrazepam Shown as Percent of Injected Dose in Frontal Cortex (F.C) and Whole Blood.

Values are the mean ± S.E.M of duplicate tissue samples from four animals.

the brain to blood ratio at 20 min was 1.06 with brain levels of this compound being more than double DPCPX. Conversion of the data from % injected dose per gram tissue to nanomolar, is shown for various brain regions and whole blood (Figure 3.8). Each drug showed similar concentrations in all brain regions tested, which decreased in a time dependent manner for DPCPX. The DPCPX concentration in brain at the 20 min time point of approximately 140 nM is similar to that measured in the radioreceptor assay (126 nM: Table 3.3) at 0.3 mg kg^{-1}. Also the DPCPX concentration in brain at the 60 min time point of about 90 nM is similar to that measured in the radioreceptor assay of 110 nM (Figure 3.6), despite the four fold difference in dose. The percentage of injected dose for flunitrazepam was approximately 2 fold higher in all brain regions compared with DPCPX.

3.3.5. Adenosine Antagonist Concentrations in Rat Brain

Having characterised this modified radioreceptor assay, the characteristics of the three lead Fujisawa antagonists, FR129946, FR160537 and FR171562 were examined. As stated above, all animals received a 30 sec transcardiac perfusion prior to removal of the cortex. FR129946 (0.01-10 mg kg^{-1}), FR160537 (0.01-1.0 mg kg^{-1}) and FR171562 (0.01-1.0 mg kg^{-1}) were administered i.p. to 3 groups of animals. These doses cover a range of doses known to reverse CPA induced hypolocomotion for each individual drug (Dr H.M. Marston, personal communication). All three drugs were examined at 1 mg kg^{-1} to determine drug concentrations in brain homogenate and serum at various time points. Standard [^{3}H]DPCPX inhibition curves, using washed P_2 membranes, were constructed in the absence and presence of denatured control brain homogenate and serum from vehicle treated rats, over an appropriate concentration range for each drug. All three drugs showed no

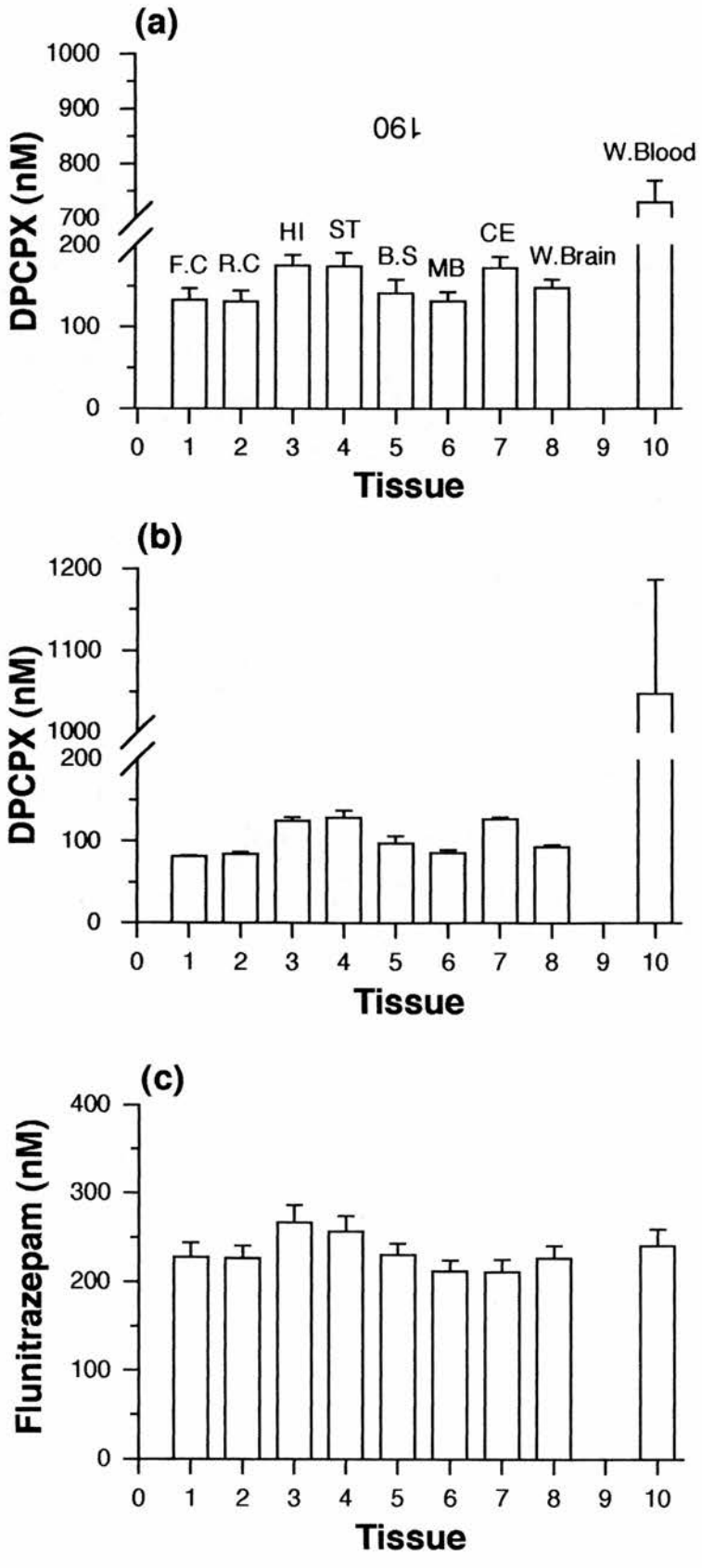

Figure 3.8 Concentration in Brain and Blood of DPCPX at (a) 20 min and (b) 60 min and Flunitrazepam at (c) 20 min.

1-Frontal Cortex: 2-Rear Cortex: 3-Hippocampus: 4-Striatum: 5-Brain stem 6-Midbrain: 7-Cerebellum: 8-Whole brain and 10-Whole blood.

alteration in affinity when incubated at 80°C, prior to determining K_i values (data not shown). FR129946, FR160537 and FR171562 all showed a dose dependent increase in concentration in brain and serum when measured 20 min after i.p. injection and a time dependent decrease (Figures 3.9, 3.10 and 3.11). Assuming the time dependent decrease is a first-order process $t_{1/2}$ values for time course studies were; 33.5 min and 26.8 min in brain and serum respectively for FR129946, 54.1 min and 21.1 min in brain and serum respectively for FR160537 and 94.9 min and 15.5 min in brain and serum respectively for FR171562. These compare with $t_{1/2}$ values of 35.2 min and 47.1 min in brain and serum respectively for DPCPX. As with DPCPX, addition of denatured control brain homogenate or serum from vehicle treated animals produced no significant alteration in affinity (in a t-test, $P < 0.05$) of the three Fujisawa compounds (Tables 3.5 & 3.6). Flushing had no significant effect on any of these compounds when measured at 1 mg kg^{-1} in brain or serum (Tables 3.5 & 3.6). As blood samples are collected before flushing no difference in the serum results would have been expected. Brain concentrations of FR160537 and FR171562 were similar to DPCPX, whereas FR129946 was undetectable at 0.01 and 0.03 mg kg^{-1} and the concentration determined at 0.1 mg kg^{-1} lower than that determined for the other three drugs (Table 3.5). This is reflected in their ED_{50} values, i.e. the dose of drug which inhibits 50% of [^{3}H]DPCPX binding (Figure 3.12). DPCPX, FR160537 and FR171562 all have similar *in vitro* affinities and ED_{50} values, whereas FR129946 has a 4-5 fold lower *in vitro* affinity and ED_{50}. A similar effect was observed for the *in vivo* dose response curves (data supplied by Dr H.M. Marston), which follow a similar profile to the *in vitro* dose response curves, with FR129946 to the right of the other 3 compounds (Figure 3.13). Serum concentrations, unlike brain, show a much larger variation for DPCPX,

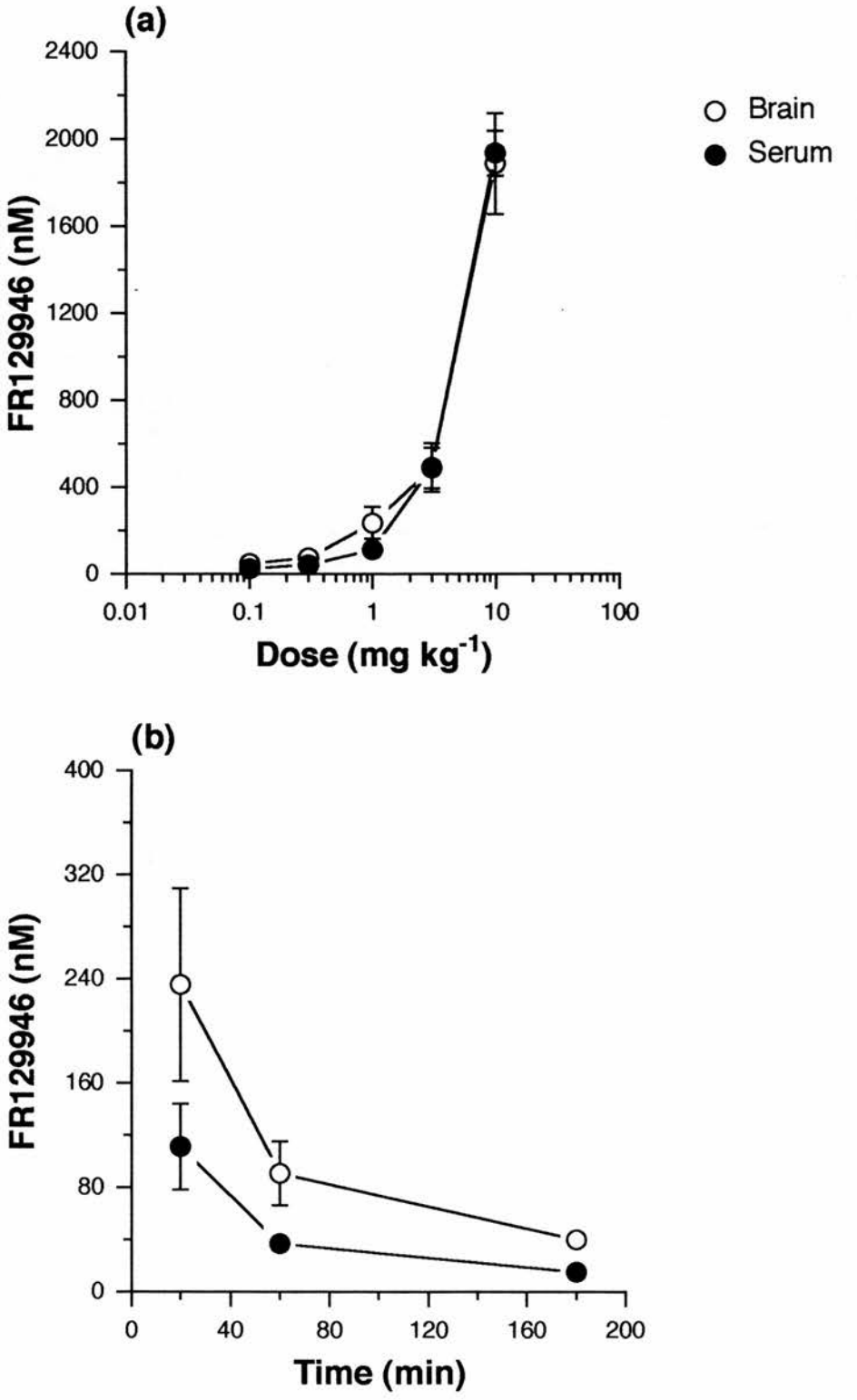

Figure 3.9 The (a) Dose and (b) Time Dependence of FR129946 Concentration in Brain and Serum.

The data represent the mean ± S.E.M. of duplicate determinations from at least three different animals for all concentrations and time points. Concentrations were determined as described in the methods at 20 min after i.p. injection in (a) and at various time points in (b).

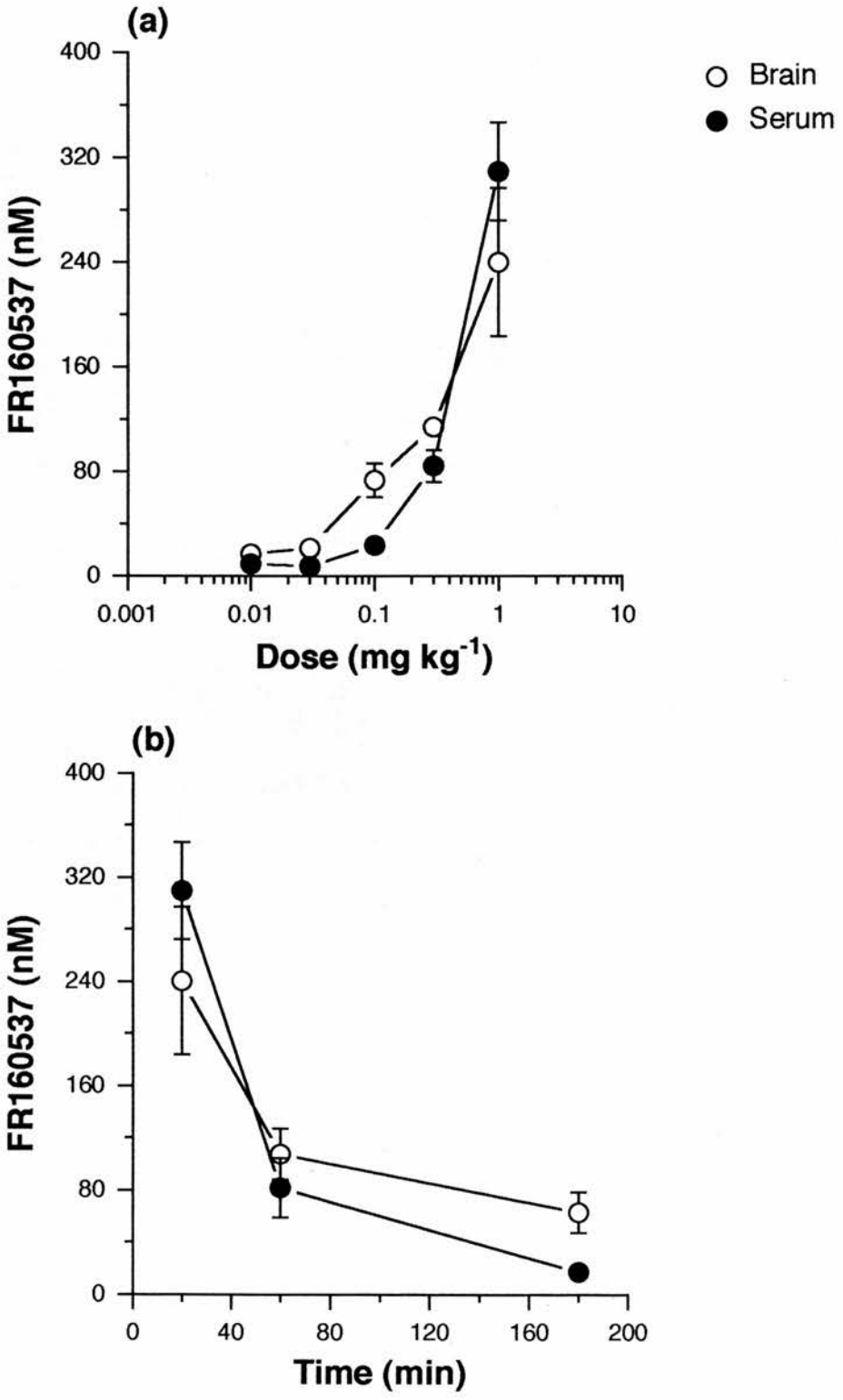

Figure 3.10 The (a) Dose and (b) Time Dependence of FR160537 Concentration in Brain and Serum.

The data represent the mean ± S.E.M. of duplicate determinations from at least three different animals for all concentrations and time points. Concentrations were determined as described in the methods at 20 min after i.p. injection in (a) and at various time points in (b).

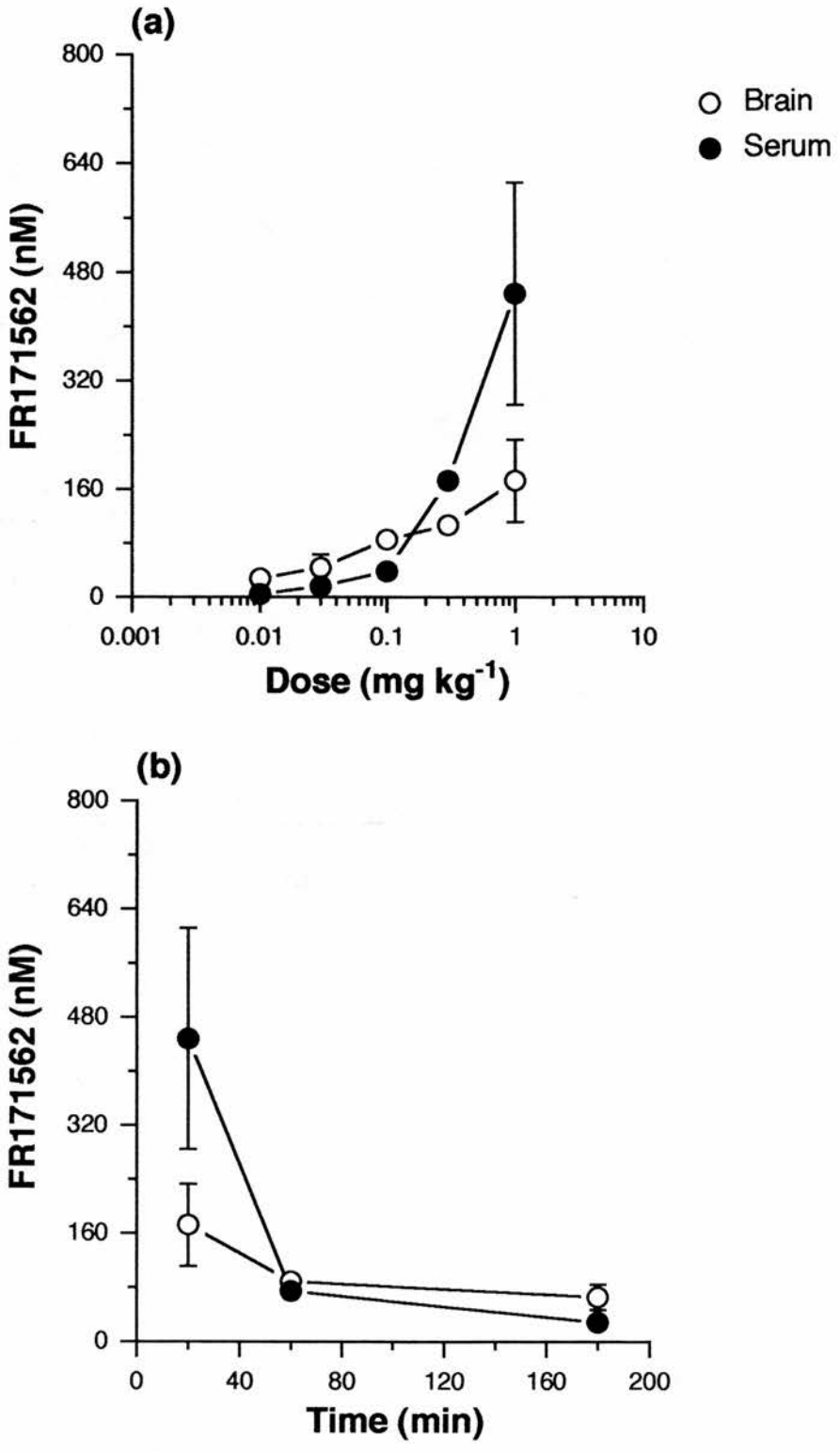

Figure 3.11 The (a) Dose and (b) Time Dependence of FR171562 Concentration in Brain and Serum.

The data represent the mean ± S.E.M. of duplicate determinations from at least three different animals for all concentrations and time points. Concentrations were determined as described in the methods at 20 min after i.p. injection in (a) and at various time points in (b).

Table 3.5 Concentration of Adenosine Antagonists in Brain Tissue

		DPCPX	FR129946	FR160537	FR171562
K_i (nM)		0.33 ± 0.02	1.12 ± 0.07	0.23 ± 0.01	0.27 ± 0.02
K_i +denatured tissue		0.35 ± 0.03	1.24 ± 0.07	0.24 ± 0.02	0.29 ± 0.03
Dose (mg kg^{-1})					
	0.01	13.8 ± 2.41	N.D.	17.0 ± 2.97	27.9 ± 4.32
	0.03	17.7 ± 2.05	N.D.	21.3 ± 2.33	43.7 ± 19.1
	0.1	87.7 ± 4.60	48.8 ± 2.31	73.5 ± 12.8	85.6 ± 15.3
	0.3	126 ± 16.0	74.1 ± 18.3	114 ± 4.56	106 ± 5.07
	1	288 ± 38.0	235 ± 74.2	240 ± 56.6	172 ± 60.9
Unflushed	1	257 ± 63.2	280 ± 58.6	198 ± 29.6	197 ± 11.5
	3	N.T.	487 ± 93.2	N.T.	N.T.
	10	N.T.	1880± 230	N.T.	N.T.

K_i values determined as in methods both in the absence and presence of denatured control brain homogenate (n≥3). Drug concentrations were measured using the [^{3}H]DPCPX radioreceptor binding assay. Values expressed as mean ± S.E.M of duplicate determinations for at least three different animals. There was no significant difference between flushed and unflushed animals for each drug at 1 mg kg^{-1} (t-test, $P < 0.05$). (N.D. - not detectable within assay limitations). (N.T. - not tested).

Table 3.6 Concentration of Adenosine Antagonists in Serum Samples

		DPCPX	FR129946	FR160537	FR171562
K_i (nM)		0.33 ± 0.07	1.01 ± 0.01	0.22 ± 0.01	0.30 ± 0.01
K_i +denatured serum		0.36 ± 0.02	0.99 ± 0.01	0.26 ± 0.02	0.29 ± 0.01
Dose (mg kg^{-1})					
	0.01	26.5 ± 2.60	N.D.	9.55 ± 2.70	4.83 ± 1.83
	0.03	26.5 ± 5.40	N.D.	7.87 ± 2.11	16.0 ± 10.9
	0.1	195 ± 72.5	23.9 ± 9.97	23.8 ± 3.70	38.6 ± 3.19
	0.3	362 ± 53.7	42.3 ± 9.08	84.5 ± 12.2	172 ± 6.98
	1	1370± 217	111 ± 32.9	310 ± 37.2	448 ± 164
Unflushed	1	1080± 350	147 ± 11.1	262 ± 70.9	478 ± 29.7
	3	N.T.	490 ± 112	N.T.	N.T.
	10	N.T.	1930± 104	N.T.	N.T.

K_i values determined as in methods both in the absence and presence of denatured control serum ($n \geq 3$). Drug concentrations were measured using the [^{3}H]DPCPX radioreceptor binding assay. Values expressed as mean ± S.E.M of duplicate determinations for at least three different animals. There was no significant difference between flushed and unflushed animals for each drug at 1 mg kg^{-1} (t-test, $P < 0.05$). (N.D. - not detectable within assay limitations). (N.T. - not tested).

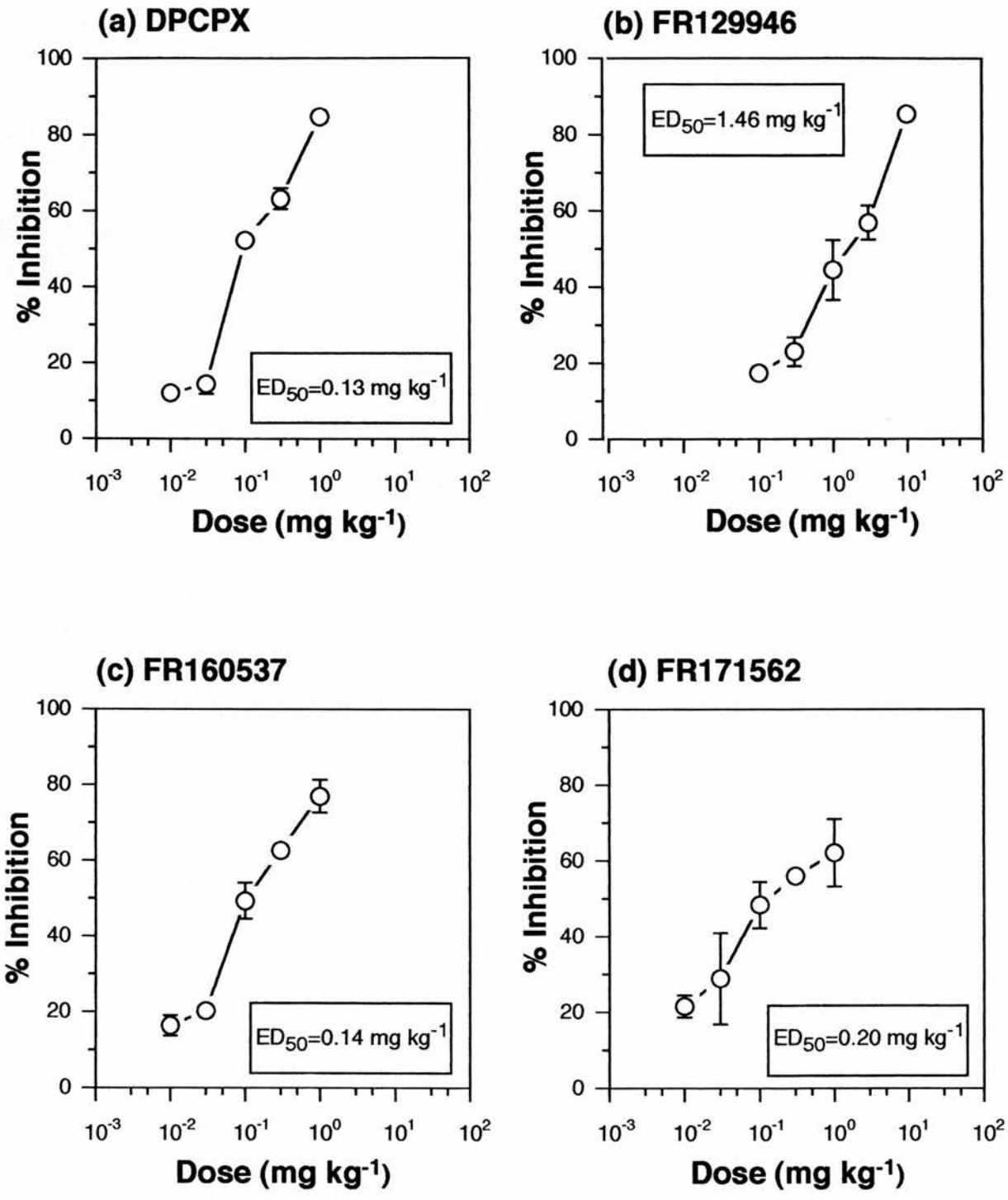

Figure 3.12 Estimation of the Dose of Drug Which Will Cause 50 Percent Inhibition (ED_{50}) of [^{3}H]DPCPX Binding.

The data was fitted to a one site logistic model and the ED_{50} determined. The data represent the mean ± S.E.M. of duplicate determinations from at least three different animals for each dose.

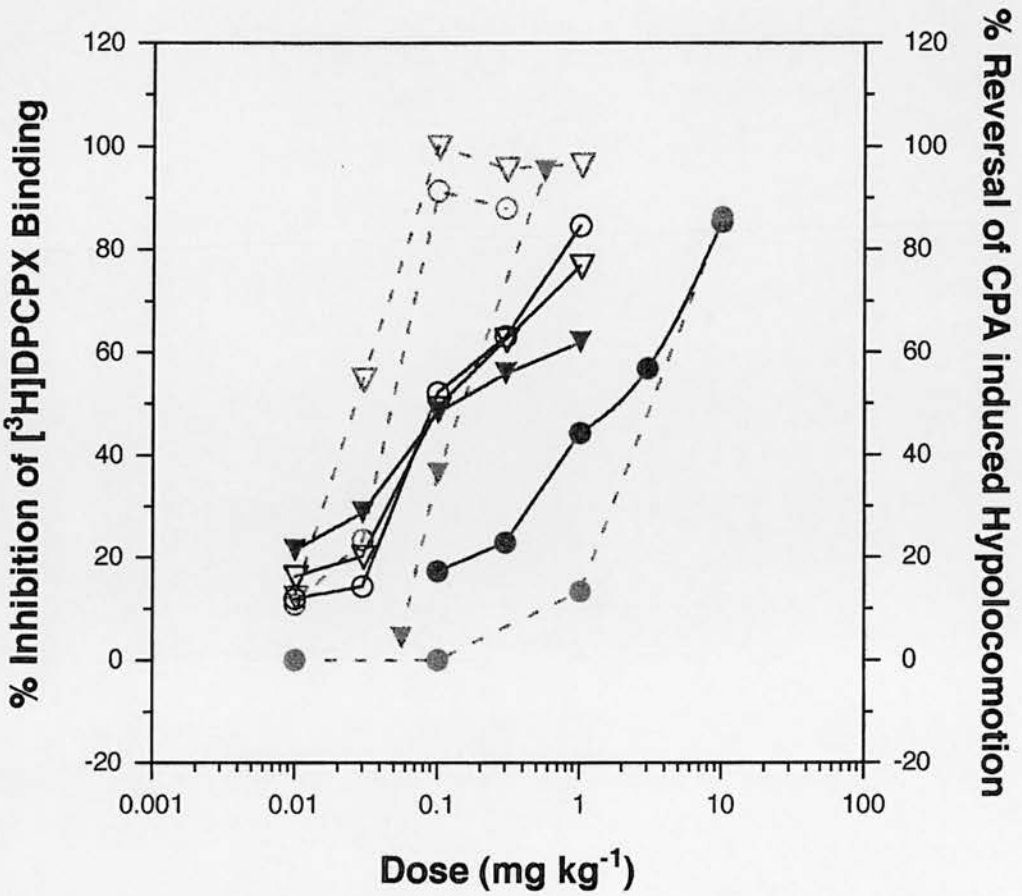

Figure 3.13 Relationship between the ED_{50} *in vitro* and the Reversal of the Behavioural Depression *in vivo*.

The values shown are the mean of duplicate determinations for at least three animals at each dose. Data shown for ○ DPCPX, ● FR129946, ▽ FR160537 and ▼ FR171562. Solid lines are for *in vitro* data and dashed lines are for *in vivo* data.

FR129946, FR160537 and FR171562 (Table 3.6); for example, at 1 mg kg^{-1} the concentrations were 1370 nM, 111 nM, 310 nM and 448 nM respectively. This is reflected in the variable brain to serum ratios (Table 3.7).

A range of adenosine antagonists known to reverse the behavioural depression induced by CPA (Dr H.M. Marston, personal communication), were measured in brain and serum at behaviourally relevant doses, in order to determine whether the antagonists could be detected in brain. All drugs were given at a behaviourally equivalent equipotent dose, i.e. a dose known to produce approximately 80% reversal of CPA-induced hypolocomotion. Six standard xanthine antagonists, 8 Fujisawa antagonists and three adenosine antagonists from other companies were tested (Table 3.8). Standard [^{3}H]DPCPX inhibition curves using washed P_2 membranes were constructed in the absence and presence of denatured control brain homogenate and serum from vehicle treated rats over an appropriate concentration range for each drug. All drugs showed no alteration in affinity when incubated at 80°C, prior to determining K_i values (data not shown). The standard xanthine antagonists DPCPX, DPX, CPT and 8-PT were all detectable in brain and serum and showed similar brain to serum ratios. The two peripheral adenosine antagonists DPSPX and 8-PST were not detectable in brain, despite micromolar serum concentrations. The Fujisawa antagonists showed a variable profile. Two drugs FK838 and FR182394, despite being given at behaviourally active doses were not measurable in brain, at 20 min post-injection. The other six Fujisawa compounds were detectable in both brain and serum. Brain to serum ratios were similar for FK453, FR129946, FR160537 and FR171562, however FK352 and FR182303 were substantially higher and lower respectively. The three adenosine antagonists from other companies were all detectable in brain but only MDL102234 was detectable in serum, with a similar ratio (0.8) to the other xanthine antagonists. For the majority of drugs,

Table 3.7 Brain to Serum Concentration Ratio of Adenosine Antagonists

Dose (mg kg^{-1})	DPCPX (U)	DPCPX (F)	FR129946	FR160537	FR171562
0.01	0.75	0.52	N.D.	1.78	5.78
0.03	0.72	0.67	N.D.	2.71	2.73
0.1	0.39	0.45	2.04	3.10	2.22
0.3	0.25	0.35	1.75	1.35	0.62
1	0.20	0.21	2.12	0.77	0.38
3	N.T.	N.T.	0.99	N.T.	N.T.
10	N.T.	N.T.	0.97	N.T.	N.T.

Brain to serum ratios shown for each drug are from the data generated in Tables 3.4 to 3.6. For DPCPX ratio shown for unflushed **(U)** and flushed **(F)** preparations. (N.D. - not detectable within assay limitations). (N.T. - not tested).

Table 3.8 Drug Concentration in Brain and Serum at the Equipotent Behavioural Dose

Drug	Dose (mg kg^{-1})	*In vitro* K_i (nM)	Detection Limit (nM)	Brain (nM)	Serum (nM)	Brain / Serum Ratio
DPCPX	0.03	0.33 ± 0.01	8.6	17.7 ± 2.0	26.5 ± 5.4	0.67
DPSPX	5.60	91.6 ± 2.73	2379	< 238	56300± 2930	< 0.004
8-PST	20.0	1380± 86.5	35800	< 3580	51960± 8260	< 0.068
DPX	0.10	29.7 ± 2.47	772	1430± 190	2160± 960	0.66
CPT	3.00	8.08 ± 0.52	211	4060± 416	10130± 925	0.40
8-PT	1.00	44.2 ± 1.41	1150	3420± 1130	2790± 344	1.22
FK838	1.00	5.62 ± 0.30	146	< 146	455 ± 91.4	< 0.32
FK352	0.10	23.5 ± 0.56	611	3220± 487	270 ± 82.6	11.9
FK453	0.10	0.53 ± 0.02	13.8	104 ± 12.2	30.1 ± 15.8	3.46
FR129946	3.00	1.10 ± 0.05	28.6	487 ± 93.0	490 ± 112	0.99
FR160537	0.03	0.22 ± 0.01	5.72	21.3 ± 2.33	7.90 ± 2.11	2.70
FR171562	0.10	0.28 ± 0.01	7.28	85.6 ± 15.3	38.6 ± 3.19	2.22
FR182303	1.00	4.10 ± 0.56	107	80.9 ± 40.7	741 ± 68.7	0.11
FR182394	0.56	2.03 ± 0.34	52.8	< 52.8	224 ± 33.8	< 0.24
KW3902	0.03	0.16 ± 0.01	4.16	17.1 ± 2.01	< 4.16	> 4.11
Takeda	1.00	8.51 ± 0.96	221	1160± 76.2	< 221	> 5.25
MDL102234	3.00	7.68 ± 0.24	200	607 ± 52.8	758 ± 195	0.80

K_i values were determined in the standard [^{3}H]DPCPX binding assay (n≥3). Detection limit is the theoretical amount of drug measurable in brain which would cause 10% inhibition of [^{3}H]DPCPX binding in the radioreceptor (1 ml) assay. For DPSPX and 8-PST brain concentrations are shown for values causing < 1% inhibition of [^{3}H]DPCPX binding in the radioreceptor assay. Drug concentrations were measured in the [^{3}H]DPCPX radioreceptor binding assay for both brain and serum samples. Values expressed as mean ± S.E.M of duplicate determinations for at least three different animals. Ratio is brain concentration divided by serum concentration .

brain concentrations were well in excess of their individual K_i values and would appear to be sufficient to account for the observed behavioural effects (Table 3.9). The anomalies shown for FK838 and FR182394 were investigated further. FK838 was given at a higher dose of 3 mg kg^{-1} and studied at both 10 and 20 min, whereas FR182394 was given at the same dose and tested at the 10 min time point. FK838 showed a dose dependent increase in serum levels from 455 ± 91.4 nM (1 mg kg^{-1}) to 4330 ± 594 nM (3 mg kg^{-1}) at 20 min post-injection and at 3 mg kg^{-1} showed a time dependent increase in serum levels from 1880 ± 173 nM at 10 min to 4330 ± 594 nM at 20 min. Despite this, FK838 (3 mg kg^{-1}) was still below the limits of detection in brain at both time points. FR182394, unlike FK838, had higher serum levels at 10 min (370 ± 47.3 nM) but was still below the limits of detection in brain at this time point.

The potential for an association between pharmacological and behavioural data was investigated. There was a very poor correlation between *in vitro* K_i and equipotent dose (Figure 3.14a), with a correlation coefficient, r^2=0.52. There was some association between brain and serum concentrations at the equipotent dose with a correlation coefficient, r^2=0.71 (Figure 3.14b). There was no association between brain concentration and equipotent dose (r^2=0.41) (Figure 3.15a). There was however a better correlation between serum concentration and equipotent dose (r^2=0.70) (Figure 3.15b). There were good correlations between brain (r^2=0.81) and serum (r^2=0.80) concentrations at the equipotent dose and the *in vitro* K_i (Figure 3.16).

Table 3.9 Relationship Between *In Vitro* K_i and Brain Concentration at the Equipotent Behavioural Dose

Drug	*In Vitro* K_i (nM)	10 x K_i (nM)	Brain (nM)	Brain / 10 x K_i Ratio
DPCPX	0.33 ± 0.01	3.3	17.7 ± 2.0	5.36
DPSPX	91.6 ± 2.73	916	< 238	--
8-PST	1380± 86.5	13800	< 3580	--
DPX	29.7 ± 2.47	297	1430± 190	4.81
CPT	8.08 ± 0.52	80.8	4060± 416	50.2
8-PT	44.2 ± 1.41	442	3420± 1130	7.74
FK838	5.62 ± 0.30	56.2	< 146	--
FK352	23.5 ± 0.56	235	3220± 487	13.7
FK453	0.53 ± 0.02	5.3	104 ± 12.2	19.6
FR129946	1.10 ± 0.05	11.0	487 ± 93.0	44.3
FR160537	0.22 ± 0.01	2.2	21.3 ± 2.33	9.68
FR171562	0.28 ± 0.01	2.8	85.6 ± 15.3	30.6
FR182303	4.10 ± 0.56	41.0	80.9 ± 40.7	1.97
FR182394	2.03 ± 0.34	20.3	< 52.8	--
KW3902	0.16 ± 0.01	1.6	17.1 ± 2.01	10.7
Takeda	8.51 ± 0.96	85.1	1160± 76.2	13.6
MDL102234	7.68 ± 0.24	76.8	607 ± 52.8	7.90

K_i values were determined in the standard [^{3}H]DPCPX binding assay ($n \geq 3$). At ten times the K_i concentration it can be calculated (in the absence of agonist) that the drug would occupy 90.9% of the receptors. Drug concentrations were measured in the [^{3}H]DPCPX radioreceptor binding assay for brain samples. Values expressed as mean ± S.E.M of duplicate determinations for at least three different animals. The ratio is equivalent to the concentration of drug in brain divided by the drug concentration required to occupy 90.9% of the receptors.

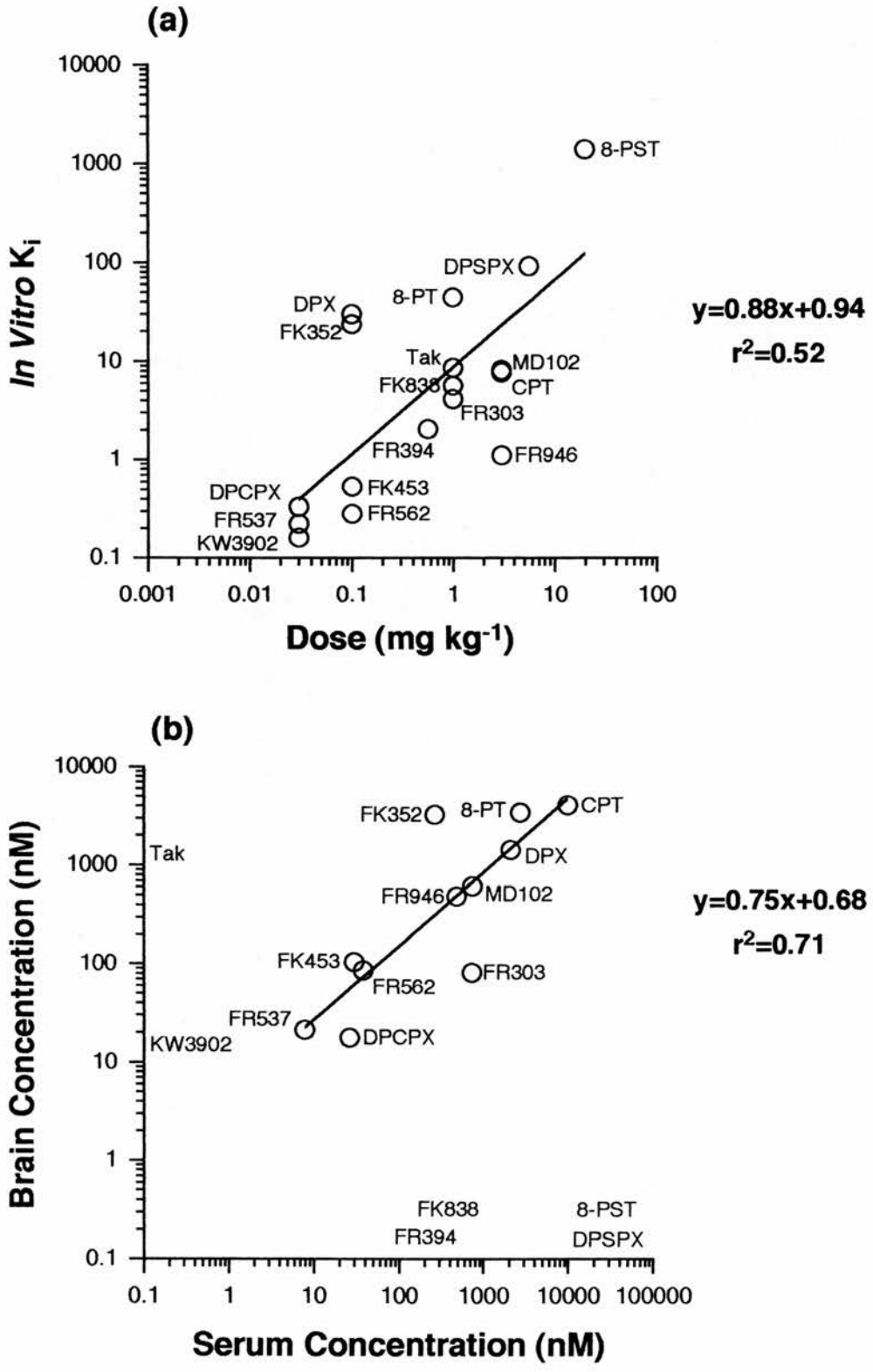

Figure 3.14 Association Between (a) the Behaviourally Equivalent Dose and *In Vitro* K_i and (b) Brain and Serum Concentrations Determined at that Dose.

K_i values determined as in methods ($n \geq 3$). Brain and serum concentrations were determined using the radioreceptor assay. Each concentration is the the mean of duplicate determinations from at least three animals.

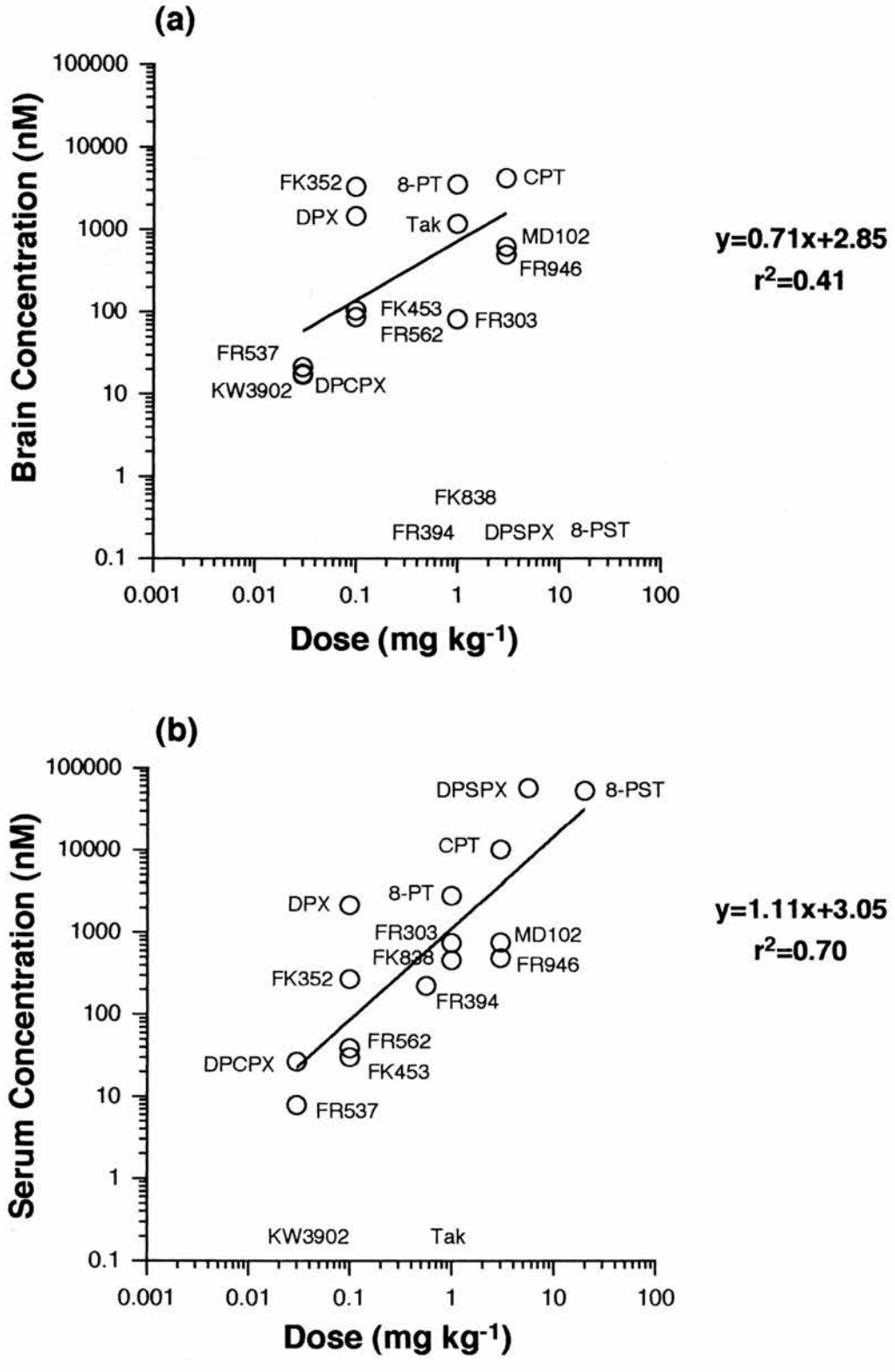

Figure 3.15 Association Between the Behaviourally Equivalent Dose and (a) Brain and (b) Serum Concentrations Determined at that Dose.

Brain and serum concentrations determined using the radioreceptor assay. Each point is the mean of duplicate determinations from at least three animals.

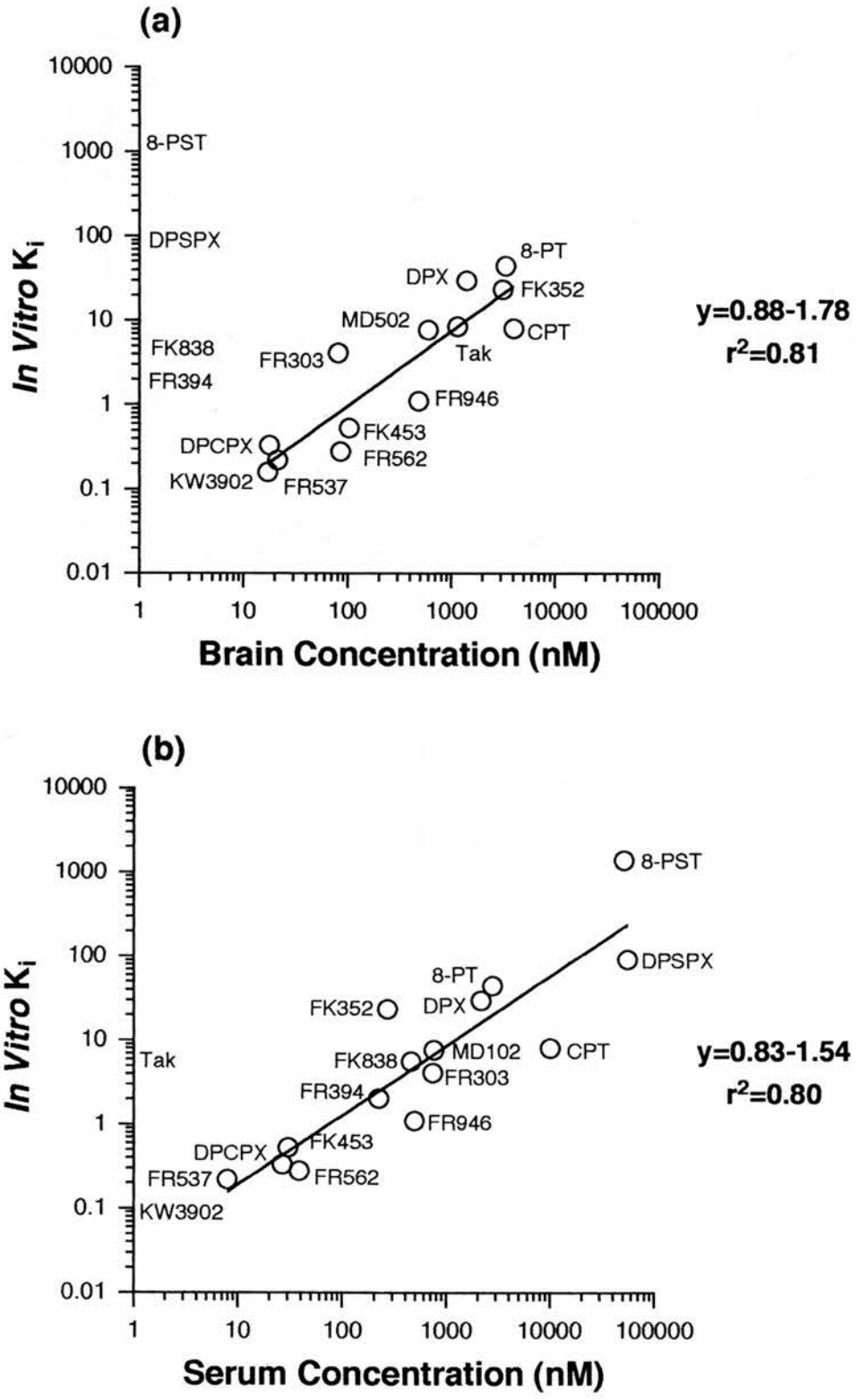

Figure 3.16 Association Between (a) Brain and (b) Serum Concentration at the Behaviourally Equivalent Dose and *InVitro* K_i.

K_i values determined as in methods (n≥3). Brain and serum concentrations were determined using the radioreceptor assay. Each concentration is the mean of duplicate determinations from at least three animals.

3.4. Discussion

Therapeutically useful CNS drugs must cross the BBB in sufficient quantities to mediate a pharmacological effect. This chapter describes the characterisation of a modified radioreceptor assay and an *ex vivo* binding assay. These assays are capable of measuring brain concentrations of adenosine receptor antagonists following i.p. drug administration. *Ex vivo* binding assays use each animal as the source of drug and receptors which could introduce potential inter-animal variation. This type of assay also requires the tissue in which the drug concentration is to be measured to have a sufficient level of binding to conduct the experiment. The radioreceptor assay avoids the biological variation inherent in *ex vivo* binding assays, by using brain homogenate from drug treated animals as a 'competing drug' in a conventional *in vitro* radioligand binding assay. This method therefore allows drug concentrations to be measured in serum which contains no endogenous receptors. These techniques detect the presence, rather than the function, of a particular compound in the brain. The final drug concentrations presented are calculated from the concentration of drug detected in the binding assay for brain homogenate and serum. These calculated values are an approximate conversion, made assuming an equal distribution of drug through tissue. This is unlikely, but in the absence of more detailed information on distribution, the estimate provides a comparison between both methods. The drug concentrations in brain homogenate probably reflect the minimum estimated concentration if most of the drug is extracellular. This is because the extracellular space represents approximately one seventh of the area in the brain and hence the concentration of drug available to the receptors could be higher.

A pilot study in which DPCPX concentration was estimated in brain homogenate using *ex vivo* binding, indicated that at behaviourally relevant

doses of DPCPX, drug was detectable in brain at 20 min post-injection. However, the lack of flexibility in the *ex vivo* binding assay, the inability to measure drug concentrations in other tissues and the potential for inter-animal variation (Heffez *et al.*, 1985; Jarvis & Williams, 1988; Florio *et al.*, 1994), prompted the development of a modified radioreceptor assay.

Contamination of brain tissue from drug present in residual cerebral blood may complicate determination of drug concentrations in both *ex vivo* binding and radioreceptor assays. A transcardiac perfusion has been used by a variety of groups to reduce the level of contribution from drug present in blood (see Introduction). [^{14}C]Inulin, a non penetrating marker for blood plasma, was used to examine the blood content of brain. Blood content of brain was maximally reduced by 62% from 21.5 μl g^{-1} to 8.15 μl g^{-1}, after perfusion with saline for 30 sec. These data are consistent with other groups (Patel *et al.*, 1994a). Assuming free penetration within tissues and a specific gravity of 1.05 g ml^{-1} this would mean the blood content of brain is reduced from 2.26% to 0.86% after a 30 sec transcardiac flush with saline. This indicates blood concentrations of drug would have to be 44.2 times higher than brain tissue before flushing and 116.3 times higher than brain tissue after flushing, before vascular contamination of brain homogenate samples could account for the drug concentration measured.

In vitro competition binding studies using a standard [^{3}H]DPCPX binding assay have demonstrated that this ligand binds to a single population of sites in rat brain that exhibit the pharmacological characteristics of the adenosine A_1 receptor (see Chapter 1; Finlayson *et al.*, 1994; Maemoto *et al.*, 1994). To add brain homogenate from drug treated animals as a 'competing drug' in the [^{3}H]DPCPX binding assay, we incorporated a denaturation step (80°C, 15 min). This removed the inherent binding capacity of these samples, without affecting the stability of any drug tested. Standard curves for

[^{3}H]DPCPX binding using washed P_2 membranes showed no alteration in affinity for any antagonists tested, following addition of denatured control brain homogenate or serum from vehicle treated animals. As expected, addition of denatured control brain homogenate but not serum produced an increase in non-specific binding with no effect on the amount of specific binding. The portion of all standard curves which are most sensitive to changes in concentration are the extremes. The range over which drug concentrations have been determined for radioreceptor, *ex vivo* binding and radioimmunoassays has varied. The portion of the standard curve used has ranged between: 30-70% (Enna, 1978), 10-70% (Janis *et al.*, 1983), 10-90% (Freedman *et al.*, 1989), 10-90% (Baumgold *et al.*, 1992) and 20-80% (Patel *et al.*, 1994a). We added known amounts of DPCPX to control brain homogenate and tested samples in the [^{3}H]DPCPX binding assay. Estimation of drug concentrations in samples which caused < 10% or > 90% inhibition of [^{3}H]DPCPX binding were less reliable. Brain and serum concentrations for drugs were subsequently determined for samples causing between 10 and 90% inhibition of [^{3}H]DPCPX binding, giving a 100 fold concentration range over which drug concentration could be determined. For DPCPX with an IC_{50}=0.43 nM, the range would be between approximately 0.043 and 4.3 nM. As brain homogenate and serum samples from drug treated animals are diluted 200 fold during sample preparation and assay procedure, the minimum detection limit for DPCPX would be approximately 8.6 nM. Assay conditions can be slightly modified for values falling outside this range. For concentrations below the detection limit, assay sensitivity can be increased by reducing assay volume, or by increasing the amount of homogenate added (Enna, 1978). Reducing the assay volume from 1 ml to 0.5 ml with no alteration in the volume of brain homogenate added, gave similar answers, therefore doubling the sensitivity of the assay. An upper limitation on addition of brain homogenate

was reached as volumes above 70 μl of 10 vol. blocked filtration. To overcome this limitation, drug treated brain homogenate was centrifuged and DPCPX concentration determined in the tissue supernatant, as described for GABA (Enna, 1978). GABA is water soluble and can be 'extracted' from brain tissue by simple centrifugation. Adenosine antagonists show varying degrees of lipophilicity, thereby complicating the procedure. This lipophilicity may be one reason why concentrations of DPCPX in tissue supernatant were only approximately 30 to 40% of their respective brain concentrations. The differences in DPCPX concentration in brain homogenate and tissue supernatant may just be methodological. As tissue supernatant was collected from brain homogenate prior to denaturation, and as the homogenate did not receive the 20 fold dilution it receives on addition to the assay, both factors may result in some DPCPX not being released from the tissue. Further experiments would be required to confirm these possibilities. For samples of brain homogenate which caused > 90% inhibition of [^{3}H]DPCPX binding, a simple 10 fold dilution in Tris-buffer prior to addition to the assay was an accurate way of determining drug concentration.

For serum samples, DPCPX concentration was determined in the same way as brain homogenate. Incubation of serum at 80°C before addition to the assay was probably not necessary as addition of control serum (diluted 10 fold before addition to the assay) from vehicle treated animals to the [^{3}H]DPCPX binding assay (data not shown) had no effect on the level of [^{3}H]DPCPX binding. For serum samples which fall below the limit of detection, unlike brain homogenate, there is no limit on the volume of serum which can be added. However, results indicate that unless control serum receives an overall dilution of 100 fold the level of [^{3}H]DPCPX binding is reduced. A similar observation has been made for human serum (Janis *et al.*, 1983).

DPCPX (0.01-1.0 mg kg^{-1}) was administered i.p. to two groups of

animals, one of which had received a transcardiac perfusion. In both groups there was a dose dependent increase in DPCPX concentration in brain and serum, with serum DPCPX consistently higher at all doses. The introduction of the transcardiac perfusion step appeared to have very little overall effect on the concentration of DPCPX in brain. This would not be unexpected for DPCPX as any contribution from drug in the blood to brain homogenate concentrations would be minimal at the brain to blood ratios measured. DPCPX concentration in brain homogenate was determined using radioreceptor and *ex vivo* binding assays, using the assay limitations characterised for the radioreceptor assay. DPCPX was not detectable at the two lowest doses in either group using *ex vivo* binding. For doses where DPCPX was detectable, there was good consistency within each group between the radioreceptor and *ex vivo* binding assays and good consistency between both groups. For the radioreceptor assay, brain to serum ratios were consistent in both groups. These data are similar to DPCPX concentrations in mouse brain determined using *ex vivo* binding (Baumgold *et al.*, 1992). Convenient storage of drug treated samples is feasible, as fresh and frozen brain and serum gave similar results.

DPCPX (1 mg kg^{-1}) exhibited a time dependent decline in brain and serum concentration from 20-180 min post injection, with $t_{1/2}$ values of 35.2 and 47.1 min respectively. Similarly, DPCPX is still detectable in mouse brain 60 min after injection (Baumgold *et al.*, 1992). The concentrations of DPCPX relative to its K_i value at this dose are likely to be sufficient at each time point (175 times the K_i at 180 min) to account for reversal of the behavioural depression induced by CPA (Marston *et al.*, 1994).

To confirm that the inhibition of [^{3}H]DPCPX binding by brain homogenate from DPCPX treated animals was due to drug present in brain tissue, DPSPX and 8-PST, two peripheral adenosine receptor antagonists,

were tested (Nikodijevic *et al.*, 1991; Baumgold *et al.*, 1992). Neither compound was detectable in brain tissue despite micromolar concentrations in serum and neither compound was capable of reversing the hypolocomotion induced by CPA (Dr H. M. Marston, personal communication). These data are consistent with those of mice for 8-PST (Baumgold *et al.*, 1992). This indicates BBB permeability is a prerequisite for detection in brain homogenates, a factor reflected by a low brain to serum ratio for these two compounds. Confirmation of the requirement to cross the BBB should be obtained in an ongoing study in which DPSPX and 8-PST are being given directly into the brain (i.c.v.), in attempting to reverse hypolocomotion induced by CPA.

DPCPX penetration into the brain was independently assessed by measuring [^{3}H]DPCPX concentrations in different brain regions following intravenous administration. There was a time dependent decrease in [^{3}H]DPCPX concentration in all brain areas measured between 20 to 60 min. [^{3}H]DPCPX was distributed equally, throughout all brain regions measured. [^{3}H]DPCPX concentration in each brain area was approximately 140 nM, consistent with data from the radioreceptor assay of 126 nM at comparable doses of 0.25 and 0.3 mg kg^{-1} respectively. Concentrations in all areas are approximately 10 fold less than those measured in a similar study in rats (Bisserbe *et al.*, 1992). They demonstrated regional differences in distribution within the brain, with brain stem levels half that of other brain regions (Bisserbe *et al.*, 1992). The similarities in the method make the differences difficult to explain (Bisserbe *et al.*, 1992).

With characterisation complete drug determinations were made in brain and serum using the radioreceptor assay. FR129946, FR160537 and FR171562, were examined over a range of doses known to reverse CPA induced hypolocomotion (Dr H.M. Marston, personal communication). All three drugs showed a dose dependent increase in brain and serum concentrations,

20 min after i.p. injection and a time dependent decrease. Brain concentrations of FR160537 and FR171562 were similar to DPCPX but FR129946 was slightly lower at equivalent doses. As with DPCPX, the concentrations of all three antagonists in brain tissue at each time point relative to their K_i values are likely to be sufficient to account for reversal of behavioural depression induced by CPA (Marston *et al.*, 1994). At 1 mg kg^{-1}, FR129946 has a similar half life in brain tissue and serum. The similarity in half life may be due to the compound being water soluble. FR129946 could have a beneficial profile with serum concentrations consistently lower than brain tissue, thus minimising potential peripheral effects. FR160537 and FR171562 are not water soluble with both compounds cleared more slowly from the brain than from serum.

Factors inherent in the radioreceptor and *ex vivo* binding assays complicate the exact determination of drug concentrations in brain tissue. Comparisons between drugs are often made by calculating ED_{50} values, i.e the dose of drug in tissue samples which inhibits 50% of radioligand binding (Sethy & Francis, 1988; Patel *et al.*, 1994a). Interestingly, the curves for the inhibition of [^{3}H]DPCPX binding and reversal of CPA induced hypolocomotion had a similar profile, with FR129946 clearly to the right of the other three compounds.

A range of adenosine antagonists known to reverse the behavioural depression induced by CPA were examined. Drugs were given at an equipotent behavioural dose and brain and serum concentrations were measured. Standard xanthines, DPCPX, DPX, CPT and 8-PT were all detectable in brain and serum and had similar brain to blood ratios. All four compounds were present in brain tissue at concentrations relative to their K_i values (Table 3.9) that are likely to be sufficient to account for reversal of behavioural depression induced by CPA (Marston *et al.*, 1994). The peripheral antagonists DPSPX and 8-PST when given at their highest soluble dose were

undetectable in brain and had no behavioural effect. The Fujisawa antagonists showed a far more variable profile. Six compounds were detectable in brain and serum. Brain to blood ratios were similar for FK453, FR129946, FR160537 and FR171562. However, they are very different for FK352 and FR182303, with the serum concentration for FK352 and the brain concentration for FR182303 being close to the limits of detection. Both compounds were only detectable in the 0.5 ml assay, where the detection limit is increased two fold. Two drugs, FR182394 and FK838, despite being given at behaviourally active doses, were not detectable in brain within the detection limits of the assay at 20 min post-injection. Brain concentrations of FR182394 when examined at 10 min post-injection still lay outside the limits of detection. FK838 was examined at a higher dose and at different time points. At the higher dose (3 mg kg^{-1}) and at 20 min post-injection where serum levels were higher, FK838 was detectable in brain tissue at approximately 80 nM. As these samples caused less than 10% inhibition in the assay, and as serum concentrations of 4330 nM could result in potential blood contamination of brain tissue equivalent to approximately 40 nM (0.86% x 4330), no conclusions can be drawn. In light of the behavioural activity of both compounds these results are difficult to explain and further experiments are required. The three adenosine antagonists from other companies were all detectable in brain but only MDL102234 was detectable in serum. MDL102234 had a similar brain to blood ratio to the other xanthine antagonists.

As drugs were given at equipotent behavioural doses, the association between pharmacological and behavioural data was investigated. In calculating correlation coefficients, compounds that were not measurable were not included in the data analysis. There was a very poor correlation between the K_i for drugs at the adenosine A_1 receptor and the equipotent dose. An association between these two variables would probably only exist if all

compounds had similar pharmacokinetic profiles. There was some association between brain and serum concentrations at the equipotent dose, which may reflect that at the doses chosen BBB permeability is similar. There was no association between brain concentration and the equipotent dose, which may again reflect the differences in the pharmacokinetics of each compound and their ability to cross the BBB. There was, however, a better correlation between serum concentration and the equipotent dose, perhaps reflecting differences in pharmacokinetics. There was a good correlation between the brain concentration at the equipotent dose and the *in vitro* K_i of drugs for the adenosine A_1 receptor. The data between these two variables was best described by the equation y=0.88-1.78 and a correlation coefficient (r^2)=0.81. The antilog of the intercept is equal to 0.017, indicating that the drugs are present in brain at approximately 60 times their respective K_i values in order to reverse this level of behavioural depression. These concentrations may be sufficient to imply a direct association between receptor occupancy and behavioural effect. It is interesting to note that despite structural similarities to other xanthines, CPT not only reverses behavioural depression but also produces hyperlocomotion in rats, an effect not seen with the other compounds. A similar effect has been described in mice for CPT (Baumgold *et al.*, 1992). With CPT present at approximately 500 times its K_i value for the adenosine A_1 receptor, the stimulation observed may be through a different mechanism. It may also be that a critical concentration of drug in relation to its K_i value for the adenosine A_1 receptor must be reached before stimulation is observed, as FR129946 which had the second highest ratio of 443 fold (Table 3.9) also produced some perceptible behavioural stimulation which did not attain significance (Dr H.M. Marston, personal communication). The good correlation between serum concentration at the equipotent dose and the *in*

vitro K_i for drugs at the adenosine A_1 receptor, is not unexpected as serum and brain ratios have already been shown to be generally related.

In conclusion, we have developed a radioreceptor assay capable of measuring the central penetration of adenosine A_1 receptor antagonists following i.p. administration. Quick, easy and reliable determinations can be made to assess whether new A_1 receptor antagonists cross the BBB, before complex and time consuming behavioural experiments are undertaken. This methodology could be applied to any receptor system and any tissue if a suitable radioligand binding assay is available.

CHAPTER FOUR

PHARMACOLOGY AND LOCALISATION OF RAT RENAL ADENOSINE A_1 RECEPTORS

4.1. Introduction

In attempting to develop an adenosine A_1 antagonist as a potential cognitive enhancer, one must consider the potential cardiotonic and diuretic effects of such compounds (Jacobson *et al.*, 1992a). A centrally selective compound devoid of such activities would be of considerable importance in conditions like Alzheimers disease, in which patients are predominantly elderly and more susceptible to these side effects, especially if given long term. Research into heart and kidney purinoreceptors is extensive and as a consequence I will concentrate on kidney purinoreceptors. For cardiovascular purinoreceptors recent reviews have been published (Olsson & Pearson, 1990; Tucker & Linden, 1993).

In kidney, adenosine is an autocoid playing an important role in regulating a variety of functions. These include renal blood flow, glomerular filtration rate, renin secretion, tubuloglomerular feedback, tubular reabsorption of water and sodium, sympathetic neurotransmitter release and erythropoeitin secretion (Spielman & Arend, 1991). In conditions such as hypoxia, when ATP is low and nephrogenic adenosine is increased, adenosine acts on the distal tubule, inhibiting the transport actions of vasopressin, parathyroid hormone and noradrenaline, reducing energy demand in the region (Spielman & Arend, 1991). Paradoxically, in the proximal tubule and cortical collecting ducts, adenosine stimulates apical sodium phosphate (Coulson *et al.*, 1991) and basolateral sodium bicarbonate transporters (Takeda *et al.*, 1993). Potential effects in glomerulus (Freissmuth *et al.*, 1987a; Toya *et al.*, 1993), medulla (Weber *et al.*, 1990b; Burnatowska-Hledin & Spielman, 1991; Weaver & Reppert, 1992) and collecting ducts (Spielman *et al.*, 1992; Schwiebert *et al.*, 1992), imply adenosine receptors are widely distributed throughout the kidney, as in brain. The overall effect of adenosine is antidiuretic, suggesting its ability to lower glomerular filtration rate and stimulate reabsorption at proximal

nephron sites, normally overwhelms decreases in distal reabsorptive transport (Spielman & Arend, 1991; Suzuki *et al.*, 1992). These effects of adenosine can be changed by altering the route of administration (Yagil, 1993).

Conflicting evidence, on the subtype and location of renal adenosine receptors, is probably in part caused by their low density in renal tissue (Williams & Risley, 1980; Murphy & Snyder, 1980; Weber *et al.*, 1990b; Gould *et al.*, 1995). Pharmacological classification of renal adenosine receptors is heavily dependent upon adenyl cyclase studies, with radioligand binding characterisation minimal (Spielman & Arend, 1991). Adenosine A_1 and A_2 receptors have been identified in the kidney of various species (Spielman & Arend, 1991), with effects mediated through multiple effectors in the case of the A_1 receptor and unifocally for the A_2 receptor (Spielman *et al.*, 1992; Coulson *et al.*, 1996). In rat kidney, adenosine A_1 receptors have been identified in medulla (Weber *et al.*, 1990b), A_2 receptors in crude membranes (Wu & Churchill, 1985) and both A_1 and A_2 receptors in basolateral membranes from cortex (Jakubowski *et al.*, 1992). The pharmacological characteristics of A_1 and A_2 receptor binding in rat kidney, although only very weakly characterised, were similar to rat brain (Wu & Churchill, 1985; Brines *et al.*, 1990; Jakubowski *et al.*, 1992). In contrast, Blanco *et al.*, (1992) found no evidence of A_1 receptors in binding studies using brush border or basolateral membranes from rat or pig kidney cortex, but did note specific binding with the A_2 agonist [^{3}H]CGS21680. However, the binding characteristics were different from classical striatal A_{2a} receptors, with effects sensitive to both cholera and pertussis toxin. Furthermore, a study in which the diuretic effects of adenosine A_1 antagonists were examined in rat showed a slightly different profile to adenosine A_1 binding in rat brain (Suzuki *et al.*, 1992). Functional studies using KW3902, a potent and selective A_1 antagonist, revealed diuretic and

renal protective effects in rat through a pertussis toxin insensitive mechanism (Mizumoto *et al.*, 1993). Adenosine A_1 receptors have been identified in rabbit glomeruli and characterised in a collecting tubule cell line (28A) and renal medullary membranes (Freissmuth *et al.*, 1987a; Spielman *et al.*, 1992). The gene for the adenosine A_1 receptor has been cloned from a rabbit kidney cDNA library and appears similar to the A_1 clone from brain (Bhattacharya *et al.*, 1993). In human kidney, A_1 receptors were identified in glomeruli and A_{2a} receptors in renal papilla (Woodcock *et al.*, 1986; Toya *et al.*, 1993). Species differences in kidney adenosine receptor pharmacology and localisation have been demonstrated using *in vitro* autoradiography. In human kidney, A_1 receptors were located in cortical tissue, in contrast to a medullary localisation in guinea pig (Palacios *et al.*, 1987). Long exposure times for [^{3}H]CHA, and low receptor density, prompted the use of [^{125}I]R-PIA to examine A_1 receptor localisation in guinea pig and rat kidney (Brines & Forrest, 1987; Weber *et al.*, 1988). In both species adenosine A_1 receptors were localised in areas of the medulla. Adenosine A_1 receptor mRNA has also been localised to the medulla of rat kidney using *in situ* hybridisation (Weaver & Reppert, 1992). This contrasts with the histochemical localisation of ecto-5′-nucleotidase activity, which was identified in brush border membranes but not medulla (Dawson *et al.*, 1989). A recent study using microdissected nephron segments has shown adenosine receptor mRNA along the whole length of the nephron (Yamaguchi *et al.*, 1995).

The potential heterogeneous distribution of adenosine receptors in rat kidney and the lack of pharmacological characterisation using radioligand binding studies requires further investigation to determine if central and peripheral adenosine A_1 receptors are identical. [^{3}H]DPCPX and [^{3}H]CGS21680 were used to investigate the properties of several rat kidney

membrane preparations. These included crude (Wu & Churchill, 1985; MacKinnon *et al.*, 1993) and renal papillary membranes (Woodcock *et al.*, 1984). Despite autoradiographic evidence to the contrary (Palacios *et al.*, 1987; Weber *et al.*, 1990b), functional studies indicate that adenosine acts on sites located on the proximal tubule (cortex) (Mizumoto & Karasawa, 1993; Nomura *et al.*, 1995; Terai *et al.*, 1995b). In view of these data, [^{3}H]DPCPX binding to a number of kidney cortical membrane preparations was also examined. In the proximal tubule of rat kidney, the luminal surface is coated with microvilli (brush border), whereas on the contraluminal side, plasma membranes form the basal (basolateral) infoldings of the cell. Various techniques have been used to isolate brush border and basolateral membranes fractions from kidney proximal tubules (Heidrich *et al.*, 1972). Techniques have involved self orienting percoll gradients (Sacktor *et al.*, 1981), sucrose gradients (Kinsella *et al.*, 1979) and magnesium precipitation (Somogyi *et al.*, 1994). Membranes from rat (Sacktor *et al.*, 1981; Cox *et al.*, 1983; Somogyi *et al.*, 1994), dog (Kinsella *et al.*, 1979), pig (Lin *et al.*, 1981) and rabbit (Podevin & Podevin, 1983) kidney, have been used to investigate transepithelial membrane transport, hormonal interactions, membrane enzyme activities and membrane binding. Using the methods of Sacktor *et al.*, (1981) and Cox *et al.*, (1983), basolateral and brush border membrane fractions were prepared for use in [^{3}H]DPCPX binding studies. Binding of [^{3}H]RX821002, an α_2 adrenoreceptor antagonist (Langin *et al.*, 1989) was also examined as a positive control.

The distribution of adenosine A_1 receptors and A_1 receptor mRNA in rat kidney was also investigated using *in vitro* autoradiography with [^{3}H]DPCPX and by *in situ* hybridisation using a riboprobe specific for the rat adenosine A_1 receptor in a manner similar to Weaver & Reppert, (1992). These methods

were used to examine whether adenosine A_1 receptors and mRNA are present in rat kidney in a highly localised manner, which may be undetectable in membrane binding studies. As the distribution of adenosine A_1 receptors in rat brain is well characterised (Goodman & Snyder, 1982; Weber *et al.*, 1990a), brain tissue was included in both autoradiographic and *in situ* hybridisation studies as a positive control.

4.2. Methods and Materials

4.2.1. Preparation of Rat Kidney Membranes

4.2.1.1. Method 1 (Mackinnon *et al.*, 1993; Crude membrane fraction)

Rats were killed by cervical dislocation, kidneys excised, decapsulated and homogenised in 25 vol. (v/w) of buffer (50 mM Tris-HCl, 5 mM (ethylenedinitrilo)tetraacetic acid (EDTA), pH 8.0) at 4°C using a Polytron P 10 disruptor (20 sec). The homogenate was centrifuged at 48000 g in a Centrikon T-2070 centrifuge for 15 min at 4°C. The supernatant was discarded, the pellet resuspended in the original volume of homogenisation buffer and recentrifuged. The pellet was washed twice by centrifugation in buffer (50 mM Tris-HCl, 0.5 mM EDTA, pH 8.0). The final pellet was resuspended in 10 vol. (v/w) of 50 mM Tris-HCl (pH 8.0) and stored at -20°C until use.

4.2.1.2. Method 2 (Wu and Churchill, 1985; Crude membrane fraction)

Rats were killed by cervical dislocation, kidneys excised, decapsulated and homogenised in 15 vol. (v/w) of buffer (50 mM sodium phosphate buffer, 250 mM sucrose, pH 7.4) at 4°C using a Polytron P 10 disruptor for three 10 sec bursts. The homogenate was centrifuged at 1000 g for 10 min at 4°C in a Beckman 2-21M/E centrifuge, and recentrifuged at 9000 g for 20 min at 4°C. The resultant supernatant was centrifuged in a Centrikon T-2070 centrifuge at

105000 g for 30 min at 4°C and the membrane containing pellet resuspended and stored in 5 vol. (v/w) of 50 mM Tris-HCl (pH 7.4) at -20°C until use.

4.2.1.3. Method 3 (Cox *et al.*, 1983; Mixed basolateral and brush border membrane fraction)

Rats were killed by cervical dislocation, kidneys excised and decapsulated. The renal cortex was dissected on ice and homogenised in 10 vol. (v/w) of isolation medium (250 mM sucrose, 10 mM triethanolamine HCl, 0.1 mM phenylmethylsulphonyl fluoride (PMSF), pH 7.4), using a glass teflon homogeniser. The homogenate was centrifuged at 700 g for 10 min at 4°C in a Beckman 2-21M/E centrifuge, the pellet discarded and supernatant recentrifuged as above. The pellet was discarded and the supernatant centrifuged at 16000 g for 20 min at 4°C. The resultant supernatant was collected and was subsequently used to homogenise the white fluffy top layer of the pellet, using a loose fitting glass teflon homogeniser and recentrifuged as above. The white fluffy top layer of the pellet was resuspended in 10 ml of isolation medium and homogenised gently. A further 10 ml of isolation medium was added before centrifugation as above. The resultant white fluffy top layer of the pellet (crude basolateral and brush border membrane fraction) was resuspended in 1 vol. (v/w) of 50 mM Tris-HCl (pH 7.4) and stored at -20°C until use.

4.2.1.4. Method 4 (Sacktor *et al.*, 1981; Basolateral and brush border membrane fraction)

Rats were killed by cervical dislocation, kidneys excised and placed in ice cold sucrose buffer (250 mM sucrose, 10 mM Tris-HCl, 0.1 mM PMSF, pH 7.6). Kidneys were decapsulated, cortices removed and thoroughly minced in 20 vol. (v/w) of sucrose buffer using a glass teflon homogeniser, followed by

three 30 sec bursts with a Polytron P 10 disruptor. The homogenate was centrifuged at 2500 g for 15 min at 4°C in a Beckman 2-21M/E centrifuge and the resultant supernatant was centrifuged at 24000 g for 20 min at 4°C. The fluffy upper layer of the pellet was resuspended in 32.2 ml of sucrose buffer and homogenised using a teflon glass homogeniser. 2.8 ml of 100% Percoll was added to the crude plasma membranes and mixed vigorously, before centrifugation in a Centrikon T-2070 centrifuge using a Beckman TH 641 swing out rotor at 30000 g for 35 min at 4°C. The resultant Percoll gradient had three layers with basolateral membranes in the middle layer and brush border membranes on the bottom layer. Each layer was gently removed with a fine tipped pasteur pipette and diluted in 4 vol. (v/v) of isolation medium containing 100 mM KCl, 100 mM mannitol and 5 mM Tris-Hepes (pH 7.2) before centrifugation at 34000 g for 30 min at 4°C. The loose fluffy membrane pellet was separated from the dense glassy Percoll pellet and centrifuged at 34000 g as before. Membranes were resuspended in 5 vol. (v/w) of 5 mM Tris-Hepes (pH 7.2) and stored at -20°C until use.

4.2.1.5. **Method 5** (Woodcock *et al.*, 1984; Rat renal papilla)

Rats were killed by cervical dislocation, kidneys excised, decapsulated, washed in ice cold saline, hemisected and the white inner papilla removed. The tissue was homogenised in 15 vol. (v/w) of sucrose buffer (250 mM sucrose, 10 mM Tris-HCl, 10 mM $MgSO_4$, pH 7.4) at 4°C using a Polytron P 10 disruptor for two 5 sec bursts. The homogenate was centrifuged in a Centrikon T-2070 centrifuge at 30000 g for 20 min at 4°C and the resulting pellet washed once with sucrose buffer. The final pellet was resuspended in 5 vol. (v/w) of sucrose buffer (pH 7.4) and stored at -20°C until use.

4.2.2. HEK 293 Cell Culture and Membrane Preparation

HEK 293 cells (European Culture Collection) were grown in culture medium (DMEM, 10% heat inactivated foetal calf serum (FCS), penicillin-streptomycin (100 u ml^{-1}) and glutamine (0.3 mg ml^{-1})) in a 37°C incubator (95% O_2/5% CO_2). All procedures were performed using aseptic tissue culture techniques. On attaining confluence, cells were split by removal of culture medium and gentle washing in 10 ml of phosphate buffered saline (PBS). Trypsin (2 ml to a 170 cm^2 flask) was added and mixed to remove cells from the flask. 8 ml of culture medium was added (FCS inactivates the trypsin), and 2.5 ml aliquots were divided into 4 flasks. Each flask was made up to 30 ml in culture medium. Approximately one week was required for the cells to regain confluence and the procedure was then repeated.

On attaining confluence, cells were split by removal of culture medium and gentle washing in 10 ml of PBS. 5 ml of PBS was added, the cells scraped and centrifuged at 1000 g for 5 min, and the pellet stored at -70°C. On the day of the assay the pellet was resuspended in 50 mM Tris-HCl (pH 7.4), homogenised using a glass teflon homogeniser and left on ice for 10 min. The homogenate was centrifuged at 50000 g for 20 min at 4°C, the pellet resuspended in Tris-buffer and recentrifuged at 50000 g for 10 min at 4°C. The final pellet was resuspended in Tris-buffer at the appropriate volume for the assay.

4.2.3. [^{3}H]DPCPX and [^{3}H]CGS21680 Binding Assays

[^{3}H]DPCPX and [^{3}H]CGS21680 binding assays were carried out as described in chapter 1 (see 1.2.3.1 & 1.2.3.3), using kidney membranes rather than brain tissue, with the following modifications. For [^{3}H]DPCPX binding, 10 μl of DMSO or R-PIA, 290 μl of Tris-buffer, 100 μl of ADA (1u ml^{-1}) and 100 μl

of either 1 or 10 nM [^{3}H]DPCPX were preincubated for 2 min at 25°C. Total binding was determined in the presence of 1% DMSO and 10 μM R-PIA was used to determine non-specific binding. Addition of kidney membrane suspension (500 μl; 40-2000 μg) to give a final volume of 1 ml, initiated a 120 min incubation at 25°C. Bound and free ligand were separated using a Brandel cell harvester and this was followed by 3 washes (3 ml) in ice cold Tris-buffer over GF/B filters. Filter disks were transferred to scintillation vials and incubated with 100 μl of 100% formic acid for 10 min, prior to addition of Emulsifier Safe scintillant (4 ml) and equilibrated overnight. Radioactivity was determined using a Packard 2500TR scintillation counter with an efficiency of approximately 50%, with samples counted for 4 min and data expressed as dpm per sample.

[^{3}H]CGS21680 binding was carried out as described for [^{3}H]DPCPX using ligand concentrations of 2 and 20 nM, except that Tris-buffer contained 10 mM $MgCl_2$ and 10 μM CADO was used to determine non-specific binding.

4.2.4. [^{3}H]RX821002 Binding Assay

[^{3}H]RX821002 ([1,4-(6,7(n)-^{3}H]benzo-dioxan-2-methoxy-2-yl)-2-imidazoline) (60 Ci mmol^{-1}; Amersham) binding was carried out under equilibrium conditions by preincubating 100 μl of test drug and 300 μl of buffer (10 mM Tris-HCl, 0.5 mM $MgCl_2$, pH 7.4) with 100 μl of 10 nM [^{3}H]RX821002 for 2 min at 25°C. Test drugs were diluted in buffer to give 10 duplicate concentrations. Total binding was determined in the presence of buffer and 100 μM adrenaline (ADR) was used to determine non-specific binding. Addition of kidney membrane suspension (500 μl; 100-1000 μg) to give a final volume of 1 ml, initiated a 60 min incubation at 25°C. Bound and free ligand were separated using a Brandel cell harvester and this was followed by 3

washes (3 ml) in ice cold buffer over GF/B filters. Filter disks were transferred to scintillation vials and radioactivity determined as above.

4.2.5. [^{3}H]DPCPX Binding To HEK 293 Cell Membranes

[^{3}H]DPCPX binding to HEK 293 cell membranes was carried as described for binding to rat kidney membranes with the following modifications. The [^{3}H]DPCPX concentration was increased to 5 nM (final 0.5 nM), HEK 293 membranes were added at 40-80 μg of protein per sample and the incubation period was 30 min.

4.2.6. *In Vitro* Autoradiography

4.2.6.1. Slide Preparation for *In Vitro* Autoradiography

Double frosted glass microscope slides for *in vitro* autoradiography were cleaned in running tap water and oven dried at 60°C. A subbing solution (10 g gelatin, 0.5 g chromic potassium sulphate in 1 l deionised water) was heat stirred to a temperature of 60-70°C and filtered through Whatman 91 filter paper. The solution was allowed to cool to below 40°C and racks containing clean slides were dipped in the subbing solution. Slides were dried overnight at 60°C in a oven containing a tray of copper sulphate dessicant. The subbing solution could be used to coat several batches of slides at once but was discarded after use.

4.2.6.2. Preparation of Brain Sections for *In Vitro* Autoradiography

For *in vitro* autoradiographic studies, rats were anaesthetised with 4% halothane in oxygen and nitrous oxide (30:70 v:v). The neck was broken, the head guillotined and the brain carefully removed and frozen in isopentane at

-45°C (temperature was maintained by cooling in a dry ice / acetone mixture). Brains were frozen onto orientating microtome chucks with Tissue Tek, dipped in Lipshaw Embedding Matrix, sprayed with cryospray and equilibrated for 30 min at -20°C. Coronal sections (20 μm) were cut at the level of the ventral hippocampus (Paxinos and Watson, 1982) on a Bright cryostat (-20°C) and thaw mounted onto gelatin coated slides. 48 continuous sections were cut (2 sections per slide) and divided into four repeating groups of six slides for receptor pharmacology. Sections were dried at room temperature and stored at -70°C prior to use.

4.2.6.3. [^{3}H]DPCPX *In Vitro* Autoradiographic Studies

A pilot experiment based on previous studies (Weber *et al.*, 1990a) was conducted to establish optimum incubation and washing conditions for [^{3}H]DPCPX autoradiography. The assay buffer used was as described for membrane binding experiments (50 mM Tris-HCl, pH 7.4), whereas the incubation time was extended to 90 min and the final [^{3}H]DPCPX concentration increased 10 fold to 1 nM.

For *in vitro* autoradiographic studies on the inhibition of [^{3}H]DPCPX binding by adenosine A_1 antagonists, tissue sections were removed from the freezer and left at room temperature for 60 min. All autoradiographic procedures were at room temperature unless otherwise stated. Sections were incubated in Coplin jars for 90 min in 50 ml of Tris-buffer containing test drug, [^{3}H]DPCPX (1 nM) and ADA (1 u ml^{-1}). Unlabelled DPCPX and FR129946 were used as competing drugs and non-specific binding was determined in the presence of 10 μM R-PIA. Following incubation, sections were washed 4 times (30 sec) in separate beakers containing Tris-buffer, dipped in distilled water, blotted, the excess liquid carefully removed under vacuum with a fine tipped

pasteur pipette and dried under a hot stream of air. For autoradiographical analysis, sections were apposed together with tritium standards to [^{3}H]-sensitive Hyperfilm in X-ray cassettes for 10 weeks at -70°C.

Cassettes were left at room temperature for 60 min before removal of the [^{3}H]-Hyperfilm and development in a darkroom. Films were bathed in Kodak D19 developer (diluted 5 fold in tap water) for 4 min, dipped in water before two 4 min washes in Kodak fixative (diluted 4 fold in tap water) and finally dipped in water containing detergent (0.1%). Films were then rinsed under cold running tap water for 30 min and dried in a cabinet at 30°C. Films were then covered and stored at room temperature prior to analysis.

Autoradiograms were analysed using a computer based image analyser (MCID, Imaging Research Inc.). After background subtraction by a matrix shading correction facility, optical density (O.D.) values were converted to binding density (fmol mg^{-1} tissue equivalent) using tritium standards ([^{3}H]Microscales) and the specific activity of the radioligand. Standard curves were calculated as O.D. versus radioactivity in moles per unit area (mm^2). O.D. measurements of each brain area were performed by selecting a measuring box of appropriate dimension, overlaying the structure in a total binding section and measuring the optical density of that area four times for both sections on each slide. Once measurements in a particular section were complete, the O.D. in corresponding structures treated with different competing drug concentrations were measured in the same way. Specific O.D. was then determined by automatic subtraction of non-specific from the respective totals. IC_{50} values for each region in the case of competition experiments were determined as for radioligand binding studies using a one site logistic model. Areas assessed were entorhinal, deep and superficial cortex and hippocampal CA1, CA3 and dentate gyrus.

4.2.7. *In Situ* Hybridisation

4.2.7.1. Riboprobe Preparation and Labelling

The plasmid pAR1639 (Figure 4.1), which contained the coding region for the rat adenosine A_1 receptor cDNA was supplied by the Fujisawa Pharmaceutical Co. Ltd. The plasmid (700 ng μl^{-1}) was in 10 μl of TE buffer (10 mM Tris-HCl, 1 mM EDTA, pH 8.0) and was constructed with pUC18 vector. The rat adenosine A_1 receptor cDNA was amplified by the Polymerase Chain Reaction (PCR) and contained the full size open reading frame of the adenosine A_1 receptor but not the 5′ and 3′ non-coding regions. Plasmid pAR1639 is relatively stable at 4°C but should be stored for longer periods at -20°C. Plasmid pAR1639 contained no RNA promoter sequences necessary for the production of a riboprobe so the insert containing the rat adenosine A_1 receptor cDNA had to be removed and cloned into a different plasmid. A general outline of the overall *in situ* hybridisation procedure is shown in Figure 4.2.

4.2.7.2. Electrical Transformation (Electroporation) and Cultivation

Plasmid pAR1639 was washed with 25 μl of TE buffer into a 500 μl microcentrifuge tube giving a plasmid solution of approximately 200 ng μl^{-1} and stored at 4°C. 1 μl of plasmid solution was added to 50 μl of Gibco electrocompetent DH10B E. coli and kept on ice. The mixture was electroporated (BioRad Gene Pulser) for 10 sec at 2.5 kV for incorporation of the plasmid into E. coli, followed by immediate addition of 800 μl of SOC medium (2% tryptone, 0.5% yeast extract, 10 mM NaCl, 2.5 mM KCl, 10 mM $MgCl_2$ and 20 mM glucose). The mixture was decanted into a 15 ml tube and left on ice to "stabilise" (the electrical shock disrupts the bacterial cell wall

Figure 4.1

Fujisawa plasmid

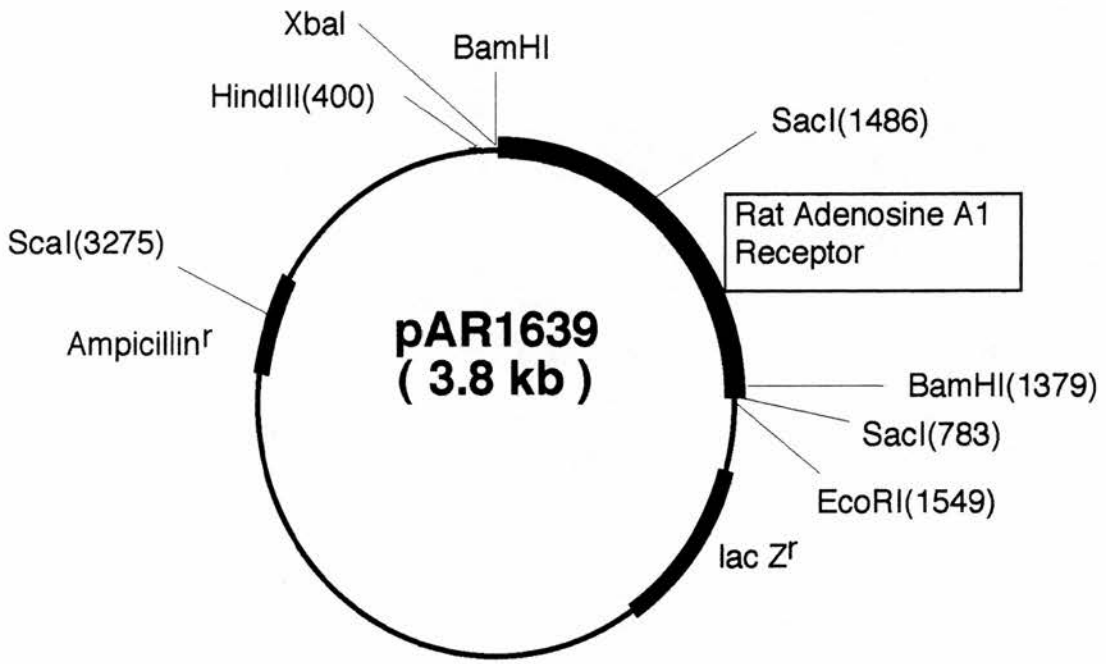

Figure 4.2 *In situ* Hybridisation

Plasmid pAR1639

↓

Electrical Transformation and Cultivation (plasmid incorporated into E. coli)

↓

DNA Purification (purification of DNA from bacterial culture)

↓

Restriction Endonuclease Digestion (to cut out appropriate area of DNA)

↓

Horizontal Agarose Electrophoresis (HAE) (to check molecular weight of DNA)

↓ Figure 4.3 - Gel 1

Polymerase Chain Reaction (amplification of the appropriate stretch of DNA)

↓ Figure 4.3 - Gel 2

TA Cloning (ligation of PCR product into new plasmid)

↓

Chemical Transformation and Cultivation (plasmid incorporated into cells)

↓

Blue/white Screening (selection of colonies containing PCR insert)

↓

DNA Purification (purification of DNA from bacterial culture)

↓ Figure 4.3 - Gels 3 & 4

DNA Sequencing (check DNA sequence of desired PCR product)

↓ Figure 4.4

[^{33}P]-Labelling of Riboprobes

↓ Figure 4.3 - Gels 5 & 6

***In situ* Hybridisation Procedure using [^{33}P]Riboprobes**

allowing the DNA to diffuse into the cell interior where it is replicated alongside the bacterial chromosomal DNA). The mixture was then incubated at 37°C for 60 min in a shaking incubator (225 rpm).

LB (Luria-Bertani) medium (1% tryptone, 0.5% yeast extract, 1% NaCl, pH 7.0) was autoclaved and stored at room temperature. LB agar (LB medium plus 15 g l^{-1} agar) was melted at low heat in a microwave (2 min) and equilibrated in a water bath at 37°C. The ampicillin resistance of the Fujisawa plasmid (Figure 4.1) was used to select E. coli which had incorporated the plasmid; ampicillin was added (50 μg ml^{-1}) to LB agar, poured onto 10 cm plates and allowed to dry. 50 μl of electroporation mix was added to the centre of a plate and spread with a flamed glass spreader. A second plate containing E. coli only was used as a control and plates were left overnight in an incubator at 37°C. The stock electroporation solution can be stored at 4°C for up to 2 weeks for re-plating, as colonies may need to be concentrated or diluted. Long term storage is possible in glycerol at -70°C.

The following day, 10 ml aliquots of LB broth containing ampicillin (50 μg ml^{-1}) were dispensed into 50 ml conical tubes. Five individual colonies were scraped from the plate using sterile plastic hoops and mixed with an aliquot of broth for inoculation, with a control tube containing broth only. The six cultures (five + control) were left overnight in a horizontal shaker (225 rpm) at 37°C and the stock plate stored at 4°C.

4.2.7.3. DNA Purification

DNA was purified using the Promega Magic™ DNA purification system. 1.5 ml aliquots of the above 5 cultures were added to 1.8 ml microcentrifuge tubes and centrifuged at 14000 rpm in a Beckman microcentrifuge for 5 min. The supernatant was decanted, a further 1.5 ml of each culture was added and recentrifuged as before. Pellets were resuspended in 200 μl of Cell

Resuspension Solution (50 mM Tris-HCl, 10 mM EDTA, RNAse A (100 μg ml^{-1})), followed by 200 μl of Cell Lysis Solution (0.2 M NaOH, 1% SDS). 200 μl of Neutralisation Solution (1.32 M potassium acetate, 6.4% glacial acetic acid, pH 4.8) was added and tubes centrifuged as above, to obtain a clear lysate. The clear lysate was transferred to a fresh microcentrifuge tube and 1 ml of Magic Miniprep DNA Purification Resin added and mixed thoroughly. The mixture was transferred to a Magic Minicolumn using a 2 ml syringe and extracted under vacuum and then washed with a further 2 ml of Column Wash Solution (200 mM NaCl, 20 mM Tris-HCl, 5 mM EDTA, pH 7.5). The minicolumn was centrifuged as above (20 sec) to dry the resin. The column was transferred to a fresh microcentrifuge tube and 50 μl of TE buffer was added, left for 1 min and DNA eluted by microcentrifugation for 20 sec. Approximately 30 μg of plasmid DNA was obtained from each of the five individual 10 ml bacterial cultures.

4.2.7.4. Restriction Endonuclease Digestion

Restriction endonucleases are enzymes found naturally in bacterial cells. They are highly specific recognising short sequences (generally palindromic in nature) in double stranded DNA. On binding to individual recognition sites, the endonucleases cleave the DNA.

The restriction map of plasmid pAR1639 (Figure 4.1) was examined and two sites on either side of the adenosine A_1 receptor insert were chosen, in order to check the molecular weight of the DNA template. The restriction digest for the five samples contained 2 μl of DNA, 0.5 μl of EcoR1, (all enzyme solutions ~8-10 u μl^{-1}), 0.5 μl of XBal, 1 μl of Buffer H and 6 μl of distilled water ($d.H_2O$) in a 500 μl microcentrifuge tube, with samples incubated at 37°C for 120 min. On removal, samples were centrifuged at 14000 rpm for 30 sec and 1.5 μl of an "electrophoresis loading dye" (10% glycerol (v/v), 0.1%

bromophenol blue, 0.1% xylene cyanol) added, which stops the samples floating away on addition to agarose gels. 10 μl of all five DNA samples were added to individual lanes on a 1% agarose gel (see below), along with two molecular weight markers (λ phage and P-gem) (Figure 4.3-Gel 1).

4.2.7.5. Horizontal Agarose Electrophoresis of DNA

DNA of varying sizes can be separated by electrophoresis through agarose gel. A 1% agarose gel is suitable for separation of products with a variety of molecular weight ranges (500-7000 bp). 50 ml of TBE buffer (0.045 M Tris-borate, 1 mM EDTA, pH 8.0) was added to 0.5 g of agarose MP and melted in a microwave at low heat for 2 min. After cooling, 0.5 μl of ethidium bromide (10 mg ml^{-1}) was added, mixed and poured while warm onto an electrophoresis tray. After the gel has solidified, the tray was placed in a electrophoretic chamber (Bioblock Consort) and TBE buffer poured over the gel. Samples were added and the gel was run at 5-10 V cm^{-1} until the dye front reached the bottom of the gel. DNA has an overall negative charge and migrates from the negative to positive terminal. The gel was examined under an ultraviolet transilluminator (Vilber Lourmat), with DNA appearing as a bright band and a polaroid photograph taken.

4.2.7.6. Polymerase Chain Reaction (PCR)

PCR originated in the mid 1980's (Mullis & Faloona, 1987) and is used to amplify a stretch of DNA between two regions of known sequence. Two amplimers (short single stranded oligonucleotides) are synthesised to complement sequences which lie on opposite strands of the DNA, flanking the segment to be amplified. Oligonucleotides were designed using Gene Jockey™ (Dr P. Taylor, Cambridge Biosoft) on an Apple Macintosh computer, to both ends of a 508 bp probe (nucleotides 359-867), from the rat adenosine

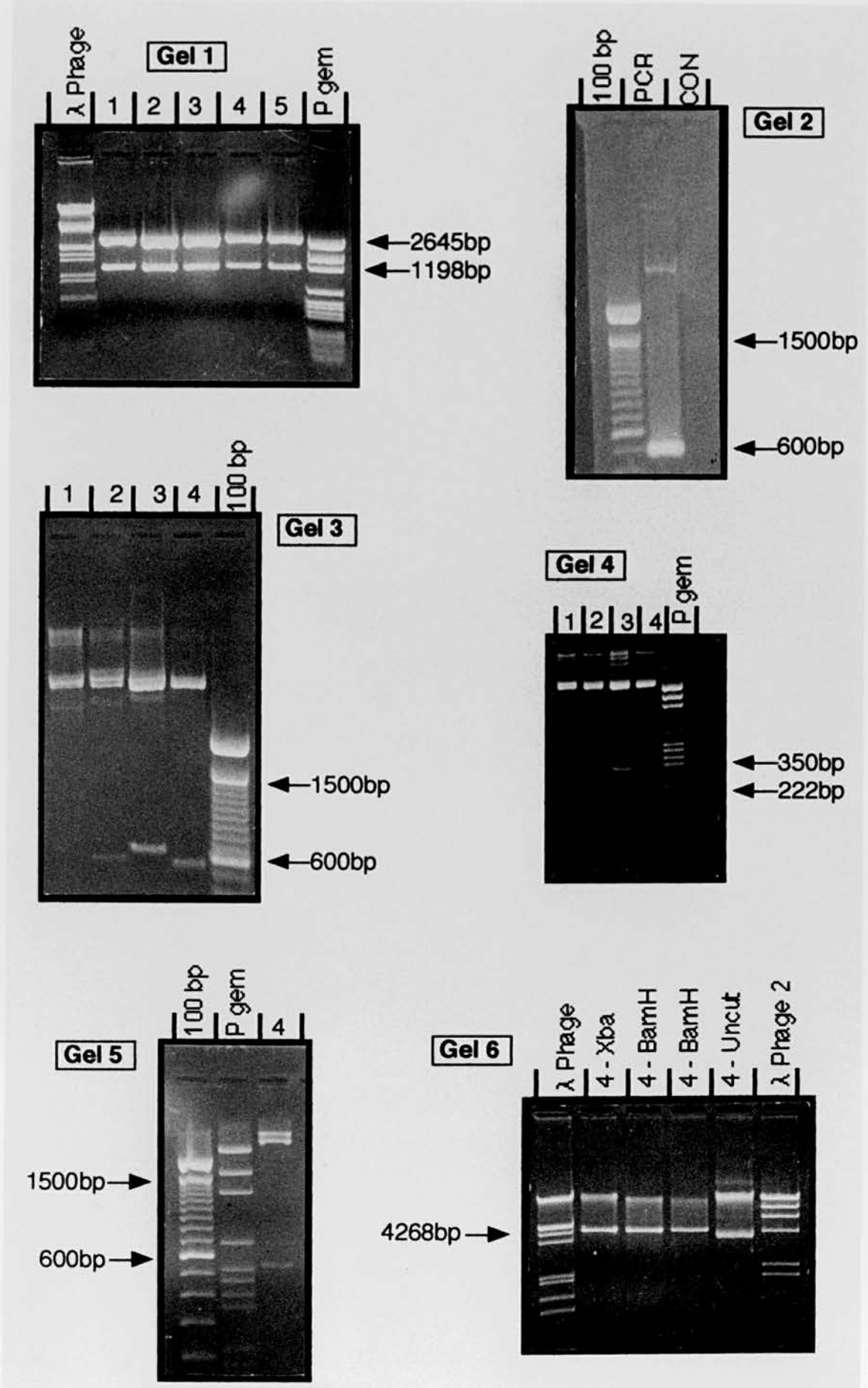

Figure 4.3 Horizontal Agarose Electrophoresis of DNA Samples

A_1 receptor cDNA, beginning in transmembrane IV and ending in domain VII. This area has low homology with the sequences of adenosine A_{2a}, A_{2b} and A_3 receptors assessed by homology matrix analysis. The 5′ probe was 22 bases (TCATTGCCTTGGTCTCTGTGCC) in length (nucleotides 359-380), with a melting temperature (Tm) of 61.9°C for double stranded DNA. The 3′ probe was 22 bases (GACGAAGAAGTTGAAGTAGACC) in length (nucleotides 846-867) with a Tm of 58.2°C for double stranded DNA. Probes were purchased from R & D Systems.

A PCR reaction was set up to amplify the desired PCR product, as the restriction digest (Figure 4.3-Gel 1) showed an insert of the correct molecular weight for all 5 samples which underwent DNA purification. The digest from lane 1 was chosen as the DNA template for the PCR reaction. The PCR reaction (1 μl 5′ of probe (20 μM), 1 μl of 3′ probe (20 μM), 10 μl of 10 x polymerase buffer (100 mM Tris-HCl, 500 mM KCl, 0.01% gelatin, pH 8.3), 10 μl of 25 mM $MgCl_2$, 1 μl of 10 mM nucleotides (DNTP's), 1 μl of Taq DNA polymerase (4 u μl^{-1}) and 75 μl of d.H_2O) was initiated by addition of 1 μl of template DNA (10-50 ng), or buffer for the control reaction, in a 500 μl microcentrifuge tube. The reaction contents were mixed and a drop of mineral oil was added to stop evaporation during the PCR process. PCR was carried out using the Hybaid Omnigene™ and a fixed protocol; a 2 min denaturation cycle at 95°C, followed by 30 repeating cycles of three procedures, denaturation (DNA separates so oligonucleotides can anneal to single strands) (95°C, 45 sec), annealing (oligonucleotides bind to the complementary sequence on single stranded DNA) (53°C, 45 sec) and polymerisation (extension by DNA polymerase which recognises and binds only double stranded DNA) (72°C, 60 sec) and finally an auto-extension (72°C, 5 min). Samples were left overnight to cool with no detrimental effect on stability.

The molecular weight of the PCR product was determined by horizontal

electrophoresis as described previously (see 4.2.7.5.). 10 μl aliquots of both PCR reactions were added to 1.5 μl of loading dye and pipetted onto a 1% agarose gel, with a molecular weight standard (100 bp marker) and a polaroid taken (Figure 4.3-Gel 2). A band with a molecular weight of approximately 500 bp matched the size of our predicted PCR product, with no bands in the control PCR reaction.

4.2.7.7. TA Cloning of PCR Reaction Product

Non-proofreading DNA polymerases such as Taq DNA polymerase, have a non-template dependent activity which adds a single deoxyadenosine (A) to the 3′ end of PCR products. TA cloning utilises this activity by creating linearised plasmid vectors with complimentary 3′ deoxythymidine (T) residues, allowing efficient ligation of PCR products into vectors. The circular construct can then be electrically or chemically transformed into E. coli and the PCR product amplified in the plasmid carrier.

4.2.7.8. Addition of (A) Overhang: Phenol/Chloroform Extraction and Ethanol Precipitation

Phenol/chloroform extraction separates nucleic acids from proteins and is widely used for the removal / inactivation of enzymes. 0.5 μl of Taq DNA polymerase (4 u μl^{-1}) was added to 50 μl of PCR reaction mixture, vortexed, a drop of mineral oil added and then incubated at 72°C for 10 min. The oil was removed and an equal volume of phenol:chloroform:isoamyl alcohol (25:24:1) was immediately added and the mixture vortexed vigorously. The phases were separated by microcentrifugation at 14000 rpm for 5 min and the top (aqueous) phase was transferred to a fresh tube. An equal volume of chloroform was added, vortexed vigorously, centrifuged for 2 min as above and the top phase again transferred to a fresh tube. Addition of sodium acetate, at a final

concentration of 0.3 M, and 2 vol. (v/v) of absolute alcohol was followed by mixing and incubation at -20°C for 120 min. The pellet was collected by microcentrifugation for 15 min as above, the ethanol decanted and the pellet washed with 70% alcohol. The pellet was lyophilised under vacuum and resuspended in 40 µl of TE buffer.

4.2.7.9. Cloning into pCR™II

Ligation of the PCR product into the Invitrogen plasmid pCR™II was performed immediately after phenol/chloroform extraction as the single (A) overhang will be removed over time. The ligation reaction contained 1 µl of PCR product, 1 µl of 10 x ligation buffer (60 mM Tris-HCl, 60 mM $MgCl_2$, 50 mM NaCl, 1 mg ml^{-1} bovine serum albumin (BSA), 70 mM ß-mercaptoethanol, 1 mM ATP, 20 mM dithiothreitol (DTT) and 10 mM spermidine), 2 µl of pCR™II vector (10 mM Tris-HCl, 1 mM EDTA, pH 7.5) (25 ng μl^{-1}), 1µl of T4 DNA ligase (4.0 Weiss u μl^{-1}) and 5 µl of sterile water. A control self ligation with no PCR product was also set up. The ligation reactions were incubated overnight at 14°C prior to transformation.

4.2.7.10. Chemical Transformation of Ligation Product

After overnight incubation, vials containing the ligation reactions were centrifuged for 30 sec at 14000 rpm. 2 µl of 0.5 M ß-mercaptoethanol was added to two independent 50 µl vials of One Shot™ TOP10F´ competent cells and mixed gently by stirring with a pipette tip. 2 µl of each ligation product were separately added to a vial of competent cells, mixed gently by stirring, and left on ice for 30 min. Stock ligations were stored at -20°C. Vials were heat shocked for 30 sec at 42°C in a water bath and placed on ice for 2 min. 450 µl of SOC medium was added and vials were shaken horizontally (225 rpm) for

60 min in a rotary shaking incubator and then placed on ice. 50 µl of the transformation reactions were spread onto LB agar plates which contained kanamycin (50 µg ml^{-1}) and had previously been spread with 40 µl of X-Gal (5-bromo-4-chloro-3-indolyl-ß-D-galactoside) (40 mg ml^{-1}) in dimethylformamide and 40 µl of IPTG (isopropyl-ß-D-thiogalactoside) (100 mM) and allowed to dry. Once the liquid was absorbed, plates were inverted and placed in an incubator at 37°C for at least 18 hr.

4.2.7.11. Blue / White Screening

After incubation at 37°C for 18 hr, plates were placed at 4°C for 2 hr to allow for proper colour development. The Invitrogen plasmid pCR™II contains a lac promoter and a lacZ∝ peptide sequence which can be functionally produced in competent cells. The resulting enzyme ß-galactosidase cleaves X-gal to give blue colonies. Correct insertion of the PCR product interrupts the reading frame of the lacZ∝ peptide and produces white colonies. Those with no insert, or the self ligation, do not alter the reading frame and colonies should be blue.

The self ligation worked well, with all colonies blue and the plate with insert had a mix of both white and blue colonies. 10 ml aliquots of LB broth containing ampicillin (50 µg ml^{-1}) was dispensed into 50 ml conical tubes. Ten individual white colonies were scraped from the plate using sterile plastic hoops, streaked onto a fresh ampicillin resistant agar plate and mixed with an aliquot of broth for inoculation. The new plate and tubes were left overnight at 37°C in an incubator and shaker (225 rpm) respectively and the stock plate stored at 4°C.

Only four of the ten colonies on the plate were still white the next day, so these four were used for DNA preparation as described previously (see

4.2.7.3.). After DNA purification, two separate restriction digests were carried out on each DNA preparation. As the Invitrogen plasmid pCR™II contains EcoR1 restriction sites on either side of the insert, the first digest should cut out the whole 508 bp PCR product. On examination of the predicted sequence of the PCR product, another restriction enzyme SacI should cut the PCR product almost in half, producing two separate fragments of 275 and 323 bp. The first digest contained 1 μl of DNA, 0.5 μl of EcoR1, 1 μl of Buffer H and 7.5 μl of d.H_2O in a 500 μl microcentrifuge tube, with samples incubated at 37°C for 90 min. The second contained 1 μl of DNA, 0.5 μl of SacI, 1 μl of Buffer J and 7.5 μl of d.H_2O in a 500 μl microcentrifuge tube, with samples incubated at 37°C for 18 hr.

Following incubation, samples were centrifuged at 14000 rpm for 30 sec and 1.5 μl of loading dye was added. Horizontal electrophoresis was carried out as described previously (see 4.2.7.5.), with 10 μl of each sample added to individual lanes on a 1% agarose gel, along with appropriate molecular weight markers (λ phage, P-gem and 100 bp). The gels were examined under ultraviolet light and polaroids taken (Figure 4.3-Gels 3 & 4). The gels indicated that three of the four digests had the correct insert.

4.2.7.12. Automated Fluorescent DNA Cycle Sequencing

The three products in the correct molecular weight range were kindly sequenced by Dr P.L. Taylor (MRC Reproductive Biology Unit, Edinburgh). Briefly, cycle sequencing is a rapid and convenient method for performing enzymatic extension reactions for DNA sequencing. The strategy of chain termination by incorporation of radiolabelled dideoxy nucleoside triphosphates (ddNTP's) originally described by (Sanger *et al.*, 1977) has recently been combined with fluorescent technology. The principles of the original radioisotopic method, and the recently developed non-radioisotopic methods,

are identical. Each method generates a population of labelled oligonucleotides that begin from a fixed point and end randomly at a fixed residue. Every base in the DNA has an equal chance of being the variable terminus, resulting in a population of oligonucleotides which differ in length by one base. The population of fragments are resolved by electrophoresis through a denaturing polyacrylamide gel.

The Sanger method requires the use of four separate reaction tubes, each with only one of the four nucleosides in the form of a radiolabelled ddNTP. Each of these four reactions are electrophoresed in individual lanes of the resolving gel, with the sequence determined by the pattern of bands observed on an autoradiogram of the resulting gel.

However, modern techniques utilise the incorporation of ddATP, ddGTP, ddCTP and ddTTP, conjugated to identifiable fluorophores and all added to a single tube. During the cycle sequencing reaction, the oligonucleotide chains synthesised are terminated by a fluorescently labelled ddNTP. When electrophoresed through a denaturing polyacrylamide gel, these oligonucleotides are separated by size. The automated sequencing apparatus (Applied Biosystems) uses a laser source to excite the fluorophores as they migrate past a detection point. Computer software subsequently constructs a screen image of the gel, with coloured bands representing each nucleotide base of the DNA chain. The actual DNA sequence is then automatically computed and can be analysed as required. DNA sequence analysis and manipulation were performed using Gene Jockey™. The data from the sequencing of all three products was accurate, with product four (Figure 4.3-Gels 3 & 4 and Figure 4.4) chosen for radioactive labelling with [^{33}P].

4.2.7.13. [^{33}P]-Labelling of the Riboprobe

150 μl of product 4 (Figure 4.3-Gels 3 & 4) was added to 30 ml of LB

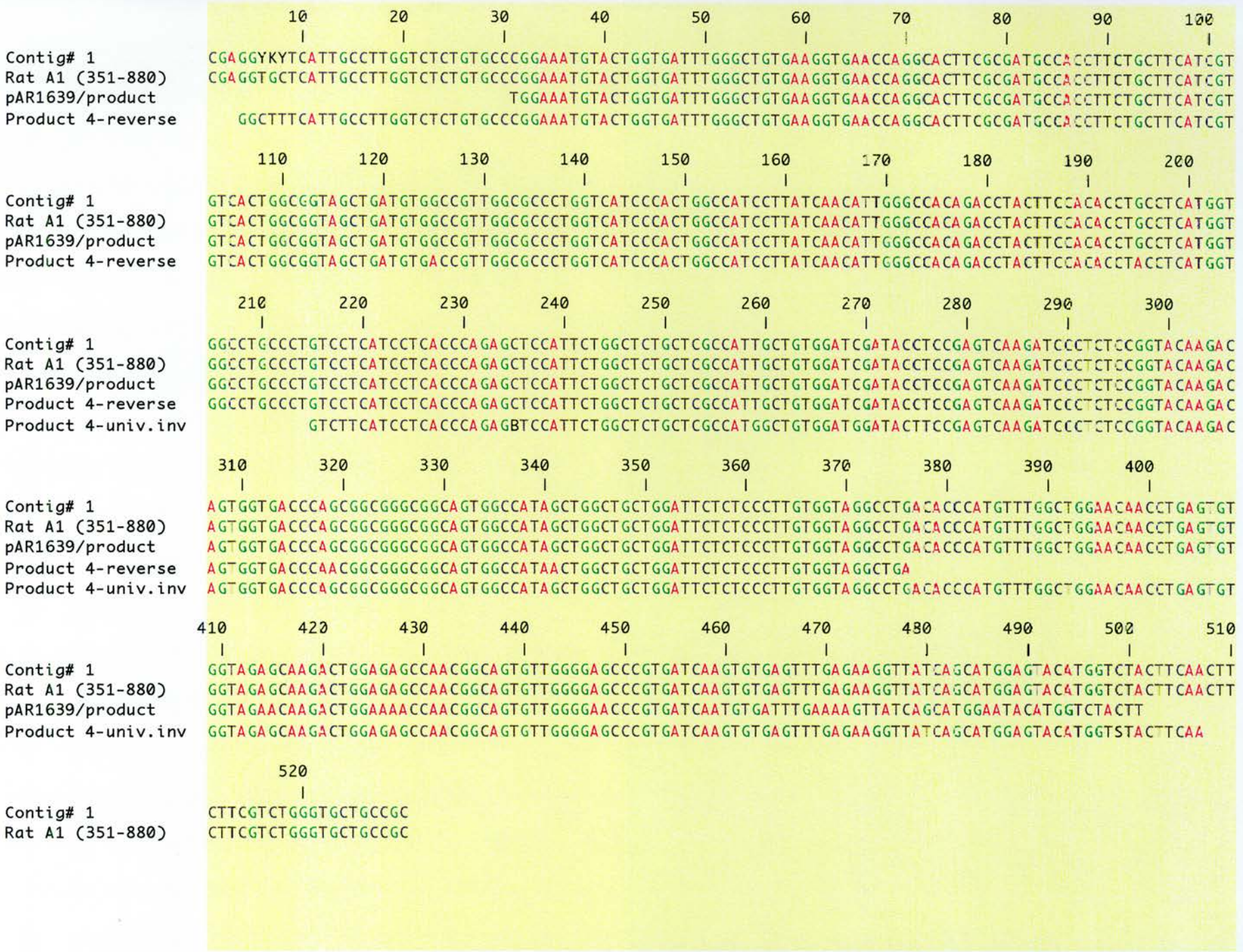

Figure 4.4 DNA Sequencing of Riboprobe for [^{33}P]Labelling

broth containing kanamycin (50 μg ml^{-1}) and ampicillin (50 μg ml^{-1}) and cultured overnight at 37°C in a rotary shaker (225 rpm). DNA was prepared using the Promega Magic™ DNA purification system as described previously (see 4.2.7.3.). After DNA purification, a restriction digest was carried out containing 1 μl of DNA, 0.5 μl of EcoR1, 1 μl of Buffer H and 7.5 μl of d.H_2O in a 500 μl microcentrifuge tube and incubated at 37°C for 90 min. The sample was centrifuged at 14000 rpm for 30 sec before 1.5 μl of loading dye was added. Horizontal electrophoresis was carried out as described previously (see 4.2.7.5.) with 10 μl of DNA added to an individual lane on a 1% agarose gel, with appropriate molecular weight markers (P-gem and 100 bp). The gel was examined under ultraviolet light and a polaroid taken (Figure 4.3-Gel 5).

The amount of DNA present in the preparation was determined using a Uvikon 860 spectrophotometer, with absorbance measured at 260 / 280 nM. The preparation contained 30 μg of DNA in 250 μl of TE buffer. For riboprobe labelling, requirements were 3 μg of DNA in 8 μl, so the DNA was precipitated by addition of 2 vol. of 100% ethanol and 0.1 vol. of 3 M sodium acetate (pH 5), and left at -20° C for 120 min. The preparation was spun at 10000 rpm at 4°C for 30 min. The pellet was washed in 70% ethanol, recentrifuged at 14000 rpm for 2 min and resuspended in TE buffer at the required concentration.

The pCR™II plasmid containing the insert must be linearised to produce the riboprobe. The restriction map of the plasmid was examined and two different restriction enzyme sites on either side of the insert were chosen for production of sense and antisense probes. The pCR™II plasmid has two RNA polymerases, SP6 and T7, which work in opposite directions, allowing synthesis of both sense and antisense riboprobes from the same product. The antisense digest contained 8 μl of DNA, 3 μl of BamH1, 2 μl of Buffer B and 7 μl of d.H_2O in a 500 μl microcentrifuge tube. The sense digest contained 8 μl of DNA, 3 μl of Xbal, 2 μl of Buffer H and 7 μl of d.H_2O in a 500 μl

microcentrifuge tube, with both samples incubated at 37°C overnight.

Samples were centrifuged at 14000 rpm for 30 sec and horizontal electrophoresis was as described previously (see 4.2.7.5.). Samples were diluted 10 fold before addition of loading dye and pipetted onto individual lanes of a 1% agarose gel, with two different λ phage molecular weight markers. The gel was examined under ultraviolet light and a polaroid taken (Figure 4.3-Gel 6).

Both sense and antisense digests underwent a proteinase K digestion to destroy the restriction endonucleases. 19 µl of each digest was added to a 500 µl microcentrifuge tube containing 7 µl of nuclease free H_2O, 3 µl of 10 x proteinase K buffer (0.1 M Tris-HCl, 0.05 M EDTA, 1% SDS, pH 7.8), 1 µl of proteinase K (10 mg ml^{-1}) and incubated at 37°C for 30 min. Digests then underwent a phenol/chloroform extraction and ethanol precipitation similar to that described previously. Briefly, 100 µl of phenol:chloroform:isoamyl alcohol (25:24:1) and 70 µl of nuclease free H_2O were added to the digest and vortexed. Phases were separated by microcentrifugation at 14000 rpm for 15 sec and the top (aqueous) phase transferred to a fresh tube. An equal volume of chloroform was added, vortexed and centrifuged as above with the top phase again transferred to a fresh tube. 10 µl of sodium acetate (3 M) (pH 5.2) and 250 µl of ice cold 100% ethanol was added, followed by mixing and incubation at -20°C for 60 min. The pellet was precipitated by centrifugation at 14000 rpm for 10 min at 4°C. The supernatant was decanted and 500 µl of 70% ethanol added and centrifuged at 14000 rpm for 2 min at 4°C. The supernatant was removed, the pellet air dried and reconstituted in 10 µl of d.H_2O.

[^{33}P]-Labelling of both sense and antisense probes was carried out at room temperature, with the following constituents added to two 500 µl

microcentrifuge tubes: 2.5 µl of 10 x Transcription buffer (TSC) (200 mM Tris-HCl, 30 mM $MgCl_2$, 10 mM spermidine, pH 7.5), 1 µl of 100 mM DTT, 1 µl of RNase inhibitor (40 u μl^{-1}), 1 µl of rATP (10 mM), 1 µl of rCTP (10 mM), 1 µl of rGTP (10 mM), 1 µl of rUTP (0.2 mM), 10 µl of DNA template, 5 µl of [^{33}P]UTP (10 $\mu Ci\ \mu l^{-1}$), 1 µl of RNA polymerase (20 u μl^{-1}) (SP6 or T7) and 0.5 µl of d.H_2O. The SP6 polymerase was used for the production of the sense probe and T7 polymerase for the antisense probe. The tubes were mixed and incubated at 37°C for 45 min. For optimal polymerisation, another 1 µl of the appropriate RNA polymerase was added to each tube, mixed and incubated as before. 2 µl of tRNA (10 mg ml^{-1}) followed by 1 µl of RNase free DNase-1 (10 u μl^{-1}) was added to remove the DNA template and the mixture was incubated for 10 min at 37°C. Both probes then underwent a phenol/chloroform extraction and ethanol precipitation as described above, with pellets resuspended in 20 µl of d.H_2O and stored at -20°C.

4.2.7.14. Preparation of Slides for [^{33}P]-Labelling

For *in situ* hybridisation, double frosted glass microscope slides were washed and baked. Slides were immersed in a 2% solution of freshly prepared 3-aminopropyltriethoxy-silane (APES) (350 ml) which can be used for 200-300 slides. Slides were dipped in 99% IMS then d.H_2O and dried overnight at 37°C. To minimise potential RNA contamination at all stages, gloves were worn and slides covered to reduce exposure to air.

4.2.7.15. Preparation of Brain and Kidney Sections for [^{33}P]-Labelling

Rats were anaesthetised as described for *in vitro* autoradiography (see 4.2.6.2.). The neck was broken, the head guillotined, the brain and kidneys

carefully removed and frozen on cardice in a sealed container. Gloves were worn at all times and tissue exposure to air minimised. Tissues were frozen on to orientating microtome chucks with Tissue Tek and dipped in Lipshaw embedding matrix. Using a Bright cryostat, 20 μm coronal sections were cut at the level of the ventral hippocampus in brain and hemisagital sections in kidney, then thaw mounted onto the appropriate slides. Sections for *in situ* hybridisation were placed in a sealed container. For each tissue, 48 continuous sections were cut (2 sections per slide) and divided into four repeating groups of six slides (slide 1 & 2 *in situ*, slide 3 & 4 cell staining and slide 5 & 6 autoradiography, see below). Sections were dried at room temperature and stored at -70°C until use.

For the comparative *in situ* hybridisation and *in vitro* autoradiographic studies using brain and kidney sections, autoradiography was performed as described previously (see 4.2.6.3.), with total binding determined in the presence of 0.1% DMSO and non-specific binding determined using 10 μM R-PIA.

4.2.7.16. *In Situ* Hybridisation Procedure Using [^{33}P]Riboprobes

All equipment for *in situ* procedures were washed and baked. All solutions were made in distilled water that had been autoclaved or treated with 0.1% diethylpyrocarbonate (DEPC). Sections were removed from the freezer and transferred quickly to sterile racks on cardice, thus preventing thawing and release of RNases. Sections were dried quickly with a hair drier and immediately transferred to a glass trough containing 350 ml of fresh 4% paraformaldehyde (pH 7.2) in DEPC treated phosphate buffered saline (PBS) for 5 min. Slides were then transferred through two troughs containing 0.1 M sodium phosphate buffer (pH 7.4) for 5 min each, with stirring and shaking,

followed by 2 min in 350 ml of DEPC-distilled water. Slides were then washed in 350 ml of 80 mM triethanolamine (TEA) buffer (pH 8.0) for 2 min, followed by a 10 min wash in TEA buffer containing 0.25% freshly added acetic anhydride. The slides were placed in 350 ml of 2 x standard sodium citrate (SSC) buffer (pH 7.0) and left soaking prior to addition of prehybridisation buffer.

Slides were individually removed and blotted using sterile gauze. 100 μl of 0.2 μM Millipore filtered prehybridisation buffer (50% deionised formamide, 4 x STE buffer (0.4 M NaCl, 40 mM Tris-HCl, 4 mM EDTA, pH 8.0), 1 x Denhardt's, yeast tRNA (0.125 mg ml^{-1}), denatured salmon sperm DNA (0.125 mg ml^{-1}), and 10 mM DTT) was added and incubated at 42°C for 60 min.

[^{33}P]-Labelled sense and antisense riboprobes were diluted in hybridisation buffer (prehybridisation buffer with 10% dextran sulphate) to give approximately 10^6 CPM per slide and incubated at 60°C for 3 min. Slides were blotted and 100 μl of riboprobe added to each section. FMC Gelbond film (hydrophilic side up), was used as a coverslip, with slides placed in 10 cm petri dishes containing small vials of sterile water to prevent dessication and incubated overnight at 50°C.

Two glass troughs containing RNase buffer (10 mM Tris-HCl, 500 mM NaCl, 1 mM EDTA, RNase (20 μg ml^{-1}), pH 8.0), one supplemented with 1 mM DTT, were placed in a water bath at 37°C. Slides were taken from the incubator and washed in 4 x SSC to remove coverslips, transferred to a new slide rack, then placed in 350 ml of 4 x SSC (plus 2 mM DTT), for 15 min at room temperature. The rack was transferred to 350 ml of RNase buffer at 37°C for 30 min and this incubation was repeated in RNase buffer containing 1 mM DTT. Slides were then taken through three sequential 30 min washes at room temperature in 4 x, 2 x and 0.1 x SSC (wash stringency can be increased by increasing the temperature and decreasing the salt concentration), followed by

three further sequential 3 min washes at room temperature in 50%, 85% and 100% IMS containing 300 mM ammonium acetate. Slides were placed on the bench and left covered overnight to dry.

In a darkroom, Kodak emulsion was preheated for 60 min in a water bath (45°C) and slides prewarmed on a hot plate. The emulsion was poured into a slide dipping chamber and slides were placed back to back, dipped twice in emulsion, blotted on a paper towel and dried in a slide rack for 10 min. The slide rack was placed in a sealed plastic box within two other boxes and left at room temperature for 120 min. Finally, slides were placed in a polacetyl box containing a perforated vial of silica gel, double wrapped in tin foil and stored at 4°C for the appropriate period of time.

4.2.7.17. Development of [^{33}P]-Labelled Sections

Slides were removed from the cold room and allowed to warm to 15°C. Four troughs containing: (a) 350 ml of Kodak D-19 developer, (b) d.H_2O, (c) 10% Kodak polymax (fixative) in d.H_2O and (d) d.H_2O were placed on ice, to attain a temperature of 15°C. Slides were washed sequentially in the four troughs for 4 min, 20 sec, 10 min and 15 min respectively. Slides were washed under running water for 20 min, dipped in haematoxylin for 2 min, rinsed in fresh running water, rinsed in 1% alcohol for 20 sec and placed in tap water. Slides were examined under light field microscopy and if nuclei staining was adequate, slides were dehydrated through three 20 sec dips in 70%, 90% and 100% ethanol. Slides were placed in histo-clear for 5 min and stored in xylene in a fume hood. Slides were removed from xylene, pertex added, coverslips placed gently over the tissue sections and left to dry.

Black and white photographs of brain and kidney sections were taken using an Olympus BH2 microscope, under light and dark field, at a magnification level of x 12 and x 35.

4.2.8. Data Analysis

Competition binding curves were constructed for binding of [^{3}H]DPCPX, [^{3}H]CGS21680 and [^{3}H]RX821002 to rat kidney membranes and HEK 293 cell membranes, as described in Chapter 1 (see 1.2.4.1). Pharmacological parameters were determined using the appropriate equations and the iterative curve fitting programme Sigma plot, as described in Chapter 1 (see 1.2.4).

4.2.9. Statistical Analysis

The data shown in the figures displayed are a representation of one experiment, all of which have been carried out at least three times, unless otherwise stated. Data in tables and text are shown as mean ± the standard error of the mean (S.E.M.) of at least three different experiments.

4.2.10. Materials

Molecular biological products used were from Invitrogen, Promega, Gibco and R & D Systems. The radioligands were; [^{3}H]DPCPX (109 Ci mmol^{-1}; NEN), [^{3}H]CGS21680 (41.2 Ci mmol^{-1}; NEN), [^{3}H]RX821002 (60 Ci mmol^{-1}; Amersham) and [^{33}P]UTP (250 μCi /10 μCi μl^{-1}; NEN). All other products used in binding studies, *in situ* hybridisation and *in vitro* autoradiography were from Sigma, Boehringer Mannheim, BDH and Kodak.

4.3. Results

4.3.1. [^{3}H]DPCPX and [^{3}H]CGS21680 Binding to Rat Kidney Membranes

In an attempt to characterise binding to adenosine receptors in rat kidney membranes, five membrane preparations were tested (see 4.2.1.). Initially crude membrane preparations were tried, followed by the isolation of membranes from particular sections of the kidney in an attempt to increase binding site density.

Method 1 (p222): No specific binding of [^{3}H]DPCPX (0.1 nM) or [^{3}H]CGS21680 (2 nM) to crude kidney membranes was detected at protein concentrations up to 0.5 mg per sample, with an incubation period of 120 min.

Method 2 (p222): No specific binding of [^{3}H]DPCPX (0.1 and 1 nM) or [^{3}H]CGS21680 (2 and 20 nM) to crude kidney membranes was detected at protein concentrations up to 0.5 mg per sample, with an incubation period of 120 min.

Method 3 (p223): No specific binding of [^{3}H]DPCPX (0.1 and 1 nM) or [^{3}H]CGS21680 (2 and 20 nM) to the mixed basolateral / brush border fraction was detected at protein concentrations up to 2 mg per sample, with an incubation period of 120 min. No specific binding of [^{3}H]DPCPX (0.1 nM) was detected in any of the individual pellet or supernatant fractions, produced during the differential centrifugation procedure.

Method 4 (p223): No specific binding of [^{3}H]DPCPX (0.1 and 1 nM) or [^{3}H]CGS21680 (2 and 20 nM) to individual basolateral or brush border fractions was detected at protein concentrations up to 2 mg per sample, with an incubation period of 120 min.

Method 5 (p224): No specific binding of [^{3}H]DPCPX (0.1 and 1 nM) or [^{3}H]CGS21680 (2 and 20 nM) to the medullary preparation was detected at

protein concentrations up to 0.5 mg per sample, with an incubation period of 120 min.

Inhibition of [^{3}H]DPCPX and [^{3}H]CGS21680 binding to rat cortical and striatal membranes respectively by adenosine agonists and antagonists was conducted simultaneously. Specific binding with the appropriate pharmacological specificity was noted in both cases (data not shown).

4.3.2. [^{3}H]RX821002 Binding to Rat Kidney Membranes

Adrenoreceptors, which have been divided into three major subtypes α_1, α_2 and β, are found throughout the body and adrenergic drugs are known to act on kidney (O'Rourke *et al.*, 1994; Bylund *et al.*, 1995). As discussed for purinoreceptors (Ch.1), IUPHAR addressed the complications of the classification of adrenoreceptor subtypes, caused by the availability of new pharmacological tools and the cloning of recombinant receptors (Bylund *et al.*, 1995). As with purinoreceptors, historical precedent makes this difficult and the guidelines for α_1 adrenoreceptor classification have already been updated (Hieble *et al.*, 1995; Vanhoutte *et al.*, 1996). Compounds available for investigating the various receptor subtypes (Bylund *et al.*, 1995) in different tissues include the α_2 adrenoreceptor radioligands [^{3}H]RX821002 (Langin *et al.*, 1989) and [^{3}H]MK912 (Uhlen *et al.*, 1992). It is thought that α_{2a} and α_{2b} adrenoreceptors are expressed in kidney, with the α_{2b} subtype predominant (Uhlen & Wikberg, 1991a, b). Uhlen and colleagues have proposed further subdivisions of α_{2a} and α_{2b} adrenoreceptors (Uhlen & Wikberg, 1991c; Uhlen *et al.*, 1993; Bylund *et al.*, 1995). The presence of adrenoreceptors in the rat kidney membrane preparations described in the previous section were

investigated using the α_2 adrenoreceptor antagonist radioligand [^{3}H]RX821002 as a positive control to prove the viability of membranes used in [^{3}H]DPCPX and [^{3}H]CGS21680 binding studies.

4.3.2.1. Effect of Protein Concentration on [^{3}H]RX821002 Binding to Rat Kidney Membranes

[^{3}H]RX821002 (1 nM) binding to rat kidney membrane preparations was carried out in parallel with [^{3}H]DPCPX and [^{3}H]CGS21680 binding studies. Kidney membranes were incubated for 60 min at 25°C, with non-specific binding determined in the presence of 100 μM adrenaline. The mixed **(Method 3)** and separate basolateral / brush border **(Method 4)** kidney membrane preparations (see 4.2.1.3 and 4.2.1.4) were used for binding studies. Unlike [^{3}H]DPCPX, an increase in specific [^{3}H]RX821002 binding was observed with increasing amounts of membrane protein in the assay for both preparations, with data shown for the separate brush border and basolateral fractions from **Method 4** (Figure 4.5); results using the mixed preparation **(Method 3)** were almost identical. No specific [^{3}H]RX821002 binding was detected when using membranes from kidney medulla (**Method 5**, see 4.2.1.5.). In all further experiments, the brush border membrane fraction (approximately 100 μg of protein per sample) **(Method 4)** was used.

4.3.2.2. Time Course of [^{3}H]RX821002 Binding to Rat Kidney Brush Border Membranes

A time course of [^{3}H]RX821002 (1 nM) binding to rat kidney membranes was carried out at 25°C, with equilibrium attained by 2 min (Figure 4.6). In all other experiments, [^{3}H]RX821002 (1 nM) binding to kidney membranes was

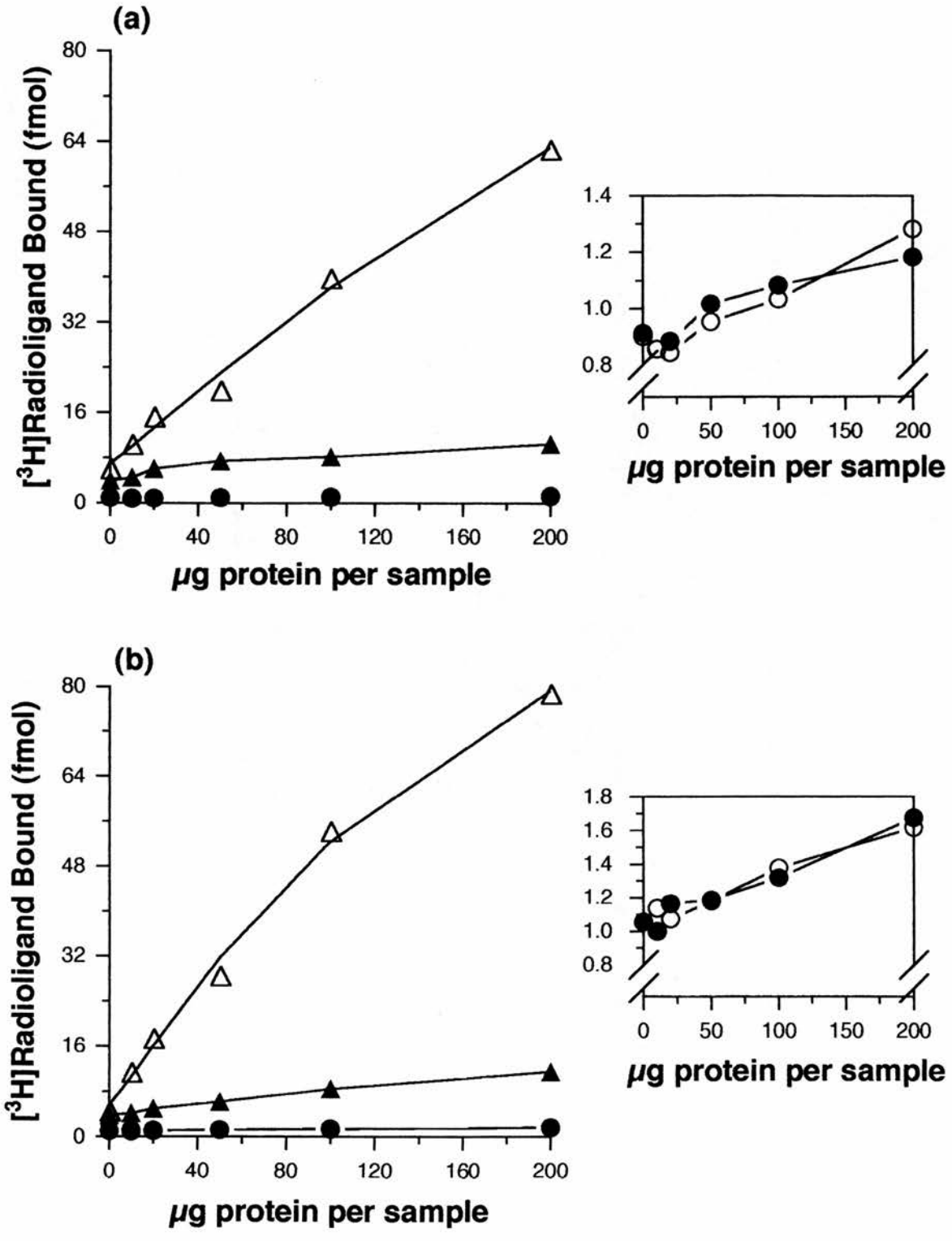

Figure 4.5 [^{3}H]DPCPX and [^{3}H]RX821002 Binding to (a) Basolateral and (b) Brush Border Membranes From Rat Kidney Cortex.

[^{3}H]DPCPX binding is represented by circles and [^{3}H]RX821002 binding by triangles. Open symbols are for total binding and filled symbols are for non-specific binding. Inset shows data for [^{3}H]DPCPX only over a compressed range.

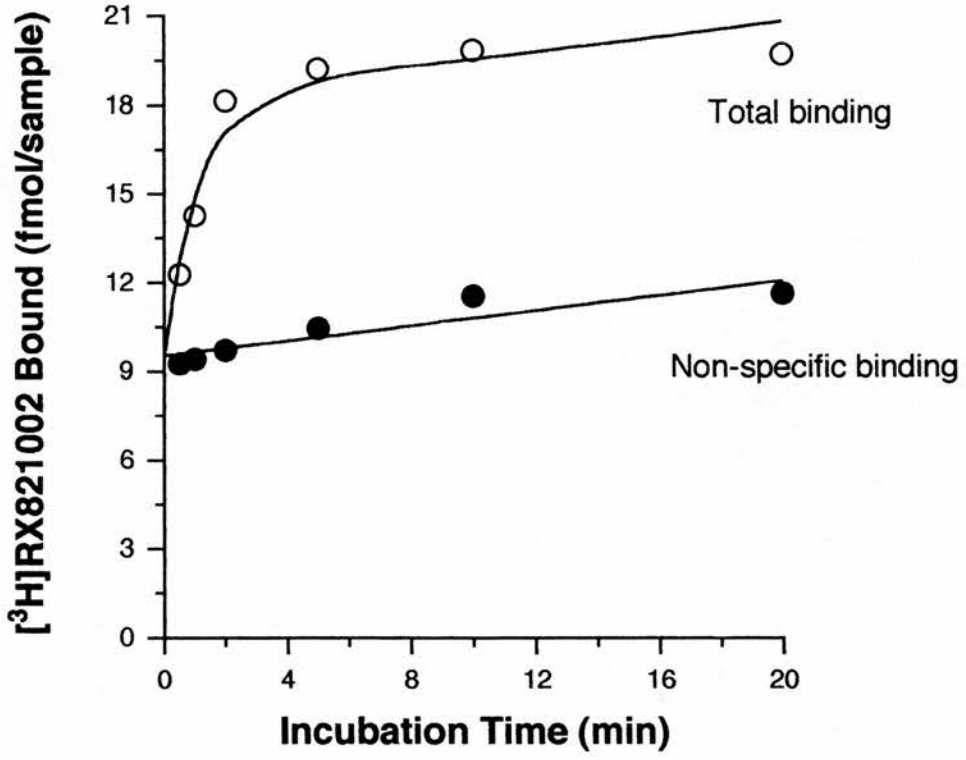

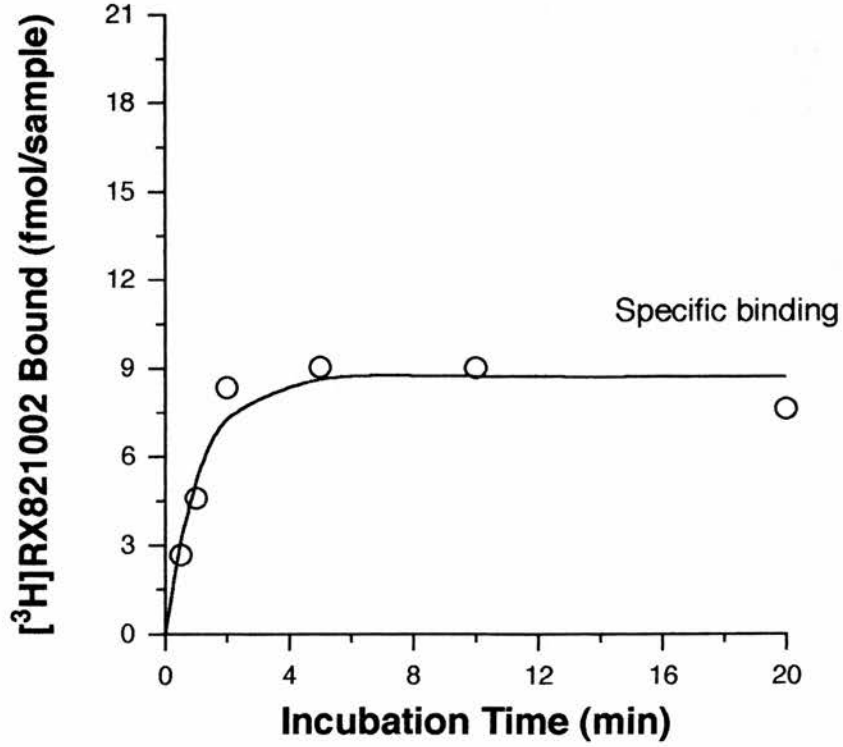

Figure 4.6 Time Course of [^{3}H]RX821002 Binding to Rat Kidney Brush Border Membranes.

The data represent a single time course experiment, with each point performed in duplicate. Membranes were incubated with 1 nM [^{3}H]RX821002 for various times at 25°C.

carried out at 25°C for 30 min.

4.3.2.3. Concentration Dependence of [^{3}H]RX821002 Binding to Rat Kidney Brush Border Membranes

Hot saturation analysis of [^{3}H]RX821002 binding to rat kidney brush border membranes was carried out once using increasing concentrations of [^{3}H]RX821002 (Figure 4.7). Curve fitting using a hyperbolic model gave an equilibrium dissociation constant (K_D) of 2.57 nM and a B_{max} of 2.68 pmol mg^{-1} protein. [^{3}H]RX821002 was used at a final concentration of 1 nM in the following experiments.

4.3.2.4. Inhibition of [^{3}H]RX821002 Binding to Rat Kidney Brush Border Membranes by Adrenergic Agonists and Antagonists

Inhibition of [^{3}H]RX821002 binding to rat kidney brush border membranes was examined using two antagonists yohimbine and prazosin and two agonists clonidine and noradrenaline. All four compounds inhibited [^{3}H]RX821002 binding (Figure 4.8), with K_i values and Hill slopes shown in Table 4.1. For the antagonists, yohimbine was more potent than prazosin, and for the agonists clonidine more potent than noradrenaline. Hill slopes for both antagonists and agonists were approximately 0.6 to 0.8.

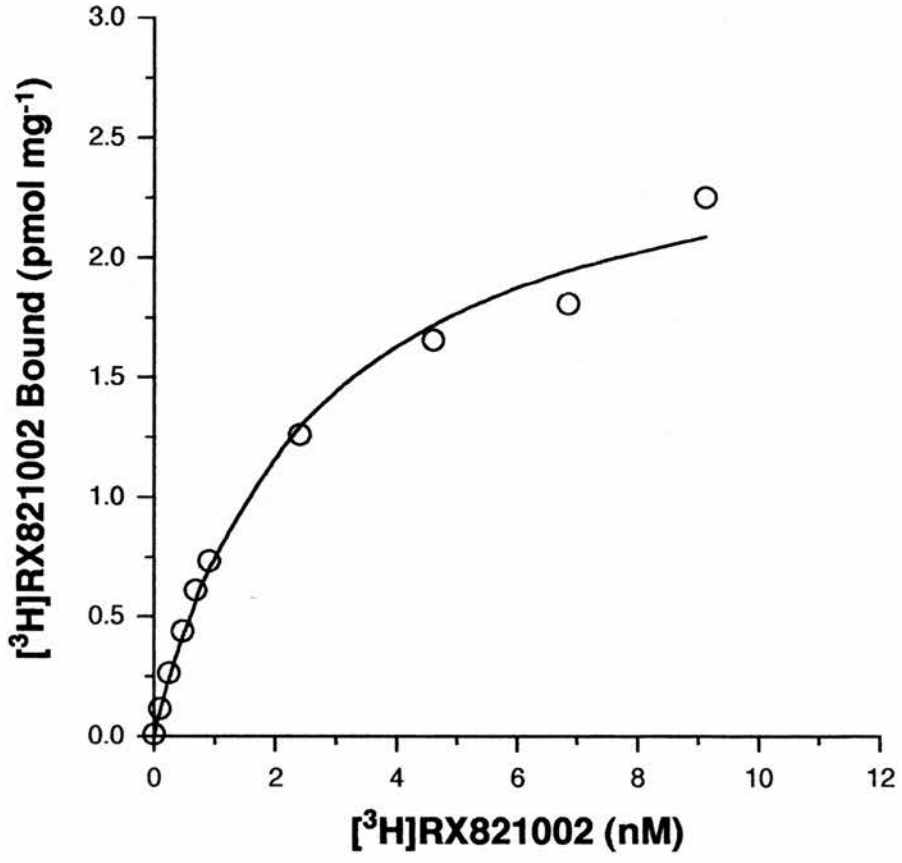

Figure 4.7 Concentration Dependence of [^{3}H]RX821002 Binding to Rat Kidney Brush Border Membranes.

The data represent a single hot saturation experiment, with each point performed in duplicate.

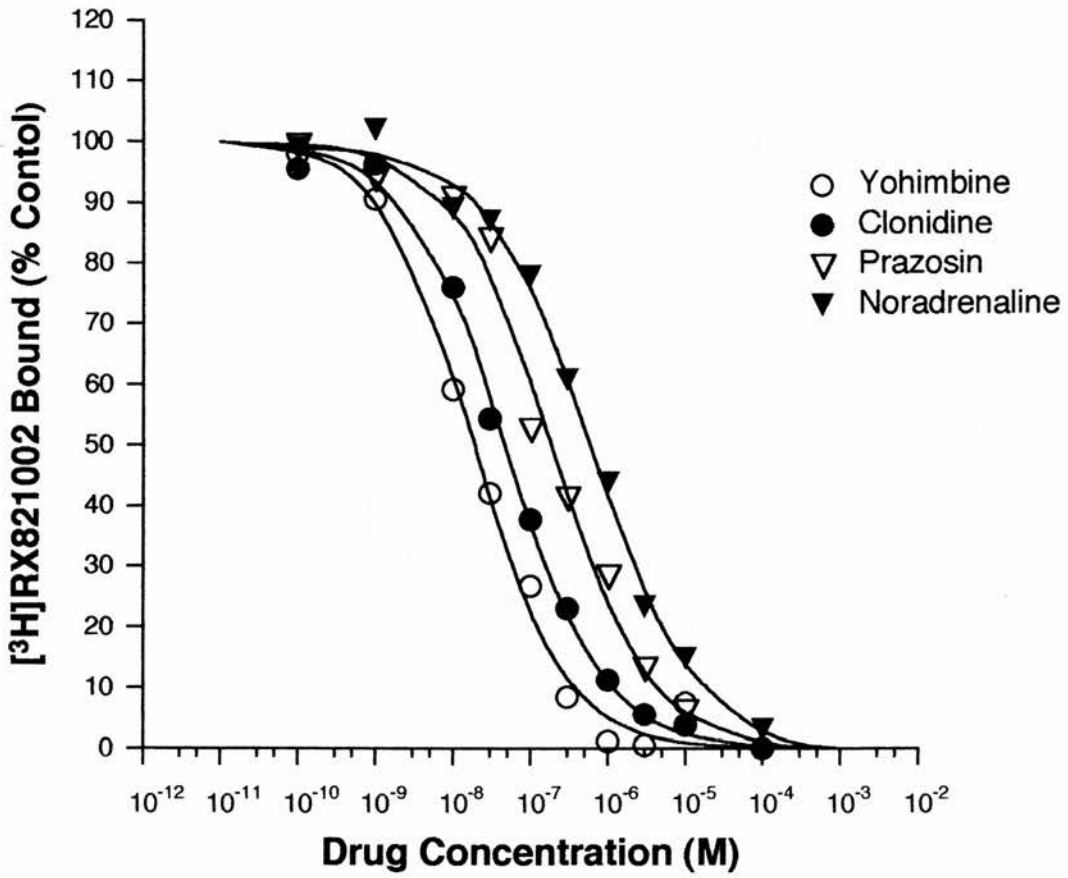

Figure 4.8 Inhibition of [^{3}H]RX821002 Binding to Rat Kidney Brush Border Membranes by Adrenergic Receptor Agonists and Antagonists.

The data represent a typical experiment, with each point performed in duplicate and with mean data obtained from three experiments (Table 4.1).

Table 4.1 Inhibition of [^{3}H]RX821002 Binding to Rat Kidney Brush Border Membranes by Adrenergic Receptor Antagonists and Agonists

Compound	K_i (nM)	(nH)
Antagonists		
Yohimbine	11.1 ± 2.14	0.78 ± 0.05
Prazosin	183 ± 22.9	0.65 ± 0.05
Agonists		
Clonidine	35.3 ± 7.37	0.84 ± 0.09
Noradrenaline	459 ± 30.6	0.62 ± 0.05

K_i values and Hill slopes determined as described in the methods for [^{3}H]RX821002 binding studies to rat kidney brush border membranes. Values expressed as mean ± S.E.M. (n=3).

4.3.3. Characterisation of [^{3}H]DPCPX Binding Sites In Rat Brain Slices Using *In Vitro* Autoradiography

Inhibition of [^{3}H]DPCPX binding to rat brain slices and the distribution of adenosine A_1 receptors was assessed using *in vitro* autoradiography. Studies were performed to provide positive control data to which results in the kidney can be compared (see below). DPCPX and the Fujisawa adenosine A_1 antagonist FR129946 were used as competitive inhibitors in a [^{3}H]DPCPX binding assay using rat brain sections. The distribution of [^{3}H]DPCPX binding sites was examined; high levels of binding were noted in hippocampal CA1, lower levels in CA3, dentate gyrus and deep cortex, minimal binding in superficial cortex and no binding in entorhinal cortex. For both DPCPX and FR129946, there was an obvious concentration dependent decrease in [^{3}H]DPCPX binding as shown in Figure 4.9 for FR129946. For DPCPX, IC_{50} values were 1.27 ± 0.09 nM in CA1, 1.29 ± 0.20 nM in dentate gyrus and 1.30 ± 0.28 nM in deep cortex. For FR129946, IC_{50} values were 10.47 ± 0.38 nM in CA1, 9.77 ± 3.39 nM in dentate gyrus and 10.2 ± 2.1 nM in deep cortex. IC_{50} values were lower than those in [^{3}H]DPCPX membrane binding studies.

4.3.4. *In vitro* [^{3}H]DPCPX Autoradiography and *In Situ* Hybridisation in Rat Kidney

In vitro autoradiography was used to examine whether a discrete localisation of [^{3}H]DPCPX binding sites, undetectable using membrane binding assays, were detectable in rat kidney. Simultaneous experiments using rat brain slices (see 4.3.3.) acted as a positive control. For *in vitro* autoradiography, slides were developed after ten weeks and analysed. The distribution of [^{3}H]DPCPX binding sites in brain was as described above,

Figure 4.9 Inhibition of [^{3}H]DPCPX Binding to Rat Brain Slices by FR129946

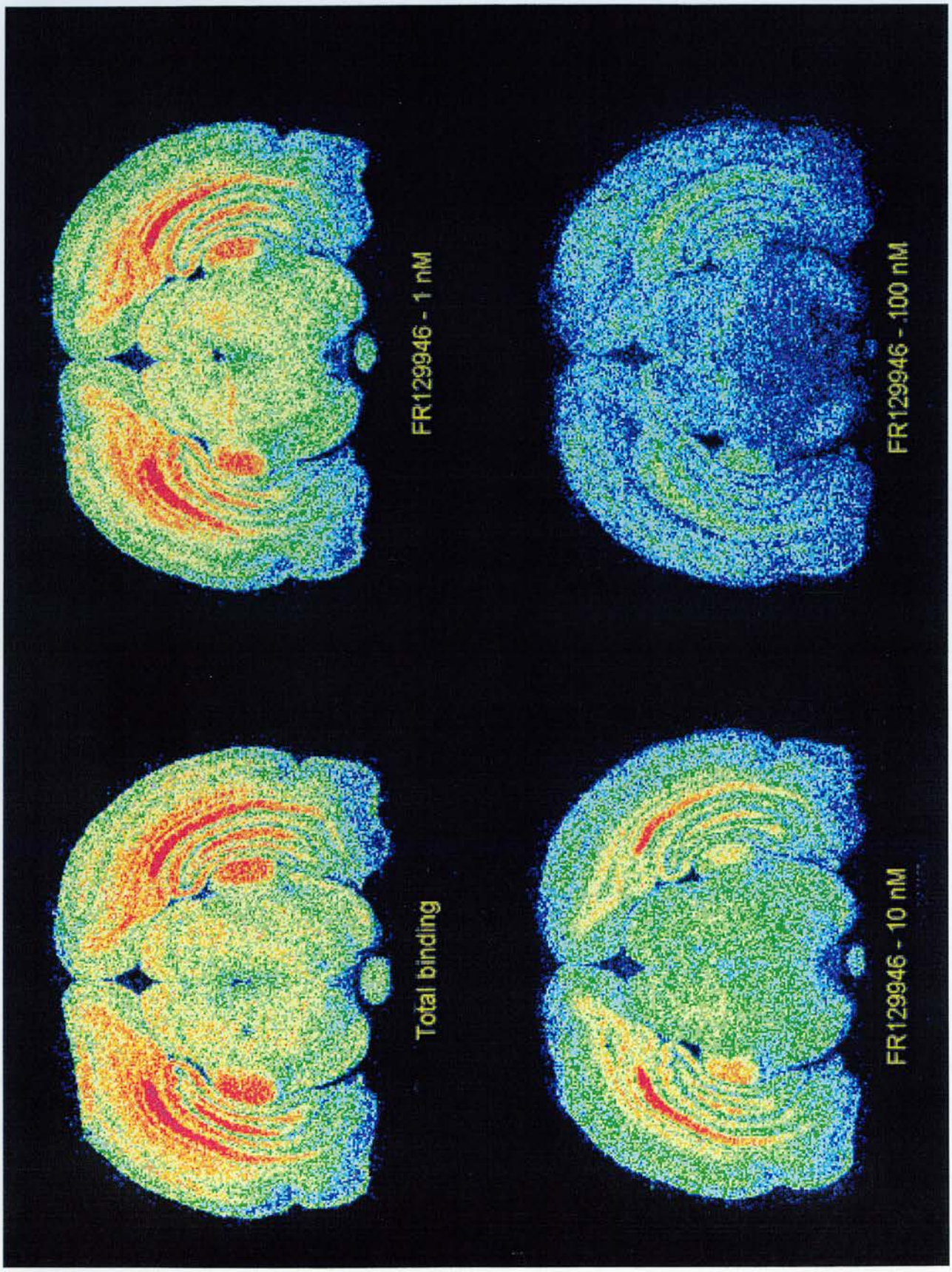

showing high levels of binding in hippocampal CA1, CA3 and dentate gyrus. Levels were also high in deep layers of cortex, the medial geniculate nucleus and negligible in entorhinal cortex. Binding in the presence of 10 μM R-PIA was undetectable (Figure 4.10). Kidney sections showed a high level of binding in cortex and very little binding in medulla. However, binding was not inhibited by R-PIA, with non-specific sections almost identical to total binding sections.

In situ hybridisation studies, conducted in parallel with *in vitro* autoradiography, were used to examine whether adenosine A_1 receptor mRNA was detectable in rat kidney, with brain tissue again used as a positive control. A preliminary set of slides were developed after 2 weeks to assess the level of receptor expression. Results using the antisense probe showed positive staining in hippocampal CA1, CA3 and dentate gyrus using dark field microscopy (Figure 4.11a), indicating adenosine A_1 receptor mRNA was located in similar regions to [^{3}H]DPCPX binding sites. Using light field microscopy, staining appeared to be localised in the pyramidal layer of CAI and the granular layer of dentate gyrus (Figure 4.11b). No distinct staining was apparent in any regions of kidney, with outer cortex shown (Figure 4.11c & d). There was a generally high level of non-specific binding in brain and kidney, which prompted the development of the remaining slides after 4 weeks. Results at four weeks were almost identical to those at two weeks. Unfortunately no conclusions could be drawn, as on examination of control slides labelled with the sense probe, the distribution and staining appeared similar to the antisense probe.

Figure 4.10 Distribution of [^{3}H]DPCPX Binding Sites in Rat Brain and Kidney

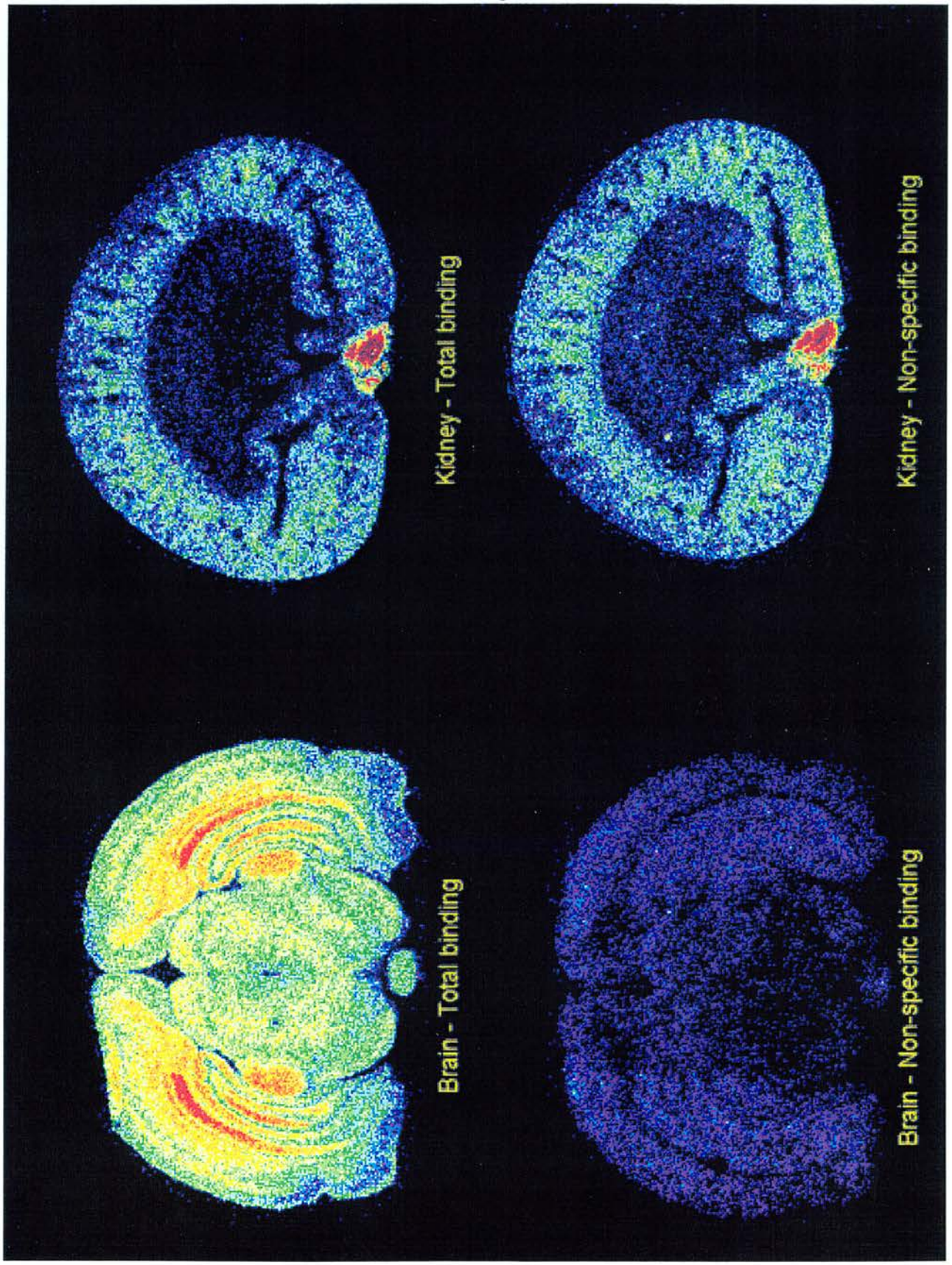

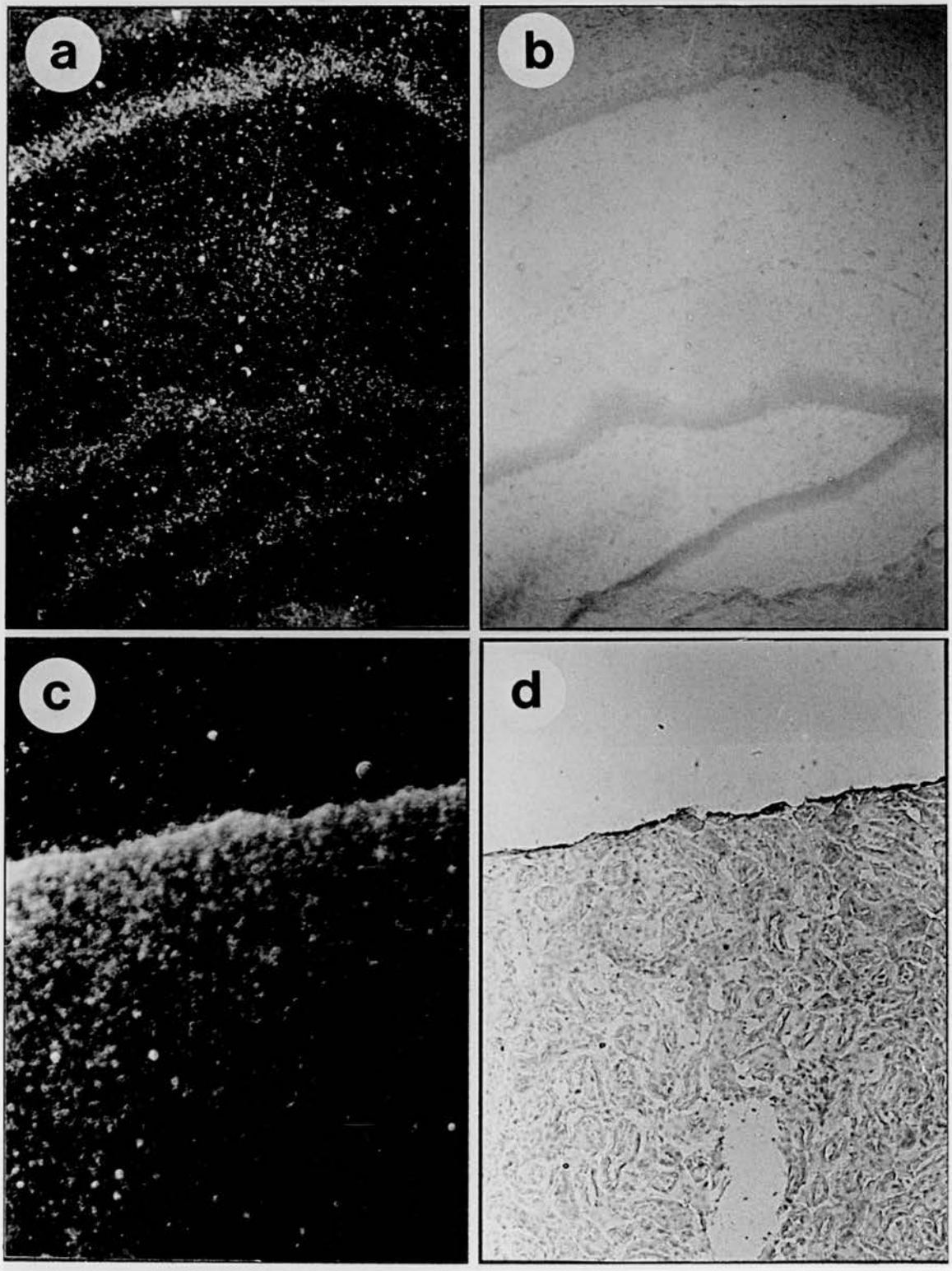

Figure 4.11 Distribution of Adenosine A_1 Receptor mRNA in Rat Brain and Kidney.

Dark and light field images of emulsion autoradiographs are shown at the level of the ventral hippocampus in brain (a & b) and shown for the outer cortical section of kidney (c & d).

4.3.5. [^{3}H]DPCPX Binding to HEK 293 Cell Membranes

Species differences in adenosine A_1 receptor pharmacology were described in Ch. 1, and were eluded to for kidney in the introduction to this chapter. The failure to identify conditions in which adenosine radioligand binding or adenosine A_1 receptor mRNA could be detected in rodent kidney, led to other options being considered. With human kidney unavailable, we investigated adenosine radioligand binding to the human embryonic kidney cell line (HEK 293). This cell line has previously been used for the stable expression of cloned receptors including adenosine (Furlong *et al.*, 1992; Aguilar *et al.*, 1995). This cell line is also known to contain endogenous β-adrenoreceptors (Aguilar *et al.*, 1995). As the non-xanthine Fujisawa antagonists retain high affinity in both rat and human brain tissue, estimating their affinity at renal receptors was of obvious interest. Preliminary investigations were performed using [^{3}H]DPCPX and [^{3}H]CGS21680 to investigate constitutive adenosine binding in this embryonic cell line.

4.3.5.1. Time Course of [^{3}H]DPCPX Binding to HEK 293 Cell Membranes

A time course of [^{3}H]DPCPX (0.5 nM) binding to HEK 293 cell membranes was carried out at 25°C, with equilibrium attained by 2 min (Figure 4.12). In all further experiments [^{3}H]DPCPX (0.5 nM) binding to HEK 293 cell membranes was carried out at 25°C for 30 min.

4.3.5.2. Concentration Dependence of [^{3}H]DPCPX Binding to HEK 293 Cell Membranes

Competition binding studies using 0.5 nM [^{3}H]DPCPX and increasing concentrations of unlabelled DPCPX gave a K_D of 97.8 ± 6.80 nM (nH=0.98 ±

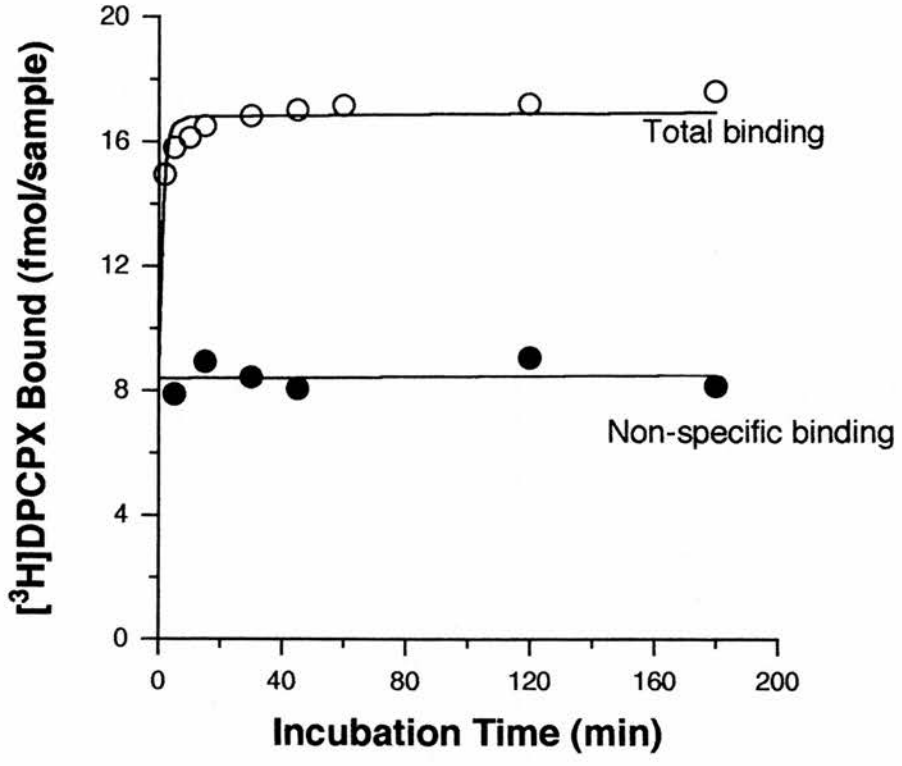

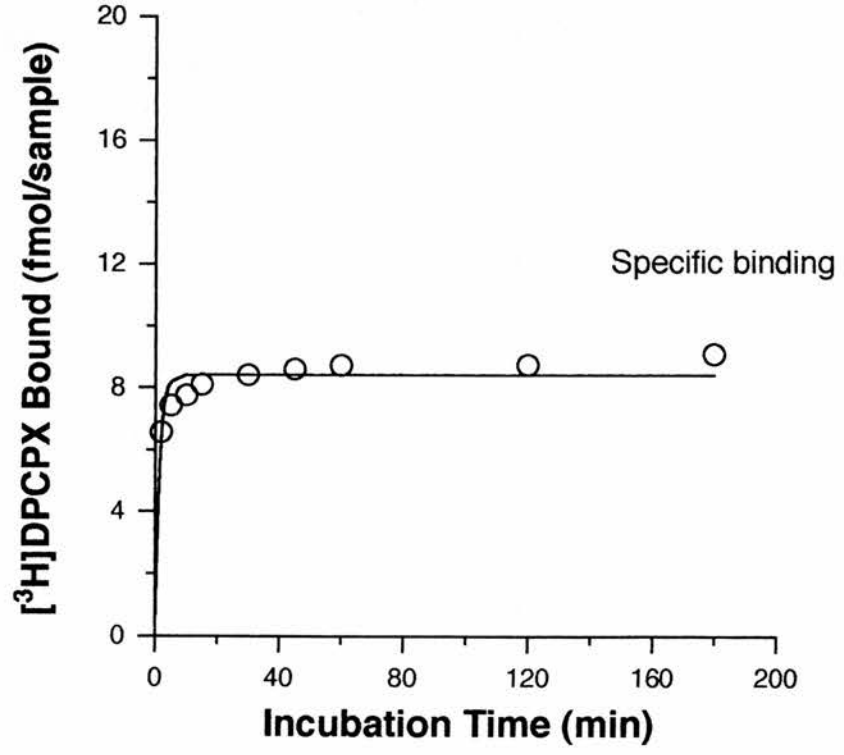

Figure 4.12 Time Course of [^{3}H]DPCPX Binding to HEK 293 Cell Membranes.

The data represent a single time course experiment, with each point performed in duplicate. Membranes were incubated with 0.5 nM [^{3}H]DPCPX for various times at 25°C.

0.05) and a B_{max} of 95.9 ± 22.5 pmol mg^{-1} protein (n=4) (Figure 4.13).

4.3.5.3. Inhibition of [^{3}H]DPCPX Binding to HEK 293 Cell Membranes by Adenosine Antagonists and Agonists

Inhibition of [^{3}H]DPCPX binding to HEK 293 cell membranes was examined using 3 antagonists and 3 agonists. All six compounds inhibited [^{3}H]DPCPX binding (Figure 4.14), with K_i values and Hill slopes shown in Table 4.2. The affinity of both antagonists and agonists was low, with Hill slopes near unity. The affinity and order of potency for both agonist and antagonists was different from that observed in brain tissue (Table 4.2). Work from within our own group (Mr T. Maemoto, personal communication) demonstrated that untransfected CHO cells developed some specific [^{3}H]DPCPX binding as the passage number increased. As the HEK 293 cells used were at a high passage number, new cells were obtained and the six compounds tested only once. The affinities of DPCPX (89.6 nM), FR160537 (1260 nM), FR129946 (10100 nM), R-PIA (529.7 nM), S-PIA (5870 nM) and NECA (15925 nM) were similar to those previously obtained using high passage cells (Table 4.2).

Potential binding of the A_{2a} agonist radioligand [^{3}H]CGS21680 to HEK 293 cell membranes was also examined. There was no specific binding to HEK 293 cell membranes detected at [^{3}H]CGS21680 concentrations of 2 and 20 nM.

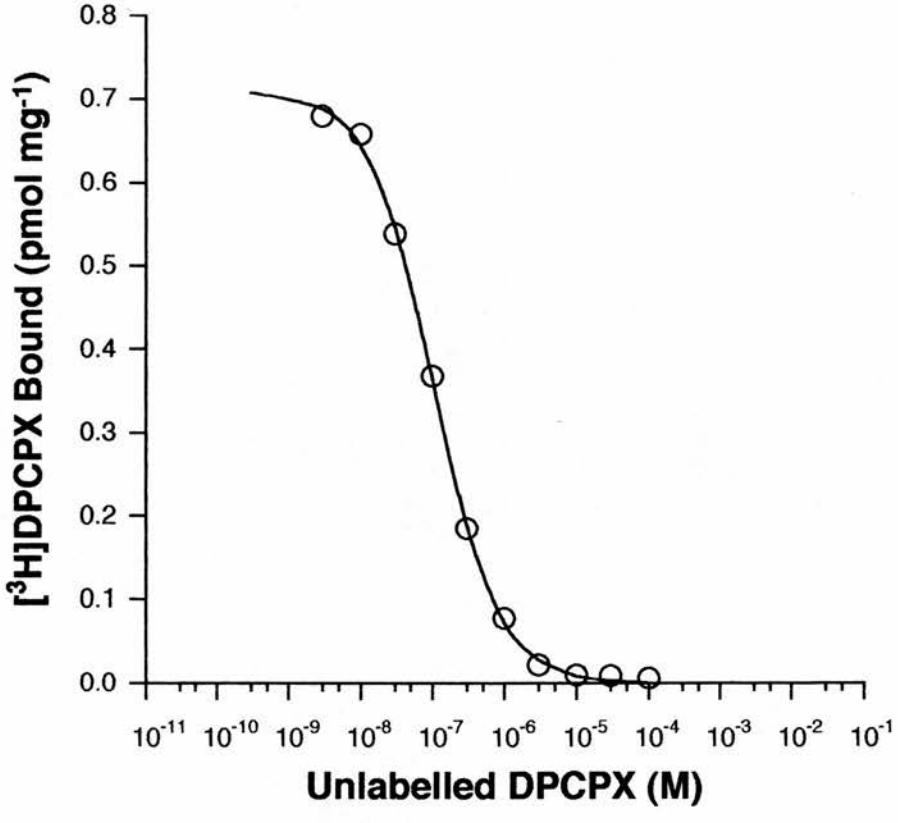

Figure 4.13 Concentration Dependence of [^{3}H]DPCPX Binding to HEK 293 Cell Membranes.

The data represent a typical experiment, with each point performed in duplicate and with mean data obtained from at least three experiments (text for mean values).

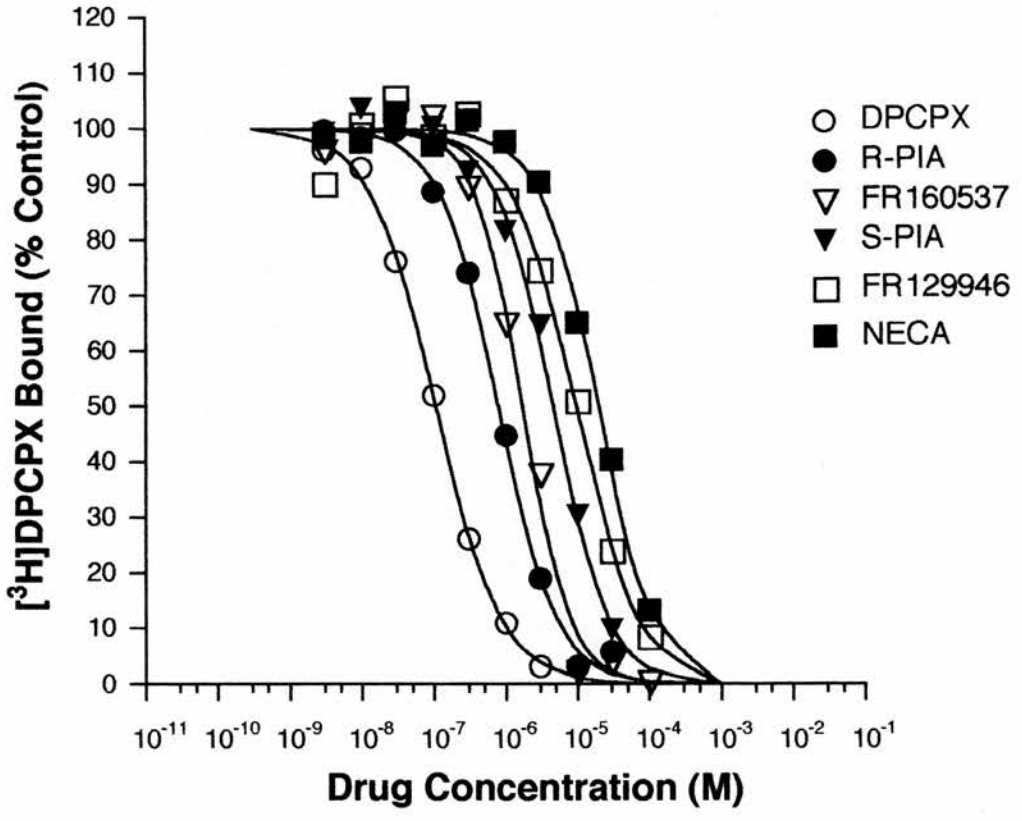

Figure 4.14 Inhibition of [^{3}H]DPCPX Binding to HEK 293 Cell Membranes by Adenosine Receptor Antagonists and Agonists.
The data represent a typical experiment, with each point performed in duplicate and with mean data obtained from at least three experiments (Table 4.2).

Table 4.2 Inhibition of [^{3}H]DPCPX Binding to HEK 293 Cell Membranes by Adenosine Receptor Antagonists and Agonists

	HEK 293 late passage		HEK 293 early passage	Human Brain	
Compound	**K_i (nM)**	**(nH)**	**K_i (nM)**	**K_i (nM)**	**(nH)**
Antagonists					
DPCPX	97.8 ± 6.80	0.98 ± 0.05	89.6	2.18 ± 0.35	0.91 ± 0.10
FR160537	2175± 248	1.18 ± 0.09	1260	0.07 ± 0.01	1.10 ± 0.09
FR129946	10780±1430	0.93 ± 0.02	10100	2.16 ± 0.43	0.78 ± 0.06
Agonists					
R-PIA	761 ± 57.8	1.04 ± 0.04	529.7	88.4 ± 20.6	0.53 ± 0.04
S-PIA	4770±86.2	1.11 ± 0.03	5870	N.T.	
NECA	19700±360	1.01 ± 0.05	15925	312 ± 67.7	0.61 ± 0.04

K_i values and Hill slopes determined as described in the methods for [^{3}H]DPCPX binding studies using HEK 293 cell membranes. Values expressed as mean ± S.E.M. (n=3). Data for [^{3}H]DPCPX binding to human brain cortical membranes taken from Chapter 1. (N.T. - not tested).

4.4. Discussion

Adenosine has a range of effects in kidney, mediated by A_1, A_2 and possibly A_3 receptors (Spielman & Arend, 1991; Zhou *et al.*, 1992; Dixon *et al.*, 1996). Adenosine receptors are reported to exist in both kidney cortex and medulla in various species. The pharmacological characterisation of these receptors has been heavily dependent on functional assays using adenyl cyclase studies, with radioligand binding studies limited. Characterisation of adenosine receptor binding sites in different areas of rat kidney was attempted using [^{3}H]DPCPX and [^{3}H]CGS21680. Two crude kidney membrane preparations were examined, with one previously used to demonstrate the existence of an A_2-like binding site using [^{3}H]CADO (Wu & Churchill, 1985). No specific binding was detectable in the two preparations using either [^{3}H]DPCPX or [^{3}H]CGS21680. The low affinity, weakly characterised binding demonstrated by Wu & Churchill, (1985) may therefore have been due to the presence of A_{2b} (Rivkees & Reppert, 1992) or A_3 (Zhou *et al*, 1992) receptors. A wealth of evidence points to the proximal tubule being the target structure responsible for the diuretic action of adenosine A_1 receptor antagonists in various species. This includes data from rat (Mizumoto & Karasawa, 1993; Nomura *et al.*, 1995; Terai *et al.*, 1995b), dog (Terai *et al.*, 1995b), rabbit (Freissmuth *et al.*, 1987b; Takeda *et al.*, 1993) and human (Buren *et al.*, 1993; Balakrishnan *et al*, 1993). In the proximal tubule of rat kidney, the luminal surface is coated with microvilli (brush border) and on the contraluminal side, plasma membranes form the basal (basolateral) infoldings of the cell. Both mixed and separate preparations of brush border and basolateral membranes were prepared from rat kidney cortex. As with the two crude membrane preparations, no specific binding was detected for either [^{3}H]DPCPX or [^{3}H]CGS21680 at various ligand and membrane protein concentrations.

Blanco *et al.*, (1992) used these two ligands to study binding to adenosine receptors in brush border and basolateral membranes from pig and rat kidney. They were also unable to detect A_1 receptor-like binding in brush border or basolateral membranes of pig cortex using [^{3}H]DPCPX, but unfortunately made no comment on binding using rat kidney membranes. They did, however, characterise a very low affinity binding site for [^{3}H]CGS21680, in brush border membranes of pig (K_D of 150 nM) and rat (K_D of 90 nM) kidney, that was different from the high affinity binding to the A_{2a} receptor in pig brain (12 nM). In the present study, the inability to detect this [^{3}H]CGS21680 binding site may have been related to the methodology used, as Blanco *et al.*, (1992) used magnesium precipitation to obtain brush border membranes. The present data also contrast with those of Jakubowski *et al*, (1992), who demonstrated the presence of A_1 and A_2 receptor-like binding sites using [^{3}H]PIA (K_D of 0.34 nM) and [^{3}H]NECA (K_D of 110 nM) in rat basolateral membranes. The lack of pharmacological data using these ligands limits further interpretation. The inability to detect A_1 binding sites in rat kidney cortical preparations is perhaps not surprising as autoradiographic (Brines & Forrest, 1987) and *in situ* hybridisation (Weaver & Reppert, 1992) studies report that adenosine A_1 binding sites and adenosine A_1 receptor mRNA are located in the medulla. Further evidence supporting this proposal was produced in a recent study in which the localisation of adenosine A_1 receptor mRNA was examined in microdissected rat nephron segments (Yamaguchi *et al.*, 1995). A diverse expression along the nephron was shown, with very low levels in the proximal convoluted tubule (Yamaguchi *et al.*, 1995). This contrasts with the histochemical localisation of ecto-5′-nucleotidase, one of the enzymes responsible for the production of adenosine (Dawson *et al.*, 1989), because enzyme activity was found in brush border and other cortical regions, with no

activity in medulla. The lack of correlation between localisation of this enzyme and autoradiographic and *in situ* hybridisation studies may not be of significance, as the correlation between adenosine receptor distribution and the presence of this enzyme was also poor in brain (Fastbom *et al.*, 1987b). The former studies (Brines & Forrest, 1987; Weaver & Reppert, 1992; Yamaguchi *et al.*, 1995) have all alluded to the presence of adenosine receptors in the medullary region of rat kidney. In an abstract, Weber *et al.*, (1990b) demonstrated [^{3}H]DPCPX binding to crude inner stripe and papillary membranes from the medulla with a K_D of 0.25 nM. The higher B_{max} of the papillary fraction led us to prepare medullary membranes in an attempt to characterise [^{3}H]DPCPX binding sites. A method was used that had previously demonstrated the presence of A_2-like receptors using an adenylate cyclase assay (Woodcock *et al.*, 1984). As with previous membrane preparations, no specific binding was detectable for either [^{3}H]DPCPX or [^{3}H]CGS21680 at various ligand and membrane protein concentrations. Although Woodcock *et al.*, (1984) used up to 2 mg of protein per sample, we would have probably expected some [^{3}H]CGS21680 binding at 0.5 mg of protein. The membrane preparation may not have been viable as [^{3}H]RX821002 binding could not be detected, in contrast to kidney cortical membrane preparations. A recent abstract identified binding in rat kidney membranes using [^{3}H]DPCPX, with a K_D of 0.58 nM and a B_{max} of 11.9 fmol mg^{-1} protein (Gould *et al.*, 1995). Gould *et al.*, (1995) preincubated membranes with 50 times more adenosine deaminase than we used, and incubated at 4°C for 5 hr. It is possible that these alterations in methodology are necessary to detect [^{3}H]DPCPX binding in rat kidney membranes.

The inability to detect specific binding of [^{3}H]DPCPX or [^{3}H]CGS21680 in both crude and complex cortical and medullary preparations prompted the

use of [^{3}H]RX821002. This α_2 adrenoreceptor antagonist radioligand was used as a positive control to confirm the viability of the membrane preparations. This ligand has been shown to bind to a variety of kidney membrane preparations and kidney cell lines, in a manner consistent with binding to α_2 adrenoreceptors (Uhlen & Wikberg, 1993; O'Rourke *et al.*, 1994). Specific binding of [^{3}H]RX821002 to basolateral and brush border membrane fractions increased linearly over the protein concentrations used. Subsequent experiments were conducted with approximately 100 μg of membrane protein, ensuring less than 10% of added ligand was bound whilst maintaining sufficient specific binding to conduct pharmacological studies. Binding was rapid with equilibrium reached by 2 min and analysis of saturation data gave a K_D of 2.57 nM. Four compounds useful in delineating the α receptor subtypes found in kidney were used to determine the nature of the binding site labelled by [^{3}H]RX821002 (O'Rourke *et al.*, 1994; Bylund *et al.*, 1995). Two agonists, noradrenaline (α/β) and clonidine (α_2) and two antagonists, yohimbine (α_2/α_1) and prazosin (α_1/α_2) inhibited [^{3}H]RX821002 binding to rat kidney membranes in a concentration dependent manner. [^{3}H]RX821002 is a selective α_2 radioligand with low affinity for α_1 and imidazoline binding sites; with nanomolar affinity for yohimbine again a classical characteristic of binding to α_2 adrenoreceptors, this would suggest negligible contamination from other binding sites (Uhlen *et al.*, 1993; Bylund *et al.*, 1995). Competition binding curves had shallow Hill slopes for agonists and antagonists indicating the presence of two binding sites. These data are consistent with those of Uhlen & Wikberg, (1991a, b) (Table 4.3), who showed [^{3}H]RX821002 labelled two

Table 4.3 [^{3}H]RX821002 Binding to Rat Kidney Membranes

	Uhlen & Wikberg, 1991a	Uhlen & Wikberg, 1991b	Present Study
K_D	2.25 nM	α_{2a}=0.68 nM α_{2b}=4.58 nM	2.57 nM
Yohimbine	α_{2a}=81.2 nM α_{2b}=9.18 nM	α_{2a}=57.7 nM α_{2b}=15.7 nM	11.1 nM
Prazosin	α_{2a}=1540 nM α_{2b}=35.9 nM	α_{2a}=1360 nM α_{2b}=52.1 nM	183 nM
Clonidine	Not tested	α_{2a}=84.4 nM α_{2b}=71.3 nM	35.3 nM
Noradrenaline	Not tested	Not tested	459 nM

distinct subtypes in rat kidney, with the characteristics of α_{2a} and α_{2b} adrenoreceptors. Further compounds would need to be tested to substantiate this hypothesis with regard to the present data. [^{3}H]RX821002 labels all four α_2 adrenoreceptor subtypes, α_{2a}, α_{2b}, α_{2c}, and α_{2d}, (O'Rourke *et al.*, 1994) and the presence of other subtypes cannot be ruled out. However, Uhlen & Wikberg (1991a) did point out that fitting a three site model provided no further improvement over a two site model.

The possibility that adenosine A_1 receptors may be discretely localised in areas of the kidney that were not detected in membrane binding studies prompted the use of *in vitro* autoradiography and *in situ* hybridisation. These techniques have been used to detect adenosine A_1 receptor-like binding and adenosine A_1 receptor mRNA in rodent kidney (Palacios *et al.*, 1987; Weaver & Reppert, 1992). For comparison with kidney, brain sections were processed simultaneously as a positive control, as the autoradiographic (Goodman & Synder, 1982; Weber *et al.*, 1990a) and immunohistochemical (Rivkees *et al.*, 1995c; Swanson *et al.*, 1995) localisation of A_1 receptors is well characterised in rat brain.

The inhibition of [^{3}H]DPCPX binding in rat brain slices by DPCPX and FR129946, two compounds with identical selectivity for the adenosine A_1 receptor, was assessed using quantitative autoradiography. The distribution of [^{3}H]DPCPX binding in rat brain was similar to that previously described (Weber *et al.*, 1990a), with high levels in hippocampal CA1, lower levels in CA3, dentate gyrus and deep cortex and no binding in entorhinal cortex. DPCPX and FR129946 inhibited [^{3}H]DPCPX binding in a concentration dependent manner, with identical affinities in both hippocampal and cortical areas. Inhibition of [^{3}H]DPCPX binding by the putative cognitive enhancer KFM19 in human hippocampus, followed a similar pattern in a variety of brain areas

(Deckert *et al.*, 1993). In comparison with membrane binding studies, the affinity of both DPCPX (3 fold) and FR129946 (5 fold) is lower. This is not uncommon in autoradiographic studies and may represent difficulty in removing endogenous adenosine from receptors, with adenosine deaminase being a large enzyme that does not penetrate deeper cell layers (Weber *et al.*, 1990a; Parkinson *et al.*, 1996). It was also important to demonstrate that Fujisawa antagonists act on these areas of the brain as autoradiographic studies in post mortem brains of Alzheimers patients show a significant decrease in adenosine receptors in CA1 and dentate gyrus (Jansen *et al.*, 1990). In an attempt to keep the conditions of autoradiographic and membrane radioligand binding studies similar, we had performed a preliminary experiment examining different radioligand concentrations, wash times and buffers. Autoradiographic studies on adenosine binding sites generally use 170 mM Tris-buffer (Goodman & Snyder, 1982; Palacios *et al.*, 1987; Weber *et al.*, 1990a; Parkinson *et al.*, 1996), however we found this provided no improvement over 50 mM Tris-buffer. It was noted, however, that [^{3}H]DPCPX binding was also localised to white matter tracts as well as the characterised areas when using the former concentration of buffer. This observation had previously been made by Weber *et al.*, (1990a) and Parkinson *et al.*, (1996) in rat and gerbil brain, respectively. Both groups associated this effect with potential axonal transport of the receptor to the presynaptic terminal. The labelling of white matter tracts had not previously been described in autoradiographic studies using the agonist [^{3}H]CHA, which predominantly labels the high affinity state of the receptor (Goodman & Snyder, 1982). This observation may, however, be of importance as recent papers on the histochemical localisation of adenosine receptors places them on axons (Swanson *et al.*, 1995; Rivkees *et al.*, 1995c). It may be interesting to postulate that under the correct conditions, [^{3}H]DPCPX is either labelling a receptor that

is being transported but which is uncoupled from a G protein and hence not recognised by agonist radioligands, or that it has in fact labelled a low affinity state/receptor in white matter tracts, that is not detectable by agonist ligands but is similar to that identified by immunohistochemical methods (Swanson *et al.*, 1995; Rivkees *et al.*, 1995c).

Having confirmed that the autoradiographic distribution of [^{3}H]DPCPX binding in rat brain was similar to that previously described by Weber *et al.*, (1990a), brain and kidney sections were examined in parallel. [^{3}H]DPCPX binding to brain sections was totally abolished by the presence of 10 μM R-PIA in the incubation medium. In contrast, there appeared to be no specific [^{3}H]DPCPX binding that was inhibited by R-PIA in any region of the kidney. The high level of non-specific binding in kidney cortex has also been reported using [^{125}I]PIA (Brines & Forrest, 1987). Labelling of the inner stripe of the outer medulla and the inner papilla was, however reported, neither of which was apparent in the present autoradiograms (Brines & Forrest, 1987). To my knowledge, this abstract appears to be the only report on the autoradiographic localisation of adenosine A_1 receptors in rat kidney. Two articles on the visualisation of peripheral adenosine A_1 receptors compare human and guinea pig kidney (Palacios *et al.*, 1987) and rat brain and guinea pig kidney (Weber *et al.*, 1988). The former demonstrated species differences with receptors located in the cortex of human kidney and the medulla of guinea pig kidney but the latter, despite using rat brain, made no mention of rat kidney. The present study, despite convincing positive control data in brain, provide no further evidence to elucidate the localisation of adenosine A_1 receptors in rat kidney. It may be that discrete localisation and low receptor density (Williams & Risley, 1980; Murphy & Snyder, 1980; Weber *et al.*, 1990b; Gould *et al.*, 1995) necessitate techniques such as nephron dissection (Yamaguchi *et al.*, 1995) to

detect A_1 receptors in binding studies. It is also possible that renal and brain A_1 receptors are different (Suzuki *et al.*, 1992), although evidence is weak, especially as the cloned rabbit adenosine A_1 receptor has high homology with the cloned brain A_1 receptor (Bhattacharya *et al.*, 1993).

Adenosine A_1 receptor gene expression in rat kidney was demonstrated by Weaver & Reppert, (1992) using Northern blot analysis and *in situ* hybridisation. We constructed a riboprobe similar to the one described by Weaver & Reppert, (1992) in an attempt to localise adenosine A_1 receptor mRNA in rat kidney. The riboprobe chosen for the A_1 receptor had very low homology with the other cloned adenosine receptors and therefore should be specific. The production of the probe was successful and sequencing of the probe confirmed that it was almost identical to the chosen sequence (Figure 4.4). The brain and kidney sections used for *in situ* hybridisation were the adjacent sections to those used for [^{3}H]DPCPX autoradiography. After completion of the labelling procedure, a preliminary set of slides were developed after two weeks and sections were viewed using dark and light field microscopy. In brain, the distribution of the adenosine A_1 receptor hybridisation signal was similar to that seen for the autoradiograms. However, in kidney no specific signal could be identified but there was a generally high level of non-specific binding in all regions. This contrasts with Weaver and Reppert, (1992), who found specific labelling in the inner and outer medulla. Results in the literature do, however vary, with some groups detecting signals for adenosine A_1 receptor mRNA in rat kidney (Reppert *et al.*, 1991; Weaver & Reppert, 1992) and others not (Mahan *et al.*, 1991; Johansson *et al.*, 1993; Dixon *et al.*, 1996.). The problem with trying to obtain any relevant information from the present *in situ* hybridisation studies was compounded by the fact that slides labelled with the sense probe gave similar results to the antisense probe in

brain and kidney. This may be due to some homology between sense and antisense probes or non-specific binding to areas of high cell density. Further studies are required to optimise the methodology.

Adenosine A_1 receptors have been identified in human kidney cortex (Palacios *et al.*, 1987), and the density of these receptors is reported to be higher in human glomeruli than in other species (Toya *et al.*, 1993). The human A_1 receptor gene consists of at least six exons and five introns and can undergo alternative splicing in the 5′-untranslated region, which effects the level of A_1 receptor expression in a tissue specific manner (Ren & Stiles, 1994a, b). Human kidney contains the correct exon sequences associated with increased levels of expression and this may account for the higher binding site densities reported (Toya *et al.*, 1993). The possibility of higher adenosine receptor density in human kidney, and the failure to establish conditions in which adenosine radioligand binding or adenosine A_1 receptor mRNA could be detected in rodent kidney, led to other options being investigated. With human kidney unavailable to compare directly to the data obtained for human brain (see 1.3.4.), we investigated adenosine radioligand binding to the human embryonic kidney cell line (HEK 293). [^{3}H]DPCPX bound specifically to membranes from HEK 293 cells, while no [^{3}H]CGS21680 binding was detectable. Experiments were conducted using approximately 40-80 μg of membrane protein, to ensure less than 10% of added ligand was bound whilst maintaining sufficient specific binding to conduct pharmacological studies. Binding was rapid with equilibrium reached by 2 min. However, the K_D of 97.8 ± 6.80 nM and the B_{max} of 95.9 ± 22.5 pmol mg^{-1} protein in HEK 293 cell membranes was different from that of human brain (K_D=2.18 ± 0.35 nM and B_{max}=4.97 ± 0.98 pmol mg^{-1} protein). In order to determine the nature of the binding site labelled by [^{3}H]DPCPX in HEK 293 cell membranes, the affinities

of three agonists and three antagonists were determined. All six compounds inhibited [^{3}H]DPCPX binding to HEK 293 cell membranes in a concentration dependent manner. For agonists the order of potency was R-PIA > S-PIA > NECA. For these three agonists, this does not resemble the order of potency used to classify any of the known adenosine receptors (Table I.1) but does, however, resemble that of the high affinity bovine A_1 receptor (Olah, *et al.*, 1992; Tucker, *et al.*, 1992). For antagonists the order of potency was DPCPX > FR160537 > FR129946, which was again different to both rat and human brain membranes. Both agonists and antagonists had very low affinities and Hill slopes near unity, indicating the existence of one low affinity site. The low affinity of NECA and the distinct agonist order of potency would appear to rule out binding to classical adenosine receptors. This is despite the fact that adenosine A_1 (Rivkees *et al.*, 1995b), A_{2a} (Salvatore *et al.*, 1993) and A_3 (Sajjedi & Firestein, 1993) transcripts have all been reported to exist in human kidney. The presence of low affinity endogenous adenosine radioligand binding in fibroblast based cell lines like HEK 293 cells does not appear uncommon, although its existence is generally ignored (Rivkees & Reppert, 1992; Pierce *et al.*, 1992; Zhou *et al.*, 1992; van Galen *et al.*, 1994). Endogenous A_{2b} mRNA has been reported to exist in monkey kidney COS6M cells and many fibroblast cell lines (Rivkees & Reppert, 1992). Human embryonic kidney fibroblasts were also reported to have a low affinity adenosine receptor but did not have A_{2b} transcripts (Pierce *et al.*, 1992). The low affinity A_{2b} receptor was first identified in human fibroblasts (Bruns, 1980), however NECA was more potent than R-PIA so this is unlikely to be the source of binding. Endogenous binding has been reported in CHO cells using the A_1/A_3 ligand [^{125}I]APNEA but it did not have the pharmacological characteristics of an adenosine receptor (van Galen *et al.*, 1994). Zhou *et al.*,

(1992) reported endogenous A_2 binding using [^{3}H]NECA in COS7 cells but none in CHO cells. In our own laboratory (Mr T. Maemoto, personal communication), it was noted that untransfected CHO cells attained some specific [^{3}H]DPCPX binding as the passage number increased. To investigate the possibility that the binding observed for [^{3}H]DPCPX to HEK 293 cell membranes was a consequence of the increasing passage number, a new cell line was obtained. However, [^{3}H]DPCPX binding to HEK 293 cell membranes was similar in the new batch of cells. The high micromolar affinity for NECA and high B_{max} seen in the present study would appear more similar to the high capacity "nonreceptor" site (Bruns *et al.*, 1986). Alternatively, the low affinity binding observed in the present study may just be an artifact associated with this embryonic cell line, as high affinity binding of adenosine A_1 receptor radioligands has been identified in human glomeruli (Toya *et al.*, 1993).

In conclusion these studies found no evidence for the presence of [^{3}H]DPCPX or [^{3}H]CGS21680 binding sites in rat kidney, although [^{3}H]RX821002 binding was detectable in kidney cortical membrane preparations. Similarly, high affinity [^{3}H]DPCPX binding sites were not detected in the human HEK 293 cell line.

GENERAL CONCLUSIONS

In this thesis a number of aspects of adenosine receptor pharmacology have been examined. This has included, investigation of species differences in adenosine A_1 receptor pharmacology in brain membranes, modulation of ligand binding to adenosine A_1 and A_{2a} receptors by magnesium and Gpp(NH)p, the establishment of a radioreceptor assay capable of measuring the central penetration of adenosine A_1 receptor antagonists, and the examination of rat renal adenosine A_1 receptor pharmacology and localisation.

In vitro radioligand binding assays were used to determine the affinity and selectivity of agonists and antagonists for adenosine A_1 and A_{2a} receptors. All antagonists had Hill slopes close to unity in both [^{3}H]DPCPX and [^{3}H]CGS21680 binding assays, with antagonists binding to a single population of sites in both cases. For agonists, Hill slopes were significantly less than unity in the [^{3}H]DPCPX binding assay, reflecting the ability of agonists to recognise two different affinity states of the receptor. This is similar to other GPCRs, with the two states representing the receptor being coupled to and uncoupled from G proteins (Gilman, 1987; Birnbaumer *et al.*, 1990). Hill slopes for agonists in the [^{3}H]CGS21680 binding assay were closer to, but still significantly less than unity for the majority of compounds, with agonists predominantly binding to the high affinity state of the receptor. The [^{3}H]DPCPX binding assay was modified for use in different species. Adenosine receptor agonists and standard xanthine antagonists had similar affinities in rat and mouse brain. In contrast these compounds were an order of magnitude less potent in guinea pig and human brain membranes. This is despite over 90% homology at the amino acid sequence level between the adenosine A_1 receptors of different species (see main introduction). For adenosine and certain other receptor types, changing a single amino acid is sufficient to produce large variations in the affinity of compounds in different species

(Oksenberg *et al.*, 1992; Link *et al.*, 1992; Kao *et al.*, 1992; Jensen *et al.*, 1993; Tucker *et al.*, 1994; Townsend-Nicholson & Schofield, 1994). In addition to single amino acids, a variety of domains throughout the structure of the adenosine A_1 receptor have been shown to be involved in both agonist and antagonist binding (Olah *et al.*, 1994; Tucker *et al.*, 1994; Townsend-Nicholson & Schofield, 1994). The novel non-xanthine adenosine A_1 antagonists from Fujisawa retained their high affinity for adenosine A_1 receptors in all species examined, including human. The non-xanthine Fujisawa antagonists appear unaffected by the changes in receptor structure, perhaps binding to an area, which is conserved within different species. These observations are of great importance, when assessing whether a compound may be useful in man. The use of rat tissue to assess the pharmacological properties of adenosine agonists and xanthine antagonists may be inappropriate, resulting in the overestimation of drug potency in man. If human tissue is unavailable to study adenosine A_1 receptors, guinea pig tissue may give a more realistic reflection of a compounds effectiveness in man. The non-xanthine Fujisawa adenosine A_1 antagonists appear unaffected by species differences in receptor structure and as a consequence, data obtained from rat studies can hopefully be extrapolated to human.

The modulation of adenosine A_1 and A_{2a} ligand binding properties by magnesium and Gpp(NH)p was complex, although similar effects have been observed for other GPCRs (Gilman, 1987; Birnbaumer *et al.*, 1990). The modulation of antagonist binding levels by magnesium and Gpp(NH)p is difficult to explain. The likeliest explanation for both effects, especially the 20% increase in [^{3}H]DPCPX binding in the presence of Gpp(NH)p, is a small alteration in antagonist affinity that was not detected. Alternative explanations postulated for the increase in antagonist binding in the presence of guanine

nucleotides have included; antagonists preferentially binding to the uncoupled form of the receptor, the presence of 'cryptic' binding sites and adenosine possibly forming pseudoirreversible complexes in the membrane (Leung & Green, 1989; Prater *et al.*, 1992; Cohen *et al.*, 1996). In common with other GPCRs, agonists bind to a high and low affinity state of the receptor, whose equilibrium can be modified by magnesium and Gpp(NH)p. The increase (on adding $MgCl_2$) and decrease (on adding Gpp(NH)p) in agonist affinity in the [^{3}H]DPCPX binding assay was examined using a two site model. The change in agonist affinity appeared to be the result of an alteration in the proportion of the high and low affinity states labelled, with no change in the affinity of either state. The adenosine A_1 agonist radioligand [^{3}H]CCPA, under the conditions used, labelled predominantly the high affinity state, with its K_D consistent with the high affinity component for CCPA recognised using [^{3}H]DPCPX. The B_{max} for [^{3}H]CCPA was also consistent with this idea as it was equivalent to the B_{max} for the high affinity state in the [^{3}H]DPCPX binding assay. The adenosine A_{2a} agonist radioligand [^{3}H]CGS21680, as with the A_1 agonist appears to predominantly label the high affinity state of the receptor. With magnesium required in the assay buffer to obtain a reasonable level of specific binding, high affinity agonist binding would be expected, as with other GPCRs (Gilman, 1987; Birnbaumer *et al.*, 1990). The increase in [^{3}H]CGS21680 binding in the presence of magnesium appeared to be the result of the increase in agonist affinity, which presumably reflects an increase in the proportion of high affinity state labelled. The decrease in binding in the presence of Gpp(NH)p was due to a decrease in affinity. The availability of the new A_{2a} antagonist radioligands [^{3}H]KF17837S (Nonaka *et al.*, 1994) and [^{3}H]SCH58261 (Zocchi *et al.*, 1996), should help elucidate the mechanisms responsible for the observed effects. It is clear for both A_1 and A_{2a} binding assays, that careful consideration must be

given to the choice of assay buffer in light of the profound effects of magnesium. Additionally, when examining binding in whole cell preparations, the effects of intracellular guanine nucleotides must be considered.

A modified radioreceptor assay, using [^{3}H]DPCPX was developed and characterised. This assay is capable of measuring the central penetration of adenosine A_1 receptor antagonists following peripheral administration. The procedure involved a transcardiac flush with saline to reduce potential contamination of brain tissue samples from drug present in cerebral blood vessels (Patel *et al.*, 1994a). A 30 sec flush with saline reduced potential contamination of brain tissue from drug in blood by 62%. The intrinsic binding capacity of drug treated brain homogenate was removed by denaturation (80°C for 15 min) and then homogenate samples were essentially added as a 'competing drug' to an *in vitro* radioligand binding assay, where one standard source of membranes is used. This avoids the complication in *ex vivo* binding assays, where each animal serves as the source of both drug and receptors and therefore assumes that the receptor density and the [^{3}H]ligand affinity is the same in vehicle and drug treated animals (Burki, 1986). Two peripheral adenosine receptor antagonists DPSPX and 8-PST were not detectable in brain despite micromolar serum concentrations, suggesting BBB permeability is a prerequisite for detection in brain homogenates (Nikodijevic *et al.*, 1991; Baumgold *et al.*, 1992). A range of adenosine antagonists were given at a behaviourally equivalent equipotent dose; i.e. a dose of antagonist known to produce an 80% reversal of CPA-induced hypolocomotion. For the drugs that were detectable in brain tissue, there was a good association between *in vitro* K_i and brain concentration at the equipotent dose. With antagonists present in brain tissue at concentrations sufficient to mediate the observed behavioural effect and with peripheral antagonists ineffective, the results indicate that the compounds are BBB permeable and capable of reversing a centrally mediated

behavioural effect. For the two compounds which were behaviourally active but which fell below the limit of detection in the assay, further studies are required. The method is simple, reliable and capable of being used as a high throughput assay for determining whether compounds cross the BBB and how long they remain there. Compounds can be measured over a minimum of a 100 fold concentration from at least 10 fold above and below the IC_{50} value of each drug for the receptor. Unlike HPLC, it also has the advantage of detecting the presence of active metabolites. If a suitable radioligand binding assay is available the method could be modified for use with other receptors and applied to different tissues and even intracellular receptor or enzyme systems.

Adenosine and its receptors are distributed widely throughout the body. It is essential to establish if central and peripheral receptors are the same. A centrally selective adenosine A_1 antagonist with limited peripheral effects may be beneficial for use as a cognitive enhancer (Jacobson *et al.*, 1992a; Suzuki *et al.*, 1993). As adenosine A_1 antagonists are potent diuretics, we examined the pharmacology and localisation of rat renal adenosine A_1 receptors, neither of which is well characterised (Spielman & Arend, 1991). A combined approach involving radioligand binding, *in vitro* autoradiography and *in situ* hybridisation was used. No specific adenosine receptor binding was found in crude or complex cortical and medullary kidney preparations, at radioligand concentrations in excess of those used to detect adenosine A_1 receptors in rat and human brain. The membrane preparations appeared viable with binding of the α_2 adrenoreceptor antagonist [^{3}H]RX821002 characterised. Even using this combined approach and despite positive signals for the adenosine A_1 receptor in brain using *in vitro* autoradiography, no signal was observed in kidney. A wealth of evidence points to multiple roles for adenosine in the kidney (Spielman & Arend, 1991). Despite this, there are conflicting reports on the

ability to detect adenosine A_1 receptor mRNA in rat kidney (see 4.4). A low receptor density and discrete localisation may be responsible, for our inability to detect adenosine A_1 receptors in rat kidney. The potential of a higher adenosine receptor density in human kidney led to the use of HEK 293 cells (Toya *et al.*, 1993; Ren & Stiles, 1994a, b). The low affinity binding characterised, may be an artifact and therefore future studies would require the use of human kidney.

Neurochemical and electrophysiological experiments have pointed to a neuromodulatory role for adenosine. In general, presynaptic adenosine A_1 receptors are responsible for inhibition of neurotransmitter release and postsynaptic A_1 receptors cause a decrease in excitability. Adenosine A_1 antagonists may reverse the inhibitory effects of adenosine, leading to synaptic facilitation at pre- and post synaptic sites and increased neurotransmitter release. Fujisawa have synthesised a range of novel non-xanthine adenosine A_1 antagonists based on the structure of FK453. These compounds are highly selective for the adenosine A_1 receptor and are potent adenosine A_1 antagonists in human brain membranes. These high affinity, blood brain barrier permeable adenosine A_1 receptor antagonists may be capable of enhancing cognition and prove to be clinically useful in conditions such as Alzheimers disease.

APPENDIX 1

Abbreviations

The abbreviations used in this thesis are in accordance with the guidelines set out in the British Journal of Pharmacology instructions to authors. Those not defined in the above publication or in the text are listed below. Mg^{2+} and Na^{+} refer to the ionic species of magnesium and sodium respectively.

Adenosine Agonists

APEC:	2-[(2-aminoethylamino)carbonylethylphenylethylamino]-5′ -N-ethylcarboxamidoadenosine
CADO:	2-Chloroadenosine
CCPA:	2-Chloro-N^6-cyclopentyladenosine
CHA:	N^6-Cyclohexyladenosine
CGS21680:	(2-*p*-carboxyethyl)phenylamino-5′-N-carboxamidoadenosine
CPA:	N^6-Cyclopentyladenosine
CSPA:	N^6-*p*-sulfophenyladenosine
NECA:	5'-N-Ethylcarboxamidoadenosine
R-PIA:	R(-)-N^6-(2-Phenylisopropyl)adenosine
S-PIA:	S(-)-N^6-(2-Phenylisopropyl)adenosine

Adenosine Antagonists

Caffeine	
CGS15943:	9-Chloro-2-(2-furyl)[1,2,4]triazolo[1,5-c]quinazolin-5-amine
CSC:	8-(3-Chlorostyryl)caffeine
CPT:	8-Cyclopentyl-1,3-dimethylxanthine
DPCPX:	8-Cyclopentyl-1,3-dipropylxanthine

DPX:	1,3-Diethyl-8-phenylxanthine
DPSPX:	1,3-Dipropyl-8-sulphophenylxanthine
FK352:	(R)-1-[(E)-3-(2-phenylpyrazolo[1,5-a]pyridin-3-yl)acryloyl]-piperidin-2-yl acetic acid
FK453:	(R)-1-((E)-3-(2-phenylpyrazolo[1,5-a]pyridin-3-yl)acryloyl)-2-piperidine ethanol)
FK838:	6-oxo-3-(2-phenylpyrazolo[1,5-a]pyridin-3-yl)acryloyl]-1(6H)-pyridazinebutylic acid
FR129946:	development compound-no name supplied
FR160537:	development compound-no name supplied
FR171562:	development compound-no name supplied
FR182303:	development compound-no name supplied
FR182394:	development compound-no name supplied
KF17837:	(FR179123): (E)-1,3-Dipropyl-8-(3,4-dimethoxystyryl)-7-methylxanthine
KW3902:	(FR144942): 8-(Noradamantan-3-yl)-1,3-dipropylxanthine
MDL102234:	(FR160502): (R)-3,7-dihydro-8-(1-phenylpropyl)-1,3-dipropyl-1*H*-purine-2,6-dione)
8-PT:	8-Phenyltheophylline
8-PST:	8-(*p* -Sulphophenyl)-theophylline
Takeda:	(FR160492) (CAS#131910-11-7): 1-Benzyl-1-6-(4-methoxyphenyl)-3-propyl-1,2,3,4-tetrahydro-5*H*-imidazol[2´,1´:5,1]pyrazolo[3,4-d]pyrimidin-2,4-dione
Theophylline	

Miscellaneous

ADP:	Adenosine 5´ diphosphate
AMP:	Adenosine 5´ monophosphate

APES:	3-aminopropyltriethoxy-silane
ATP:	Adenosine 5´ triphosphate
BSA:	Bovine serum albumin
cAMP:	Adenosine 3´ 5´ cyclic monophosphate
cDNA:	Complementary DNA
DEPC:	Diethylpyrocarbonate
d.H_2O:	Distilled water
DMSO:	Dimethylsulphoxide
DMEM:	Dulbecco's modified eagles medium
DNA:	Deoxyribonucleic acid
DNTP's:	Deoxynucleoside triphosphates
dpm:	Disintegrations per minute
DTT:	Dithiothreitol
EDTA:	(Ethylenedinitrilo)tetraacetic acid
FCS:	Foetal calf serum
G protein:	Guanyl nucleotide binding protein
GPCRs:	G protein coupled receptors
Gpp(NH)p:	5´-Guanylimidodiphosphate
GTP:	Guanosine 5´ triphosphate
IMS:	Industrial methylated spirits
IPTG:	Isopropyl-β-D-thiogalactoside
LB:	Luria Bertani (medium or agar)
O.D.:	Optical density
PCR:	Polymerase chain reaction
PBS:	Phosphate buffered saline
PMSF:	Phenylmethylsulphonyl fluoride
rpm:	Revolutions per minute
SSC:	Standard sodium citrate

TE:	Tris-EDTA buffer
TEA:	Triethanolamine buffer
X-GAL:	5-bromo-4-chloro-3-indolyl-β-D-galactoside

REFERENCES

ABBRACCHIO, M.P. & BURNSTOCK, G. (1994). Purinoreceptors: Are there families of P_{2X} and P_{2Y} purinoreceptors?. *Pharmacol. Ther.*, **64**, 445-475.

ABBRACCHIO, M.P., CATTABENI, F., FREDHOLM, B.B. & WILLIAMS, W. (1993). Purinoreceptor nomenclature: A status report. *Drug Dev. Res.*, **28**, 207-213.

ABBRACCHIO, M.P., BRAMBILLA, R., CERUTI, S., KIM, H.O., VON LUBITZ, D.K.J.E., JACOBSON, K.A. & CATTABENI, F. (1995). G protein-dependent activation of phospholipase C by adenosine A_3 receptors in rat brain. *Mol. Pharmacol.*, **48**, 1038-1045.

AGUILAR, J.S., TAN, F., DURAND, I. & GREEN, R.D. (1995). Isolation and characterisation of an avian A_1 adenosine receptor gene and a related cDNA clone. *Biochem. J.*, **307**, 729-734.

AKBAR, M., OKAJIMA, F., TOMURA, H., SHIMEGI, S. & KONDO, Y. (1994). A single species of A_1 adenosine receptor expressed in chinese hamster ovary cells not only inhibits cAMP accumulation but also stimulates phospholipase C and arachidonate release. *Mol. Pharmacol.*, **45**, 1036-1042.

ALEXANDER, S.P.H. & REDDINGTON, M. (1989). The cellular localisation of adenosine receptors in rat neostriatum. *Neurosci.*, **28**, 645-651.

ALEXANDER, S.P.H., CURTIS, A.R., KENDALL, D.A. & HILL, S.J. (1994). A_1 adenosine receptor inhibition of cyclic AMP formation and radioligand binding in the guinea pig cerebral cortex. *Br. J. Pharmacol.*, **113**, 1501-1507.

ALLENDE, G., FRANCO, R., MALLOL, J., LLUIS, C. & CANELA, E.I. (1991). N-ethylmaleimide affects agonist binding to A_1 adenosine receptors differently in the presence than in the absence of the ligand. *Biochem. Biophys. Res. Commn.*, **181**, 213-218.

ARAKI, T., KATO, H., KOGURE, K., SHUTO, K. & ISHIDA, Y. (1992). Autoradiographic mapping of neurotransmitter system receptors in mammalian brain. *Pharmacol. Biochem. Behav.*, **41**, 539-542.

ARVIN, B., NEVILLE, L.F., PAN, J. & ROBERTS, P.J. (1989). 2-Chloroadenosine attenuates kainic acid-induced toxicity within the rat striatum: relationship to release of glutamate and Ca^{2+} influx. *Br. J. Pharmacol.*, **98**, 225-235.

ASANO, T., SHINOHARA, H., MORISHITA, R., NOROTA, I., KATO, K. & ENDOH, M. (1995). The G-protein G_o in mammalian cardiac muscle: Localisation and coupling to A_1 adenosine receptors. *J. Biochem.*, **117**, 183-189.

ASKALAN, R. &. RICHARDSON, P.J. (1994). Role of histidine residues in the adenosine A_{2a} receptor ligand binding site. *J. Neurochem.*, **63**, 1477-1484.

BALAKRISHNAN, V.S., COLES, G.A. & WILLIAMS. J.D. (1993). A potential role for endogenous adenosine in control of human glomerular and tubular function. *Am. J. Physiol.*, **265**, F504-F510.

BALAKRISHNAN, V.S., VON RUHLAND, C.J., GRIFFITHS, D.F.R., COLES, G.A. & WILLIAMS, J.D. (1996). Effects of a selective adenosine A_1 receptor antagonist on the development of cyclosporin nephrotoxicity. *Br. J. Pharmacol.*, **117**, 879-884.

BARBER, A., BARTOSZYK, G.D., GREINER, H.E., MAULER, F., MURRAY, R.D., SEYFRIED, C.A., SIMON, M., GOTTSCHLICH, R., HARTING, J. & LUES, I. (1994). Central and peripheral actions of the novel k-opioid receptor agonist, EMD 60400. *Br. J. Pharmacol.*, **111**, 843-851.

BARLOW, R.B. (1983). In: Biodata handling with microcomputers. Elsevier, Cambridge.

BARNES, J.C., BROWN, J.D., CLARKE, N.P., CLAPHAM, J., EVANS, D.J. & O'SHAUGHNESSY, C.T. (1993). Pharmacological activity of VUF 9153, an isothiourea histamine H_3 receptor antagonist. *Eur. J.* Pharmacol., **250**, 147-152.

BARRINGTON, W.W., JACOBSON, K.A. & STILES, G.L. (1990). Glycoprotein nature of the A_2 receptor binding subunit. *Mol. Pharmacol.*, **38**, 177-183.

BAUMGOLD, J., NIKODIJEVIC, O. & JACOBSON, K.A. (1992). Penetration of adenosine antagonists into mouse brain as determined by *ex-vivo* binding. *Biochem. Pharmacol.*, **43**, 889-894.

BEAVEN, M.A., RAMKUMAR, V. & ALI, H. (1994). Adenosine A_3 receptors in mast cells. *Trends Pharmacol. Sci.*, **15**, 13-14.

BERNE, R. M. (1963). Cardiac nucleotides in hypoxia: possible role in regulation of coronary blood flow. *Am. J. Physiol.*, **204**, 317-323.

BHATTACHARYA, S., DEWITT, D.L., BURNATOWSKA-HLEIDIN, M., SMITH, W.L. & SPIELMAN, W.S. (1993). Cloning of an adenosine A_1 receptor encoding gene from rabbit. *Gene*, **128**, 285-288.

BIRNBAUMER, L. (1992). Receptor-to-effector signalling through G proteins: Roles for $\beta\gamma$ dimers as well as α subunits. *Cell*, **71**, 1069-1072.

BIRNBAUMER, L., ABRAMOWITZ, J. & BROWN, A.M. (1990). Receptor-effector coupling by G proteins. *Biochim. Biophys. Acta.*, **1031**, 163-224.

BISSERBE, J.C., PASCAL, O., DECKERT, J. & MAZIERE, B. (1992). Potential use of DPCPX as probe for *in-vivo* localisation of brain A_1 adenosine receptors. *Brain Res.*, **599**, 6-12.

BLACK, J.W. & SHANKLEY, N.P. (1995). Inverse agonists exposed. *Nature*, **374**, 214-215.

BLANCO, J., CANELA, E.I., MALLOL, J., LLUIS, C. & FRANCO, R. (1992). Characterisation of adenosine receptors in brush-border membranes from pig kidney. *Br. J. Pharmacol.*, **107**, 671-678.

BOARDER, R. M., WEISMAN, G.A., TURNER, J.T. & WILKINSON, G.F. (1995). G protein-coupled P_2 purinoreceptors: from molecular biology to functional responses. *Trends Pharmacol. Sci.*, **16**, 133-139.

BOETTGE, K., JAEGER, K.H. & MITTENZWEI, H. (1957). Das adenylsauresystem. Neuere ergebnisse und probleme. *Arnzeim. Forsch.*, **7**, 24-59.

BOND, R.A., LEFF, P., JOHNSON, T.D., MILANO, C.A., ROCKMAN, H.A., McMINN, T.R., APPARSUNDARAM, S., HYEK, M.F., KENAKIN, T.P., ALLEN, L.F. & LEFKOWITZ, R.J. (1995). Physiological effects of inverse agonists in transgenic mice with myocardial overexpression of the β_2-adrenoreceptor. *Nature*, **374**, 272-276.

BOREA, P.A., VARANI, K., MALAGUTI, V. & GILLI, G. (1991). Receptor binding at two different temperatures to discriminate agonist and antagonist behaviour of adenosine A_1 receptor ligands in rat brain. *J. Pharm. Pharmacol.*, **43**, 866-868.

BRADFORD, M.M. (1976). A rapid and sensitive method for the quantification of microgram quantities of protein utilising the principle of protein dye binding. *Anal. Biochem.*, **72**, 710-716.

BRINES, M.L. & FORREST, J.N. (1987). Autoradiographic localisation of A_1 adenosine receptors to tubules in the red medulla and papilla of the rat kidney. *Kid. Intl.*, **33**, 256.

BRUNS, R.F. (1980). Adenosine receptor activation in human fibroblasts: nucleoside agonists and antagonists. *Can. J. Physiol. Pharmacol.*, **58**, 673-691.

BRUNS, R.F. (1981). Adenosine antagonism by purines, pteridines and benzopteridines in human fibroblasts. *Biochem. Pharmacol.*, **30**, 325-333.

BRUNS, R.F. (1990). Adenosine Receptors. *Ann. N.Y. Acad. Sci.*, **603**, 211-216.

BRUNS, R.F., DALY, J.W. & SNYDER, S.H. (1980). Adenosine receptors in brain membranes: Binding of N^6-cyclohexyl[^{3}H]adenosine and 1,3-diethyl-8-[^{3}H]phenylxanthine. *Proc. Natl. Acad. Sci.*, **77**, 5547-5551.

BRUNS, R.F., LU, G.H. & PUGSLEY, T.A. (1986). Characterisation of the A_2 adenosine receptor labelled by [^{3}H]NECA in rat striatal membranes. *Mol. Pharmacol.*, **29**, 331-346.

BRUNS, R.F., FERGUS, J.H., BADGER, E.W., BRISTOL, J.A., SANTAY, L.A., HARTMAN, J.D., HAYS, S.J. & HUANG, C.C. (1987). Binding of the A_1-selective adenosine antagonist 8-cyclopentyl-1,3-dipropylxanthine to rat brain membranes. *Naunyn-Schmiedeberg's Arch. Pharmacol.*, **335**, 59-63.

BUREN, M., KOOMANS, H.A., VAN RIJN, H.J.M., RESTORICK, J. & ACTON, G. (1993). Adenosine A_1-receptor blockade with oral FK453 in essential hypertensives increases sodium excretion and lowers blood pressure, without an effect on renal haemodynamics. *Kid. Intl.*, **43**, 967.

BURKI, H.R. (1986). Binding of psychoactive drugs to rat brain amine receptors, measured *ex-vivo*, and their effects on the metabolism of biogenic amines. *Naunyn-Schmiedeberg's Arch. Pharmacol.*, **332**, 258-266.

BURNATOWSKA-HLEDIN, M.A. & SPIELMAN, W.S. (1991). Effects of adenosine on cAMP production and cystolic Ca^{2+} in cultured rabbit medullary thick limb cells. *Am. J. Physiol.*, **260**, C143-C150.

BURNSTOCK, G. (1972). Purinergic nerves. *Pharmacol. Rev.*, **24**, 509-581.

BURNSTOCK, G. (1978). A basis for distinguishing two types of purinergic receptor. In: Cell membrane receptors for drugs and hormones: A multidisciplinary approach: 107-118. Eds, Straub, R.W. & Bolis, L. Raven Press, New York.

BURNSTOCK, G. (1993). Physiological and pathological roles of purines: An update. *Drug Dev. Res.*, **28**, 195-206.

BYLUND, D.B. & YAMAMURA, H.I. (1990). Methods for receptor binding. In: Methods in neurotransmitter receptor analysis, 1-36. Eds, H.I. Yamamura, S.J. Enna & M.J. Kuhar. Raven Press, New York.

BYLUND, D.B., EIKENBURG, D.C., HIEBLE, J.P., LANGER, S.Z., LEFKOWITZ, R.J., MINNEMAN, K.P., MOLINOFF, P.B., RUFFOLO, R.R. & TRENDELENBURG, U. (1995). IV. International union of pharmacology nomenclature of adrenoreceptors. *Pharmacol. Rev.*, **46**, 121-136.

BYMASTER, F.P., HEATH, I., HENDRIX, J.C. & SHANNON, H.E. (1993a). Comparative behavioural and neurochemical activities of cholinergic antagonists in rats. *J. Pharmacol. Exp.Ther.*, **267**, 16-24.

BYMASTER, F.P., WONG, D.T., MITCH, C.H., WARD, J.S., CALLIGARO, D.O., SCHOEPP, D.D., SHANNON, H.E., SHEARDOWN, M.J., OLESEN, P.H., SUZDAK, P.D., SWEDBERG, M.D.B. & SAUERBERG, P. (1993b). Neurochemical effects of the M_1 muscarinic agonist xanomeline (LY246708/NNC11-0232). *J. Pharmacol. Exp. Ther.*, **269**, 282-289.

CAHILL, C.M., WHITE, T.D. & SAWYNOK, J. (1993). Involvement of calcium channels in depolarisation-evoked release of adenosine from spinal cord synaptosomes. *J. Neurochem.*, **60**, 886-893.

CARRUTHERS, A.M. & FOZARD, J.R. (1993). Adenosine A_3 receptors: two into one won't go. *Trends Pharmacol. Sci.*, **14**, 290-291.

CASADO, V., CANTI, C., MALLOL, J., CANELA, E.I., LLUIS, C. & FRANCO, R. (1990). Solubilisation of A_1 adenosine receptor from pig brain: Characterisation and evidence of the role of the cell membrane on the coexistence of high- and low-affinity states. *J. Neurosci. Res.*, **26**, 461-473.

CASADO, V., MALLOL, J., CANELA, E.I., LLUIS, C. & FRANCO. R. (1991). The binding of [^{3}H]R-PIA to A_1 adenosine receptors produces a conversion of the high- to the low-affinity state. *FEBS Lett.*, **286**, 221-224.

CASADO, V., MALLOL, J., FRANCO, R., LLUIS, C. & CANELA, E.I. (1994). A_1 adenosine receptors can occur manifesting two kinetic components of 8-cyclopentyl-1,3-[^{3}H]dipropylxanthine ([^{3}H]DPCPX) binding. *Naunyn-Schmiedeberg's Arch. Pharmacol.*, **349**, 485-491.

CHENG, Y.C. & PRUSOFF, W.H. (1973). The relationship between the inhibition constant (K_i) and the concentration of inhibitor which causes 50% inhibition (IC_{50}) of an enzymatic reaction. *Biochem. Pharmacol.*, **22**, 3099-3108.

CHERN, Y., KING, K., LAI, H.L. & LAI, H.T. (1992). Molecular cloning of a novel adenosine receptor gene from rat brain. *Biochem. Biophys. Res. Commn.*, **185**, 304-309.

CIRUELA, F., CASADO, V., MALLOL, J., CANELA, E.I., LLUIS, C. & FRANCO, R. (1995). Immunological identification of A_1 adenosine receptors in brain cortex. *J. Neurosci. Res.*, **42**, 818-828.

CIRUELA, F., SAURA, C., CANELA, E.I., MALLOL, J., LLUIS, C. & FRANCO, R. (1996). Adenosine deaminase affects ligand-induced signalling by interacting with cell surface adenosine receptors. *FEBS Lett.*, **380**, 219-223.

CLARK, E.A. & HILL, S.J. (1995). Differential effect of sodium ions and guanine nucleotides on the binding of thioperamide and clobenpropit to histamine H_3-receptors in rat cerebral cortical membranes. *Br. J. Pharmacol.*, **114**, 357-362.

COHEN, F.R., LAZARENO, S. & BIRDSALL, N.J.M. (1996). The effects of saponin on the binding and functional properties of the human adenosine A_1 receptor. *Br. J. Pharmacol.*, **117**, 1521-1529.

COLLIS, M.G. & HOURANI, S.M.O. (1993). Adenosine receptor subtypes. *Trends Pharmacol. Sci.*, **14**, 360-366.

COULSON, R., JOHNSON, R.A., OLSSON, R.A., COOPER, D.R. & SCHEINMAN, S.J. (1991). Adenosine stimulates phosphate and glucose transport in opposum kidney epithelial cells. *Am. J. Physiol.*, **260**, F921-F928.

COULSON, R., PROCH, P.S., OLSSON, R.A., CHALFANT, C.E. & COOPER, D.R. (1996). Upregulated renal adenosine A_1 receptors augment PKC and glucose transport but inhibit proliferation. *Am. J. Physiol.*, **270**, F263-F274.

COX, H.M., MUNDAY, K.A. & POAT, J.A. (1983). The binding of [^{125}I]-angiotensin to rat renal epithelial cell membranes. *Br. J. Pharmacol.*, **79**, 063-070.

CUNHA, R.A., JOHANSSON, B., CONSTANTINO, M.D., SEBASTIAO, A.M. & FREDHOLM, B.B. (1996). Evidence for high-affinity binding sites for the adenosine A_{2a} receptor agonist [^{3}H]CGS21680 in the rat hippocampus and cerebral cortex that are different from striatal A_{2a} receptors. *Naunyn-Schmiedeberg's Arch. Pharmacol.*, **353**, 261-271.

DALY, J.W. (1982). Adenosine receptors: Targets for future drugs. *J. Med. Chem.*, **25**, 197-207.

DALY, J.W., BRUNS, R.F. & SNYDER, S.H. (1981). Adenosine receptors in the central nervous system: Relationship to the central actions of methylxanthines. *Life Sci.*, **28**, 2083-2097.

DALY, J.W., BUTTS-LAMB, P. & PADGETT, W. (1983). Subclasses of adenosine receptors in the central nervous system: interaction with caffeine and related methylxanthines. *Cell Mol. Neurobiol.*, **3**, 69-80.

DALY, J.W., PADGETT, M.T., BUTTS-LAMB, P. & WATERS, J. (1985). 1,3-dialkyl-8-(*p*-sulfophenyl)xanthines: potent water-soluble antagonists for A_1 and A_2-adenosine receptors. *J. Med. Chem.*, **28**, 487-492.

DALZIEL, H.H. & WESTFALL, D.P. (1994). Receptors for adenine nucleotides and nucleosides: Subclassification, distribution, and molecular characterisation. *Pharmacol. Rev.*, **46**, 449-466.

DAVAL, J.L., NEHLIG, A. & NICOLAS, F. (1991). Physiological and pharmacological properties of adenosine: Therapeutic implications. *Life Sci.*, **49**, 1435-1453.

DAWSON, T.P., GANDHI, R., LE HIR, M. & KAISSLING, B. (1989). Ecto-5'-Nucleotidase: Localisation in rat kidney by light microscopic histochemical and immunohistochemical methods. *J. Histochem. Cytochem.*, **37**, 39-47.

DE GUBAREFF, T. &. SLEATOR, W. (1965). Effects of caffeine on mammalian atrial muscle and its interaction with adenosine and calcium. *J. Pharmacol. Exp. Ther.*, **148**, 202-214.

DE LEAN, A., HANCOCK, A.A. & LEFKOWITZ, R.J. (1981). Validation and statistical analysis of a computer modelling method for quantitative analysis of radioligand binding data for mixtures of pharmacological receptor subtypes. *Mol. Pharmacol.*, **21**, 5-16.

DE MEY, J.G. & VANHOUTTE, P.M. (1981). Role of the intima in cholinergic and purinergic relaxation of isolated canine femoral arteries. *J. Physiol.*, **316**, 347-355.

DECKERT, J., BERGER, W., KLEOPA, K., HECKERS, S., RANSMAYR, G., HEINSEN, H., BECKMANN, H. & RIEDERER, P. (1993). Adenosine A_1 receptors in human hippocampus: inhibition of [^{3}H]8-cyclopentyl-1,3-dipropylxanthine binding by antagonist drugs. *Neurosci. Lett.*, **150**, 191-194.

DECKERT, J., NOTHEN, M.M., BRYANT, S.P., REN, H., WOLF, H.K., STILES, G.L., SPURR, N.K. & PROPPING, P. (1995). Human adenosine A_1 receptor gene: Systematic screening for DNA sequence variation and linkage mapping on chromosome 1q31-32.1 using a silent polymorphism in the coding region. *Biochem. Biophys. Res. Comm.*, **214**, 614-621.

DIXON, A.K., GUBITZ, A.K., SIRINATHSINGHJI, D.J.S., RICHARDSON, P.J. & FREEMAN, T.C. (1996). Tissue distribution of adenosine receptor mRNAs in the rat. *Br. J. Pharmacol.*, **118**, 1461-1468.

DRURY, A.D. & SZENT-GYöRGYI, A. (1929). The physiological activity of adenine compounds with especial reference to their action upon the mammalian heart. *J. Physiol.*, **68**, 213-237.

ENNA, S.J. (1978). Radioreceptor assay techniques for neurotransmitter drugs. In: Neurotransmitter receptor binding, 127-141. Eds, H.I. Yamamura, S.J. Enna & M.J. Kuhar. Raven Press, New York.

ENNA, S.J. & SNYDER, S.H. (1976). A simple, sensitive and specific radioreceptor assay for endogenous GABA in brain tissue. *J. Neurochem.*, **26**, 221-224.

FASTBOM, J. &. FREDHOLM, B.B. (1990). Regional differences in the effect of guanine nucleotides on agonist and antagonist binding to adenosine A_1-receptors in rat brain, as revealed by autoradiography. *Neurosci.*, **34**, 759-769.

FASTBOM, J., PAZOS, A., PROBST, A. & PALACIOS, J.M. (1986). Adenosine A_1-receptors in human brain: Characterisation and autoradiographic visualisation. *Neurosci.Lett.*, **65**, 127-132.

FASTBOM, J., PAZOS, A., PROBST, A. & PALACIOS, J.M. (1987a). Adenosine A_1 receptors in the human brain: A quantitative autoradiographic study. *Neurosci.*, **22**, 827-839.

FASTBOM, J., PAZOS, A. & PALACIOS, J.M. (1987b). The distribution of adenosine A_1 receptors and 5'-nucleotidase in the brain of some commonly used experimental animals. *Neurosci.*, **22**, 813-826.

FERKANKY, J.W., VALENTINE, H.L., STONE, G.A. & WILLIAMS, M. (1986). Adenosine A_1 receptors in mammalian brain: species differences in their interactions with agonists and antagonists. *Drug Dev. Res.*, **9**, 85-93.

FINK, J.S., WEAVER, D.R., RIVKEES, S.A., PETERFREUND, R.A., POLLACK, A.E., ADLER, E.M. & REPPERT, S.M. (1992). Molecular cloning of the rat A_2 adenosine receptor: selective co-expression with D_2 dopamine receptors in rat striatum. *Mol. Brain Res.*, **14**, 186-195.

FINLAYSON, K., MAEMOTO, T., OLVERMAN, H.J. & BUTCHER. S.P. (1994). The effect of Gpp(NH)p on adenosine A_1 receptor binding in rat cortical membranes. *Br. J. Pharmacol. Proc. Suppl*, **113**, 108P

FLORIO, C., ROSATI, A.M., TRAVERSA, U. & VERTUA, R. (1994). Strain-related differences in adenosine receptor density and behavioural sensitivity to adenosine analogues in mice. *Pharmacol. Biochem. Behav.*, **49**, 271-276.

FREDHOLM, B.B. & DUNWIDDIE, T.V. (1988). How does adenosine inhibit transmitter release?. *Trends Pharmacol. Sci.*, **9**, 130-134.

FREDHOLM, B.B., ABBRACCHIO, M.P., BURNSTOCK, G., DALY, J.W., KENDALL-HARDEN, T., JACOBSON, K.A., LEFF, P & WILLIAMS, M. (1994). Nomenclature and classification of purinoreceptors. *Pharmacol. Rev.*, **46**, 143-156.

FREEDMAN, S.B., HARLEY, E.A. & PATEL, S. (1989). Direct measurement of muscarinic agents in the central nervous system of mice using *ex-vivo* binding. *Eur. J. Pharmacol.*, **174**, 253-260.

FREISSMUTH, M., HAUSLEITHNER, V., TUISL, E., NANOFF, C. & SCHUTZ, W. (1987a). Glomeruli and microvessels of the rabbit kidney contain both A_1- and A_2-adenosine receptors. *Naunyn-Schmiedeberg's Arch. Pharmacol.*, **335**, 438-444.

FREISSMUTH, M., NANOFF, C., TUISL, E. & SCHUTZ, W. (1987b). Stimulation of adenylate cyclase activity via A_2-adenosine receptors in isolated tubules of the rabbit renal cortex. *Eur. J. Pharmacol.*, **138**, 137-140.

FREISSMUTH, M., SELZER, E. & SCHUTZ, W. (1991a). Interactions of purified bovine brain A_1-adenosine receptors with G proteins. *Biochem. J.*, **275**, 651-656.

FREISSMUTH, M., SCHUTZ, W. & LINDER, M.E. (1991b). Interactions of the bovine brain A_1-adenosine receptor with recombinant G protein α-subunits. *J. Biol. Chem.*, **266**, 17778-17783.

FREUND, S., UNGERER, M. & LOHSE, M.J. (1994). A_1 adenosine receptors expressed in CHO-cells couple to adenylyl cyclase and phospholipase C. *Naunyn-Schmiedeberg's Arch. Pharmacol.*, **350**, 49-56.

FURLONG, T.J., PIERCE, K.D., SELBIE, L.A. & SHINE, J. (1992). Molecular characterisation of a human brain adenosine A_2 receptor. *Mol. Brain Res.*, **15**, 62-66.

GAARDER, A., JONSEN, J., LALAND, S., HELLEM, A. & OWREN, P.A. (1961). Adenosine diphosphate in red cells as a factor in the adhesiveness of human blood platelets. *Nature*, **192**, 531-532.

GAVISH, M., GOODMAN, R.R. & SNYDER, S.H. (1982). Solubilised adenosine receptors in the brain: Regulation by guanine nucleotides. *Science*, **215**, 1633-1635.

GERLACH, E., DEUTICKE, B. & DREISBACH, R.H. (1963). Der nucleotid-abbau im herzmuskel bei sauerstoffmangel und seine mogliche. Bedeutung fur die coronardurchblutung. *Naturwissenschaften*, **50**, 228-229.

GERWINS, P., NORDSTEDT, C. & FREDHOLM, B.B. (1990). Characterisation of adenosine A_1 receptors in intact DDT_1MF-2 smooth muscle cells. *Mol. Pharmacol.*, **38**, 660-666.

GILMAN, A.G. (1987). G proteins: Transducers of receptor-generated signals. *Ann. Rev. Biochem.*, **56**, 615-649.

GINSBORG, B.L. & HIRST, G.D.S. (1972). The effect of adenosine on the release of the transmitter from the phrenic nerve of the rat. *J. Physiol.*, **224**, 629-645.

GLASS, M., FAULL, R.L.M. & DRAGUNOW, M. (1996). Localisation of the adenosine uptake site in human brain: a comparison with the distribution of adenosine A_1 receptors. *Brain Res.*, **710**, 79-91.

GOODMAN, R.R. & SNYDER, S.H. (1982). Autoradiographic localisation of adenosine receptors in rat brain using [^{3}H]cyclohexyladenosine. *J. Neurosci.*, **2**, 1230-1241.

GOODMAN, R.R., COOPER, M.J., GAVISH, M. & SNYDER, S.H. (1982). Guanine nucleotide and cation regulation of the binding of [^{3}H]cyclohexyladenosine and [^{3}H]diethylphenylxanthine to adenosine A_1 receptors in brain membranes. *Mol. Pharmacol.*, **21**, 329-335.

GOULD, R.J., MURPHY, K.M.M. & SNYDER, S.H. (1983). A simple sensitive radioreceptor assay for calcium antagonist drugs. *Life Sci.*, **33**, 2665-2672.

GOULD, J., BOWMER, C.J. & YATES, M.S. (1995). Renal adenosine receptors in rats with acute renal failure. *Br. J. Pharmacol.*, **115**, 5P.

GREEN, N.H. & STONER, H.B. (1950). Biological actions of the adenine nucleotides. H.K. Lewis, London.

GRIEBEL, J., SAFFROY-SPITTLER, M., MISSLIN, R., REMMY, D., VOGEL, E. & BOUGUIGNON, J.J. (1991). Comparison of the behavioural effects of an adenosine A_1/A_2-receptor antagonist, CGS 15943A, and an A_1-selective antagonist, DPCPX. *Pyschopharm.*, **103**, 541-544.

GU, J.G., FOGA, O., PARKINSON, F.E. & GEIGER, J.D. (1995). Involvement of bidirectional adenosine transporters in the release of L-[^{3}H]adenosine from rat brain synaptosomal preparations. *J. Neurochem.*, **64**, 2105-2110.

GURDEN, M.F., COATES, J., ELLIS, F., EVANS, B., HORNBY, E., KENNEDY, I., MARTIN, D.P., STRONG, P., VARDEY, C.J. & WHEELDON, A. (1993). Functional characterisation of three adenosine receptor subtypes. *Br. J. Pharmacol.*, **109**, 693-698.

HASLAM, R.J. & CUSACK, N.J. (1981). Blood platelet receptors for ADP and for adenosine. In: Purinergic receptors 221-285. Eds, G. Burnstock. Chapman & Hall, London.

HEFFEZ, D.S., NOWAK, T.S. & PASSONNEAU, J.V. (1985). Nimodipine levels in gerbil brain following parenteral drug administration. *J. Neurosurg.*, **63**, 589-592.

HEIDRICH, H.G., KINNE, R., KINNE-SAFFRAN, E. & HANNIG, K. (1972). The polarity of the proximal tubule cell in rat kidney. *J. Cell Biol.*, **54**, 232-245.

HENDERSON, R., BALDWIN, J.M., CESKA, T.A., ZEMLIN, F., BECKMANN, E. & DOWNING, K.H. (1990). Model for the structure of bacteriorhodopsin based on high resolution electron cryo-microscopy. *J .Mol. Biol.*, **213**, 899-929.

HIDE, I., PADGETT, W.L., JACOBSON, K.A. & DALY, J.W. (1991). A_{2a} adenosine receptors from rat striatum and rat pheochromocytoma PC12 cells: Characterisation with radioligand binding and by activation of adenylate cyclase. *Mol. Pharmacol.*, **41**, 352-359.

HIEBLE, J.P., BYLUND, D.B., CLARKE, D.E., EIKENBURG, D.C., LANGER, S.Z., LEFKOWITZ, R.J., MINNEMAN, K.P. & RUFFOLO, R.R. (1995). International union of pharmacology X. recommendations for nomenclature of α_1 adrenoreceptors: Consensus update. *Pharmacol. Rev.*, **47**, 267-270.

HOLTON, P. (1959). The liberation of adenosine triphosphate on antidromic stimulation of sensory nerves. *J. Physiol.*, **145**, 494-504.

HULME, E.C., BIRDSALL, N.J.M. & BUCKLEY, N.J. (1990). Muscarinic receptor subtypes. *Ann. Rev. Pharmacol. Toxicol.*, **30**, 633-673.

HUTCHISON, A.J., WEBB, R.L., OEI, H.H., GHAI, G.R., ZIMMERMAN, M.B. & WILLIAMS, M. (1989). CGS21680, an A_2 selective adenosine receptor agonist with preferential hypotensive activity. *J. Pharmacol. Exp. Ther.*, **251**, 47-55.

HUTCHISON, K.A., NEVINS, B., PERINI, F. & FOX, I.H. (1990). Soluble and membrane-associated human low-affinity adenosine binding protein (Adetonin): Properties and homology with mammalian and avian stress proteins. *Biochemistry*, **29**, 5138-5144.

HYTTEL, J., NEILSEN, J.B. & NOWAK, G. (1992). The acute effect of sertindole on brain 5-HT_2, D_2 and α_1 receptors (*ex-vivo* radioreceptor binding studies). *J. Neural Trans.*, **89**, 61-69.

IREDALE, P.A., ALEXANDER, S.P.H. & HILL, S.J. (1994). Coupling of a transfected human brain A_1 adenosine receptor in CHO-K1 cells to calcium mobilisation via a pertussis toxin-sensitive mechanism. *Br. J. Pharmacol.*, **111**, 1252-1256.

JACOBSON, K.A., VAN GALEN, P.J.M. & WILLIAMS, M. (1992a). Adenosine receptors: Pharmacology, structure-activity relationships and therapeutic potential. *J. Med. Chem.*, **35**, 406-423.

JACOBSON, K.A., NIKODIJEVIC, O., SHI, D., GALLO-RODRIGUEZ, C., OLAH, M.E., STILES, G.L. & DALY, J.W. (1992b). A role for central A_3-adenosine receptors. *FEBS Lett.*, **336**, 57-60.

JACOBSON, K.A., NIKODIJEVIC, O., PADGETT, W.L., GALLO-RODRIGUEZ, C., MAILLARD, M. & DALY, J.W. (1993). 8-(-3-Chlorostyryl)caffeine (CSC) is a selective A_2-adenosine antagonist *in vitro* and *in vivo*. *FEBS Lett.*, **323**, 141-144.

JACOBSON, M.A., JOHNSON, R.G., LUNEAU, C.J. & SALVATORE, C.A. (1995). Cloning and chromosomal localisation of the human A_{2b} adenosine receptor gene (ADORA2B) and its pseudogene. *Genomics*, **27**, 374-376.

JACOBSON, K.A., VON LUBITZ, D.K.J.E., DALY, J.W. & FREDHOLM, B.B. (1996). Adenosine receptor ligands: differences with acute versus chronic treatment. *Trends Pharmacol. Sci.*, **17**, 108-113.

JAKUBOWSKI, Z., SKOWRONSKI, R., MATECKI, A., MOHUCZY, D., PAWELCZYK, T., STEPINSKI, J. & ANGIELSKI, S. (1992). Adenosine receptors in basolateral membranes of rat renal cortex. *Pol. J. Pharmacol. Pharm.*, **44**, 373-382.

JANIS, R.A., KROL, G.J., NOE, A.J. & PAN, M. (1983). Radioreceptor and high-performance liquid chromatographic assays for the calcium channel antagonist nitrendipine in serum. *J. Clin. Pharmacol.*, **23**, 266-273.

JANSEN, K.L.R., FAULL, R.L.M., DRAGUNOW, M. & SYNEK, B.L. (1990). Alzheimers disease: Changes in hippocampal N-methyl-D-aspartate, quisqualate, neurotensin, adenosine, benzodiazepine, serotonin and opioid receptors-an autoradiographic study. *Neurosci.*, **39**, 613-627.

JARVIS, M.F. & WILLIAMS, M. (1988). Differences in adenosine A-1 and A-2 receptor density revealed by autoradiography in methylxanthine-sensitive and insensitive mice. *Pharmacol. Biochem. Behav.*, **30**, 707-714.

JARVIS, M.F., SCHULZ, R., HUTCHISON, A.J., DO, U.H., SILLS, M.A. & WILLIAMS, M. (1989a). [^{3}H]CGS21680, a selective A_2 adenosine receptor agonist directly labels A_2 receptors in rat brain. *J. Pharmacol. Exp. Ther.*, **251**, 888-893.

JARVIS, M.F., JACKSON, R.H. & WILLIAMS, M. (1989b). Autoradiographic characterisation of high-affinity adenosine A_2 receptors in the rat brain. *Brain Res.*, **484**, 111-118.

JARVIS, M.F., JACKSON, R.H & WILLIAMS, M. (1989c). Direct autoradiographic localisation of adenosine A_2 receptors in rat brain using the A_2 selective agonist [^{3}H]CGS21680. *Eur. J. Pharmacol.*, **168**, 243-246.

JENSEN, C.J., GERARD, N.P., SCHWARTZ, T.W. & GETHER, U. (1993). The species selectivity of chemically distinct tachykinin nonpeptide antagonists is dependent on common divergent residues of the rat and human neurokinin-1 receptors. *Mol. Pharmacol.*, **45**, 294-299.

JI, X.D., VON LUBITZ, D.K.J.E., OLAH, M.E., STILES, G.L. & JACOBSON, K.A. (1994). Species differences in ligand affinity at central A_3-adenosine receptors. *Drug Dev. Res.*, **33**, 51-59.

JOCKERS, R.A., LINDER, M.E., HOHENEGGER, M., NANOFF, C., BERTIN, B., STOSBERG, A.D., MARULLO, S. & FREISSMUTH, M. (1994). Species differences in the G protein selectivity of the human and bovine A_1-adenosine receptor. *J. Biol. Chem.*, **269**, 32077-32084.

JOHANSSON, B. & FREDHOLM, B.B. (1995). Further characterisation of the binding of the adenosine receptor agonist [^{3}H]CGS21680 to rat brain using autoradiography. *Neuropharmacol.*, **34**, 393-403.

JOHANSSON, B., PARKINSON, F.E. & FREDHOLM, B.B. (1992). Effects of mono- and divalent ions on the binding of the adenosine analogue CGS21680 to adenosine A_2 receptors in rat striatum. *Biochem. Pharmacol.*, **44**, 2365-2370.

JOHANSSON, B., AHLBERG, S., VAN DER PLOEG, I., BRENE, S., LINDEFORS, N., PERSSON, H. & FREDHOLM, B.B. (1993). Effect of long term caffeine treatment on A_1 and A_2 adenosine receptor binding and on mRNA levels in rat brain. *Naunyn-Schmiedeberg's Arch. Pharmacol.*, **347**, 407-414.

KAO, H.T., ADHAM, N., OLSEN, M.A., WEINSHANK, R.L., BRANCHECK, T.A. & HARTIG, P.R. (1992). Site-directed mutagenesis of a single residue changes the binding properties of the serotonin 5-HT_2 receptor from a human to a rat pharmacology. *FEBS Lett.*, **307**, 324-328.

KENAKIN, T.P., BOND, R.A. & BONNER, T.I. (1992). Definition of pharmacological receptors. *Pharmacol. Rev.*, **44**, 351-361.

KENNEDY, C. &. LEFF, P. (1995). How should P_{2x} purinoreceptors be classified pharmacologically. *Trends Pharmacol. Sci.*, **16**, 168-174.

KIM, H.O., JI, X.D., MELMAN, N., OLAH, M.E., STILES, G.L. & JACOBSON, K.A. (1994). Structure-activity relationships of 1,3-dialkylxanthine derivatives at rat A_3 adenosine receptors. *J. Med. Chem.*, **37**, 3373-3382.

KIM, J., WESS, J., VAN RHEE, A.M., SCHOENBERG, T. & JACOBSON, K.A. (1995). Site-directed mutagenesis identifies residues involved in ligand recognition in the human A_{2a} adenosine receptor. *J. Biol. Chem.*, **270**, 13987-13997.

KINSELLA, J.L., HOLOHAN, P.D., PESSAH, N.I. & ROSS, C.R. (1979). Isolation of luminal and antiluminal membranes from dog kidney cortex. *Biochim. Biophys. Acta.*, **552**, 468-477.

KIRK, I.P. & RICHARDSON, P.J. (1995). Further characterisation of [^{3}H]-CGS21680 binding sites in the rat striatum and cortex. *Br. J. Pharmacol.*, **114**, 537-543.

KLOTZ, K.N., CRISTALLI, G., GRIFANTINI, M., VITTORI, S. & LOHSE, M.J. (1985). Photoaffinity labelling of A_1-adenosine receptors. *J. Biol. Chem.*, **260**, 14659-14664.

KLOTZ, K.N., LOHSE, M.J. & SCHWABE, U. (1986). Characterisation of the solubilised A_1 adenosine receptor from rat brain membranes. *J. Neurochem.*, **46**, 1528-1534.

KLOTZ, K.N., LOHSE, M.J. & SCHWABE, U. (1988). Chemical modification of A_1 adenosine receptors in rat brain membranes. *J. Biol. Chem.*, **263**, 17522-17526.

KLOTZ, K.N., LOHSE, M.J., SCHWABE, U., CRISTALLI, G., VITTORI, S. & GRIFANTINI, M. (1989). 2-Chloro-N^6-[^{3}H]cyclopentyladenosine ([^{3}H]CCPA) - a high affinity agonist radioligand for A_1 adenosine receptors. *Naunyn-Schmiedeberg's Arch. Pharmacol.*, **340**, 679-683.

KLOTZ, K.N., KEIL, R., ZIMMER, F.J. & SCHWABE, U. (1990). Guanine nucleotide effects on 8-cyclopentyl-1,3-[^{3}H]dipropylxanthine binding to membrane bound and solubilised A_1 adenosine receptors of rat brain. *J. Neurochem.*, **54**, 1988-1994.

KLOTZ, K.N., VOGT, H. & TAWFIK-SCHLIEPER, H. (1991). Comparison of A_1 adenosine receptors in brain from different species by radioligand binding and photoaffinity labelling. *Naunyn-Schmiedeberg's Arch. Pharmacol.*, **343**, 196-201.

KWONG, F.Y.P., DAVIES, A., TSE, C.M., YOUNG, J.D., HENDERSON, P.J.F. & BALDWIN, S.A. (1988). Purification of the human erythrocyte nucleoside transporter by immunoaffinity chromatography. *Biochem. J.*, **255**, 243-249.

LANGIN, D., LAFONTAN, M., STILLINGS, M.R. & PARIS, H. (1989). [^{3}H]RX821002: A new tool for the identification of α_{2a}-adrenoreceptors. *Eur. J. Pharmacol.*, **167**, 95-104.

LEFF, P. (1995). The two-state model of receptor activation. *Trends Pharmacol. Sci.*, **16**, 89-97.

LEID, M., FRANKLIN, P.H. & MURRAY, T.F. (1988). Labelling of A_1 adenosine receptors in porcine atria with the antagonist radioligand 8-cyclopentyl-1,3-[^{3}H]dipropylxanthine. *Eur. J. Pharmacol.*, **147**, 141-144.

LEUNG, E. &. GREEN, R.D. (1989). Density gradient profiles of A_1 adenosine receptors labelled by agonist and antagonist radioligands before and after detergent solubilisation. *Mol. Pharmacol.*, **36**, 412-419.

LEUNG, E., KWATRA, M.M., HOSEY, M. & GREEN, R.D. (1988). Characterisation of cardiac A_1 adenosine receptors by ligand binding and photoaffinity labelling. *J. Pharmacol. Exp. Ther.*, **244**, 1150-1156.

LEUNG, E., JACOBSON, K.A. & GREEN, R.D. (1990). Analysis of agonist-antagonist interactions at A_1 adenosine receptors. *Mol. Pharmacol.*, **38**, 72-83.

LIBERT, F. (1994). *Errata. Genomics*, **23**, 305.

LIBERT, F., PARMENTIER, M., LEFORT, A., DINSART, C., VAN SANDE, J., MAENHAUT, C., SIMONS, M.J., DUMONT, J.E. & VASSART, G. (1989). Selective amplification and cloning of four new members of the G protein-coupled receptor family. *Science*, **244**, 569-572.

LIBERT, F., SCHIFFMANN, S.N., LEFORT, A., PARMENTIER, M., GERARD, C., DUMONT, J.E., VANDERHAEGHEN, J.J. & VASSART, G. (1991a). The orphan receptor cDNA RDC7 encodes an adenosine A_1 receptor. *EMBO*, **10**, 1677-1682.

LIBERT, F., PASSAGE, E., PARMENTIER, M., SIMONS, M.J., VASSART, G. & MATTEI, M.G. (1991b). Chromosomal mapping of A_1 and A_2 adenosine receptors, VIP receptor, and a new subtype of serotonin receptor. *Genomics*, **11**, 225-227.

LIBERT, F., VAN SANDE, J., LEFORT, A., CZERNILOFSKY, A., DUMONT, J.E., VASSART, G., ENSINGER, H.A. & MENDLA, K.D. (1992). Cloning and the functional characterisation of a human A_1 adenosine receptor. *Biochem. Biophys. Res. Comm.*, **187**, 919-926.

LIN, J.T., DA CRUZ, M.E.M., RIEDEL, S. & KINNE, R. (1981). Partial purification of hog kidney sodium-D-glucose cotransport system by affinity chromatography on a phlorizin polymer. *Biochim. Biophys. Acta.*, **640**, 43-54.

LINDEN, J. (1991). Structure and function of A_1 adenosine receptors. *FASEB J.*, **5**, 2668-2676.

LINDEN, J. (1994). Cloned adenosine A_3 receptors: pharmacological properties, species differences and receptor functions. *Trends Pharmacol. Sci.*, **15**, 298-306.

LINDEN, J., TAYLOR, H.E., ROBEVA, A.S., TUCKER, A.L., STEHLE, J.H., RIVKEES, S.A., FINK, J.S. & REPPERT, S.M. (1993). Molecular cloning and functional expression of a sheep A_3 adenosine receptor with widespread tissue distribution. *Mol. Pharmacol.*, **44**, 524-532.

LINK, R., DAUNT, D., BARSH, G., CHRUSCINSKI, A. & KOBILKA, B. (1992). Cloning of two mouse genes encoding α-adrenergic receptor subtypes and identification of a single amino acid in the mouse α2-C10 homolog responsible for an interspecies variation in antagonist binding. *Mol. Pharmacol.*, **42**, 16-27.

LOHSE, M.J., LENSCHOW, V. & SCHWABE, U. (1984). Two affinity states of R_i adenosine receptors in brain membranes. *Mol. Pharmacol.*, **26**, 1-9.

LOHSE, M.J., KLOTZ, K.N. & SCHWABE, U. (1986). Agonist photoaffinity labelling of A_1 adenosine receptors: persistent activation reveals spare receptors. *Mol. Pharmacol.*, **30**, 403-409.

LOHSE, M.J., KLOTZ, K.N., LINDENBORN-FOTINOS, J., REDDINGTON, M., SCHWABE, U. & OLSSON, R.A. (1987). 8-cyclopentyl-1,3-dipropylxanthine (DPCPX) - a selective high affinity antagonist radioligand for A_1 adenosine receptors. *Naunyn- Schmeideberg's Arch. Pharmacol.*, **336**, 204-210.

LOHSE, M.J., KLOTZ, K.N., SCHWABE, U., CRISTALLI, G., VITTORI, S. & GRIFANTINI, M. (1988). 2-Chloro-N^6-cyclopentyladenosine: a highly selective agonist at A_1 receptors. *Naunyn-Schmeideberg's Arch. Pharmacol.*, **337**, 687-689.

LONDOS, C. &. WOLFF, T. (1977). Two distinct adenosine sensitive sites on adenylate cyclase. *Proc. Natl. Acad. Sci.*, **74**, 5482-5486.

LONDOS, C., COOPER, D.M.F. & WOLFF, T. (1980). Subclasses of external adenosine receptors. *Proc. Natl. Acad. Sci.*, **77**, 2551-2554.

LORENZEN, A., FUSS, M., VOGT, H. & SCHWABE, U. (1993). Measurement of guanine nucleotide-binding protein activation by A_1 adenosine receptor agonists in bovine brain membranes: Stimulation of guanosine-5'-O-(3-[^{35}S]thio)triphosphate binding. *Mol. Pharmacol.*, **44**, 115-123.

LORENZEN, A., GUERRA, L., VOGT, H. & SCHWABE, U. (1996). Interaction of full and partial agonists of the A_1 adenosine receptor with receptor/G protein complexes in rat brain. *Mol. Pharmacol.*, **49**, 915-926.

LUPICA, C.R., CASS, W.A., ZAHNISER, N.R. & DUNWIDDIE, T.V. (1989). Effects of the selective adenosine A2 receptor agonist CGS21680 on *in vitro* electrophysiology, cAMP formation and dopamine release in rat hippocampus and striatum. *J. Pharmacol. Exp. Ther.*, **252**, 1134-1141.

LUTHIN, D.R. & LINDEN, J. (1995). Comparison of A_4 and A_{2a} binding sites in striatum and COS cells transfected with adenosine A_{2a} receptors. *J. Pharmacol. Exp. Ther.*, **272**, 511-518.

LUTHIN, D.R., OLSSON, R.A., THOMPSON, R.D., SAWMILLER, D.R. & LINDEN, J. (1995). Characterisation of two affinity states of adenosine A_{2a} receptors with a new radioligand, 2-[2-(4-amino-3-[^{125}I]iodophenyl)ethylamino]adenosine. *Mol. Pharmacol.*, **47**, 307-313.

MacKINNON, A.C., STEWART, M., OLVERMAN, H.J., SPEDDING, M. & BROWN, C. (1993). [^{3}H]p-aminoclonidine and [^{3}H]idazoxan label different populations of imidazoline sites on rat kidney. *Eur. J. Pharmacol.*, **232**, 79-87.

MAEMOTO, T., FINLAYSON, K., ATKINS, J.M., PERRY, R.C., OLVERMAN, H.J. & BUTCHER, S.P. (1994). Regional and species differences in [^{3}H]DPCPX binding to brain adenosine A_1 receptors. *Br. J. Pharmacol.*, **113**, 53P.

MAENHAUT, C., VAN SANDE, J., LIBERT, F., ABRAMOWICZ, M., PARMENTIER, M., VANDERHAEGHEN, J.J., DUMONT, J.E., VASSART, G. & SCHIFFMANN, S. (1990). RDC8 codes for an adenosine A_2 receptor with physiological constitutive activity. *Biochem. Biophys. Res. Comm.*, **173**, 1169-1178.

MAHAN, L.C., McVITTIE, L.D., SMYK-RANDALL, E.M., NAKATA, H.M., MONSMA, F.J., GERFEN, C. & SIBLEY. D. (1991). Cloning and expression of an A_1 adenosine receptor from rat brain. *Mol. Pharmacol.*, **40**, 1-7.

MARQUARDT, D.L., WALKER, L.L. & HEINEMANN, S. (1994). Cloning of two adenosine receptor subtypes from mouse bone marrow-derived mast cells. *J. Immunol.*, **152**, 4508-4515.

MARSHALL, F.A., CLARK, S.A., MICHEL, A.D. & BARNES, J.C. (1993). Binding of angiotensin antagonists to rat liver and brain membranes measured *ex-vivo*. *Br. J. Pharmacol.*, **109**, 760-764.

MARSTON, H.M., BAIRD, A.L. & BUTCHER, S.P. (1994). Functional dissociation of adenosine A_1 and A_2 receptor directed drugs using a behavioural index. *Br. J. Pharmacol.*, **113**, 110P.

MARTINEZ-MIR, M.I., PROBST, A. & PALACIOS, J.M. (1991). Adenosine A_2 receptors: Selective localisation in the human basal ganglia and alterations with disease. *Neurosci.*, **42**, 697-706.

MAZZONI, M.R., MARTINI, C. & LUCACCHINI, A. (1993). Regulation of agonist binding to A_{2a} adenosine receptors: effects of guanine nucleotides (GDP[S] and GTP[S]) and Mg^{2+} ion. *Biochim. Biophys. Acta.*, **1220**, 76-84.

MAZZONI, M.R., BUFFONI, R.S., GIUSTI, L. & LUCACCHINI, A. (1995). Characterisation of a low affinity binding site for N^6-substituted adenosine derivatives in rat testis membranes. *J. Rec. Sig. Trans. Res.*, **15**, 905-929.

MCILWAIN, H. (1972). Regulatory significance of the release and action of adenine derivatives in cerebral systems. *Biochem. Soc. Symp.*, **36**, 69-85.

MENG, F., XIE, G., CHALMERS, D., MORGAN, C., WATSON, S.J. & AKIL, H. (1994a). Cloning and characterisation of a pharmacologically distinct A_1 adenosine receptor from guinea pig brain. *Mol. Brain Res.*, **26**, 143-155.

MENG, F., XIE, G., CHALMERS, D., MORGAN, C., WATSON, S.J. & AKIL, H. (1994b). Cloning and expression of the A_{2a} adenosine receptor from guinea pig brain. *Neurochem. Res.*, **19**, 613-621.

MEYERHOF, W., MULLER-BRECHLIN, R. & RICHTER, D. (1991). Molecular cloning of a novel putative G-protein coupled receptor expressed during rat spermiogenesis. *FEBS Lett*, **284**, 155-160.

MILLIGAN, G., BOND, R.A. & LEE, M. (1995). Inverse agonism: pharmacological curiosity or potential therapeutic strategy. *Trends Pharmacol. Sci.*, **16**, 10-13.

MIZUMOTO, H. & KARASAWA, A. (1993). Renal tubular site of action of KW3902, a novel adenosine A_1-receptor antagonist, in anaesthetised rats. *Jpn. J. Pharmacol.*, **61**, 251-253.

MIZUMOTO, H., KARASAWA, A. & KUBO, K. (1993). Diuretic and renal protective effects of 8-(noradamantan-3-yl)-1,3-dipropylxanthine (KW3902), a novel adenosine A_1-receptor antagonist, via pertussis toxin insensitive mechanism. *J. Pharmacol. Exp. Ther.*, **266**, 200-206.

MOGUL, D.J., ADAMS, M.E. & FOX, A.P. (1993). Differential activation of adenosine receptors decrease N-type but potentiates P-type Ca^{2+} current in hippocampal CA3 neurons. *Neuron*, **10**, 327-334.

MONITTO, C.L., LEVITT, R.C., DISILVESTRE, D. & HOLROYD, K.J. (1995). Localisation of the A_3 adenosine receptor gene (ADORA3) to human chromosome 1p. *Genomics*, **26**, 637-638.

MONOPOLI, A., CONTI, A., DIONISOTTI, S., CASATI, C., CAMAIONI, E., CRISTALLI, G. & ONGINI, E. (1994). Pharmacology of the highly selective A_1 adenosine receptor agonist 2-chloro-N^6-cyclopentyladenosine. *Arzneim. Forsch. Drug Res.*, **44**, 1305-1312.

MOSER, G.H., SCHARDER, J. & DEUSSEN, A. (1989). Turnover of adenosine in plasma of human and dog blood. *Am. J. Physiol.*, **256**, C799-C806.

MULLIS, K.B. & FALOONA, F.A. (1987). Specific synthesis of DNA *in vitro* via a polymerase-catalysed chain reaction. *Methods Enzymol.*, **155**, 335-350.

MURPHY, K.M.M. & SNYDER, S.H. (1980). Adenosine receptors in rat testis: Labelling with ^{3}H-cyclohexyladenosine. *Life Sci.*, **28**, 917-920.

MURPHY, K.M.M. & SNYDER, S.H. (1982). Heterogeneity of adenosine A_1 receptor binding in brain tissue. *Mol. Pharmacol.*, **22**, 250-257.

MURRISON, E.M., GOODSON, S.J., HARRIS, C.A. & EDBROOKE, M.R. (1995). The human A_3 adenosine receptor gene. *Biochem. Soc. Trans.*, **23**, 270S.

MURRISON, E.M., GOODSON, S.J., EDBROOKE, M.R. & HARRIS, C.A. (1996). Cloning and characterisation of the human adenosine A_3 receptor gene. *FEBS Lett.*, **384**, 243-246.

MURTHY, K.S. & MAKHLOUF, G.M. (1995). Adenosine A_1 receptor-mediated activation of phospholipase C-β_3 in intestinal muscle: dual requirement for α and $\beta\gamma$ subunits of G_{i3}. *Mol. Pharmacol.*, **47**, 1172-1179.

NAKATA, H. (1990). A_1 adenosine receptor of rat testis membranes. *J. Biol. Chem.*, **265**, 671-677.

NAKATA, H. (1992). Biochemical and immunological characterisation of A_1 adenosine receptors purified from human brain membranes. *Eur. J. Biochem.*, **206**, 171-177.

NAKATA, H. (1993). Development of an antiserum to rat-brain A_1 adenosine receptor: application for immunological and structural comparison of A_1 adenosine receptors from various tissues and species. *Biochim. Biophys. Acta.*, **1177**, 93-98.

NANOFF, C. & STILES, G.L. (1993). Solubilisation and characterisation of the A_2-adenosine receptor. *J. Rec. Res.*, **13**, 961-973.

NANOFF, C., MITTERAUER, T., ROKA, F., HOHENEGGER, M. & FREISSMUTH, M. (1995). Species differences in A_1 adenosine receptor/G protein coupling: Identification of a membrane protein that stabilises the association of the receptor/G protein complex. *Mol. Pharmacol.*, **48**, 806-817.

NIKODIJEVIC, O., SARGES, R., DALY, J.W. & JACOBSON, K.A. (1991). Behavioural effects of A_1- and A_2- selective adenosine agonists and antagonists: Evidence for synergism and antagonism. *J. Pharmacol. Exp. Ther.*, **259**, 286-294.

NOMURA, H., NAGASHIMA, K., KUSAKA, H. & KARASAWA, A. (1995). Antihypertensive effects of KW3902, an adenosine A_1-receptor antagonist, in dahl salt-sensitive rats. *Jpn. J. Pharmacol.*, **68**, 389-396.

NONAKA, H., SHIMADA, J., NONAKA, Y., KOIKE, N., AOKI, N., KOBAYASHI, H., KASE, H., YAMAGUCHI, K. & SUZUKI, F (1993). Photoisomerisation of a potent and selective A_2 antagonist, *(E)*-1,3-dipropyl-8-(3,4-dimethoxystyryl)-7-methylxanthine. *J. Med. Chem.*, **36**, 3731-3733.

NONAKA, H., MORI, A., ICHIMURA, M., SHINDOU, T., YANAGAWA, K., SHIMADA, J. & KASE, H. (1994). Binding of [^{3}H]KF17837S, a selective adenosine A_{2a} receptor antagonist, to rat brain membranes. *Mol. Pharmacol.*, **46**, 817-822.

NONAKA, H., ICHIMURA, M., TAKEDA, M., KANDA, T., SHIMADA, J., SUZUKI, F. & KASE, H. (1996). KW-3902, a selective high affinity antagonist for adenosine A_1 receptors. *Br. J. Pharmacol.*, **117**, 1645-1652.

OKSENBERG, D., MARSTERS, S.A, O'DOWD, B.F., JIN, H., HAVLIK, S., PEROUTKA, S.J. & ASHKENAZI, A. (1992). A single amino-acid difference confers major pharmacological variation between human and rodent 5-HT_{1b} receptors. *Nature*, **360**, 161-163.

OLAH, M.E. & STILES, G.L. (1990). Agonists and antagonists recognise different but overlapping populations of A_1 adenosine receptors: Modulation of receptor number by $MgCl_2$, solubilisation, and guanine nucleotides. *J. Neurochem.*, **55**, 1432-1438.

OLAH, M.E. & STILES, G.L. (1992). Adenosine receptors. *Ann. Rev. Physiol.*, **54**, 211-225.

OLAH, M.E. & STILES, G.L. (1995). Adenosine receptor subtypes: Characterisation and therapeutic regulation. *Ann. Rev. Pharmacol. Toxicol.*, **35**, 581-606.

OLAH, M.E., REN, H., OSTROWSKI, J., JACOBSON, K.A. & STILES, G.L. (1992). Cloning, expression and characterisation of the unique bovine A_1 adenosine receptor: studies on the ligand binding site by site directed mutagenesis. *J. Biol. Chem.*, **267**, 10764-10770.

OLAH, M.E., JACOBSON, K.A. & STILES, G.L. (1994). Role of the second extracellular loop of adenosine receptors in agonist and antagonist binding. *J. Biol. Chem.*, **269**, 24692-24698.

OLIVEIRA, J.C., SEBASTIAO, A.M. & RIBEIRO, J.A. (1991). Solubilised rat brain adenosine receptors have two high-affinity binding sites for 1,3-dipropyl-8-cyclopentylxanthine. *J. Neurochem.*, **57**, 1165-1171.

OLSSON, R.A. & PEARSON, J.D. (1990). Cardiovascular purinoreceptors. *Physiol. Rev.*, **70**, 761-845.

O'ROURKE, M.F., BLAXALL, H.S., IVERSEN, L.J. & BYLUND, D.B. (1994). Characterisation of [^{3}H]RX821002 binding to alpha-2 adrenergic receptor subtypes. *J. Pharmacol. Exp. Ther.*, **268**, 1362-1367.

OSTROWSKI, J., KJELSBERG, M.A., CARON, M.G. & LEFKOWITZ, R.J. (1992). Mutagenesis of the β_2 adrenergic receptor: how structure elucidates function. *Ann. Rev. Pharmacol. Toxicol.*, **32**, 167-183.

PALACIOS, J.M., FASTBOM. J., WIEDERHOLD, K.H. & PROBST, A. (1987). Visualisation of adenosine A_1 receptors in the human and guinea pig kidney. *Eur. J. Pharmacol.*, **138**, 273-276.

PALMER, T.M. & STILES, G.L. (1995). Adenosine Receptors. *Neuropharmacol.*, **34**, 683-694.

PALMER, T.M., BENOVIC, J.L. & STILES, G.L. (1995a). Agonist-dependent phosphorylation and desensitisation of the rat A_3 adenosine receptor. *J. Biol. Chem.*, **270**, 29607-29613.

PALMER, T.M., GETTYS, T.W. & STILES, G.L. (1995b). Differential interaction with and regulation of multiple G-proteins by the rat A_3 adenosine receptor. *J. Biol. Chem.*, **270**, 16895-16902.

PALMER, T.M., POUCHER, S.M., JACOBSON, K.A. & STILES, G.L. (1995c). ^{125}I-4-(2-[7-amino-2-{2-furyl}{1,2,4}triazolo{2,3-a}{1,3,5} triazin-5-yl-amino]ethyl)phenol, a high affinity antagonist radioligand selective for the A_{2a} adenosine receptor. *Mol. Pharmacol.*, **48**, 970-974.

PARKINSON, F.E. & FREDHOLM, B.B. (1992). Magnesium dependent enhancement of endogenous agonist binding to A_1 adenosine receptors: A complicating factor in quantitative autoradiography. *J. Neurochem.*, **58**, 941-950.

PARKINSON, F.E., JOHANSSON, B., LINDSTROM, K. & FREDHOLM, B.B. (1996). Adenosine A_1 and A_{2a} receptors and nitrobenzylthioinosine-sensitive transporters in gerbil brain: no changes following long term treatment with the adenosine transport inhibitor propentoffyline. *Neuropharmacol.*, **35**, 79-89.

PATEL, S., CHAPMAN, K.L., HEALD, A., SMITH, A.J. & FREEDMAN, S.B. (1994a). Measurement of central nervous system activity of systemically administered CCK_B receptor antagonists by *ex-vivo* binding. *Eur. J. Pharmacol.*, **253**, 237-244.

PATEL, S., SMITH, A.J., CHAPMAN, K.L., FLETCHER, A.E., KEMP, J.A., MARSHALL, G.R., HARGREAVES, R.J., RYECROFT, W., IVERSEN, L.L., IVERSEN, S.D., BAKER, R., SHOWELL, G.A., BOURRAIN, S., NEDUVELIL, J.G., MATTASSA, V.G. & FREEDMAN, S.B. (1994b). Biological properties of the benzodiazepine amidine derivative L-740,093, a cholecystokinin-B/Gastrin receptor antagonist with high affinity *in-vitro* and high potency *in-vivo*. *Mol. Pharmacol.*, **46**, 943-948.

PAXINOS, G. & WATSON, C. (1982). *The rat brain in stereotaxic coordinates.* Academic Press: New York.

PEACHEY, J.A., HOURANI, S.M.O. & KITCHEN, I. (1994). The binding of 1,3-[^{3}H]-dipropyl-8-cyclopentylxanthine to adenosine A_1 receptors in rat smooth muscle preparations. *Br. J. Pharmacol.*, **113**, 1249-1256.

PEET, N.P., LENTZ, N.L., DUDLEY, M.W., OGDEN, A.M.L., McCARTY, D.R. & RACKE, M.M. (1993). Xanthines with C^8 chiral substituents as potent and selective adenosine A_1 antagonists. *J. Med. Chem.*, **36**, 4015-4020.

PETERFREUND, R.A., MACCOLLIN, M., GUSELLA, J. & FINK, S. (1996). Characterisation and expression of the human A_{2a} adenosine receptor gene. *J. Neurochem.*, **66**, 362-368.

PIERCE, K.D., FURLONG, T.J., SELBIE, L.A. & SHINE, J. (1992). Molecular cloning and expression of an adenosine A_{2b} receptor from human brain. *Biochem. Biophys. Res. Comm.*, **187**, 86-93.

PIERSEN, C.E., TRUE, C.D. & WELLS, J.N. (1994). A carboxyl-terminally truncated mutant and nonglycosylated A_{2a} adenosine receptors retain ligand binding. *Mol. Pharmacol.*, **45**, 861-870.

PODEVIN, E.F.B. & PODEVIN, R.A. (1983). Isolation of basolateral and brush border membranes from the rabbit kidney cortex. *Biochim. Biophys. Acta.*, **735**, 86-94.

PRATER, M.N., TAYLOR, H., MUNSHI, R. & LINDEN, J. (1992). Indirect effect of guanine nucleotides on antagonist binding to A_1 adenosine receptors: Occupation of cryptic binding sites by endogenous vesicular adenosine. *Mol. Pharmacol.*, **42**, 765-772.

PUFFINBARGER, N.K., HANSEN, K.R., RESTA, R., LAURENT, A.B., KNUDSEN, T.B., MADARA, J.L. & THOMPSON, L.F. (1995). Production and characterisation of multiple antigenic peptide antibodies to the adenosine A_{2b} receptor. *Mol. Pharmacol.*, **47**, 1126-1132.

RAMKUMAR, V. & STILES, G.L. (1988). Reciprocal modulation of agonist and antagonist binding to A_1 adenosine receptors by guanine nucleotides is mediated via a pertussis toxin-sensitive G Protein. *J. Pharmacol. Exp. Ther.*, **246**, 1194-1200.

REDDINGTON, M., KLOTZ, K.N., LOHSE, M.J. & HIETEL, B. (1989). Radiation inactivation analysis of the A_1 adenosine receptor of rat brain. *FEBS Lett.*, **252**, 125-128.

REN, H. & STILES, G.L. (1994a). Characterisation of the human A_1 adenosine receptor gene: evidence for alternative splicing. *J. Biol. Chem.*, **269**, 3104-3110.

REN, H. & STILES, G.L. (1994b). Posttranscriptional mRNA processing as a mechanism for regulation of human A_1 adenosine receptor expression. *Proc. Natl. Acad. Sci.*, **91**, 4864-4866.

REN, H. & STILES, G.L. (1995). Separate promoters in the human A_1 adenosine receptor gene direct the synthesis of distinct messenger RNAs that regulate receptor abundance. *Mol. Pharmacol.*, **48**, 975-980.

REPPERT, S.M., WEAVER, D.R., STEHLE, J.H. & RIVKEES, S.A. (1991). Molecular cloning and characterisation of a rat A_1 adenosine receptor that is widely expressed in brain and spinal cord. *Mol. Endocrinol.*, **5**, 1037-1048.

RIBEIRO, J.A. & SEBASTIAO, A.M. (1986). Adenosine receptors and calcium: basis for proposing a third (A_3) adenosine receptor. *Prog. Neurobiol.*, **26**, 179-209.

RIBEIRO, J.A. & SEBASTIAO, A.M. (1994). Further evidence for adenosine A_3 receptors. *Trends Pharmacol. Sci.*, **15**, 13.

RICHARDS, M.L. & SADEE, W. (1985). *In-vivo* opiate receptor binding of oripavines to mu, delta and kappa sites in rat brain as determined by an *ex-vivo* labelling method. *Eur. J. Pharmacol.*, **114**, 343-353.

RIVKEES, S.A. (1994). Localisation and characterisation of adenosine receptor expression in rat testis. *Endocrinology*, **135**, 2307-2313.

RIVKEES, S.A. & REPPERT, S.M. (1992). RFL9 encodes an A_{2b} adenosine receptor. *Mol. Endocrinol.*, **6**, 1598-1604.

RIVKEES, S.A., LASBURY, M.E. & BARBHAIYA, H. (1995a). Identification of domains of the human A_1 adenosine receptor that are important for binding receptor subtype-selective ligands using chimeric A_1/A_{2a} adenosine receptors. *J. Biol. Chem.*, **270**, 20485-20490.

RIVKEES, S.A., LASBURY, M.E., STILES, G.L., HENEGARIU, O., CURTIS, C. & VANCE, G. (1995b). The human A_1 adenosine receptor: ligand binding properties, sites of somatic expression and chromosomal localisation. *Endocrine*, **3**, 623-629.

RIVKEES, S.A., PRICE, S.L. & ZHOU, F.C. (1995c). Immunohistochemical detection of A_1 adenosine receptors in rat brain with emphasis on localisation in the hippocampal formation, cerebral cortex, cerebellum and basal ganglia. *Brain Res.*, **677**, 193-203.

SACKTOR, B., ROSENBLOOM, I.L., LIANG, C.T. & CHENG, L. (1981). Sodium gradient- and sodium plus potassium gradient-dependent L-glutamate uptake in renal basolateral membrane vesicles. *J. Mem. Biol.*, **60**, 63-71.

SAJJADI, F.G. & FIRESTEIN, G.S. (1993). cDNA cloning and sequence analysis of the human A_3 adenosine receptor. *Biochim. Biophys. Acta.*, **1179**, 105-107.

SALVATORE, C.A., JACOBSON, M.A., TAYLOR, H.E., LINDEN, J. & JOHNSON, R.J. (1993). Molecular cloning and characterisation of the human A_3 adenosine receptor. *Proc. Natl. Acad. Sci.*, **90**, 10365-10369.

SAMAMA, P., COTECCHIA, S., COSTA, T. & LEFKOWITZ, R.J. (1993). A mutation-induced activated state of the β_2-adrenergic receptor. *J. Biol. Chem.*, **268**, 1625-4636.

SANGER, F., NICKLEN, S. & COULSON, A.R. (1977). DNA sequencing with chain-terminating inhibitors. *Proc. Natl. Acad. Sci.*, **74**, 5463-5467.

SATTIN, A. & RALL, T.W. (1970). The effect of adenosine and adenine nucleotides on the cyclic adenosine 3'5' phosphate content of guinea pig cerebral cortex slices. *Mol. Pharmacol.*, **6**, 13-23.

SCHUTZ, W. & FREISSMUTH, M. (1992). Reverse intrinsic activity of antagonists on G protein-coupled receptors. *Trends Pharmacol. Sci.*, **13**, 376-380.

SCHWABE, U., LORENZEN, A. & GRUN, S. (1991). Adenosine receptors in the central nervous system. *J. Neural Trans.*, **34**, 149-155.

SCHWIEBERT, E.M., KARLSON, K.H., FRIEDMAN, P.A., DIETL, P., SPIELMAN, W.S. & STANTON, B.A. (1992). Adenosine regulates a chloride channel via protein kinase C and a G protein in a rabbit cortical collecting duct cell line. *J. Clin. Invest.*, **89**, 834-841.

SETHY, V.H. & FRANCIS, J.W. (1988). Regulation of brain acetylcholine concentration by muscarinic receptors. *J. Pharmacol. Exp. Ther.*, **246**, 243-248.

SHIMADA, J., SUZUKI, F., NONAKA, H., ISHII, A. & ICHIKAWA, S. (1992). *(E)*-1,3-dialkyl-7-methyl-8-(3,4,5-trimethoxy-styryl)xanthines: Potent and selective A_2 antagonists. *J. Med. Chem.*, **35**, 2342-2345.

SNYDER, S.H. (1985). Adenosine as a neuromodulator. *Ann. Rev. Neurosci.*, **8**, 103-124.

SOMOGYI, A.A., SIMMONS, N. & GROSS, A.S. (1994). *In-vitro* potencies of histamine H_2-receptor antagonists on tetraethylammonium uptake in rat renal brush-border membrane vesicles. *J. Pharm. Pharmacol.*, **46**, 375-377.

SPIELMAN, W.S. & AREND, L.J. (1991). Adenosine receptors and signalling in the kidney. *Hypertension*, **17**, 117-130.

SPIELMAN, W.S., KLOTZ, K.N., AREND, L.J., OLSON, B.A., LEVIER, D.G. & SCHWABE, U. (1992). Characterisation of adenosine A_1 receptor in a cell line (28A) derived from rabbit collecting tubule. *Am. J. Physiol.*, **263**, C502-C508.

STEHLE, J.H., RIVKEES, S.A., LEE, J.J., WEAVER, D.R., DEEDS, J.D. & REPPERT, S.M. (1992). Molecular cloning and expression of the cDNA for a novel adenosine A_2 adenosine receptor subtype. *Mol. Endocrinol.*, **6**, 384-393.

STILES, G.L. (1985). The A_1 adenosine receptor. *J. Biol. Chem.*, **260**, 6728-6732.

STILES, G.L. (1986). Photoaffinity crosslinked A_1 adenosine receptor binding subunits: homologous glycoprotein expression by different tissues. *J. Biol. Chem.*, **261**, 10839-10843.

STILES, G.L. (1988). A_1 adenosine receptor-G protein coupling in bovine brain membranes: Effects of guanine nucleotides, salt, and solubilisation. *J. Neurochem.*, **51**, 1592-1598.

STILES, G.L. (1990). Adenosine receptors and beyond: Molecular mechanisms of physiological regulation. *Clin. Res.*, **38**, 10-18.

STILES, G.L. (1992). Adenosine receptors. *J. Biol. Chem.*, **267**, 6451-6454.

STONE, G.A., JARVIS, M.F., SILLS, M.A., WEEKS, B., SNOWHILL, E.W. & WILLIAMS, M. (1998). Species differences in the high affinity A_2 binding sites in striatal membranes from mammalian brain. *Drug Dev. Res.*, **15**, 31-46.

STRADER, C.D., FONG, T.M., TOTA, M.R. & UNDERWOOD, D. (1994). Structure and function of G protein-coupled receptors. *Ann. Rev. Biochem.*, **63**, 101-132.

STROHER, M., NANOFF, C. & SCHUTZ, W. (1989). Differences in the GTP-regulation of membrane-bound and solubilised A_1-adenosine receptors. *Naunyn-Schmiedeberg's Arch. Pharmacol.*, **340**, 87-92.

SUZUKI, F., SHIMADA, J., MIZUMOTO, H., KARASAWA, A., KUBO, K., NONAKA, H., ISHII, A. & KAWAKITA, T. (1992). Adenosine A_1 antagonists. 2. Structure-activity relationships on diuretic activities and protective effects against acute renal failure. *J. Med. Chem.*, **35**, 3066-3075.

SUZUKI, F., SHIMADA, J., SHIOZAKA, S., ICHIKAWA, S., ISHII, A., NAKAMURA, J., NONAKA, H., KOBAYASHI, H. & FUSE, E. (1993). Adenosine A_1 antagonists. 3. Structure-activity relationships on amelioration against scopolamine- or N^6-((R)-phenylisopropyl)adenosine-induced cognitive disturbance. *J. Med. Chem.*, **36**, 2508-2518.

SWANSON, T.H., DRAZBA, J.A. & RIVKEES, S.A. (1995). Adenosine A_1 receptors are located predominantly on axons in the rat hippocampal formation. *J. Comp. Neurology*, **363**, 517-531.

SWEENEY, M.I. (1996). Adenosine release and uptake in cerebellar granule neurons both occur via an equilibrative nucleoside carrier that is modulated by G proteins. *J. Neurochem.*, **67**, 81-88.

TAKEDA, M., YOSHITOMI, K. & IMAI, M. (1993). Regulation of Na^+-$3HCO_3^-$ cotransport in rabbit proximal convoluted tubule via adenosine A_1 receptor. *Am. J. Physiol.*, **265**, F511-F519.

TANG, W.J. & GILMAN, A.G. (1992). Adenylyl cyclases. *Cell*, **70**, 869-872.

TAYLOR, S.J., MICHEL, A.D. & KILPATRICK, G.J. (1992). *In-vivo* occupancy of histamine H_3 receptors by thioperamide and (R)-alpha-methylhistamine measured using histamine turnover and an *ex-vivo* labelling technique. *Biochem. Pharmacol.*, **44**, 1261-1267.

TERAI, T., KITA, Y., KUSUNOKI, T., SHIMAZAKI, T., ANDOH. T., HORAI, H., AKAHANE, A., SHIOKAWA, Y. & YOSHIDA, K. (1995a). A novel non-xanthine adenosine A_1 receptor antagonist. *Eur. J. Pharmacol.*, **279**, 217-225.

TERAI, T., KITA, Y., KUSUNOKI, T., ANDOH. T., NAGATOMI, I., HORAI, H., AKAHANE, A., SHIOKAWA, Y. & YOSHIDA, K. (1995b). Renal effects of FK453: A potent non-xanthine adenosine A_1 receptor antagonist. *Drug Dev. Res.*, **36**, 25-34.

TOTA, M.R., CANDELORE, M.R., DIXON, R.A.F. & STRADER, C.D. (1991). Biophysical and genetic analysis of the ligand-binding site of the β-adrenoreceptor. *Trends Neurosci.*, **12**, 4-6.

TOWNSEND-NICHOLSON, A &. SHINE, J. (1992). Molecular cloning and characterisation of a human brain A_1 adenosine receptor cDNA. *Mol. Brain Res.*, **16**, 365-370.

TOWNSEND-NICHOLSON, A. & SCHOFIELD, P.R. (1994). A threonine residue in the seventh transmembrane domain of the human A_1 adenosine receptor mediates specific agonist binding. *J. Biol. Chem.*, **269**, 2373-2376.

TOWNSEND-NICHOLSON, A., BAKER, E., SCHOFIELD, P.R. & SUTHERLAND, G.R. (1995). Localisation of the adenosine A_1 receptor subtype gene (ADORA1) to chromosome 1q32.1. *Genomics*, **26**, 423-425.

TOYA, Y., UNEMURA, S., IWAMOTO, T., HIRAWA, N., KIHARA, M., TAKAGI, N. & ISHII, M. (1993). Identification and characterisation of adenosine A_1 receptor-cAMP system in human glomeruli. *Kid. Intl.*, **43**, 928-932.

TRAVERSA, U., ROSATI, A.M., FLORIO, C. & VERTUA, R. (1994). Effects of divalent cations on adenosine agonist binding to A_1 receptors and non-A_1/non-A_2 sites in rat cerebral cortex. *Pharmacol. Toxicol.*, **75**, 28-35.

TUCKER, A.L. & LINDEN, J. (1993). Cloned receptors and cardiovascular responses to adenosine. *Cardiovascular Res.*, **27**, 62-67.

TUCKER, A.L., LINDEN, J., ROBEVA, A.S., D'ANGELO, D.D. & LYNCH, K.R. (1992). Cloning and expression of a bovine adenosine A_1 receptor cDNA. *FEBS Lett.*, **297**, 107-111.

TUCKER, A.L., ROBEVA, A.S., TAYLOR, H.E., HOLETON, D., BOCKNER, M., LYNCH, K.R. & LINDEN, J. (1994). A_1 adenosine receptors. *J. Biol. Chem.*, **269**, 27900-27906.

UHLEN, S. & WIKBERG, J.E.S. (1991a). Delineation of rat kidney α_{2a} and α_{2b}-adrenoreceptors with [^{3}H]RX821002 radioligand binding: computer modelling reveals that guanfacine is an α_2-selective compound . *Eur. J. Pharmacol.*, **202**, 235-243.

UHLEN, S. & WIKBERG, J.E.S. (1991b). Rat spinal cord α_2-adrenoreceptors are of the α_{2a}- subtype: Comparison with α_{2a} and α_{2b}-adrenoreceptors in rat spleen, cerebral cortex and kidney using [^{3}H]RX821002 ligand binding . *Pharmacol. Toxicol.*, **69**, 341-350.

UHLEN, S. & WIKBERG, J.E.S. (1991c). Delineation of three pharmacological subtypes of α_2-adrenoreceptor in the rat kidney. *Br. J. Pharmacol.*, **104**, 657-664.

UHLEN, S., XIA, Y., CHAJILANI, V., FELDER, C.C. & WIKBERG, J.E.S. (1992). [^{3}H]MK912 binding delineates two α_2-adrenoreceptor subtypes in rat CNS, one of which is identical with the cloned pA2d α_2-adrenoreceptor. *Br. J. Pharmacol.*, **106**, 986-995.

UHLEN, S., XIA, Y., CHAJILANI, V., LIEN, E.J. & WIKBERG, J.E.S. (1993). Evidence for the existence of two forms of α_{2a}-adrenoreceptors in the rat. *Naunyn-Schmeideberg's Arch. Pharmacol.*, **347**, 280-288.

UKENA, D., JACOBSON, K.A., PADGETT, W.L., AYALA, C., SHAMIM, M.T., KIRK, K.L., OLSSON, R.A. & DALY, J.W. (1986). Species differences in structure-activity relationships of adenosine agonists and xanthine antagonists at brain A_1 adenosine receptors. *FEBS Lett.*, **209**, 122-128.

UMEMIYA, M. & BERGER, A.J. (1994). Activation of adenosine A_1 and A_2 receptors differentially modulates calcium channels and glycinergic synaptic transmission in rat brainstem. *Neuron*, **13**, 1439-1446.

UNGERER, M., OBERMAIER-SKROBRANEK, B. & LOHSE, M.J. (1992). Adenosine A_1 receptor gene structure and regulation in normotensive and spontaneously hypertensive rats. *Mol. Pharmacol.*, **226**, 381-382.

VAN CALKER, D., MULLER, M. & HAMPRECHT, B. (1979). Adenosine regulates, via two different types of receptors, the accumulation of cAMP in cultured brain cells. *J. Neurochem.*, **33**, 999-1005.

VAN GALEN, P.J.M., VAN BERGEN, A.H., GALLO-RODRIGUEZ, C., MELMAN, N., OLAH, M.E., IJZERMAN, A.P., STILES, G.L. & JACOBSON, K.A. (1994). A binding site model and structure-activity relationships for the rat A_3 adenosine receptor. *Mol. Pharmacol.*, **45**, 1101-1111.

VANHOUTTE, P.M., HUMPHREY, P.P.A. & SPEDDING, M. (1996). X. International union of pharmacology recommendations for nomenclature of new receptor subtypes. *Pharmacol. Rev.*, **48**, 1-2.

VON LUBITZ, D.K.J.E., PAUL, I.A., BARTUS, R.T. & JACOBSON, K.A. (1993). Effects of chronic administration of adenosine A_1 receptor agonist and antagonist on spatial learning and memory. *Eur. J. Pharmacol.*, **249**, 271-280.

VON LUBITZ, D.K.J.E., CARTER, M.F., DEUTSCH, S.I., LIN, R.C.S., MASTROPAOLO, J., MESHULAM, Y. & JACOBSON, K.A. (1995). The effects of adenosine A_3 receptor stimulation on seizures in mice. *Eur. J. Pharmacol.*, **275**, 23-29.

VON LUBITZ, D.K.J.E., CARTER, M.F., BEENHAKKER, M., LIN, R.C.S. & JACOBSON, K.A. (1996). Adenosine: a prototherapeutic concept in neurodegeneration. *Ann. NY. Acad. Sci.*, **765**, 163-179.

WAN, W., SUTHERLAND, G.R. & GEIGER, J.D. (1990). Binding of the adenosine A_2 receptor ligand [^{3}H]CGS21680 to human and rat brain: Evidence for multiple affinity states. *J. Neurochem.*, **55**, 1763-1771.

WATSON, W.P., MISRA, A., CROSS, A.J., GREEN, A.R. & LITTLE, H.J. (1994). The differential effects of felodipine and nitrendipine on cerebral dihydropyridine binding *ex-vivo* and the ethanol withdrawal syndrome in mice. *Br. J. Pharmacol.*, **112**, 1017-1024.

WEAVER, D.R. (1993). A_{2a} adenosine receptor gene expression in developing rat brain. *Mol. Brain Res.*, **20**, 313-327.

WEAVER, D.R. & REPPERT, S.M. (1992). Adenosine receptor gene expression in rat kidney. *Am. J. Physiol.*, **263**, F991-995.

WEBER, R.G., JONES, C.R., PALACIOS, J.M. & LOHSE, M.J. (1988). Autoradiographic visualisation of A_1-adenosine receptors in brain and peripheral tissues of rat and guinea pig using ^{125}I-HPIA. *Neurosci. Lett.*, **87**, 215-220.

WEBER, R.G., JONES, R.C., LOHSE, M.J. & PALACIOS, J.M. (1990a). Autoradiographic visualisation of A_1 adenosine receptors in rat brain with [^{3}H]8-cyclopentyl-1,3-dipropylxanthine. *J. Neurochem.*, **54**, 1344-1353.

WEBER, R.G., BRINES, M.L., HEBERT, S.C. & FORREST, J.N. (1990b). Demonstration of A_1 adenosine receptors on rat medullary thick ascending limb tubules by radioligand binding. *Kid. Intl.*, **37**, 380.

WIENER, H.L. & MAAYANI, S. (1991). Species-dependent attenuation of adenosine A_1 agonist binding by guanine nucleotides. *Eur. J. Pharmacol.*, **208**, 271-272.

WILLIAMS, M. (1987). Purine receptors in mammalian tissues: Pharmacology and functional significance. *Ann. Rev. Pharmacol. Toxicol.*, **27**, 315-345.

WILLIAMS, M. (1993). Purinergic Drugs: opportunities in the 1990s. *Drug Dev. Res.*, **28**, 438-444.

WILLIAMS, M. & RISLEY, E.A. (1980). Biochemical characterisation of putative central purinergic receptors by using 2-chloro[^{3}H]adenosine, a stable analog of adenosine. *Proc. Natl. Acad. Sci.*, **77**, 6892-6896.

WOODCOCK, E.A., LOXLEY, R., LEUNG, E. & JOHNSTON, C.I. (1984). Demonstration of R_A-adenosine receptors in rat renal papillae. *Biochem. Biophys. Res. Comm.*, **121**, 434-440.

WOODCOCK, E.A., LEUNG, E. & JOHNSTON, C.I. (1986). Adenosine receptors in papilla of human kidneys. *Clin. Sci.*, **70**, 353-357.

WU, P.H. & CHURCHILL, P.C. (1985). 2-Chloro-[^{3}H]-adenosine binding in isolated rat kidney membranes. *Arch. Intl. Pharmacodyn.*, **273**, 83-87.

YAGIL, Y. (1993). The effects of adenosine on water and sodium excretion. *J. Pharmacol. Exp. Ther.*, **268**, 826-835.

YAMAGUCHI, S., UMEMURA,S., TAMURA, K., IWAMOTO, T., NYUI, N., ISHIGAMA, T. & ISHII, M. (1995). Adenosine A_1 receptor mRNA in microdissected rat nephron segments. *Hypertension*, **26**, 1181-1185.

YAWO, H. & CHUHMA, N. (1993). Preferential inhibition of ω-conotoxin-sensitive presynaptic Ca^{2+} channels by adenosine autoreceptors. *Nature*, **365**, 256-258.

YEUNG, S.M.H. & GREEN, R.D. (1983). Agonist and antagonist affinities for inhibitory adenosine receptors are reciprocally affected by 5'-guanylylimidodiphosphate or *N*-ethylmaleimide. *J. Biol. Chem.*, **258**, 2334-2339.

YEUNG, S.M.H. & GREEN, R.D. (1984). [^{3}H]5'-N-ethylcarboxamide adenosine binds to both R_a and R_i adenosine receptors in rat striatum. *Naunyn-Schmiedeberg's Arch. Pharmacol.*, **325**, 218-225.

ZHAO, Z., RAVID, S. & RAVID, K. (1995). Chromosomal mapping of the mouse A_3 adenosine receptor gene, ADORA3. *Genomics*, **30**, 118-119.

ZHOU, Q-Y., LI, C., OLAH, M.E., JOHNSON, R.A., STILES, G.L. & CIVELLI, O. (1992). Molecular cloning and characterisation of an adenosine receptor: the A_3 adenosine receptor. *Proc. Natl. Acad. Sci.*, **89**, 7432-7436.

ZOCCHI, C., ONGINI, E., FERRARA, S., BARALDI, P.G. & DIONISOTTI, S. (1996). Binding of the radioligand [^{3}H]-SCH58261, a new non-xanthine A_{2A} adenosine receptor antagonist, to rat striatal membranes. *Br. J. Pharmacol.*, **117**, 1521-1529.